

Washington University in St. Louis

Washington University Open Scholarship

Arts & Sciences Electronic Theses and
Dissertations

Arts & Sciences

Summer 8-15-2016

Functions of the DNA Polymerase Delta Replicase in Lagging Strand Replication

Joseph L. Stodola

Washington University in St. Louis

Follow this and additional works at: https://openscholarship.wustl.edu/art_sci_etds



Part of the [Biochemistry Commons](#)

Recommended Citation

Stodola, Joseph L., "Functions of the DNA Polymerase Delta Replicase in Lagging Strand Replication" (2016). *Arts & Sciences Electronic Theses and Dissertations*. 727.
https://openscholarship.wustl.edu/art_sci_etds/727

This Dissertation is brought to you for free and open access by the Arts & Sciences at Washington University Open Scholarship. It has been accepted for inclusion in Arts & Sciences Electronic Theses and Dissertations by an authorized administrator of Washington University Open Scholarship. For more information, please contact digital@wumail.wustl.edu.

WASHINGTON UNIVERSITY IN ST. LOUIS

Division of Biology and Biomedical Sciences

Biochemistry

Dissertation Examination Committee:

Peter Burgers, Chair

Roberto Galletto

Tim Lohman

Sheila Stewart

Heather True

Functions of the DNA Polymerase Delta Replicase in Lagging Strand
Replication

By

Joseph L. Stodola

A dissertation presented to the
Graduate School of Arts and Sciences
of Washington University in
partial fulfillment of the
requirements for the degree
of Doctor of Philosophy

August 2016
St. Louis, Missouri

© 2016, Joseph Stodola

Table of Contents

List of Figures	iii
Acknowledgments	iv
Abstract	v
Chapter I: Introduction	1
Chapter II: Analysis of metal-binding domains in the catalytic subunit of DNA polymerase δ	33
Chapter IIA: Eukaryotic DNA polymerases require an iron-sulfur cluster for the formation of active complexes	35
Chapter IIB: Identification and characterization of PCNA mutants that Suppress Pol δ-CysA lethality	66
Chapter III: A four-subunit DNA polymerase ζ complex containing Pol δ accessory subunits is essential for PCNA-mediated mutagenesis	83
Chapter IV: Proficient replication of the yeast genome by a viral DNA polymerase	99
Chapter V: Resolving individual steps of Okazaki-fragment maturation at a millisecond timescale	115
Chapter VI: Sequential switching of binding partners on PCNA during in vitro Okazaki fragment maturation	136
Chapter VII: Pif1 removes a Rap1-dependent barrier to the strand displacement activity of DNA polymerase δ	153
Chapter VIII: Future Directions	167
References	172

List of Figures

Figure 1: Steps of origin firing and replication initiation in budding yeast.	24
Figure 2: Organization of the eukaryotic replication fork.	25
Figure 3: Subunit organization of the eukaryotic B-family DNA polymerases.	26
Figure 4: Structure of B-family polymerases.	27
Figure 5: Structures of C-terminal domain and accessory subunits of eukaryotic B-family polymerases.	28
Figure 6: Model of Okazaki fragment maturation.	29
Figure 7: Structure of <i>S. cerevisiae</i> PCNA.	30
Figure 8: Structure of a sliding clamp–clamp loader–DNA complex in the “notched-screw cap” conformation.	31
Figure 9: Structure of the RPA–single-stranded DNA complex.	32

Acknowledgments

I am indebted to many people who have provided guidance, assistance, and support throughout my time at Washington University. To my mentor, Peter, thank you for being a great graduate advisor. You are a thoughtful scientist and have pushed me to tackle projects that I could not have imagined accomplishing at the outset. Even more than your scientific expertise, though, I thank you for truly caring about the well-being of your students, postdocs, and staff. I am lucky to have trained in your lab. To Bonnie, thank you for your relentless optimism. You are always able to find a bright spot in a lab meeting full of negative data, and willing to help out when my day is full and I need an extra set of hands.

I have had the opportunity with many wonderful people and great scientists in the Burgers' lab. Carrie Stith has been in the lab since my first day as a rotation student, and few days go by in which she does not either save my experiment or save time by finding the elusive reagent I've been looking for. Justin Sparks and Sarem Hailemariam have been my fellow graduate students in the lab over the years. Both are incredible colleagues, willing to spend time walking through a confusing piece of data, but also quick to share a good laugh in the lab. Also, many postdocs have passed through the lab during my time: Sara, Sandeep, Alena, Paulina, Sjoerd, Rachel, Elias, and Tanumoy. They have been a valuable resource of scientific expertise, as well as offering me the opportunity to learn much about the world through sharing their experiences living and studying all over the globe. To Kim, thanks for all of your encouraging words during your summer stints in the lab.

The Biochemistry department has provided a great environment to perform my thesis work. Everyone is quick to lend a reagent, piece of equipment, or some technical advice. I need to specially thank Roberto Galletto; not only a member of my thesis committee, but someone who both taught me the quench-flow kinetic technique and generously lent me his machine indefinitely, without which the work described here could not have been possible. He has also been a great collaborator in several projects in the past and hopefully in the future.

Finally, I am thankful to the National Institutes of Health for funding the work in the lab, and the United States-Israel Binational Science foundation for funding my work specifically.

ABSTRACT OF THE DISSERTATION

Functions of the DNA Polymerase Delta Replicase in Lagging Strand Replication

Joseph L. Stodola

Doctor of Philosophy in Biology and Biomedical Sciences

Biochemistry

Washington University in St. Louis, 2016

Professor Peter Burgers, Chair

The work described in this dissertation focuses on several aspects of DNA replication in the model organism *Saccharomyces cerevisiae*, with particular attention paid to the function of the replicative DNA polymerases. The majority of the work focuses on the lagging strand polymerase DNA polymerase δ (Pol δ) and its functions in Okazaki fragment synthesis and maturation. The first major theme of this dissertation is investigating the role that metal binding motifs play in the structure and function of Pol δ and other budding yeast polymerases. First, in Chapter II, I discuss the role that two metal binding motifs within the catalytic subunit of Pol δ play in creating the multi-subunit polymerase complex and in promoting crucial interactions with the replication sliding clamp, proliferating cell nuclear antigen, or PCNA. In Chapter III I describe work defining the importance of similar metal binding motifs in the translesion DNA polymerase ζ (Pol ζ). This yielded the observation that the two accessory subunits of Pol δ , Pol31 and Pol32, are also constitutive members of a four-subunit Pol ζ complex. In Chapter IV, I describe the creation of a chimeric DNA polymerase comprising the bacteriophage RB69 DNA

polymerase fused to the metal binding domain of the Pol δ catalytic subunit. We show that this chimeric polymerase can form a multimeric complex containing the Pol δ accessory subunits, interact with PCNA, and support DNA replication *in vivo*. This data provided insight into the structural requirements of the lagging strand replication machinery.

The second major theme is Pol δ 's crucial role in synthesizing Okazaki fragments and participating in the removal of initiator RNA, called Okazaki fragment maturation. Chapter V describes my work developing a system to study the activity of Pol δ in higher kinetic detail than previous studies, using rapid-quench techniques. This work yielded insights into how Pol δ performs DNA synthesis and strand displacement synthesis, as well as accomplishes nick translation, requiring collaboration between Pol δ and the flap-endonuclease FEN1. Chapter VI describes the production and characterization of engineered PCNA heterotrimers. These proteins were produced to test the 'toolbelt' model, which is the hypothesis that PCNA binds multiple enzymes simultaneously to increase the efficiency of DNA metabolism processes involving multiple enzymes. Finally, there has been a growing interest among those studying lagging strand synthesis into how potential impediments to the Okazaki fragment maturation machinery are resolved. Chapter VII shows that although the transcription factor Rap1 can block strand displacement synthesis by Pol δ when it is bound to DNA, this block can be resolved through the action of the helicase Pif1.

CHAPTER I

Introduction

In all organisms, DNA replication is required for the copying of genetic information during each cell cycle. In order to faithfully maintain genetic information, the genome must be completely and accurately copied before cell division. In eukaryotes, DNA replication occurs during the synthesis (S) phase of the cell cycle. To accomplish complete duplication of the genome, eukaryotes employ a dynamic, multi-protein complex called the replisome. A fundamental component of the replisome are replicative DNA polymerases, which perform template-directed DNA synthesis, creating a complete copy of genetic information in each cell.

The unwinding of the two strands of the DNA duplex at replication origins creates the classical bi-directional replication fork, and the polarity of each DNA strand requires that replication of each side of the fork proceed by a different mechanism. After priming, the leading strand of the fork can be synthesized continuously by a 5' to 3' polymerase. However, the opposite, the lagging strand, must be replicated discontinuously. Primers are synthesized continuously throughout replication on the lagging strand, which are then extended by lagging strand DNA polymerases. The result of this discontinuous replication is many short stretches of DNA on the lagging strand known as Okazaki fragments. To make continuous, double-stranded DNA on the lagging strand, the RNA initiating each of the Okazaki fragments must be removed and the resulting nick ligated, a process known as Okazaki fragment maturation.

In eukaryotic cells, the lagging strand is replicated by DNA polymerase delta (Pol δ), a three-subunit polymerase complex. All known functions of this polymerase are reliant on interaction with PCNA, a donut-shaped factor that encircles double-stranded DNA. Binding to PCNA greatly increases the efficiency by which Pol δ replicates, and their pairing is essential to completing DNA replication. This introduction will review current knowledge on how DNA replication occurs in eukaryotic cells. Particular emphasis will be placed on

lagging strand synthesis in budding yeast, the focus of this thesis.

Replication initiation and organization of the eukaryotic replication fork

Initiation of replication in eukaryotic systems requires the regulated, ordered assembly of multiple protein complexes at origins of replication. Of all eukaryotic DNA replication systems studied, the replication origins in budding yeast are the best understood, likely because its origins are the best defined to specific origin sequences. Replication in *S. cerevisiae* initiates from sequences known as autonomously replicating sequences (ARS), named such because of their ability to support the replication of plasmid DNA in yeast (Masai et al., 2010). Each ARS consists of three to four short (10-15 base pair) conserved sequences spread over 100-150 bp of chromosomal DNA (Bell and Dutta, 2002). These short sequences include the highly conserved Autonomously-replicating-sequence Conserved Sequence (ACS), along with other, less conserved elements. The key feature of origins in all eukaryotes, including budding yeast, is that they are binding sites for the origin recognition complex (ORC), which begins the process of origin firing when it binds to origin DNA.

The complex process of replication initiation has been studied by many groups since the development of molecular biology techniques, and remains an active area of research. To briefly summarize and simplify this complex process (**Fig. 1**), replication initiation and origin firing can be divided into two main steps (Bell and Dutta, 2002; Masai et al., 2010; Weinreich, 2015). First, during late M and early G1 phase, the ORC complex binds origin DNA and, together with other protein factors (Cdc6 and Cdt1), recruits the MCM2-7 complex, the replicative helicase. The ordered assembly of these factors results in the loading of the MCM complex onto the origin DNA so that its binding is stable. The loaded MCMs, in complex with ORC, are known as the prereplicative complex (pre-RC). In the second major step, phosphorylation events (by the

kinases DDK and CDK) allow the recruitment of two further protein factors (Cdc45 and GINS) to the loaded MCMs at the G1 to S phase transition. These three factors, Cdc45, the MCMs, and GINS form what is known as the CMG. Through the formation of the CMG, the MCM helicase is activated, allowing for initial strand separation and the formation of the classical bi-directional replication fork (Bell and Dutta, 2002; Fragkos et al., 2015; Weinreich, 2015; Yeeles et al., 2015). Additionally, the CMG acts as a platform upon which further protein complexes are formed, resulting in the recruitment of the replicative DNA polymerases (Pols ϵ , α , and δ) and accessory factors (including RPA, RFC, and PCNA) to the newly formed fork.

In eukaryotes, including budding yeast, three main polymerases perform replicative DNA synthesis, Pol α , Pol δ , and Pol ϵ (Johansson and Dixon, 2013; Johansson and Macneill, 2010). The Pol α complex contains both polymerase and primase activities, and primes synthesis on both the leading and lagging strand. Pol α is additionally required to initiate each of the Okazaki fragments on the lagging strand. Pol δ and Pol ϵ have long been recognized as the major replicative polymerases, together performing the vast majority of DNA synthesis. Despite this knowledge, many groups sought to define roles for Pol δ and Pol ϵ in replication more specifically, i.e. which polymerase synthesizes DNA on which strand (leading and lagging) of the replication fork? A large body of evidence is consistent with a division of labor model of the eukaryotic replication fork (Burgers, 2009; Nick McElhinny et al., 2008). In this model (**Fig. 2**), DNA on the leading strand is synthesized by Pol ϵ , and the lagging strand is replicated by Pol δ . This conclusion has been supported by genetic data examining asymmetric mismatch generation by Pol δ and Pol ϵ (Larrea et al., 2010; Nick McElhinny et al., 2008; Pursell et al., 2007), studies of polymerase localization on replication forks (Yu et al., 2014), and rNMP incorporation in the two DNA strands (Reijns et al., 2015). *In vitro* work using purified CMG helicase complex

and the three replicative polymerases to more closely simulate *in vivo* replication has also supported this model; Pol ϵ and Pol δ were found to spontaneously replicate the leading and lagging strands, respectively, consistent with the conclusions from genetic studies. These recent studies have additionally suggested that Pol ϵ and Pol δ are in fact inhibited from replicating on their ‘incorrect’ strand (Georgescu et al., 2014; 2015). For these reasons, the model placing Pol ϵ on the leading strand and Pol δ on the lagging strand has become widely accepted.

Despite the preponderance of evidence supporting the organization of the replication fork as detailed above, a recent study has suggested an alternate arrangement of replicative polymerases at the fork (Johnson et al., 2015). The authors of this study conclude that Pol δ is the major replicative polymerase on *both* strands of the replication fork. They argue that Pol ϵ is localized to the leading strand, but playing a largely non-catalytic role. Despite raising concerns that must be addressed by the field as a whole, discussion of this study will be limited due to technical and data analysis concerns raised by several groups (Burgers et al., 2016; Johnson et al., 2016).

It is important to note that Johnson et al. makes no argument against the persisting agreement that Pol δ is the main replicative polymerase of the lagging strand (Johnson et al., 2015; Nick McElhinny et al., 2008). This has been supported by many of the studies cited above, and is additionally supported by genetic and biochemical evidence linking Pol δ with Okazaki fragment maturation (Garg et al., 2004; Jin et al., 2001; 2003; Stith et al., 2008).

The eukaryotic B-family polymerases: organization and structure

In budding yeast and higher eukaryotes, each of the replicative DNA polymerases, Pol α ,

Pol δ , and Pol ϵ , is a multi-subunit complex consisting of a polymerase subunit and additional accessory subunits. Pol δ contains three subunits (Pol3, Pol31, and Pol32), Pol α , four subunits (Pol1, Pol12, Pri1, Pri2), and Pol ϵ , four as well (Pol2, Dpb2, Dpb3, Dpb4) (Johansson and Dixon, 2013; Johansson and Macneill, 2010). The subunit composition and organization of these polymerase complexes is diagrammed in **Fig. 3**. The catalytic subunits containing polymerase activity (Pol1, Pol2, and Pol3) are phylogenetically related, and are members of the Family B polymerases (Doubl   and Zahn, 2014). Eukaryotes also contain a fourth B-family DNA polymerase, the translesion DNA polymerase Pol ζ (Makarova and Burgers, 2015). Like the other family members, Pol ζ is a multi-subunit complex consisting of the catalytic subunit Rev3 as well as accessory subunits Rev7, Pol31, and Pol32 (the latter two shared with Pol δ) (Makarova et al., 2012).

The Family B polymerases are one of seven described DNA polymerase families, and are found not only in eukaryotes but also in archaea, viruses, and proteobacteria (Doubl   and Zahn, 2014; Fil  e et al., 2002; Ito and Braithwaite, 1991). These polymerases are classified as such according to the structural organization of their polymerase domain, into five subdomains: the palm, finger, thumb, exonuclease, and N-terminal domain (NTD) (**Fig. 4**) (Doubl   and Zahn, 2014; Franklin et al., 2001; Hopfner et al., 1999). The first three, the palm, finger, and thumb domains, contain the polymerase activity of the enzymes. This common polymerase fold is conserved among not only the B-family polymerases, but among all DNA polymerases and even polymerases with different activities (i.e. RNA polymerases and reverse transcriptases).

The exonuclease domain is present in all four eukaryotic, B-family polymerases, but is only active in the catalytic subunits of Pol δ and Pol ϵ . This activity, a 3' to 5' nuclease activity,

is the proofreading activity of the enzyme, correcting for incorrectly incorporated nucleotides. In Pol α and Pol ζ , the critical residues required for exonucleolytic cleavage have been lost, and these enzymes are not able to proofread for misincorporations. As the original function of the exonuclease domain has not been preserved in these polymerases, the overall structure of this domain in Pol α is not as well-conserved as the exonuclease domains of Pol δ and Pol ϵ (Doubl   and Zahn, 2014).

The N-terminal domain of each eukaryotic, B-family polymerase does not contain an enzymatic activity, and its function in each polymerase is largely undefined. The structure of the Pol3-NTD contains motifs that resemble an OB fold, found in proteins that bind single-stranded DNA, and also an RNA-binding motif (Swan et al., 2009). This structural homology has led to the proposal that the N-terminal domain may be involved in binding template DNA upstream of the 3'-primer terminus. However, this hypothesis remains unconfirmed, and a specific role for the NTD in Pol δ or the other B-family polymerases has yet to be described.

What distinguishes the B-family polymerases in eukaryotes from those found in simpler organisms is the presence of an additional subdomain, the C-terminal domain (CTD). Although part of the same polypeptide chain as the polymerase subunits, the C-terminal domains have been predicted to be physically separated from the main catalytic core of these polymerases, connected by a linker peptide lacking significant structure (Jain et al., 2009). The main function of the CTD in the eukaryotic polymerases is to mediate interactions between the polymerase subunit and the B-subunits of each polymerase (either Pol12, Dpb2, or Pol31) (Netz et al., 2012). Since all four polymerases contain phylogenetically conserved CTDs and B-subunits, it is likely that the CTD/B-subunit pair in each polymerase adopts a similar, conserved structure. Direct structural evidence for this hypothesis is currently unavailable. The only CTD/B-subunit

structure solved to date is the yeast Pol1-CTD in complex with its B-subunit Pol12 (Klinge et al., 2009) (**Fig. 5a**). Bound to Pol12, the Pol1-CTD adopts an “elongated, bilobal shape” (Klinge et al., 2009). Each lobe contains four conserved metal-binding cysteine residues, a structural feature present in all four CTDs. In Pol1/Pol12, the second of these four-cysteine motifs, along with a conserved α helix, makes extensive contacts with the B-subunit Pol12, suggesting that the interaction between these two proteins is constitutive. Chapter II takes this line of research further, by investigating the function of the metal-binding clusters in these polymerases.

In addition to the Pol12 structure, a structure of the Pol δ B-subunit (p50, the human homologue of yeast Pol31) has been solved, in complex with a portion of the third subunit (p66, homologue of yeast Pol32) (Baranovskiy et al., 2008a; 2008b) (**Fig. 5b**). Comparing these two B-subunit structures has revealed common structural features. Both Pol12 and p50 contain two main domains: an N-terminal OB-like fold, and a C-terminal phosphodiesterase-like scaffold. The OB-like motif is analogous to DNA-binding folds found in single-stranded DNA binding proteins, and may help the polymerase complex bind nucleic acid. It is thought that the inactivated phosphodiesterase motif, forming the bulk of both Pol12 and p50, has been optimized to form extensive protein-protein interactions with the polymerase CTDs.

The p50 structure also contains a fragment of p66, the third subunit of Pol δ (Pol32 in budding yeast). The p66 fragment forms a winged helix-turn-helix (wHTH) domain, and makes extensive contacts with the C-terminal end of p50. The authors hypothesize that the structure solved in this study represents the true “B-subunit” core, even though it is spread over two separate polypeptides in Pol δ . They note that the primary structure of the Pol δ B-subunit differs from that of Pol ϵ and Pol α (Dpb2 and Pol12, respectively), both of which contain an N-

terminal region of unknown structure not found in Pol δ . Computational predictions of this region in both Dpb2 and Pol12 are consistent with a wHTH, suggesting that the OB-fold/phosphodiesterase/wHTH structure observed in the Pol δ accessory subunits (pictured in **Fig. 5b**) may be a structural feature found in all the B-family polymerases. While each of the B-family polymerases contain more than just two subunits, the additional accessory subunits spread among the polymerases are not conserved like the catalytic and B-subunits, and I will focus further discussion on Pol δ .

Current understanding of the overall structure of the Pol3-Pol31-Pol32 complex remains incomplete. No high-resolution structure of the entire polymerase complex has been solved to date. Nevertheless, some insight has been gained by other techniques. A small angle X-ray scattering study examined the full, three-subunit budding yeast complex (Jain et al., 2009), finding that the polymerase overall forms an elongated structure. This paper proposes a structure in which the globular core of Pol3 forms one structural unit, while Pol3-CTD-Pol31-Pol32 form a second, elongated, structural unit. This was consistent with sedimentation velocity analysis of the complex (Johansson et al., 2001). However, both analyses were performed in the absence of both DNA and Pol δ 's obligate partner in DNA replication, PCNA. It is plausible and even likely that when bound to PCNA and template-primer DNA, Pol δ does not adopt an elongated structure like it may in solution (and in SAXS analysis), but may appear more compact overall. Future study is required to address what structures the PCNA-Pol δ -DNA complex adopts, and how this may differ from when Pol δ is in solution.

Processivity of PCNA-Pol δ

Processivity is the ability of an enzyme to catalyze successive reactions without dissociating from its substrate. It was recognized soon after its discovery that Pol δ polymerizes

DNA with low processivity (Bauer and Burgers, 1988; Burgers, 1988; Downey et al., 1990; Prelich et al., 1987), meaning that the number of nucleotides incorporated by the polymerase in a single polymerase-DNA binding event is low (<10 nucleotides). As alluded to previously, processive DNA synthesis by Pol δ requires an additional replication factor, proliferating cell nuclear antigen (PCNA). This factor, which forms a toroidal structure that can be loaded around double-stranded DNA, stabilizes Pol δ on DNA and allows the polymerase to replicate hundreds of nucleotides in a single DNA-binding event. Although PCNA is now recognized to have many functions in DNA replication and repair (detailed further below), it was first purified from calf thymus and yeast as a factor able to stimulate processive DNA synthesis by Pol δ (Bauer and Burgers, 1988; Tan et al., 1986).

The *POL3* and *POL31* genes encoding the first two subunits of Pol δ are essential in budding yeast (Gerik et al., 1998; Hartwell, 1976; Sugimoto et al., 1995). The third subunit Pol32, however, is not essential for growth (Gerik et al., 1998). These observations can be explained in the context of Pol δ 's interactions with PCNA. Over the years, motifs responsible for interactions between Pol δ and PCNA have been found in all three subunits of Pol δ (Acharya et al., 2011; Johansson et al., 2004; Netz et al., 2012); the most well-characterized is a conserved, PCNA-interacting protein (PIP) motif at the extreme C-terminus of Pol32. A Pol3-Pol31 complex can also be purified from budding yeast, known as Pol δ^* (Burgers and Gerik, 1998). This complex retains the ability to synthesize DNA processively in a PCNA-dependent manner, as opposed to Pol3 alone, which inefficiently replicates even in the presence of PCNA (Acharya et al., 2011). Retention of PCNA-dependent processivity likely explains why *POL32* is dispensable for cell viability but *POL31* is not. However, *pol32 Δ* cells are sensitive to DNA damaging agents (Johansson et al., 2004), consistent with the observation that Pol δ^* does not

replicate as efficiently *in vitro* as the full, three-subunit complex.

Subunit composition of Pol δ in other eukaryotes

Polymerases delta from other eukaryotes contain a fourth subunit, known as Cdm1 in fission yeast and PolD4 in humans (Johansson and Dixon, 2013). This subunit displays limited sequence conservation across evolution (Johansson and Macneill, 2010), and most effort has been dedicated to understanding this subunit's function in the context of the human Pol δ . No structural information is available for PolD4, but it is thought to interact directly with both the catalytic and B-subunit of the Pol δ complex (Li et al., 2006). In keeping with its complete absence in some organisms, this subunit has been found to be dispensable for polymerase activity (Lin et al., 2013). In fact, it is possible that the polymerase complex actually functioning in human DNA replication is the three-subunit Pol δ . Levels of the fourth subunit have been shown to drop during S phase (Chea et al., 2012; Lee et al., 2012), and PolD4 has also been shown to be degraded in response to several types of DNA damage (Zhang et al., 2007). The absence of the fourth subunit has been linked to some changes in activity, most notably in the processes that govern Okazaki fragment maturation. Three-subunit human Pol δ exhibits less strand displacement synthesis activity (Lin et al., 2013), which may be preferable in the context of normal DNA replication to prevent the formation of potentially-damaging long flaps. As the authors of this study note, the three-subunit human Pol δ seems ideally suited to performing DNA replication during S phase (this form also exhibits more efficient proofreading activity), and seems to be the predominant complex present during S phase. It remains to be determined, then, what the cellular function of the four-subunit Pol δ complex is in human cells.

Okazaki fragment maturation – short flap pathway

In addition to DNA synthesis on the lagging strand, each of the RNA primers that initiate the Okazaki fragments must be removed, and the resulting nick ligated to yield continuous double-stranded DNA. This multi-step process is known as Okazaki fragment maturation (**Fig. 6**). Given the current size estimates for eukaryotic Okazaki fragments, approximately 100,000 fragments must be matured during each cell cycle in budding yeast, and millions in the much larger human genome (Balakrishnan and Bambara, 2013a). Despite this challenge, it is essential for each Okazaki fragment to be correctly processed, as either DNA nicks or flap intermediates resulting from incomplete processing can lead to expansion mutations, duplications, or double-stranded DNA breaks (Gordenin et al., 1997). The core enzymatic machinery sufficient to observe Okazaki fragment maturation *in vitro* consists of three enzymes, Pol δ , flap endonuclease 1 (FEN1), and DNA ligase I (Stith et al., 2008). All three enzymes interact with PCNA, which localizes and stabilizes each enzyme on lagging strand replication intermediates.

The maturation process begins when the 5'-end of the preceding Okazaki fragment interrupts Pol δ as it is extending a lagging strand primer. When it encounters the 5'-end of a DNA that blocks polymerase progress, Pol δ has the intrinsic ability to displace the proximal 5'-nucleotides and incorporate across from the newly exposed template bases, an activity called strand displacement synthesis (Garg et al., 2004). With the wild-type polymerase, the limited amount of strand displacement synthesis that occurs when the polymerase first encounters a 5'-block is balanced by the activity of the polymerase's 3'-5' exonuclease activity. After incorporating a few nucleotides, the wild-type Pol δ moves the primer end to its exonuclease and cuts out the newly incorporated bases back to the nick position. When allowed to continue indefinitely, these activities, incorporation and exonucleolytic cleavage, will cycle, which is

known as idling (Garg et al., 2004; Stith et al., 2008). Idling by Pol δ limits strand displacement, allowing the nick to be maintained and preventing the formation of long flaps that cannot be processed by the next enzyme in the pathway, FEN1. When the exonuclease activity of Pol δ is inactivated by mutation in biochemical experiments, the polymerase no longer idles and can only move forward in incorporation mode. Such a mutation results in more extensive strand displacement synthesis than the wild-type polymerase and generates longer 5'-flaps, but provides a clearer way of observing strand displacement by Pol δ , which we have exploited in our biochemical studies (Stith et al., 2008).

Strand displacement by Pol δ generates a distribution of short 5'-flaps, which become the substrate for the next core maturation enzyme, FEN1. Flap endonuclease 1 is a structure-specific endonuclease that can thread the 5'-end of flaps into its helical arch to cut flaps of varying lengths (Balakrishnan and Bambara, 2013b). FEN1 cuts the short 5'-flaps produced by Pol δ , removing a few bases of RNA primer, moving the nick position. The current view of Okazaki fragment maturation is that complete removal of the RNA that initiates Okazaki fragments is achieved through the repeated action of Pol δ strand displacement and FEN1 cleavage, in a cycle known as nick translation (Stith et al., 2008).

FEN1 was first implicated in Okazaki fragment maturation through genetic studies in *Saccharomyces cerevisiae* that noted the formation of duplications flanked by repeat sequences in *rad27 Δ* strains (Jin et al., 2001; Tishkoff et al., 1997). These authors hypothesized that the duplications were the result of ligation of an unprocessed 5'-flap to the 3'-end of the downstream Okazaki fragment, linking FEN1 to the proper maturation of Okazaki fragments. Soon after, *in vitro* experiments showed that FEN1 was able to process Pol δ -created flaps to yield a ligatable

nick (Ayyagari et al., 2003; Maga et al., 2001), further linking FEN1 to Okazaki fragment maturation.

Much effort has been dedicated to understanding what the optimal DNA substrate for FEN1 cleavage is. The current view in the field is that FEN1 prefers substrates with a double-flap structure, containing both a 3'- and 5'-flap. Specifically, FEN1 best cuts substrates that contain a single nucleotide 3'-flap. Regardless of the length of the 5'-flap, FEN1 will cut one base into the upstream duplex. With the 3'-flap then able to anneal, cleavage yields a ligatable nick. Such a model is consistent with biochemical and structural data (Balakrishnan and Bambara, 2013b; Kao et al., 2002; Tsutakawa et al., 2011). As only 5'-flaps are produced during Okazaki fragment maturation from Pol δ strand displacement, nascent flaps would need to rearrange to form the optimal FEN1 substrate, with a single 3'-extrahelical nucleotide. It is unclear as to whether this would occur from random re-equilibration of the flap or in an active process by one of the Okazaki fragment maturation enzymes.

The final step of Okazaki fragment maturation is ligation, which is performed by DNA ligase I. This enzyme cannot seal RNA-DNA nicks, and only ligates after complete removal of initiator RNA. In eukaryotic replication systems, this enzyme is less dependent on PCNA, even though it contains a PCNA-binding domain (Vijayakumar et al., 2007). One function of this domain is to recruit ligase to replication foci (Montecucco et al., 1998). However, other studies have shown that ligase acts distributively, with the position of ligation following RNA removal largely dependent on ligase concentration (Ayyagari et al., 2003). As such, the currently prevailing model states that PCNA-interaction is important for generally localizing DNA ligase to replication forks, with the actual ligation step being much less dependent on PCNA.

Long-flap processing of Okazaki fragments

The previously described Okazaki fragment maturation pathway is the major pathway functioning to remove initiator RNA on the lagging strand. However, there are instances where this pathway is not sufficient. Critically, if FEN1 becomes disengaged from PCNA or is not present at a particular Okazaki fragment, extended strand displacement synthesis by Pol δ can result in a flap that is able to bind to RPA. RPA can stably bind flaps that are greater than ~20 nt (Rossi et al., 2008). FEN1 is unable to cleave flaps containing RPA, and other enzymatic activities are required for processing (Bae et al., 2001). The 5'-3' helicase Pif1 has also been implicated in long-flap formation (Stith et al., 2008); it functions in mitochondrial DNA maintenance and telomere homeostasis (Boulé and Zakian, 2006). The potential danger of Pif1-generated flaps is the same; once they are large enough to bind RPA, FEN1 is unable to cut. Since the traditional processing pathway dependent on FEN1 can only process flaps of a few nucleotides in length, this pathway is alternatively known as the “short-flap processing pathway” (Balakrishnan and Bambara, 2013a).

In budding yeast, the long-flap processing pathway largely relies on the activity of Dna2, a multi-functional enzyme with nuclease, helicase, and ATPase activities (Budd et al., 1995; Kang et al., 2010). Dna2 can remove RPA from long flaps and, in a similar mechanism to FEN1, binds the flap base and threads the 5'-end of the flap to cleave at the correct position (Stewart et al., 2010). It was previously thought that Dna2 was unable to cleave flaps at their base like FEN1, and so it was hypothesized that even when Dna2 was engaged to process a long flap, FEN1 action would be required to fully process the flap to a ligatable nick. However, a recent report has provided evidence that Dna2 can in fact cleave RPA-coated flaps at their base, yielding a structure that can be ligated (Levikova and Cejka, 2015). Such a mechanism would

completely bypass the requirement of FEN1 in the processing of long flaps to double-stranded DNA.

***In vitro* studies of eukaryotic lagging strand replication**

Over many years of study, the work of the Burgers lab has defined the minimal enzymatic machinery required to observe efficient *in vitro* replication. For processive replication, Pol δ requires that the sliding clamp PCNA is loaded onto primer termini. Loading of PCNA requires cracking open the ring-shaped protein between two monomer interfaces and placing it around double-stranded DNA, which is accomplished by a protein complex called Replication Factor C (RFC). Finally, on DNA templates that are single-stranded, the single-stranded DNA binding protein Replication Protein A (RPA) stimulates the processivity of PCNA-Pol δ by removing secondary structures that can form in the template strand. These proteins form the critical machinery required by Pol δ to replicate DNA efficiently. The structural and biochemical properties of PCNA, RFC, and RPA are discussed below.

Proliferating Cell Nuclear Antigen

Proliferating Cell Nuclear Antigen, or PCNA, is an essential eukaryotic replication factor (Maga and Hubscher, 2003; Majka and Burgers, 2004; Moldovan et al., 2007). As discussed previously, this protein was first identified in eukaryotes as a factor that could increase the processivity of replicative polymerases, specifically Pol δ . PCNA is a member of a structurally and functionally conserved family of proteins known as the β clamps, members of which are found in all domains of life. Each of the β clamp proteins forms a ring-shaped complex that encircles and slides along DNA, despite large differences in amino acid sequence. The subunit composition of the β clamps varies across life forms, with eubacterial clamps existing as

homodimers, archaeal clamps as a heterotrimer, and as a homotrimer in the T4 bacteriophage and eukaryotes. Despite these differences, each of the β clamps possess very similar structures (Gulbis et al., 1996; Kong et al., 1992; Krishna et al., 1994).

Each of the monomers of PCNA, overall a homotrimeric complex (**Fig. 7**), contains two similar domains, each comprising a curved β sheet (Majka and Burgers, 2004). This creates a ring-shaped β sheet scaffold around the PCNA ring, and gives the entire complex a pseudo six-fold symmetry. On the inner portion of these β sheets are twelve alpha helices, creating a rough cylinder inside the complex. These helices outline an inner cavity that is 30 angstroms in diameter, an appropriate size to encircle double-stranded DNA (with a 20-angstrom diameter). The inner alpha helices also contain a high number of positively charged residues, and likely form favorable electrostatic interactions with the negatively charged phosphodiester backbone of DNA. The flat PCNA ring has distinct front and back faces, allowing greater functionality of the ring. The front face, also known as the C-terminal face, is the face where most protein-protein interactions take place (Jónsson et al., 1998).

The ability of PCNA and the other β clamps to encircle double-stranded DNA and slide along it makes it an ideal platform localizing DNA replication and metabolism proteins to where they are required. As discussed, PCNA is known as the polymerase processivity clamp in the context of DNA replication. However, PCNA also interacts with dozens of other DNA replication and metabolism proteins, and acts as a master regulator of DNA synthesis and repair (Majka and Burgers, 2004; Moldovan et al., 2007). The majority of these interactions are dependent on a single region of PCNA, the Interdomain Connection Loop (ICL). The ICL is a 16 amino acid long loop residing on the front face of PCNA that connects the β sheet domains present in each monomer. Although the sequence of this loop as a whole diverges across species,

an invariant leucine and isoleucine residue form an exposed hydrophobic cleft. This cleft is the primary binding pocket for the many protein-protein interactions PCNA makes. Specifically, proteins containing a PCNA Interacting Protein (PIP) box bind to PCNA in the ICL. The consensus PIP box sequence is Qxx(L/M/I)xx(F/Y)(F/Y), with the hydrophobic residues of the PIP binding to the hydrophobic pocket created by the ICL.

As the PIP motifs of various DNA metabolism proteins bind to the same region of PCNA, it is likely that each PCNA monomer is only able to bind to a single protein at one time, suggesting that competition for PCNA access may occur in the cell. Different PIP motifs have been shown to bind to PCNA with differing affinities; in one study, affinity of PIP peptides for PCNA spanned an order of magnitude (from ~ 0.1 - $3 \mu\text{M}$). In the same study, the authors showed that, in the budding yeast system, altering the balance of PIP box affinities for PCNA impacts DNA metabolism processes (Fridman et al., 2010). For example, increasing the Pol δ subunit Pol32's affinity for PCNA above normal levels results in an increase in spontaneous mutation rate and sensitivities to DNA damaging agents. Increased affinity between FEN1 and PCNA resulted in synthetic lethality, suggesting significant problems in completing DNA replication. These results suggest that the balance of affinities between different PCNA-interacting proteins is evolutionarily maintained, and that competition for PCNA must be carefully equilibrated.

The presence of three identical monomers in the PCNA ring has led to the hypothesis that more than one PCNA-interacting protein could bind a single heterotrimer ring simultaneously. This model is frequently referred to as the toolbelt model (Dovrat et al., 2014), and provides a potentially elegant explanation as to how PCNA may regulate multi-step processes involving more than one PCNA-binding enzyme. Most work to date evaluating this hypothesis has been in systems other than budding yeast, in which the homotrimeric nature of PCNA has made

biochemical studies difficult. In the archaeon *Sulfolobus solfataricus*, PCNA exists as a heterotrimer (subunits denoted PCNA1, PCNA2, and PCNA3), with each of the three major Okazaki fragment processing enzymes PolB1 (the replicative polymerase), Fen1, and Lig1 binding preferentially to different PCNA subunits, PCNA2, PCNA1, and PCNA3, respectively (Beattie and Bell, 2012). Biochemical data from this system suggests that PCNA-dependent Okazaki fragment maturation occurs most efficiently when each enzyme is able to bind to *Sulfolobus* PCNA simultaneously. Additionally, multiple groups have shown in the *E. coli* replication system that the replicative polymerase Pol III and the Y-family translesion DNA polymerase Pol IV are able to simultaneously bind the bacterial β clamp, leading to more efficient lesion bypass (Indiani et al., 2005; Kath et al., 2014). However, eukaryotic DNA replication and genome maintenance is more complicated than either of these model systems, with many more sliding clamp binding proteins identified for PCNA. As such, more work is required to better understand how PCNA participates in so many DNA metabolism processes.

Replication Factor C (RFC)

RFC is a heteropentameric protein complex that loads PCNA onto template-primer junctions (Hedglin et al., 2013a; Majka and Burgers, 2004). All domains of life rely on replication sliding clamps to complete DNA replication. As such, clamp loader complexes remarkably similar to RFC exist in prokaryotes, bacteriophage, and archaea. In budding yeast and higher eukaryotes, RFC consists of five subunits from five separate polypeptides, termed Rfc1, Rfc2, Rfc3, Rfc4, and Rfc5. All are essential for cell survival in budding yeast. These subunits share significant sequence homology with each other and with clamp loader subunits from simpler organisms. All clamp loaders described are heteropentameric, but not all are made from five distinct polypeptides. Some RFC-like complexes from simpler organisms contain

fewer than five distinct subunits, with multiple copies of certain proteins making up the pentamer.

Loading of PCNA onto primer-template DNA by RFC is an ATP-dependent process (for structural model of clamp loading, see **Fig. 8**). RFC and analogous clamp loaders belong to the diverse AAA+ ATPase family, which comprise many oligomeric complexes that couple ATP hydrolysis to modulation of protein-protein interactions through the production of mechanical force (Neuwald et al., 1999). In order to effectively place PCNA on primer-template DNAs, RFC must stably bind PCNA, locate the correct DNA substrate, open the PCNA ring and load it onto DNA, finally dissociating from PCNA and DNA to allow access to the replication clamp by proteins such as the replicative polymerases. Work by many groups has outlined how the clamp loaders accomplish this task, in a mechanism that appears to be largely conserved over the diverse class of clamp loaders.

In the absence of ATP, RFC binds with low affinity to both primer-template junctions and PCNA. Upon binding ATP, the clamp loader undergoes a conformational change that orders the complex and permits the optimal interaction between RFC and PCNA, cracking open the PCNA ring in the process. Once formed, the ATP-dependent PCNA-RFC complex specifically recognizes and binds a primer-template junction, adopting a “notched screw cap” structure that is pseudo-helical, matching the helical character of duplex DNA (Bowman et al., 2004; Kelch et al., 2011). The specific orientation of the “screw cap” structure (interacting with DNA in the minor groove) binds the last turn of the DNA double helix in a manner so that further extension of the double-stranded DNA is blocked at the 3'-end of the primer strand by a barrier within the RFC complex known as the C-terminal collar. In contrast, the template strand can clearly exit through a channel in the complex. Such a binding mechanism allows specific recognition of primer-template DNA.

When adopting the “screw cap” conformation on DNA, the ATPase sites formed between subunit interfaces within RFC are aligned for highest efficiency ATP hydrolysis. Upon ATP hydrolysis, RFC reverts back to its low-affinity DNA-binding conformation and dissociates from PCNA and DNA, leaving the PCNA ring encircling the primer-template DNA. The bound ADP can then be exchanged for ATP, allowing RFC to bind and subsequently load additional PCNA rings onto primer-template DNAs. There is some evidence, however, that complete dissociation of RFC following ATP hydrolysis is slow compared to other steps in the cycle (Hedglin et al., 2013b). This allows RFC to re-bind PCNA and unload it from primer-template DNA. Hedglin et al. observed an equilibrium, intermediate level of PCNA occupancy on primer-template DNAs when RFC was allowed to load and unload the clamp in the presence of excess ATP. The unloading activity of RFC could be inhibited, however, by trapping PCNA on DNA with Pol δ , providing insight into how PCNA unloading may be prevented when the lagging strand replicase is being assembled.

In eukaryotes, several RFC-like complexes (RLCs) have been identified. In budding yeast, each of these complexes contain the Rfc2-5 subunits contained in RFC, but contain a different subunit in place of Rfc1, either Rad24, Ctf18, or Elg1. The Rad24-RLC complex loads the PCNA-like 9-1-1 clamp, which participates in checkpoint activation. Ctf18-RLC is important for the establishment of chromatid cohesion, knowledge gained from genetic studies. It has also been shown to possess PCNA unloading activity *in vitro* (Bylund and Burgers, 2005; Majka and Burgers, 2004). However, it is still unclear whether this biochemical activity is related to the *in vivo* phenotypes observed. The most relevant alternative clamp loader to the understanding of lagging strand replication is the Elg1-RLC. Although previously thought to lack PCNA unloading activity (Bylund and Burgers, 2005), a recent series of studies has provided evidence

that Elg1-RLC unloads PCNA from the lagging strand following completion of Okazaki fragment maturation (Kubota et al., 2015; 2013a; 2013b), possibly allowing recycling of PCNA for Okazaki fragment synthesis. Cells lacking Elg1 exhibit a higher level of genomic instability, both in budding yeast and higher eukaryotes. While the various phenotypes observed could reasonably be explained by insufficient recycling of PCNA, it remains to be seen whether inefficient PCNA unloading directly results in the defects observed in *elg1Δ* cells.

Replication Protein A (RPA)

RPA was first identified as a protein factor required for replication in the *in vitro* SV40 replication system (Weinberg et al., 1990; Wold and Kelly, 1988). Since that time, it has come to be recognized as the primary single-stranded DNA binding protein in eukaryotic cells, and is involved in all aspects of DNA metabolism, including replication, recombination, and repair. Additionally, it is involved in the cellular response to DNA damage and plays a role in the activation of checkpoints. The common feature between all of these pathways is the presence of single-stranded DNA intermediates, which RPA binds very tightly, with sub-nanomolar affinity (Kim et al., 1994; Kumaran et al., 2006). A structural model of an RPA homologous to that found in budding yeast is shown in **Fig. 9**.

RPA is composed of three subunits, RPA1, RPA2, and RPA3, with sizes of 70-, 32-, and 14-kDa, respectively (structure and functions of RPA discussed in (Chen and Wold, 2014; Prakash and Borgstahl, 2012)). All three subunits contain domains that interact with single-stranded DNA. The primary structural motif involved in DNA binding is the oligonucleotide/oligosaccharide-binding fold (OB-fold). The heterotrimeric RPA complex contains six OB-folds throughout the complex, four within RPA1, and one each in RPA2 and

RPA3. This structural unit is used by other ssDNA binding proteins, such as those from T4 bacteriophage and *E. coli*, even though those proteins adopt an overall architecture that is distinct from that of the eukaryotic RPAs.

RPA can bind single-stranded DNA stably in different modes, differentiated by the number of nucleotides of DNA bound in each. Each OB-fold within RPA has the potential to bind 4-6 nucleotides of ssDNA, so engagement with a different number of OB-folds would alter the RPA binding site size. Two stable DNA-binding modes have been identified, one engaging 18-20 nucleotides and another engaging 28-30 nucleotides, representing DNA-binding with three and four OB-folds, respectively (Kumaran et al., 2006). These different binding modes likely contribute to the ability of RPA to bind DNA in a dynamic, rather than static, manner. RPA has been shown to diffuse rapidly along single-stranded DNA (Nguyen et al., 2014), and also to readily and rapidly exchange with free RPA or other DNA binding proteins in solution (Gibb et al., 2014). These results suggest that the individual OB-folds within RPA dynamically bind and dissociate from DNA. Since RPA contains multiple OB-folds, the whole complex can retain high-affinity binding to DNA even while diffusing or resolving secondary DNA structures.

As noted above, RPA is involved in a diverse array of DNA metabolism processes, but I will focus on its role in DNA replication. During S phase, RPA accumulates at replication foci, and coats the single-stranded DNA produced by the replicative helicase. The primary functions of RPA at the replication fork are: first, to protect the exposed ssDNA from nucleases, and second, to resolve secondary structures that may form on unwound DNA. Secondary structures in the template strand are an obstacle to the replicative DNA polymerases, and can become a source of deletions. If the secondary structure is not resolved, the end of the replicating strand can realign, yielding a deletion as the polymerase continues replicating.

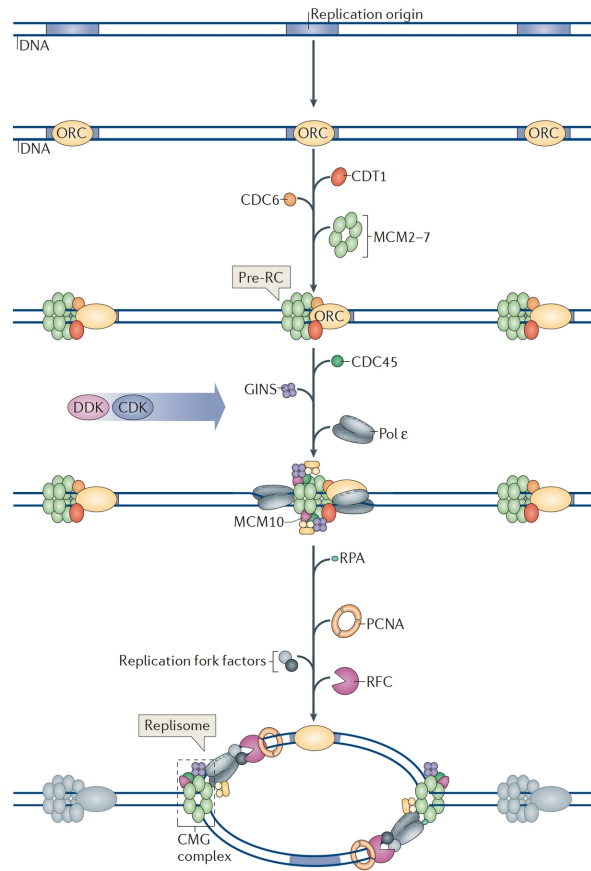


Figure 1: Steps of origin firing and replication initiation in budding yeast. Adapted from (Fragkos et al., 2015).

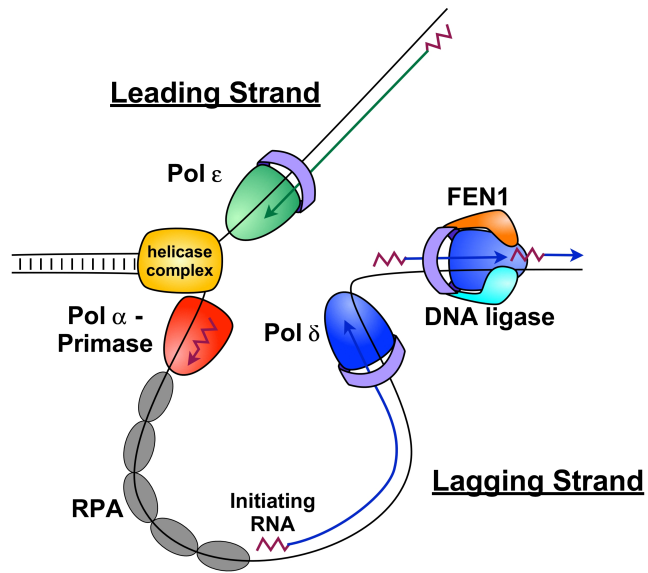


Figure 2: Organization of the eukaryotic replication fork. Adapted from (Burgers, 2009; Nick McElhinny et al., 2008).

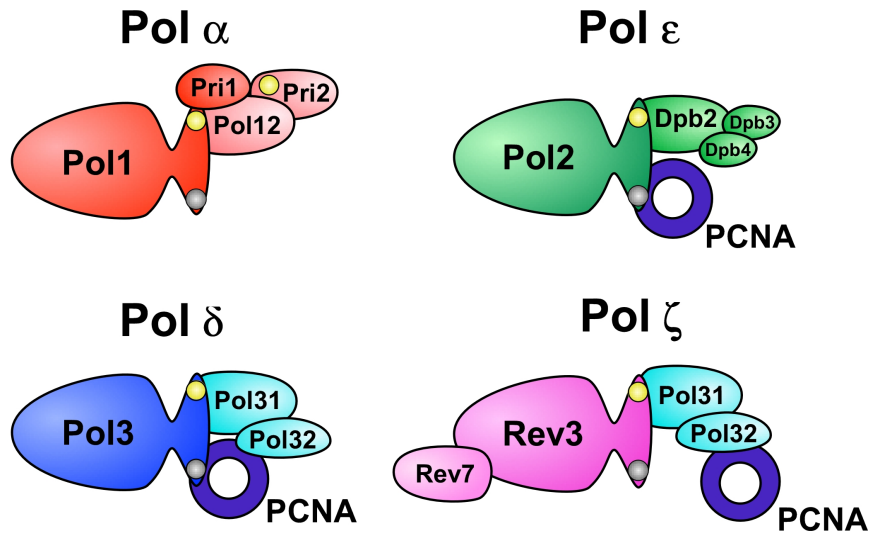


Figure 3: Subunit organization of the eukaryotic B-family DNA Polymerases. The B-family polymerases found in budding yeast are multi-subunit enzymes. Each contains a structurally conserved catalytic subunit (Pol1, Pol2, Pol3 and Rev3), consisting of a polymerase domain and a C-terminal domain that mediates interactions with additional subunits. The zinc ribbon and iron-sulfur cluster motifs within the CTDs are represented by grey and yellow circles, respectively. The iron-sulfur cluster motifs within the CTDs mediate interactions between the catalytic and second subunits. The sliding clamp PCNA stimulates three of these enzymes, and interacts with Pol ε, δ and ζ in different manners.

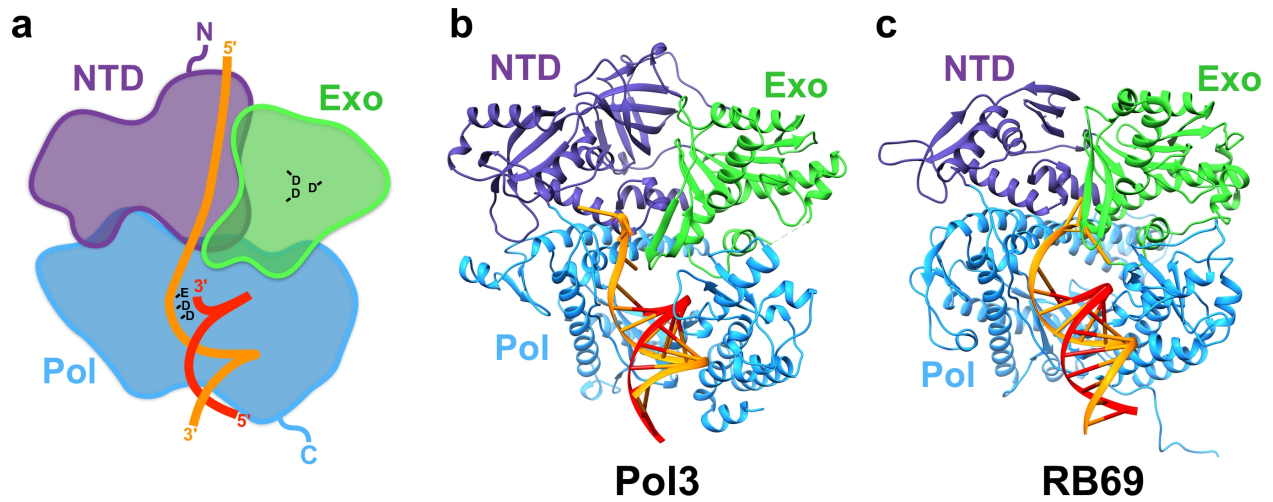


Figure 4: Structure of B-family polymerases. (a) Model of catalytic subunit of B-family polymerases. The catalytic core of all B-family polymerases is made up of five subdomains, the N-terminal domain (NTD, purple), exonuclease domain (Exo, green) and the palm, finger, and thumb domains that collectively are the polymerase domain (Pol, blue). Template-primer DNA is shown in the approximate position according to structural data. The predicted path of the template DNA (orange), between the NTD and exonuclease domains is shown. Polymerase activity relies on two catalytic aspartates and a glutamate; exonuclease activity relies on three catalytic aspartates. (b) Structure of catalytic core of Pol3 (Swan et al., 2009), catalytic subunit of *S. cerevisiae* Pol δ . (c) Structure of the bacteriophage RB69 gp43 polymerase, a close structural homologue of Pol3 (Wang et al., 2011).

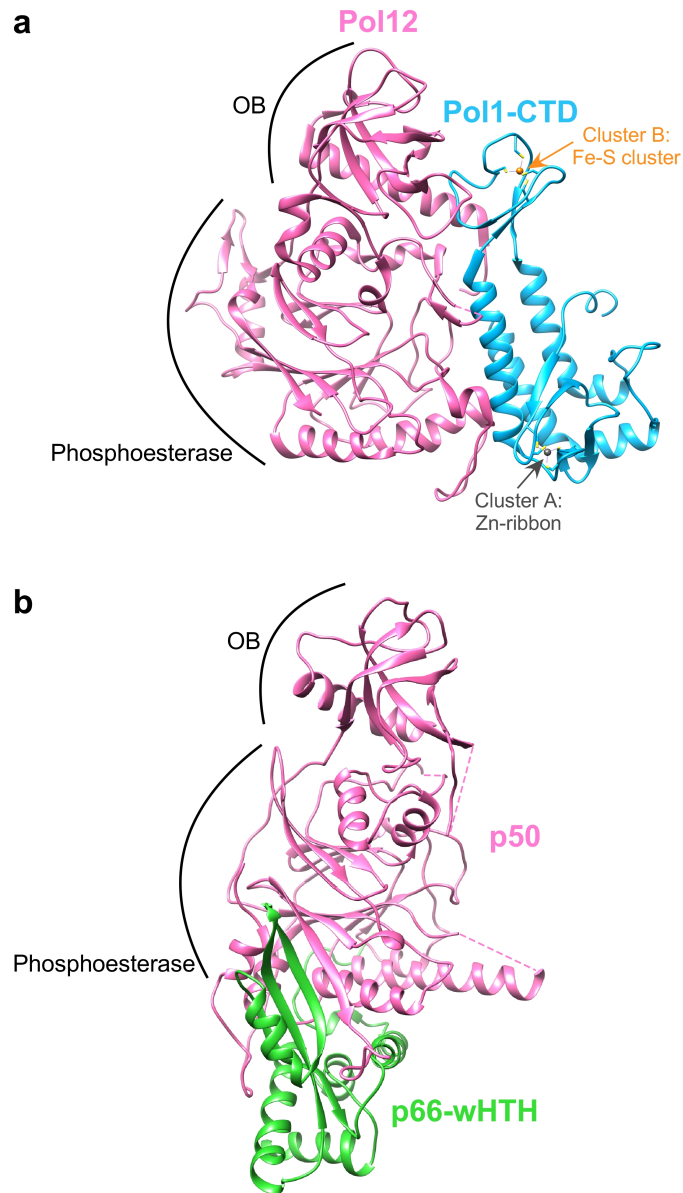


Figure 5: Structures of C-terminal domain and accessory subunits of eukaryotic B-family polymerases. (a) Structure of the Pol1-CTD (blue) in complex with Pol12 (pink), both members of the Pol α complex (Klinge et al., 2009). The two four-cysteine clusters chelating metal ions are highlighted (Cluster A and B). Structure was solved with zinc in both positions, but was labeled as an Fe-S cluster according to (Netz et al., 2012). This is also discussed in Chapter II. General domains within Pol12 containing homology to either an OB-fold or a phosphodiesterase motif are labeled. **(b)** Structure of human p50 (pink) in complex with a fragment of p66 (green) (Baranovskiy et al., 2008a). The fragment of p66 crystallized adopts a winged-helix-turn-helix (wHTH) structure.

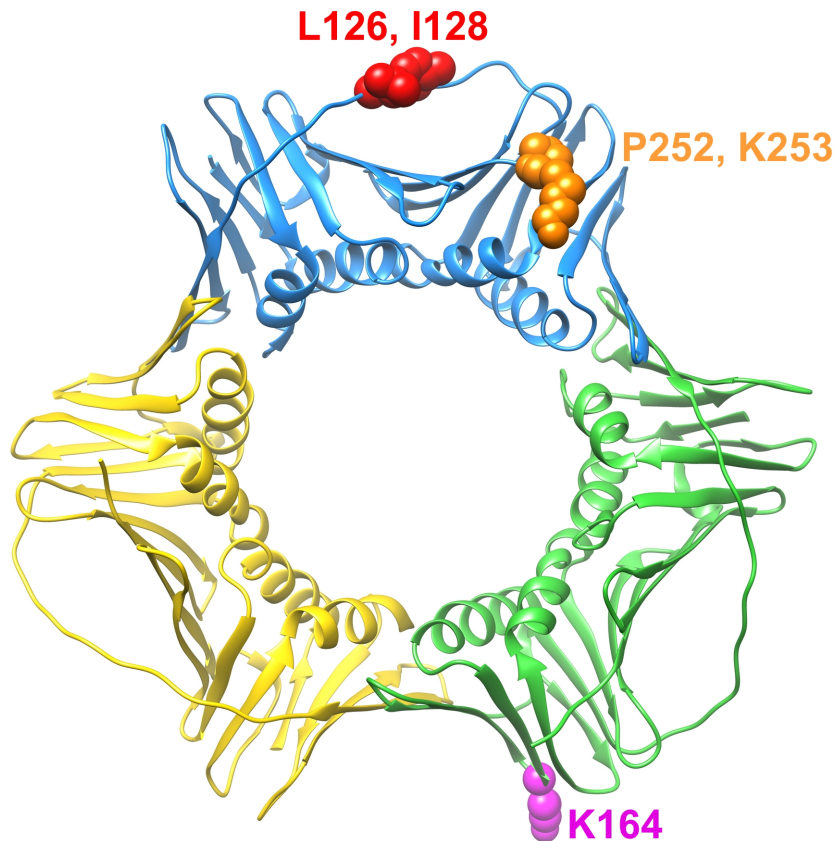


Figure 7: Structure of *S. cerevisiae* PCNA. The PCNA ring consists of three identical subunits, shown in blue, green, and yellow (Krishna et al., 1994). Residues important for protein-protein interactions and post-translational modifications are indicated. Leucine-126 and Isoleucine-128 (in red) in the interdomain connection loop form a hydrophobic pocket in which PIP box-containing proteins bind. Proline-252 and Lysine-253 are important for FEN1 interaction, specifically when PCNA is loaded onto DNA. Lysine-164 is the most important site of post-translational modification to PCNA; K164 has been shown to be a site for both ubiquitination and sumoylation of PCNA.

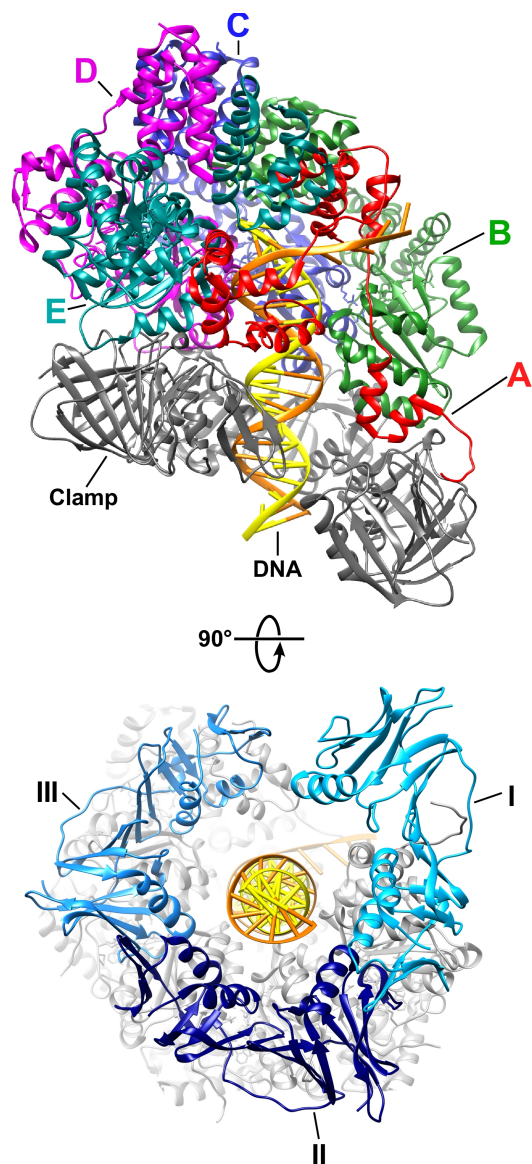


Figure 8: Structure of a sliding clamp–clamp loader–DNA complex in the “notched-screw cap” conformation. The structure shown was generated using the T4 bacteriophage sliding clamp and clamp loader complexes (Kelch et al., 2011). The clamp loader complex from T4 is made up of only two separate polypeptides. The A subunit is gp62, and subunits B-E are gp44. This complex is related to the eukaryotic RFC, containing five separate polypeptides. In RFC, the A subunit is Rfc1, B subunit is Rfc2, C subunit is Rfc3, D subunit is Rfc4, and E subunit is Rfc5. The T4 sliding clamp, like eukaryotic PCNA, is a homotrimer, comprising three copies of gp45. Co-crystallization of proteins with primer-template junction DNA and an ATP analogue allowed capture of the “notched-screw cap” conformation (top), in which the sliding clamp is opened at a subunit-subunit interface, being held by the clamp loader in a conformation that matches the DNA helix. In the lower structure, the complex has been rotated 90° to look down the DNA helix. The individual clamp subunits (I, II, and III) are colored individually to highlight the opening between subunits induced by the clamp loader.

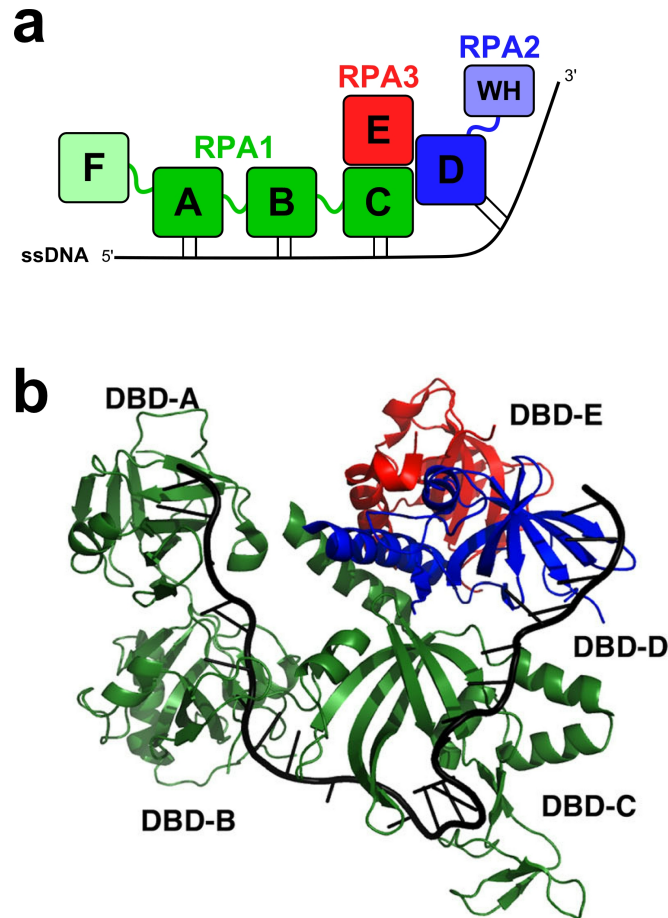


Figure 9: Structure of the RPA–single-stranded DNA complex. (a) Schematic representation of RPA in its 30 nucleotide binding mode. DNA-Binding Domains (DBDs) A-F are labeled, and are spread between the three RPA subunits, as indicated. These domains adopt a conserved OB-fold structure. In RPA2, WH denotes winged-helix domain. Linkers between structured domains are denoted with lines. OB-fold F in RPA1 and the winged helix in RPA2 are shaded to denote that they were not resolved in the structure in **b**. Diagram adapted from (Chen and Wold, 2014). (b) Structure of *Ustilago maydis* RPA in complex with single-stranded DNA (Fan and Pavletich, 2012). Specific DNA-Binding Domains within the larger structure are indicated. RPA1 is shown in green, RPA2 in blue, and RPA3 in red. Representation of structure adapted from (Chen and Wold, 2014).

CHAPTER II

Analysis of metal-binding domains in the catalytic subunit of DNA polymerase δ

PREFACE TO THE CHAPTER

This chapter contains biochemical and functional analysis of the metal-binding domain in the Pol δ catalytic subunit, Pol3. The catalytic subunits of each of the eukaryotic B-family DNA polymerases contain a small, conserved C-terminal domain (CTD). In each polymerase, this domain contains two, conserved, cysteine-rich metal-binding motifs. Prior to the work described here, each motif was thought to bind zinc, and the functional significance of these motifs was unclear.

Section IIA provides evidence that in each of the B-family polymerases, one of the cysteine-rich motifs binds an Fe-S cluster while the other binds zinc. In the case of DNA polymerase δ , the Fe-S cluster was shown to be required for interactions between the catalytic subunit Pol3 and the Pol δ accessory subunits. The Zn-binding motif was found to be important for mediating interactions between the Pol δ complex and the replication sliding clamp PCNA. This work was a collaboration between our group and two groups at Philipps-Universität in Marburg, Germany. My role in this work was performing *in vitro* replication assays, with particular emphasis on characterizing the functional significance of the Zn-binding motif in Pol3.

Section IIB is an extension of the work in IIA. Budding yeast cells cannot tolerate mutations in the Zn-binding motif in Pol3, presumably due to a PCNA-dependent replication defect. To better understand this phenotype, we sought to identify PCNA mutants that suppress this lethality. I identified two mutants; the characterization of these mutants and their relationship to the activity of Pol δ is discussed. While this work remains an incomplete story, in the future these mutants may provide a tool to study the link between PCNA and the response to replication stress. The initial genetic screen was performed in collaboration with Carrie Stith. I performed all subsequent genetic and biochemical experiments.

CHAPTER IIA

Eukaryotic DNA polymerases require an iron-sulfur cluster for the formation of active complexes.

Eukaryotic DNA polymerases require an iron-sulfur cluster for the formation of active complexes

Daili J A Netz¹, Carrie M Stith², Martin Stümpfig¹, Gabriele Köpf¹, Daniel Vogel¹, Heide M Genau¹, Joseph L Stodola², Roland Lill^{1*}, Peter M J Burgers^{2*} & Antonio J Pierik^{1*}

The eukaryotic replicative DNA polymerases (Pol α , δ and ϵ) and the major DNA mutagenesis enzyme Pol ζ contain two conserved cysteine-rich metal-binding motifs (CysA and CysB) in the C-terminal domain (CTD) of their catalytic subunits. Here we demonstrate by *in vivo* and *in vitro* approaches the presence of an essential [4Fe-4S] cluster in the CysB motif of all four yeast B-family DNA polymerases. Loss of the [4Fe-4S] cofactor by cysteine ligand mutagenesis in Pol3 destabilized the CTD and abrogated interaction with the Pol31 and Pol32 subunits. Reciprocally, overexpression of accessory subunits increased the amount of the CTD-bound Fe-S cluster. This implies an important physiological role of the Fe-S cluster in polymerase complex stabilization. Further, we demonstrate that the Zn-binding CysA motif is required for PCNA-mediated Pol δ processivity. Together, our findings show that the function of eukaryotic replicative DNA polymerases crucially depends on different metalcenters for accessory subunit recruitment and replisome stability.

Replication of double-stranded nuclear DNA in eukaryotes is performed through the coordinated work of three DNA polymerase complexes, Pol α , Pol δ and Pol ϵ (ref. 1). Pol α together with the primase complex initiates the synthesis of short RNA primers, which are subsequently extended by Pol δ and Pol ϵ for processive synthesis of the lagging and leading strands, respectively^{2,3}. In *Saccharomyces cerevisiae*, Pol α has four subunits (Pol1, Pol12, Pri1, Pri2), Pol δ has three (Pol3, Pol31, Pol32) and Pol ϵ has four (Pol2, Dpb2, Dpb3 and Dpb4). The catalytic subunits Pol1, Pol2 and Pol3 are phylogenetically related and belong to the class B DNA polymerases⁴. They are tightly associated with the so-called B subunits Pol12, Dpb2 and Pol31, respectively. The B subunits are all essential and share both phosphodiesterase-like and oligosaccharide-binding domains^{5,6}. Eukaryotes contain a fourth class B DNA polymerase, Pol ζ , which is the major enzyme responsible for mutagenesis in response to DNA damage^{7,8}. Pol ζ , composed of the catalytic subunit Rev3 and the accessory subunit Rev7, is not essential for growth in yeast, but disruption of *REV3L* in mice causes embryonic lethality⁹.

Eight conserved cysteine residues are present in the CTD of all four eukaryotic class B DNA polymerases (**Supplementary Results, Supplementary Fig. 1**). This domain is absent in the other classes of DNA polymerases such as bacterial or mitochondrial DNA polymerases. The first set of four cysteine residues (CysA) resembles a zinc ribbon motif (C-X₂-C-X₇₋₃₁-C-X₂-C)¹⁰, whereas the C-terminal set (CysB) has an atypical pattern. This CTD is not present in B-family DNA polymerases of bacteriophages, herpes viruses, proteobacteria and archaea. However, phylogenetic analysis has indicated that a motif similar to CysB is present in the CTD of euryarchaeal D-family polymerases¹¹. The crystal structure of the yeast class B Pol3 has been determined, yet it lacks the entire CTD as full-length Pol3 isolated from yeast is prone to aggregation¹². Two three-dimensional structures of the CTD of DNA polymerase α have been reported. A Zn²⁺-reconstituted synthetic oligopeptide corresponding to the CysB region of human Pol1 was structurally characterized by NMR spectroscopy¹³. Recently, the crystal structure of the yeast Pol1-CTD in complex with Pol12 was reported¹⁴.

This complex was purified from *Escherichia coli* after heterologous expression, and it contains a Zn²⁺ ion in both the CysA and CysB motifs. This study provided structural information for earlier biochemical studies, which had described interactions between the CTDs and their corresponding B-subunits¹⁵⁻¹⁷.

Intriguingly, the *pol3-13* allele of yeast, in which the second cysteine of CysB (C1074) in Pol3 is mutated to serine, is synthetically lethal with mutations in the essential genes *NBP35*, *DRE2* and *TAH18* (ref. 18). These genes encode components of the cytosolic Fe-S protein assembly (CIA) machinery, which is required for maturation of most cytosolic and nuclear Fe-S proteins¹⁹⁻²². Nbp35 together with Cfd1 serves as a scaffold complex that assembles a transiently bound Fe-S cluster in an early step of the biosynthesis process^{23,24}. Dre2, an Fe-S protein, and the diflavin reductase Tah18 form an electron transfer chain using NADPH for Tah18-dependent reduction of one of the two Fe-S clusters of Dre2 (ref. 22). CIA components acting later in biogenesis encompass the Fe-only hydrogenase-like Nar1 and the β -propeller protein Cia1^{25,26}. Remarkably, the CIA machinery requires a sulfur-containing compound exported by mitochondria after synthesis by the cysteine desulfurase complex Nfs1-Isd11 and other components of the mitochondrial Fe-S cluster (ISC) assembly machinery^{19,27}.

Although it is widely believed that both CysA and CysB of Pol3 bind Zn²⁺ ions, the synthetic lethality resulting from the combination of the *pol3-13* allele and mutations in CIA components pointed to the presence of a hitherto unrecognized Fe-S cluster in Pol3. We therefore addressed the question of whether the CTD of polymerases coordinate an Fe-S cluster and what the physiological role of such a cofactor might be. We provide *in vivo* and *in vitro* evidence that a [4Fe-4S] cluster rather than Zn²⁺ is bound to the CysB motif in all yeast B-family DNA polymerases. Assembly of this essential Fe-S cluster was strictly dependent on the function of mitochondrial Nfs1 and cytosolic Nbp35, explaining the synthetic lethality of the *pol3-13* allele and Fe-S biosynthetic genes¹⁸. The findings also indicate a so-far-unknown dependence of nuclear DNA synthesis on mitochondrial function. Finally, our study reveals the physiological importance of the two different metal cofactors, the [4Fe-4S]

¹Institut für Zytobiologie und Zytopathologie, Philipps-Universität Marburg, Marburg, Germany. ²Department of Biochemistry and Molecular Biophysics, Washington University School of Medicine, St. Louis, Missouri, USA. *e-mail: lill@staff.uni-marburg.de, burgers@biochem.wustl.edu or pierik@staff.uni-marburg.de

cluster in CysB and Zn²⁺ in CysA, in the stabilization of DNA polymerase interactions with different accessory proteins essential for processive DNA synthesis at the replication fork.

RESULTS

Eukaryotic DNA polymerases bind an Fe-S cluster *in vivo*

To investigate the presumed presence of Fe-S clusters in eukaryotic DNA polymerases, we used a sensitive *in vivo* radiolabeling assay, which measures the incorporation of ⁵⁵Fe into newly synthesized proteins in baker's yeast. The coding information for a C-terminal Myc tag was fused by chromosomal integration to Pol1, Pol2, Pol3 and Rev3, the catalytic subunits of the Pol α , Pol ϵ , Pol δ and Pol ζ complexes, respectively. No negative effects on cell growth were caused by introducing these tags. A significant ($P < 0.05$) amount of ⁵⁵Fe was associated with Pol1, Pol2 and Pol3 immunoprecipitated with Myc-specific beads (1.01 ± 0.19 pmol, 1.34 ± 0.17 pmol and 2.6 ± 0.2 pmol per gram of cells above respective control levels; **Fig. 1a** and **Supplementary Fig. 2**). The radiolabeling was not due to adventitious binding of iron to cysteine-rich proteins, as negligible amounts of ⁵⁵Fe bound to transcription factor IIIA (TFIIIA), which contains nine conserved zinc fingers (**Fig. 1a**). The presence of Fe-S clusters rather than other forms of iron was tested by measuring the dependence of ⁵⁵Fe binding on the mitochondrial and cytosolic Fe-S protein assembly machineries. Depletion of the cysteine desulfurase Nfs1 (refs. 19,27) of the galactose-regulatable strain Gal-NFS1 by growth on glucose almost completely abolished ⁵⁵Fe binding to the polymerases. Proper assembly of the ⁵⁵Fe-S cluster requires mitochondria-localized Nfs1 because a cytosolic version of Nfs1 fails to support radiolabeling of Pol3 (**Supplementary Fig. 3**). Similarly, depletion of the CIA machinery components Nbp35 and Nar1 in regulatable yeast strains (Gal-NBP35 (ref. 20) and Gal-NAR1 (ref. 25)) abrogates Fe-S cluster formation on the polymerases (**Fig. 1a** and **Supplementary Figs. 2,4**). As Pol1 is associated with primase, which contains a [4Fe-4S] cluster in its Pri2 subunit²⁸, we examined the Pri2 contribution to the binding of ⁵⁵Fe to Pol1. Although the amount of ⁵⁵Fe copurified with hemagglutinin (HA)-tagged Pri2 (1.12 ± 0.28 pmol ⁵⁵Fe per gram of cells) was similar to that measured in Pol1-Myc (1.01 ± 0.19 pmol ⁵⁵Fe per gram of cells), only 20% of HA-Pri2 immunoprecipitated together with Pol1-Myc and vice versa (**Supplementary Fig. 5**). Thus, a major contribution from Pri2 to Pol1-associated ⁵⁵Fe radioactivity could be excluded. A similar reservation does not hold for Pol δ or Pol ϵ . None of the small subunits of Pol ϵ have conserved cysteine residues that can serve as potential ligands for an Fe-S cluster. Structural studies of the small subunits of Pol δ do not indicate the presence of potential metal

binding sites⁶. Taken together, our data clearly suggest the presence of a hitherto unrecognized Fe-S cluster in all three replicative DNA polymerases *in vivo*.

The CTD of the catalytic subunit binds the Fe-S cluster

We next tested whether the Fe-S cluster is associated with the CTD, as suggested by the synthetic lethality of the *pol3-13* allele¹⁸ and the strict conservation of the cysteine residues. As Pol3 is an essential gene and episomal copies of full-length polymerases have deleterious effects on cell growth²⁹, we expressed only the CTD of Pol3 (residues 982–1097) with an N-terminal HA epitope tag from a plasmid. HA-Pol3-CTD bound significant ($P < 0.05$) amounts of ⁵⁵Fe (4.1 ± 0.9 pmol g⁻¹; **Fig. 1b** and **Supplementary Fig. 6**), which dropped to background values in both Nfs1- and Nbp35-depleted cells. This behavior closely resembles that of full-length Pol3 (**Fig. 1a**). As no significant ($P > 0.05$) ⁵⁵Fe binding to full-length Rev3 could be detected, apparently because of Rev3's low abundance (**Supplementary Fig. 7**), we examined ⁵⁵Fe binding to HA-tagged Rev3-CTD (residues 1374–1504). In this case, a significant ($P < 0.05$) amount of ⁵⁵Fe (0.9 ± 0.3 pmol g⁻¹) was detected, which dropped to background values upon Nfs1 and Nbp35 depletion (**Fig. 1b**). These results provide evidence that *in vivo*, all yeast class B DNA polymerases bind Fe-S clusters in their CTD. Considering the high amino acid sequence conservation of the CTDs of all eukaryotic B-class polymerases¹¹ (**Supplementary Fig. 1**), we anticipate that the presence of an Fe-S cluster in polymerase CTDs extends to all eukaryotes, including humans.

Accessory subunits stabilize the Fe-S cluster in CysB

To identify which of the eight conserved cysteine residues of the polymerase CTDs are responsible for Fe-S cluster coordination, we used Pol3 as a prototype polymerase and introduced cysteine-to-alanine substitutions. In principle, the CysA and CysB motifs may independently bind an Fe-S cluster, as the corresponding segments are structurally well separated (47-Å Zn-Zn distance) by a three-helix bundle in the zinc-bound form of Pol1-CTD¹⁴. All cysteine residues of CysB are required for Fe-S cluster binding *in vivo* because their substitution by alanine completely abolishes ⁵⁵Fe incorporation into Pol3-CTD (**Fig. 2a**, right). In contrast, the amount of ⁵⁵Fe binding was significantly ($P < 0.05$) above background values for all cysteine-to-alanine exchanges in CysA, suggesting that some Fe-S cluster may remain bound to CysB (**Fig. 2a**, left). The weakened Fe-S cluster binding efficiency of CysA mutant proteins could be caused by a lack of polymerase complex stabilization by Pol31, even though this subunit interacts primarily with the CysB region¹⁷.

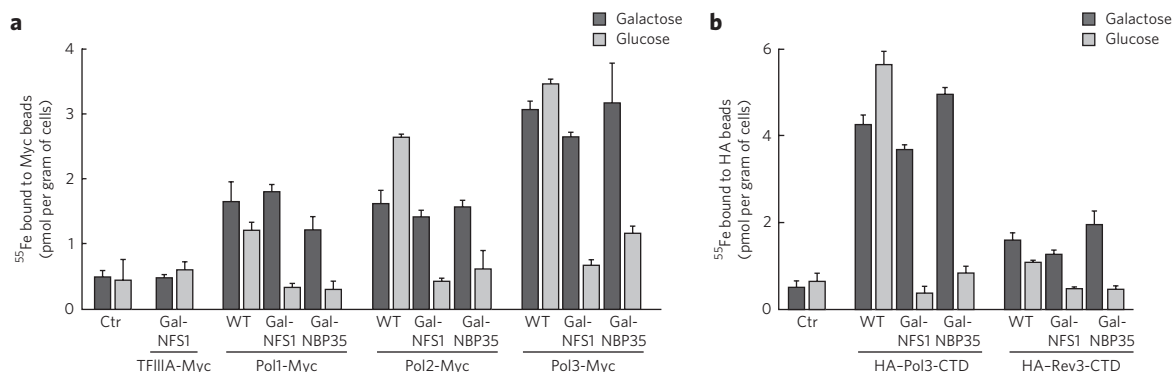


Figure 1 | Yeast replicative DNA polymerases and Rev3 contain Fe-S clusters *in vivo*. (a) Wild-type (WT), Gal-NFS1 or Gal-NBP35 cells harboring genomically Myc-tagged Pol1, Pol2 and Pol3 were grown in galactose- or glucose-containing medium to induce or repress, respectively, production of Nfs1 or Nbp35. After ⁵⁵Fe radiolabeling of cells, polymerases were immunoprecipitated from cell extracts, and bound ⁵⁵Fe was quantified by scintillation counting. TFIIIA-Myc expressed in Gal-NFS1 and WT cells without tagged polymerases (Ctr) served as controls. (b) ⁵⁵Fe incorporation into plasmid-encoded HA-Pol3-CTD and HA-Rev3-CTD as in **a**. Western blots for the cell extracts are presented in **Supplementary Figures 2 and 6 for a and b**, respectively. Error bars, s.d. ($n \geq 3$).

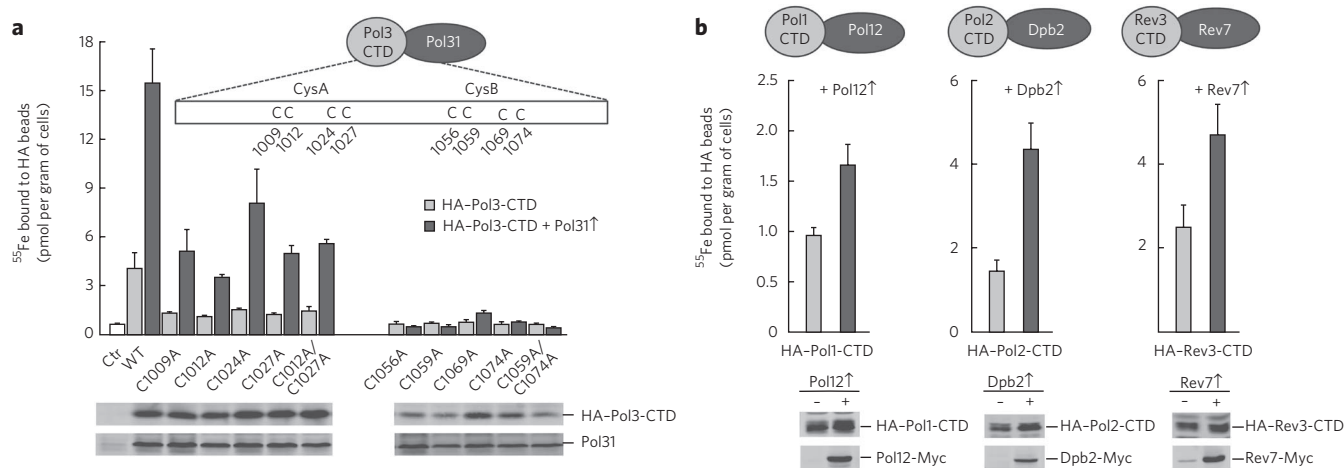


Figure 2 | The Fe-S cluster is coordinated by the CysB motif and is stabilized by accessory-subunit binding. (a) ^{55}Fe incorporation into plasmid-encoded HA-Pol3-CTD and cysteine-to-alanine substitutions thereof (cartoon), with (Pol31 \uparrow) or without Pol31 overexpression in wild-type yeast cells grown in galactose-containing medium. Western blots are for cell extracts with Pol31 overexpression. (b) ^{55}Fe incorporation into indicated plasmid-encoded polymerase CTDs, with (\uparrow) or without overexpression of the accessory subunits (cartoon) in wild-type yeast cells grown in galactose-containing medium. Western blots are shown for indicated cell extracts. Full-length blots are presented in **Supplementary Figure 8**. Error bars, s.d. ($n \geq 3$).

Indeed, overexpression of Pol31 resulted in a four- to eight-fold higher ^{55}Fe binding to both wild-type and CysA mutant Pol3-CTDs (**Fig. 2a** and **Supplementary Fig. 8**) but not to CysB mutant proteins. Nevertheless, the greater abundance of Pol31 could not completely compensate for the Fe-S cluster binding deficit caused by cysteine exchanges in CysA. We attribute the lower ^{55}Fe content of the CysA mutant proteins to an indirect effect of the disruption of CysA motif structure due to the lack of zinc binding. This may affect the efficiency of Fe-S cluster formation in CysB. The decreased amount of protein of the CysB-mutated CTD found in immunostains of cell extracts, even upon Pol31 overexpression (**Supplementary Fig. 8a,c**), can be explained by the absence of the Fe-S cluster in CysB. This absence renders the protein sensitive to degradation, as frequently seen for Fe-S proteins. Together, these findings imply that only CysB is responsible for Fe-S cluster binding, whereas CysA may bind zinc¹⁴. We infer that Pol3–Pol31 complex formation is intrinsically linked to the presence of an intact Fe-S cluster, explaining its physiological importance for Pol δ function.

Next, we tested whether the functional connection between the presence of an Fe-S cluster on the DNA polymerase and its interaction with the respective accessory subunits also holds for the other class B family members. Overexpression of Pol12, Dpb2 and Rev7 with the CTDs of Pol1, Pol2 and Rev3, respectively, significantly

($P < 0.05$) increased the amounts of ^{55}Fe coisolated in the absence of the overproduced accessory subunits (**Fig. 2b**). Thus, the increase in the efficiency of Fe-S cluster binding to the polymerase CTDs by the respective accessory subunits appears to extend to all members of the class B family, suggesting a stabilization of Fe-S cluster binding by these subunits and vice versa.

The [4Fe-4S] cluster is required for complex formation

To characterize the type and stoichiometry of Fe-S cluster binding to DNA polymerases, we performed biochemical and spectroscopic studies. Expression of the yeast Pol1-, Pol2-, Pol3- and Rev3-CTD in *E. coli* resulted in the formation of dark inclusion bodies, which gave brownish solutions upon treatment with chaotropic agents (**Fig. 3a**). Soluble brown Pol2-, Pol3- and Rev3-CTDs could be obtained in the absence of chaotropic agents after modifications of the protocol (**Supplementary Fig. 9**). Pol1-CTD and Pol2-CTD were aggregation prone. A low yield of Pol1-CTD holoform was obtained (~0.1 Fe and S per monomer; **Supplementary Fig. 10**). This apparent lability of Fe-S cluster binding to purified Pol1-CTD may have precluded its earlier discovery in structural studies¹⁴. The other CTDs contained 2.0–2.6 mol non-heme iron and acid-labile sulfide per CTD, and their UV-visible (UV-vis) spectra showed a broad absorption maximum centered at 400 nm, indicative of [4Fe-4S]

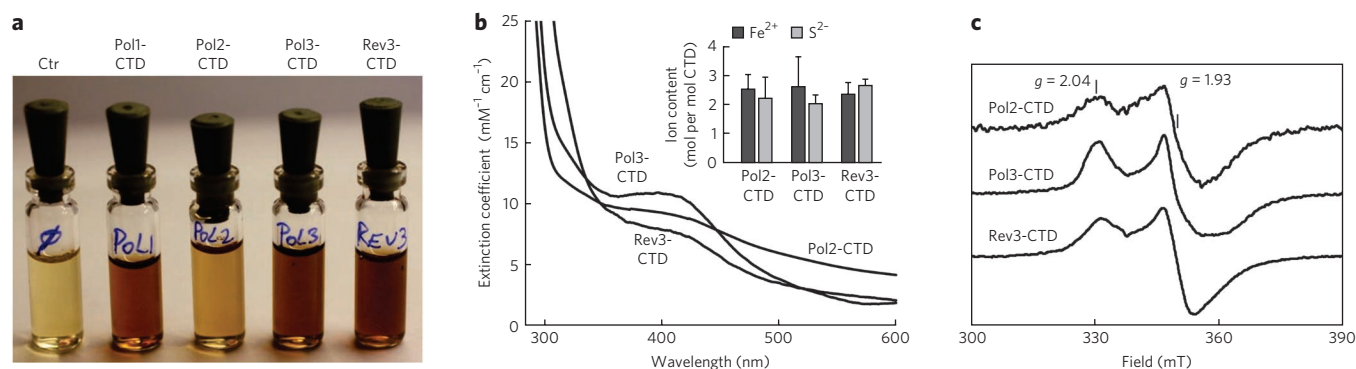


Figure 3 | Recombinant purified CTDs of Pol1, Pol2, Pol3 and Rev3 harbor a [4Fe-4S] cluster. (a) Solubilized inclusion bodies of indicated CTDs obtained after expression in *E. coli*. (b) UV-vis and (c) X-band EPR spectra of purified soluble Pol2-, Pol3- and Rev3-CTDs in absence of chaotropic agents. The inset in **b** shows non-heme iron and acid-labile sulfide contents. Error bars, s.d. ($n \geq 3$). Samples in **c** were reduced with 2 mM sodium dithionite (2 min). EPR conditions: 9.458 GHz, 10 K and 2 mW microwave power.

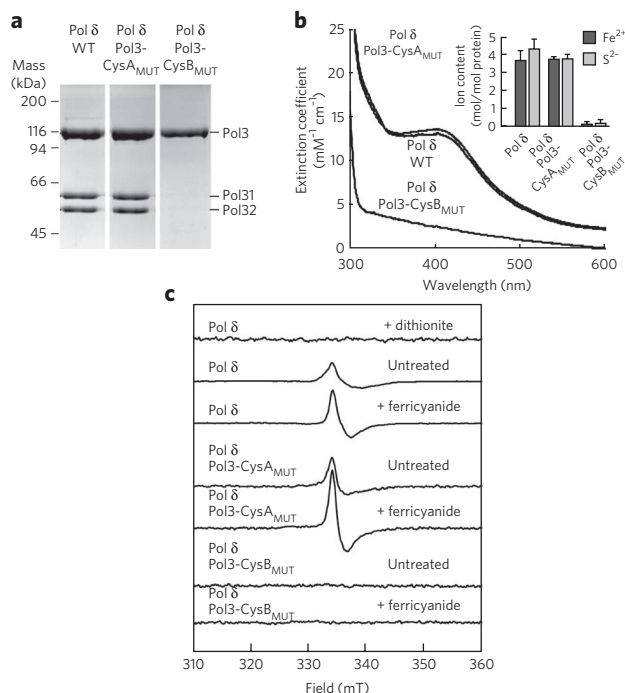


Figure 4 | Functional integrity of purified Pol δ complex depends on binding of an Fe-S cluster to Pol3. (a–c) Pol δ complex purified from yeast coexpressing wild-type (WT), CysA_{MUT} (C1012S C1027S) or CysB_{MUT} (C1059S C1074S) Pol3 with Pol31 and Pol32 was analyzed by (a) Coomassie blue-stained SDS-PAGE (b) UV-vis spectroscopy and chemical analysis (inset) or (c) EPR spectroscopy. EPR conditions and treatments with ferricyanide (2 mM) or dithionite are as in **Figure 3c**. The full-length gel for **a** is presented in **Supplementary Figure 11c**. Error bars, s.d. ($n \geq 3$).

clusters (**Fig. 3b**). These soluble CTDs did not show electron paramagnetic resonance (EPR) signals, even after oxidation with ferricyanide, excluding the presence of [3Fe-4S] clusters³⁰. However, upon reduction with dithionite, EPR signals with $g = 2.04$ and $g = 1.93$ characteristic of [4Fe-4S]¹⁺ clusters were detected (**Fig. 3c**). Together, these results provide evidence for a single [4Fe-4S]²⁺ cluster bound to the purified CTDs.

As no Fe-S cluster has been detected in any isolated DNA polymerase complex, we investigated the native Pol δ complex for such a metal center after its expression was induced and it was purified from *S. cerevisiae* (**Supplementary Fig. 11a,b**). Isolated Pol δ was olive yellow and contained Pol3, Pol31 and Pol32 in stoichiometric ratios (**Fig. 4a** and **Supplementary Fig. 11c**). UV-vis spectroscopy of Pol δ showed broad absorption in the 400-nm region, and chemical analysis detected approximately 4 mol of non-heme iron and acid-labile sulfide ions per mol of Pol δ (**Fig. 4b**, inset). Thus, the Fe-S content, the UV-vis spectrum and the extinction coefficient of 13 mM⁻¹cm⁻¹ at 400 nm indicate the presence of a single [4Fe-4S]²⁺ or a single [3Fe-4S]¹⁺ cluster in purified Pol δ complex (**Fig. 4b**). EPR spectroscopy showed a weak signal centered at $g = 2.02$, characteristic of [3Fe-4S]¹⁺ clusters. Spin quantification of the EPR signal, however, accounted for only $5 \pm 1\%$ of the total Fe-S cluster content (**Fig. 4c**). This signal increased two-fold upon oxidation with ferricyanide, corresponding to just 10 \pm 2% of the Fe-S cluster content. After dithionite treatment of the wild-type Pol δ complex, the [3Fe-4S]¹⁺ cluster EPR signal at $g = 2.02$ disappeared because of reduction to the EPR-silent [3Fe-4S]⁰ state. However, native Pol δ treated with dithionite did not show a [4Fe-4S]¹⁺ EPR signal (**Fig. 4c**, top trace). These findings are in contrast to the results for the soluble CTDs, in which the [4Fe-4S]²⁺ cluster may be reduced

to the [4Fe-4S]¹⁺ form. The absence of an EPR signal in dithionite-treated polymerase δ could be explained by the lower redox potential of the [4Fe-4S]²⁺ cluster in the intact complex in comparison to that of Pol3-CTD. Dithionite can only reduce the cluster if the midpoint potential is above -500 mV, which is apparently the case for the CTDs. Alternatively, the [4Fe-4S]¹⁺ cluster may have a high spin state with an EPR spectrum too broad to be detectable. A third explanation would be conversion of the [4Fe-4S]¹⁺ cluster to the EPR silent [3Fe-4S]⁰ form. Breakdown of the cluster upon dithionite treatment is unlikely as processivity remained unaltered. Many other [4Fe-4S]²⁺ cluster-containing proteins have EPR and redox properties similar to those of native Pol δ . For example, aconitase has a labile [4Fe-4S]²⁺ cluster that is converted to the [3Fe-4S]¹⁺ form during isolation³¹, and the [4Fe-4S]²⁺ cluster is difficult to reduce with dithionite. Regardless of the behavior upon dithionite treatment, our analysis provides evidence that Pol δ isolated from yeast contains a [4Fe-4S]²⁺ cluster, which upon purification partially (5–10%) breaks down to a [3Fe-4S]¹⁺ or [3Fe-4S]⁰ cluster.

To verify the specificity and physiological relevance of Fe-S cluster binding to polymerases, we studied the effect of mutations in CysA or CysB on both Fe-S cluster binding and functionality of isolated Pol δ . The lethal double mutation C1059S C1074S in CysB of Pol3 disrupted its binding to both Pol31 and Pol32 upon isolation of Pol3 from cell extracts and in yeast two-hybrid experiments (**Fig. 4a** and **Supplementary Fig. 12**). The mutation further abrogated Fe-S cluster binding, as seen from chemical analysis and the loss of UV-vis and EPR signals (**Fig. 4b,c**). In marked contrast, lethal double mutation of CysA (C1012S C1027S) did not alter the subunit composition of the purified Pol δ complex and did not affect the Pol3 interactions in the two-hybrid analysis. Likewise, the Fe-S content, the UV-vis and EPR spectra were unchanged in comparison to the wild-type situation. These data further support the view that CysB binds a [4Fe-4S] cluster, whereas no evidence was obtained for Fe-S cluster binding to CysA. Hence, on the basis of the consensus zinc ribbon motif of CysA (C-X₂-C-X₇₋₃₁-C-X₂-C)¹⁰ and the crystallographic data, CysA may bind zinc¹⁴. Neither set of mutations in the CTD of Pol3 affected its basal DNA polymerase activity (**Supplementary Fig. 13**), in agreement with Pol3 truncation mapping studies and structural comparisons with other B-family DNA polymerases that localize the catalytic domain N-terminal of the CTD¹².

CysA is an important determinant for PCNA binding

We then asked what the physiological function of the zinc-binding CysA motif may be. Processive DNA replication can be tested *in vitro* and depends on multiple protein and protein-DNA interactions, including those involving the processivity factor PCNA^{32,33}. The latter protein is a circular homotrimeric clamp that coordinates DNA replication, recombination and repair processes and endows both stability and processivity to the replicating machinery. To address the role of the CysA motif in processive, lagging-strand DNA replication, we used isolated Pol δ preparations (Pol3, Pol31 and Pol32; **Supplementary Fig. 11**) for *in vitro* DNA synthesis in the presence of PCNA (**Supplementary Fig. 14**). Mutation of two cysteine residues of CysA (C1012S and C1027S) severely decreased PCNA-dependent replication processivity, documenting the importance of this metal center for polymerase function (**Fig. 5a**). An interaction between Pol δ and PCNA has previously been mapped to a C-terminal segment of the accessory subunit Pol32 and termed PIP (PCNA interaction protein) motif³³. However, the Pol32- Δ PIP mutant form of Pol δ was almost fully proficient for processive DNA replication, underscoring its minor functional importance. The relative effects observed for the Pol3-CysA and Pol32- Δ PIP mutants shows the much higher importance of the CysA site compared to PIP for stability of the PCNA-polymerase complex on DNA. Hence, the CysA structural motif may represent the key binding site for PCNA on Pol δ ,

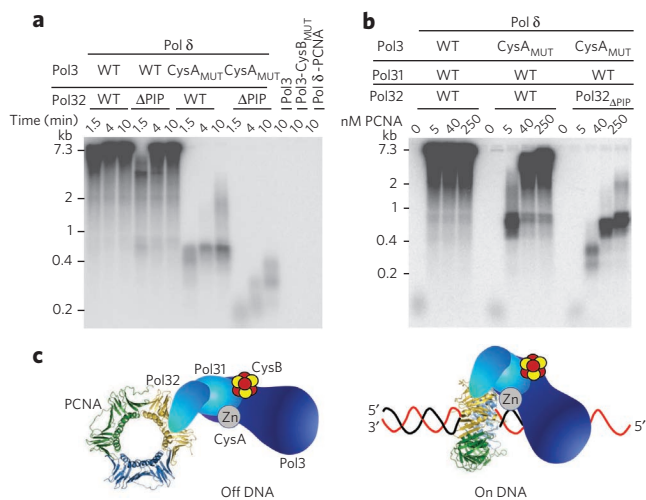


Figure 5 | The CysA motif of Pol δ is critical for processive DNA replication with PCNA.

(a) Alkaline agarose gel electrophoresis of DNA replication products of assay with purified proteins as indicated. A phosphorimaging scan is shown. ΔPIP refers to truncated Pol32 (Supplementary Fig. 11). All complexes contain wild-type Pol31. The right-most lane is a control with wild-type Pol δ but without PCNA. Size markers are indicated on the left. (b) Assay as in a was carried out for 10 min with the indicated PCNA concentrations. (c) Model for the roles of the PIP and CysA motifs for PCNA interaction with Pol δ in solution (Off DNA) and in assembly with substrate (On DNA).

whereas the PIP motif may have an ancillary function. Consistent with this view, PCNA-dependent replication activity of Pol δ was almost completely abolished when both CysA and PIP binding sites were mutated (Fig. 5a). Used as controls for these experiments, the catalytic subunit Pol3 alone, the CysB mutant protein or a sample lacking PCNA showed no discernible processive DNA replication. To further substantiate the relative importance of the two PCNA binding sites of Pol δ, we varied the PCNA concentration in the *in vitro* replication assay containing either wild-type or CysA mutant Pol3 together with wild-type or ΔPIP-Pol32. Increasing PCNA concentrations relieved the replication defect of the CysA mutant, suggesting that under these conditions, interactions between PCNA and PIP partially rescue the replication defect (Fig. 5b). Indeed, when PIP was also absent, hardly any processive replication was observed. Taken together, these findings suggest a crucial role of CysA in PCNA–Pol δ complex formation, stability or both during on-DNA processive DNA replication (Fig. 5c). In contrast, the PIP binding site may be more relevant for off-DNA complex formation, such as recruitment of the enzyme to replication foci in the nucleus, as has been observed with other PIP box-containing proteins^{33,34}.

DISCUSSION

Our study identifies a previously unrecognized essential Fe-S cluster in the CTD of all yeast class B DNA polymerases, in addition to a Zn²⁺ ion bound on the other side of CTD¹⁴. Hence, this class of enzymes contains two different metal centers, which were shown to have distinct physiological roles. The presence of the Fe-S cluster was demonstrated by several *in vivo* and *in vitro* methods such as ⁵⁵Fe radiolabeling and purification of the DNA polymerase complex after induced expression of the enzyme in yeast, the native organism. Mutational and spectroscopic studies allowed us to define it as a [4Fe-4S] cluster that is coordinated by CysB, the second cysteine-rich motif in the CTD. The presence of an Fe-S cluster rather than Zn²⁺, as originally suggested by a crystal structure of the CTD of Pol1, changes our understanding of DNA polymerase function and

raises several questions regarding the precise physiological role of this Fe-S cluster. Our data clearly demonstrate that Pol3 becomes unstable in the absence of the Fe-S cluster (for example, upon Nfs1 depletion, as shown in western blots in Supplementary Fig. 2) and that the replication function is severely compromised owing to loss of accessory subunits essential for function at the replication fork (Fig. 4). This functional impairment caused by decreased complex stability may extend to the other DNA polymerases because the interaction between the various CTDs and their respective accessory proteins is a key determinant for the stability of the bound Fe-S cluster. It is likely that euryarchaeal D-family polymerases also bind an Fe-S cluster in the CysB motif. Interestingly, these polymerases contain a B subunit that has both phosphodiesterase-like and oligosaccharide-binding domains⁶ and are thus predicted to share the principle of Fe-S cluster binding for accessory subunit recruitment with the eukaryotic polymerases. In the case of the translesion polymerase Pol ζ, the accessory protein Rev7 has a fold that is completely different from those of the B subunits of the other polymerases, and therefore a firm conclusion by analogy with Pol δ cannot be made and requires direct experimentation. However, the data do suggest that the Rev3-CTD may also be involved in Rev3-Rev7 interactions in addition to the interaction of the N-terminal region of the polymerase domain of Rev3 with Rev7 (ref. 35). Together, our findings assign essential roles to the Fe-S cluster: stabilization of the CTD to enable complex formation, maintenance of the catalytic polymerase subunit with its respective accessory proteins, or both. As an Fe-S cluster is intrinsically sensitive to oxidative stress, oxidative damage of the cluster may lead to gradual dissociation of the accessory subunits and decreased processivity at the replication fork. An attenuated rate of DNA replication during oxidative stress conditions may serve as a regulatory mechanism for polymerase activity.

In retrospect, the lability and complexity of Fe-S clusters may explain the previous difficulties in obtaining purified polymerase complex that is suitable for functional studies and crystallography. Purification of the catalytic subunit on its own invariably resulted in low yields and aggregation (detailed in Methods), possibly explaining why Pol3 could only be crystallized after truncation of the C terminus¹². The Pol1-CTD in complex with Pol12 was crystallized with a Zn²⁺ ion in CysB after heterologous expression and purification from *E. coli*¹⁴. Our own purification experiments after expression in *E. coli* showed extreme lability of the Fe-S cluster of Pol1-CTD, necessitating anaerobic purification conditions to isolate the Fe-S cluster together with the protein. In general, misincorporation of non-native metal centers into metalloproteins is not unusual and has been encountered previously, especially upon overproduction or heterologous expression. For instance, replacement of Fe or an Fe-S cluster by Zn in *E. coli* has been reported

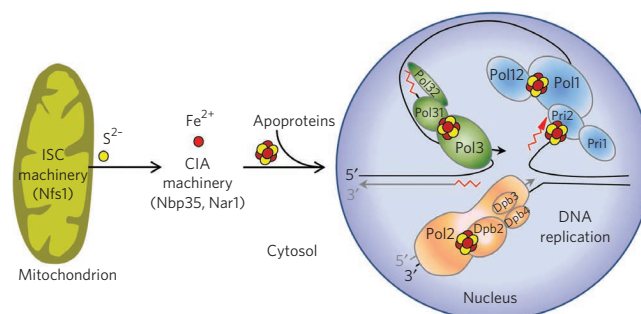


Figure 6 | Role of mitochondria and Fe-S cluster biogenesis in nuclear DNA replication.

Assembly of Fe-S clusters on nuclear replicative DNA polymerases requires Fe-S protein biogenesis machineries located in the mitochondria (ISC machinery, iron-sulfur cluster assembly) and cytosol (CIA machinery, cytosolic iron-sulfur protein assembly), providing an explanation for the essential function of mitochondria for cell viability.

for *Clostridium pasteurianum* rubredoxin³⁶ or for the Fe-S cluster-containing scaffold protein IscU from *Haemophilus influenzae*³⁷, respectively. Likewise, the CIA protein Nar1, containing two Fe-S clusters, does not contain its native metal centers after it is expressed in *E. coli*³⁸. Zinc can be erroneously incorporated into the copper-binding protein azurin³⁹. Ribonucleotide reductases of various bacteria, upon overexpression in *E. coli*, contain a dinuclear iron center, yet in their native state they have a dimanganese center^{40,41}. Hence, these data imply that a number of proteins isolated as zinc-binding proteins may exist as Fe-S proteins inside the cell, emphasizing the importance of assessing the metal occupancy of a protein in its native organism.

Our data provide evidence for a previously unknown crucial function for the CysA zinc-binding segment in mediating DNA-dependent interactions between PCNA and the catalytic subunit of Pol δ (Fig. 5c). This protein interaction seems to operate alongside an earlier defined binding determinant, the C-terminal PIP motif of the accessory subunit Pol32. Because mutation of CysA was more detrimental to *in vitro* processive DNA replication than deletion of the PIP segment, CysA may be the major determinant for PCNA interaction with Pol δ on DNA. Notably, the function of the CysA motif may be more divergent than that of CysB, which seems to be conserved among all replicative DNA polymerases as a structural motif for the interaction with their respective essential accessory subunits. In Pol δ , Pol ϵ and Pol ζ , the CysA motif may serve a similar function, that is, mediating DNA-dependent interactions with PCNA, as all of these polymerases require PCNA for processive synthesis^{42,43}. However, functional interactions between PCNA and Pol α have not been demonstrated^{32,44}, and therefore the functional role of the CysA motif in this enzyme awaits further investigation.

Our findings indicate that insertion of the Fe-S cluster into nuclear DNA polymerases depends on the function of not only the cytosolic but also the mitochondrial Fe-S protein biogenesis machineries (Fig. 6). The cysteine desulfurase Nfs1, if located only in the cytosol and nucleus, could not assist in the assembly of the Fe-S cluster into Pol3 (Supplementary Fig. 3). Thus, Nfs1, and presumably other members of the mitochondrial ISC assembly machinery¹⁹, need to operate inside mitochondria to support Fe-S cluster insertion into polymerases. This finding shows, surprisingly, that mitochondria are essential for nuclear DNA replication, presumably because they act as sulfur donors for the DNA polymerase Fe-S cluster insertion here. This crucial task of mitochondria explains their indispensability for cell viability in virtually all eukaryotes and may be more basic than even respiration, which is dispensable in some organisms¹⁹. Interestingly, other steps of eukaryotic DNA and RNA metabolism involve Fe-S proteins including factors required for ribosome function in protein translation (Rli1), nucleotide excision repair and transcription (Rad3, named XPD in humans), DNA double strand break repair (FancJ) and chromosome segregation (Chl1)¹⁹. On one hand, the involvement of these proteins may explain the role of mitochondrial function in several DNA metabolism-related, neurodegenerative and cancer-linked phenotypes, including nuclear genome instability⁴⁵. At least a subset of these disorders could originate from impaired Fe-S cluster assembly on these proteins and on the B-family DNA polymerases. On the other hand, the indispensable role of mitochondria in nuclear DNA and RNA metabolism suggests that eukaryotes, at some point in evolution, became dependent on these endosymbiotic organelles to express their genome.

METHODS

Yeast strains and plasmids. *Saccharomyces cerevisiae* W303-1A (*MATa*, *ura3-1*, *ade2-1*, *trp1-1*, *his3-11,15* and *leu2-3,112*) was used as wild type and as a background strain for cells with genes under the control of galactose-regulatable promoters and/or encoding N- or C-terminally epitope-tagged proteins. Details of strains and plasmid constructs are in Supplementary Methods and Supplementary Tables 1 and 2.

Expression in *E. coli* and purification of CTDs. The pASK-IBA43plus plasmids (IBA) encoding the C-terminally Strep-tagged CTDs of Pol1, Pol2, Pol3 and Rev3 were transformed into BL21 *E. coli* cells. Induction with anhydrotetracycline hydrochloride (AHT, 4.3 μ M) took place at $D_{600\text{nm}}$ of 0.5–0.7, at 30 °C for 16 h. Under these conditions, Pol1, Pol2 and Rev3 were totally insoluble. Inclusion bodies were solubilized in purification buffer (100 mM Tris-Cl, pH 8.0, 150 mM NaCl) containing 8 M urea. For Pol2, 6 M guanidinium hydrochloride was used instead of urea. To yield soluble CTDs, an overnight culture of *E. coli*, HMS174 (DE3) pLysS transformed with pASK-IBA43plus encoding the C-terminally Strep-tagged CTDs of Pol1, Pol2, Pol3 or Rev3 was diluted 100-fold into Terrific broth (24 g of yeast extract, 12 g of bactotryptone, 4 ml of glycerol, 12.5 g K_2HPO_4 and 2.31 g of KH_2PO_4 per liter) containing 3% (v/v) ethanol and was allowed to grow to a $D_{600\text{nm}}$ of 0.5 at 37 °C. The cultures were cooled down to 20 °C (~30 min), and benzyl alcohol (0.1 % v/v), betaine hydrochloride (1 mM), FeCl_3 (50 μ M) and α -cysteine (100 μ M) were added, followed by AHT. After ~16 h of expression at 20 °C, the cells were harvested and resuspended in anaerobic purification buffer. All subsequent steps were conducted in an anaerobic chamber (Coy), maintaining samples at 4 °C. The cell suspension was treated with 0.5 mg lysozyme per gram of cells for 30 min and was disrupted by sonication (three 30-s bursts, with 1-min cooling periods). After centrifugation at 100,000g for 45 min, the supernatant was mixed with one-tenth of its volume of high-capacity Strep-Tactin agarose (IBA) and homogenized for 1 h. The slurry was poured into a column and washed with 10 bed volumes of cold purification buffer, followed by elution with the same buffer containing 2 mM desthiobiotin. The proteins were analyzed by UV-vis spectroscopy and were frozen for EPR spectroscopy immediately after purification. For chemical analysis and SDS-PAGE, samples were shock-frozen and stored at –80 °C.

Purification of yeast Pol δ from yeast cells. Pol δ was purified from a yeast overproduction system⁴⁶. *POL3* containing a cleavable N-terminal GST-purification tag, *POL31* and *POL32* were overexpressed from the galactose-inducible *GAL1-10* promoter in protease-deficient strain BJ2168 (*MATa*, *ura3-52*, *trp1-289*, *leu2-3,112*, *prb1-1122*, *prc1-407*, *pep4-3*). After affinity purification on glutathione beads and removal of the GST tag by rhinoviral 3C protease, the preparation was further purified on a MonoS column. The SDS-PAGE shown in Figure 4a and Supplementary Figure 11c is of the MonoS eluates. Single and double cysteine-to-serine mutants were made using the QuikChange (Stratagene) protocol. Mutants were subjected to the same purification protocol. Because GST-tagged Pol3 was used for affinity purification, the presence of Pol31 and Pol32 in the Pol3-CysA mutant preparation and their absence from the Pol3-CysB mutant preparation indicates retention and defect in Pol3-Pol31 interactions in the mutants, respectively. After concentration to >2 mg ml⁻¹ using Centricon filters, preparations of the wild-type and the CysA mutant, but not of the CysB mutant, showed an olive-yellow color. The Pol3 catalytic subunit on its own was prepared as described above, but after overexpression using only the pBL335 plasmid in BJ2168. The yield was invariably low, and the protein was aggregation prone. Contaminating three-subunit enzyme was removed by two consecutive MonoS column steps (the single Pol3 subunit elutes before Pol δ). Pol δ preparations with Pol32- Δ PIP containing either the wild-type or CysA form of Pol3 were overproduced in strain PY117 (*MATa*, *ura3-52*, *trp1-289*, *leu2-3,112*, *his3-11,15*, *prb1-1122*, *pep4-3*, *pol32- Δ :HIS3*), a *pol32A* derivative of BJ2168 (ref. 33). Complex purification was performed in the same way as for wild-type.

Single-strand DNA replication assays. PCNA, RFC and RPA were purified as described^{47–49}. Assays (60 μ l) contained 20 mM Tris-HCl pH 7.8, 1 mM DTT, 100 μ g ml⁻¹ bovine serum albumin, 8 mM magnesium acetate, 0.5 mM ATP, 100 μ M each of dCTP, dGTP and dTTP, 10 μ M of [α -³²P]dATP, 100 mM NaCl, 2 nM of singly primed (36 base pairs, complementary to nucleotides 6330–6295) single-stranded M13mp18 DNA, 500 nM of RPA and 5 nM of PCNA (or PCNA concentration indicated in Fig. 5). PCNA was loaded onto the primed DNA by incubation with 5 nM RFC at 30 °C for 1 min, and replication was started by adding (mutant) Pol δ or Pol3. Aliquots (18 μ l) were taken at various time points, and replication was stopped by the addition of 2 μ l 100 mM EDTA and 3% SDS. After incubating at 50 °C for 10 min, 45 μ l of precipitation solution (2.5 M ammonium acetate, 20 μ g ml⁻¹ sonicated salmon sperm DNA, 1 mM EDTA and 0.05 mg ml⁻¹ linear acrylamide (Ambion Technologies)) was added, followed by ethanol precipitation. The dissolved pellet was analyzed by electrophoresis on a 1% alkaline agarose gel. Gels were dried and documented by PhosphorImager analysis (GE Healthcare).

EPR and UV-vis spectroscopy. EPR spectra were recorded with a Bruker EMX-6/1 X-band spectrometer containing an ER-041 XG microwave bridge, ER-041-1161 frequency counter, EMX-1101 power supply, ER-070 magnet, EMX-032T Hall field probe, ER-4102 Universal TE102 rectangular cavity and Oxford Instruments helium flow cryostat ESR-900. Data acquisition and manipulation were performed with the Bruker WINEPR software. For spin quantification, 1 mM CuSO_4 in 2 M NaClO₄ and 10 mM HCl was used. UV-vis spectra were recorded on a Jasco V-550 spectrophotometer. For EPR and UV-vis spectroscopy, the proteins were in anaerobic purification buffer and treated with sodium dithionite (2 mM) or potassium

ferricyanide (2 mM) when applicable. Samples were transferred inside the anaerobic chamber to stoppered anaerobic quartz cuvettes (Hellma) or Ilmasil-PN high-purity quartz EPR tubes. EPR samples were capped with rubber seals and shock-frozen outside the anaerobic chamber in liquid nitrogen.

Additional methods. ⁵⁵Fe incorporation, cloning, yeast two-hybrid analysis, cysteine mutagenesis, and chemical analysis of iron and acid-labile sulfide are described in the **Supplementary Methods**.

Received 19 July 2011; accepted 3 October 2011;
published online 27 November 2011

References

- Johansson, E. & Macneill, S.A. The eukaryotic replicative DNA polymerases take shape. *Trends Biochem. Sci.* **35**, 339–347 (2010).
- Nick McElhinny, S.A., Gordenin, D.A., Stith, C.M., Burgers, P.M. & Kunkel, T.A. Division of labor at the eukaryotic replication fork. *Mol. Cell* **30**, 137–144 (2008).
- Pursell, Z.F., Isoz, I., Lundström, E.B., Johansson, E. & Kunkel, T.A. Yeast DNA polymerase ϵ participates in leading-strand DNA replication. *Science* **317**, 127–130 (2007).
- Burgers, P.M. *et al.* Eukaryotic DNA polymerases: proposal for a revised nomenclature. *J. Biol. Chem.* **276**, 43487–43490 (2001).
- Mäkinen, M. *et al.* A novel family of DNA-polymerase-associated B subunits. *Trends Biochem. Sci.* **24**, 14–16 (1999).
- Baranovskiy, A.G. *et al.* X-ray structure of the complex of regulatory subunits of human DNA polymerase δ . *Cell Cycle* **7**, 3026–3036 (2008).
- Nelson, J.R., Lawrence, C.W. & Hinkle, D.C. Thymine-thymine dimer bypass by yeast DNA polymerase ζ . *Science* **272**, 1646–1649 (1996).
- Prakash, S., Johnson, R.E. & Prakash, L. Eukaryotic translesion synthesis DNA polymerases: specificity of structure and function. *Annu. Rev. Biochem.* **74**, 317–353 (2005).
- Bemark, M., Khamlichi, A.A., Davies, S.L. & Neuberger, M.S. Disruption of mouse polymerase ζ (Rev3) leads to embryonic lethality and impairs blastocyst development *in vitro*. *Curr. Biol.* **10**, 1213–1216 (2000).
- Krishna, S.S., Majumdar, I. & Grishin, N.V. Structural classification of zinc fingers: survey and summary. *Nucleic Acids Res.* **31**, 532–550 (2003).
- Tahirov, T.H., Makarova, K.S., Rogozin, I.B., Pavlov, Y.I. & Koonin, E.V. Evolution of DNA polymerases: an inactivated polymerase-exonuclease module in Pol ϵ and a chimeric origin of eukaryotic polymerases from two classes of archaeal ancestors. *Biol. Direct* **4**, 11 (2009).
- Swan, M.K., Johnson, R.E., Prakash, L., Prakash, S. & Aggarwal, A.K. Structural basis of high-fidelity DNA synthesis by yeast DNA polymerase δ . *Nat. Struct. Mol. Biol.* **16**, 979–986 (2009).
- Evanics, F., Maurmann, L., Yang, W.W. & Bose, R.N. Nuclear magnetic resonance structures of the zinc finger domain of human DNA polymerase- α . *Biochim. Biophys. Acta* **1651**, 163–171 (2003).
- Klinge, S., Núñez-Ramírez, R., Llorca, O. & Pellegrini, L. 3D architecture of DNA Pol α reveals the functional core of multi-subunit replicative polymerases. *EMBO J.* **28**, 1978–1987 (2009).
- Mizuno, T., Yamagishi, K., Miyazawa, H. & Hanaoka, F. Molecular architecture of the mouse DNA polymerase α -primase complex. *Mol. Cell. Biol.* **19**, 7886–7896 (1999).
- Dua, R., Levy, D.L. & Campbell, J.L. Analysis of the essential functions of the C-terminal protein/protein interaction domain of *Saccharomyces cerevisiae* pol ϵ and its unexpected ability to support growth in the absence of the DNA polymerase domain. *J. Biol. Chem.* **274**, 22283–22288 (1999).
- Sanchez Garcia, J., Ciufu, L.F., Yang, X., Kearsey, S.E. & MacNeill, S.A. The C-terminal zinc finger of the catalytic subunit of DNA polymerase δ is responsible for direct interaction with the B-subunit. *Nucleic Acids Res.* **32**, 3005–3016 (2004).
- Chanet, R. & Heude, M. Characterization of mutations that are synthetic lethal with *pol3-13*, a mutated allele of DNA polymerase delta in *Saccharomyces cerevisiae*. *Curr. Genet.* **43**, 337–350 (2003).
- Lill, R. Function and biogenesis iron-sulphur proteins. *Nature* **460**, 831–838 (2009).
- Hausmann, A. *et al.* The eukaryotic P-loop NTPase Nbp35: an essential component of the cytosolic and nuclear iron-sulfur protein assembly machinery. *Proc. Natl. Acad. Sci. USA* **102**, 3266–3271 (2005).
- Zhang, Y. *et al.* Dre2, a conserved eukaryotic Fe/S cluster protein, functions in cytosolic Fe/S protein biogenesis. *Mol. Cell. Biol.* **28**, 5569–5582 (2008).
- Netz, D.J.A. *et al.* Tah18 transfers electrons to Dre2 in cytosolic iron-sulfur protein biogenesis. *Nat. Chem. Biol.* **6**, 758–765 (2010).
- Roy, A., Solodovnikova, N., Nicholson, T., Antholine, W. & Walden, W.E. A novel eukaryotic factor for cytosolic Fe-S cluster assembly. *EMBO J.* **22**, 4826–4835 (2003).
- Netz, D.J.A., Pierik, A.J., Stümpfig, M., Mühlhoff, U. & Lill, R. The Cfd1-Nbp35 complex acts as a scaffold for iron-sulfur protein assembly in the yeast cytosol. *Nat. Chem. Biol.* **3**, 278–286 (2007).
- Balk, J., Pierik, A.J., Netz, D.J.A., Mühlhoff, U. & Lill, R. The hydrogenase-like Nar1p is essential for maturation of cytosolic and nuclear iron-sulphur proteins. *EMBO J.* **23**, 2105–2115 (2004).
- Balk, J., Netz, D.J.A., Tepper, K., Pierik, A.J. & Lill, R. The essential WD40 protein Cia1 is involved in a late step of cytosolic and nuclear iron-sulfur protein assembly. *Mol. Cell. Biol.* **25**, 10833–10841 (2005).
- Kispal, G., Csere, P., Prohl, C. & Lill, R. The mitochondrial proteins Atm1p and Nfs1p are required for biogenesis of cytosolic Fe/S proteins. *EMBO J.* **18**, 3981–3989 (1999).
- Klinge, S., Hirst, J., Maman, J.D., Krude, T. & Pellegrini, L. An iron-sulfur domain of the eukaryotic primase is essential for RNA primer synthesis. *Nat. Struct. Mol. Biol.* **14**, 875–877 (2007).
- Burgers, P.M. & Gerik, K.J. Structure and processivity of two forms of *Saccharomyces cerevisiae* DNA polymerase δ . *J. Biol. Chem.* **273**, 19756–19762 (1998).
- Orme-Johnson, W.H. & Orme-Johnson, A.R. Iron-sulfur proteins: the problem of determining cluster type. in *Iron-Sulfur Proteins* (ed. Spiro, T.G.) 67–95 (Wiley, 1982).
- Kent, T.A. *et al.* Mössbauer studies of beef heart aconitase: evidence for facile interconversions of iron-sulfur clusters. *Proc. Natl. Acad. Sci. USA* **79**, 1096–1100 (1982).
- Tsurimoto, T. & Stillman, B. Multiple replication factors augment DNA synthesis by the two eukaryotic DNA polymerases, α and δ . *EMBO J.* **8**, 3883–3889 (1989).
- Johansson, E., Garg, P. & Burgers, P.M. The Pol32 subunit of DNA polymerase δ contains separable domains for processive replication and proliferating cell nuclear antigen (PCNA) binding. *J. Biol. Chem.* **279**, 1907–1915 (2004).
- Montecucco, A. *et al.* DNA ligase I is recruited to sites of DNA replication by an interaction with proliferating cell nuclear antigen: identification of a common targeting mechanism for the assembly of replication factories. *EMBO J.* **17**, 3786–3795 (1998).
- Hara, K. *et al.* Crystal structure of human REV7 in complex with a human REV3 fragment and structural implication of the interaction between DNA polymerase ζ and REV1. *J. Biol. Chem.* **285**, 12299–12307 (2010).
- Dauter, Z., Wilson, K.S., Sieker, L.C., Moulis, J.M. & Meyer, J. Zinc- and iron-rubredoxins from *Clostridium pasteurianum* at atomic resolution: a high-precision model of a ZnS₄ coordination unit in a protein. *Proc. Natl. Acad. Sci. USA* **93**, 8836–8840 (1996).
- Ramelot, T.A. *et al.* Solution NMR structure of the iron-sulfur cluster assembly protein U (IscU) with zinc bound at the active site. *J. Mol. Biol.* **344**, 567–583 (2004).
- Urzica, E., Pierik, A.J., Mühlhoff, U. & Lill, R. Crucial role of conserved cysteine residues in the assembly of two iron-sulfur clusters on the CIA protein Nar1. *Biochemistry* **48**, 4946–4958 (2009).
- Nar, H. *et al.* Characterization and crystal structure of zinc azurin, a by-product of heterologous expression in *Escherichia coli* of *Pseudomonas aeruginosa* copper azurin. *Eur. J. Biochem.* **205**, 1123–1129 (1992).
- Abbouni, B., Oehlmann, W., Stolle, P., Pierik, A.J. & Auling, G. Electron paramagnetic resonance (EPR) spectroscopy of the stable-free radical in the native metallo-cofactor of the manganese-ribonucleotide reductase (Mn-RNR) of *Corynebacterium glutamicum*. *Free Radic. Res.* **43**, 943–950 (2009).
- Boal, A.K., Cotruvo, J.A. Jr., Stubbe, J. & Rosenzweig, A.C. Structural basis for activation of class Ib ribonucleotide reductase. *Science* **329**, 1526–1530 (2010).
- Burgers, P.M.J. *Saccharomyces cerevisiae* replication factor C. II. Formation and activity of complexes with the proliferating cell nuclear antigen and with DNA polymerases δ and ϵ . *J. Biol. Chem.* **266**, 22698–22706 (1991).
- Garg, P., Stith, C.M., Majka, J. & Burgers, P.M.J. Proliferating cell nuclear antigen promotes translesion synthesis by DNA polymerase ζ . *J. Biol. Chem.* **280**, 23446–23450 (2005).
- Wong, S.W. *et al.* DNA polymerases α and δ are immunologically and structurally distinct. *J. Biol. Chem.* **264**, 5924–5928 (1989).
- Veatch, J.R., McMurray, M.A., Nelson, S.W. & Gottschling, D.E. Mitochondrial dysfunction leads to nuclear genome instability via an iron-sulfur cluster defect. *Cell* **137**, 1247–1258 (2009).
- Fortune, J.M., Stith, C.M., Kissling, G.E., Burgers, P.M. & Kunkel, T.A. RPA and PCNA suppress formation of large deletion errors by yeast DNA polymerase δ . *Nucleic Acids Res.* **34**, 4335–4341 (2006).
- Ayyagari, R., Impellizzeri, K.J., Yoder, B.L., Gary, S.L. & Burgers, P.M. A mutational analysis of the yeast proliferating cell nuclear antigen indicates distinct roles in DNA replication and DNA repair. *Mol. Cell. Biol.* **15**, 4420–4429 (1995).
- Gomes, X.V., Gary, S.L. & Burgers, P.M. Overproduction in *Escherichia coli* and characterization of yeast replication factor C lacking the ligase homology domain. *J. Biol. Chem.* **275**, 14541–14549 (2000).
- Henricksen, L.A., Umbricht, C.B. & Wold, M.S. Recombinant replication protein A: expression, complex formation, and functional characterization. *J. Biol. Chem.* **269**, 11121–11132 (1994).

Acknowledgments

We thank B. Yoder for yeast two-hybrid analysis and M. Reuter for help with cloning. This work was supported by grant GM032431 from the US National Institutes of Health (P.M.J.B.), the Deutsche Forschungsgemeinschaft (SFB 593, Gottfried-Wilhelm Leibniz program, and GRK 1216), Rhön Klinikum, von Behring-Röntgen Stiftung, LOEWE-Program of State Hessen, Max-Planck Gesellschaft and Fonds der Chemischen Industrie.

Author contributions

All authors performed experiments. D.J.A.N., R.L., P.M.J.B. and A.J.P. designed experiments, analyzed data and wrote the manuscript.

Competing financial interests

The authors declare no competing financial interests.

Additional information

Supplementary information is available online at <http://www.nature.com/naturechemicalbiology/>. Reprints and permissions information is available online at <http://www.nature.com/reprints/index.html>. Correspondence and requests for materials should be addressed to R.L. (lill@staff.uni-marburg.de), P.M.J.B. (burgers@biochem.wustl.edu) or A.J.P. (pierik@staff.uni-marburg.de).

SUPPLEMENTARY INFORMATION

Eukaryotic DNA polymerases require an iron-sulfur cluster
for the formation of active complexes

Daili J. A. Netz¹, Carrie M. Stith², Martin Stümpfig¹, Gabriele Köpf¹,
Daniel Vogel¹, Heide M. Genau¹, Joseph L. Stodola²,
Roland Lill^{1*}, Peter M. J. Burgers^{2*} & Antonio J. Pierik^{1*}

¹Institut für Zytobiologie und Zytopathologie, Philipps-Universität Marburg,
Robert-Koch-Strasse 6, D-35033 Marburg, Germany.

²Department of Biochemistry and Molecular Biophysics, Washington
University School of Medicine, St. Louis, Missouri 63110, USA.

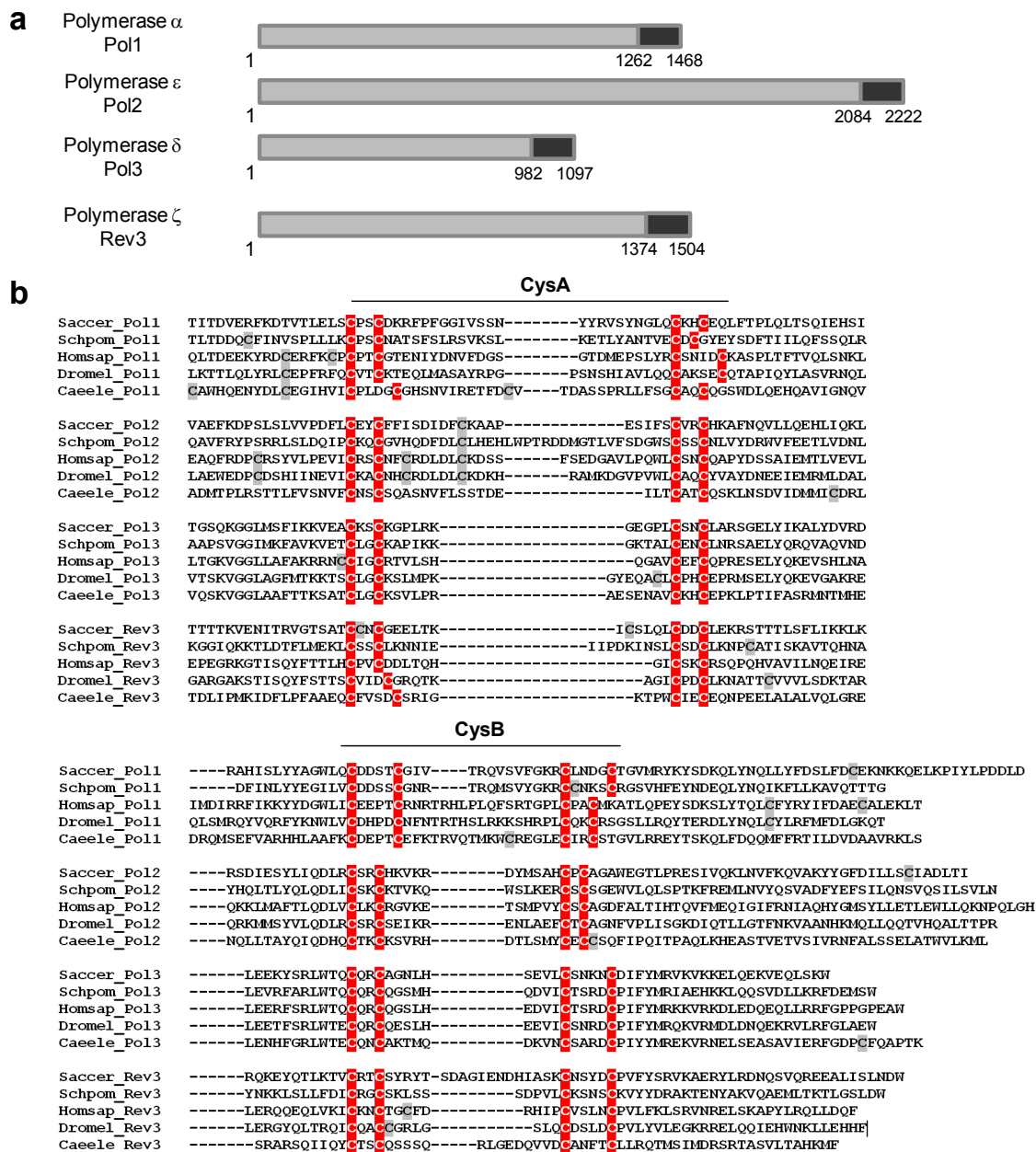
* To whom correspondence should be addressed. E-mail: lill@staff.uni-marburg.de,
burgers@biochem.wustl.edu, pierik@staff.uni-marburg.de

Supplementary Figures 1-14

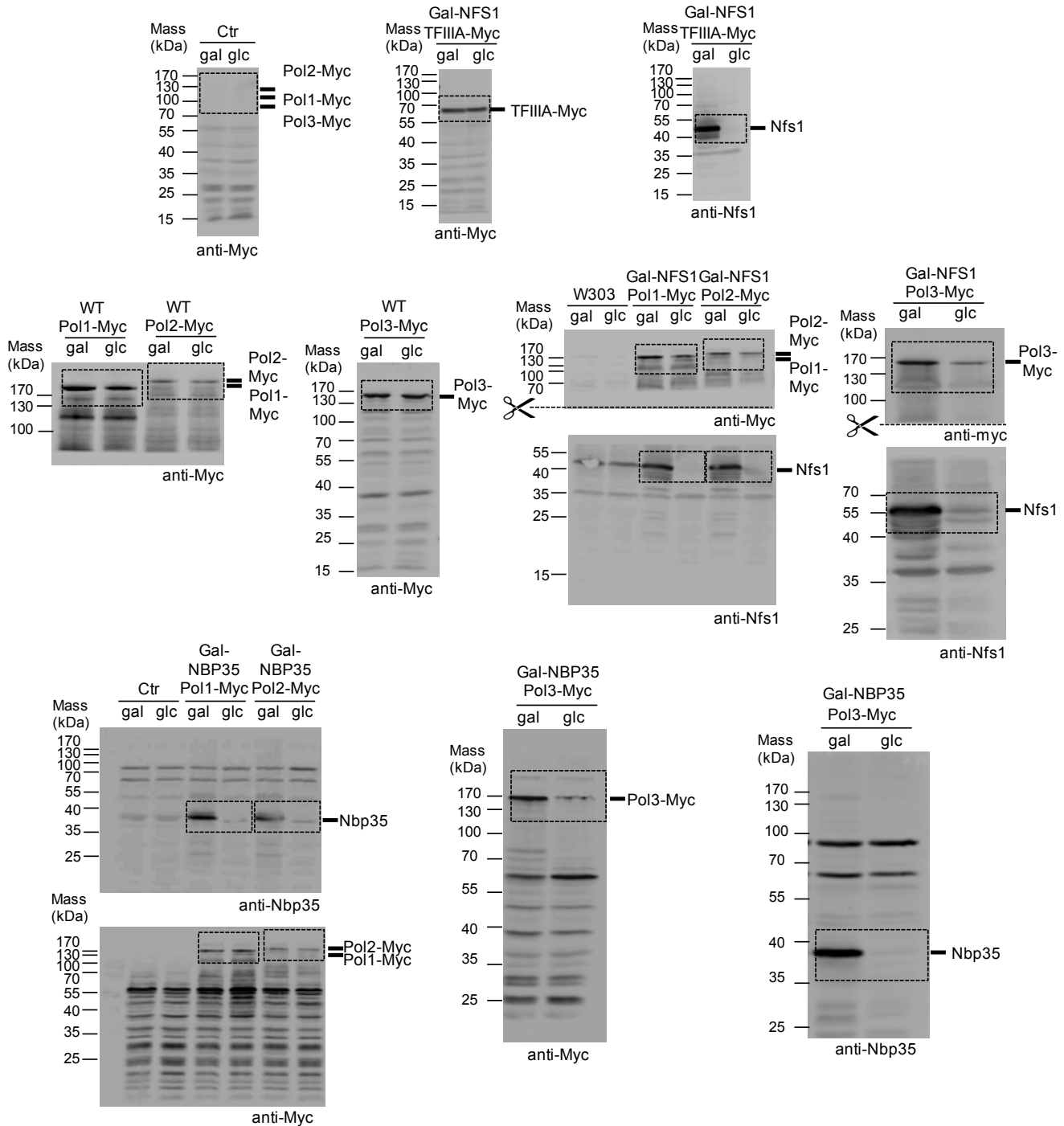
Supplementary Tables 1-2

Supplementary Methods and References

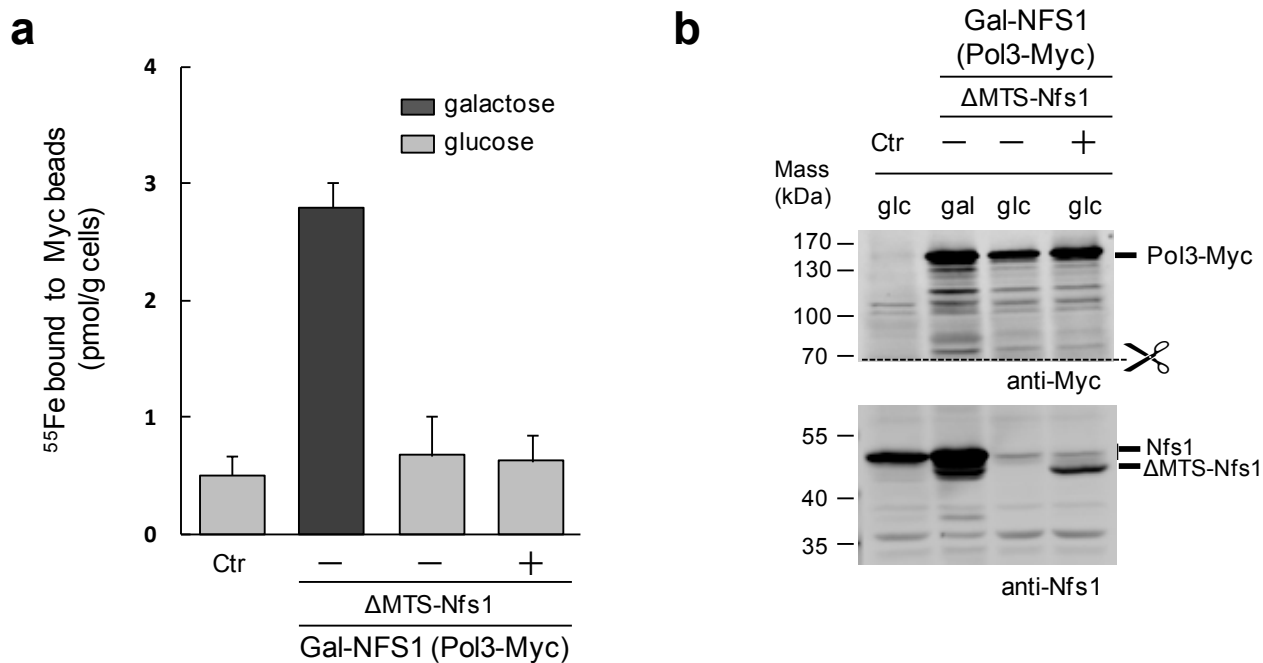
Supplementary Results



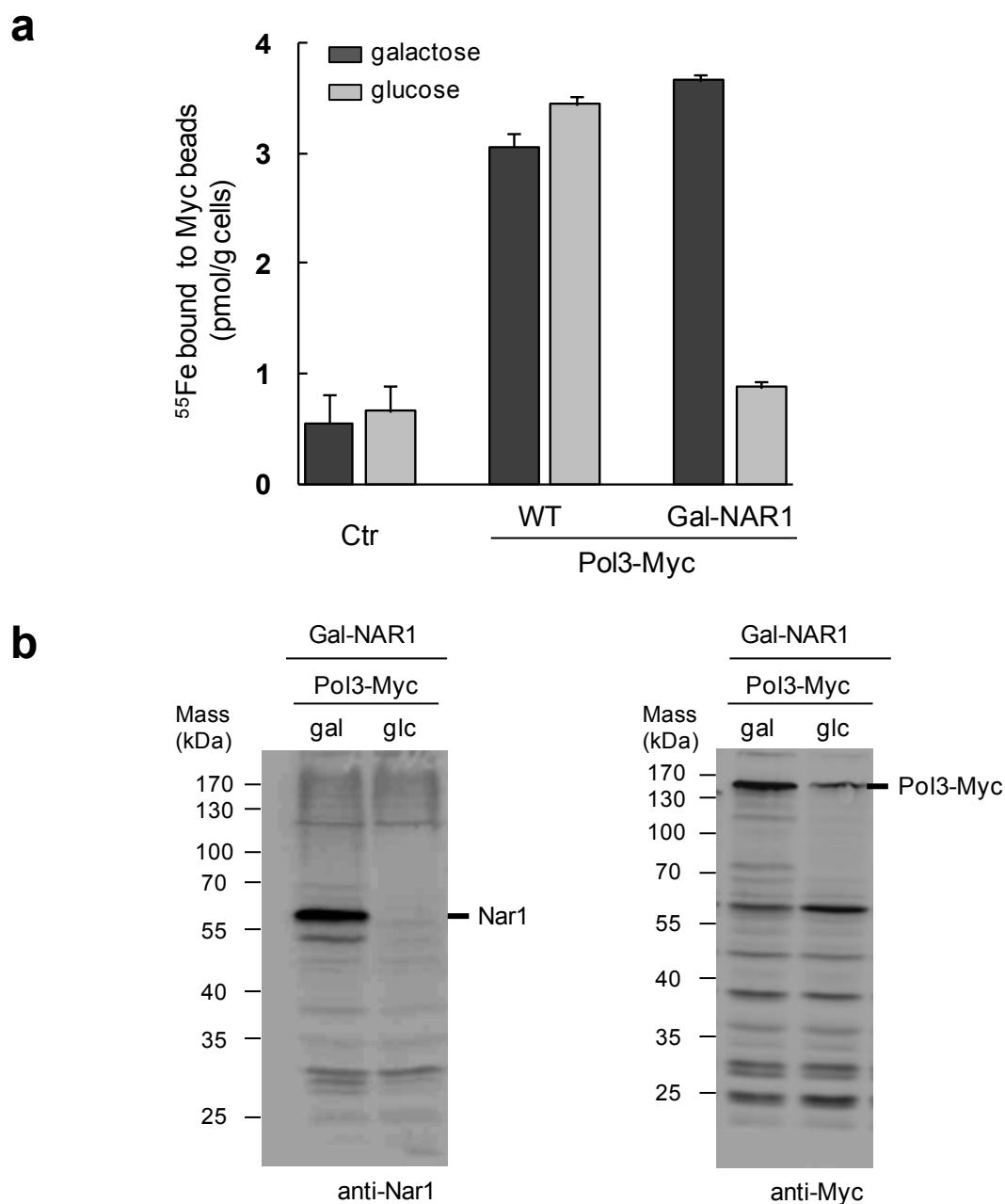
Supplementary Figure 1. Eukaryotic B-family DNA polymerases contain eight conserved cysteine residues in their C-terminal domain (CTD). **a**, Schematic representation of the *Saccharomyces cerevisiae* B-family DNA polymerases with amino acid positions demarking the CTDs (in brown). **b**, Amino acid sequence alignment of the CTDs shows two motifs of four cysteine residues, CysA and CysB which are involved in metal binding. Abbreviations: Saccer, *S. cerevisiae*; Schpom, *Schizosaccharomyces pombe*; Homsap, *Homo sapiens*; Dromel, *Drosophila melanogaster*; Caeele, *Caenorhabditis elegans*. Cysteine residues which are considered to coordinate metal ions have been highlighted in red, other cysteine residues in grey.



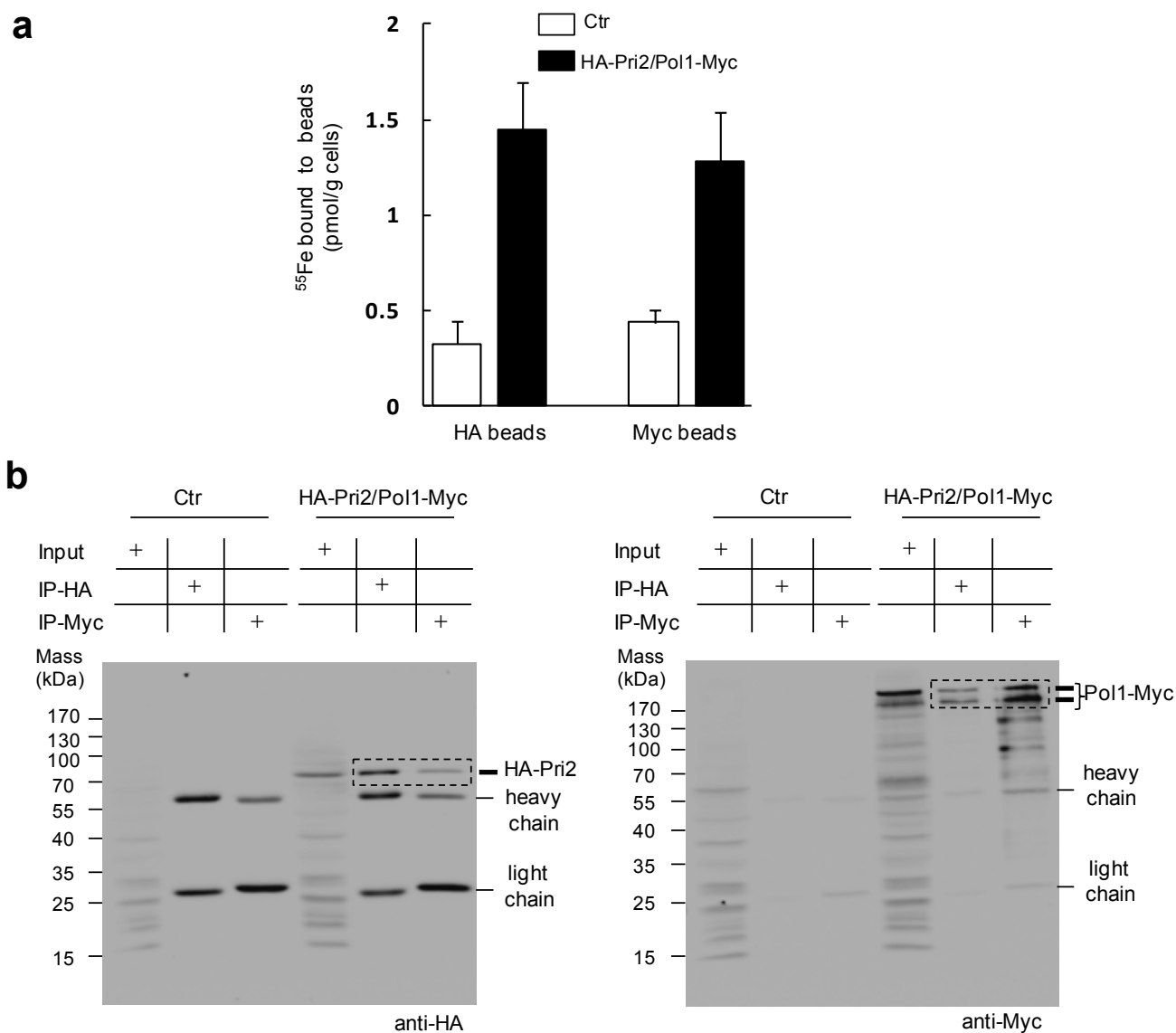
Supplementary Figure 2. Immunoblots for the indicated (tagged) proteins in the cell extracts subjected to ^{55}Fe incorporation in Figure 1a. Proteins were visualized by immunostaining using specific antibodies and chemiluminescence detection by a CCD camera. Hatched boxes denote areas of particular interest (target of immunoprecipitation or protein depleted). The positions of molecular mass markers are indicated.



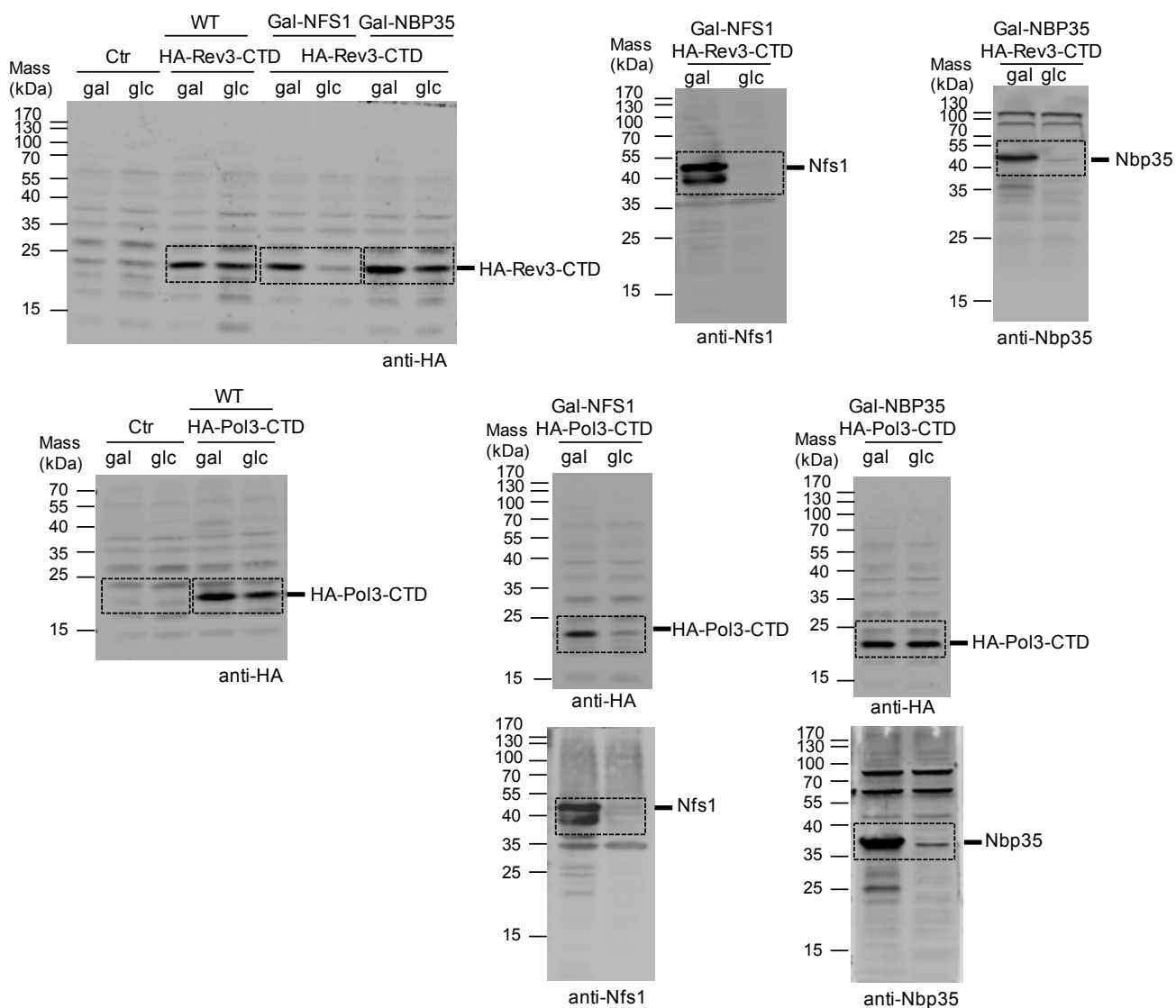
Supplementary Figure 3. A cytosolic version of cysteine desulfurase Nfs1 does not support Fe-S cluster assembly on Pol3-Myc. Gal-NFS1 cells with the *NFS1* gene under the control of the *GAL1-10* (Gal) promoter were transformed with a plasmid (+) encoding a cytosolic form¹ of Nfs1 (lacking amino acid residues 1-94, ΔMTS-Nfs1) or with an empty plasmid (-). **a**, ⁵⁵Fe radiolabelling and immunoprecipitation was performed as in Fig. 1 using wild-type cells (Ctr) or the indicated Gal-NFS1 cells carrying genomically Myc-tagged Pol3. The data for wild-type cells and the galactose bar correspond to Fig. 1a in the main text. **b**, Cell extracts from **a** were analyzed by immunoblotting to show the presence of Pol3-Myc, the depletion of mitochondrial Nfs1, and the synthesis of the slightly shorter ΔMTS-Nfs1 protein. Error bars, s.d. (n ≥ 3).



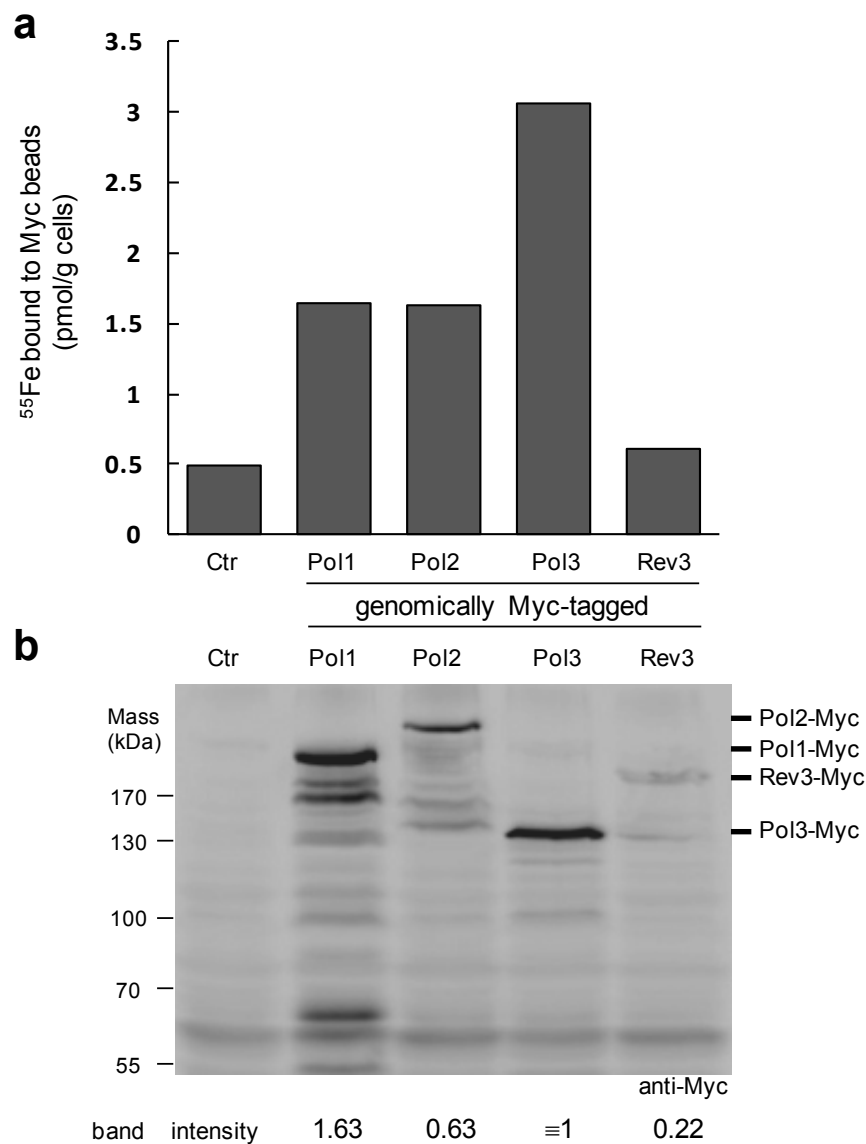
Supplementary Figure 4. Depletion of the cytosolic CIA protein Nar1 leads to loss of radioactive iron associated with Pol3-Myc. a, ⁵⁵Fe radiolabelling and immunoprecipitation was performed as in Fig. 1 using wild-type cell extracts (Ctr), or extracts from wild-type (WT) and Gal-NAR1 cells carrying genomically Myc-tagged Pol3. Gal-NAR1 cells express the *NAR1* gene under the control of the *GALI-10* (Gal) promoter. The data for Ctr and WT correspond to Fig. 1a in the main text. **b,** Immunoblots of cell extracts from a. The indicated (tagged) proteins were visualized by immunostaining using specific antibodies and chemiluminescence detection by a CCD camera. The positions of molecular mass markers are indicated. Error bars, s.d. (n ≥ 3).



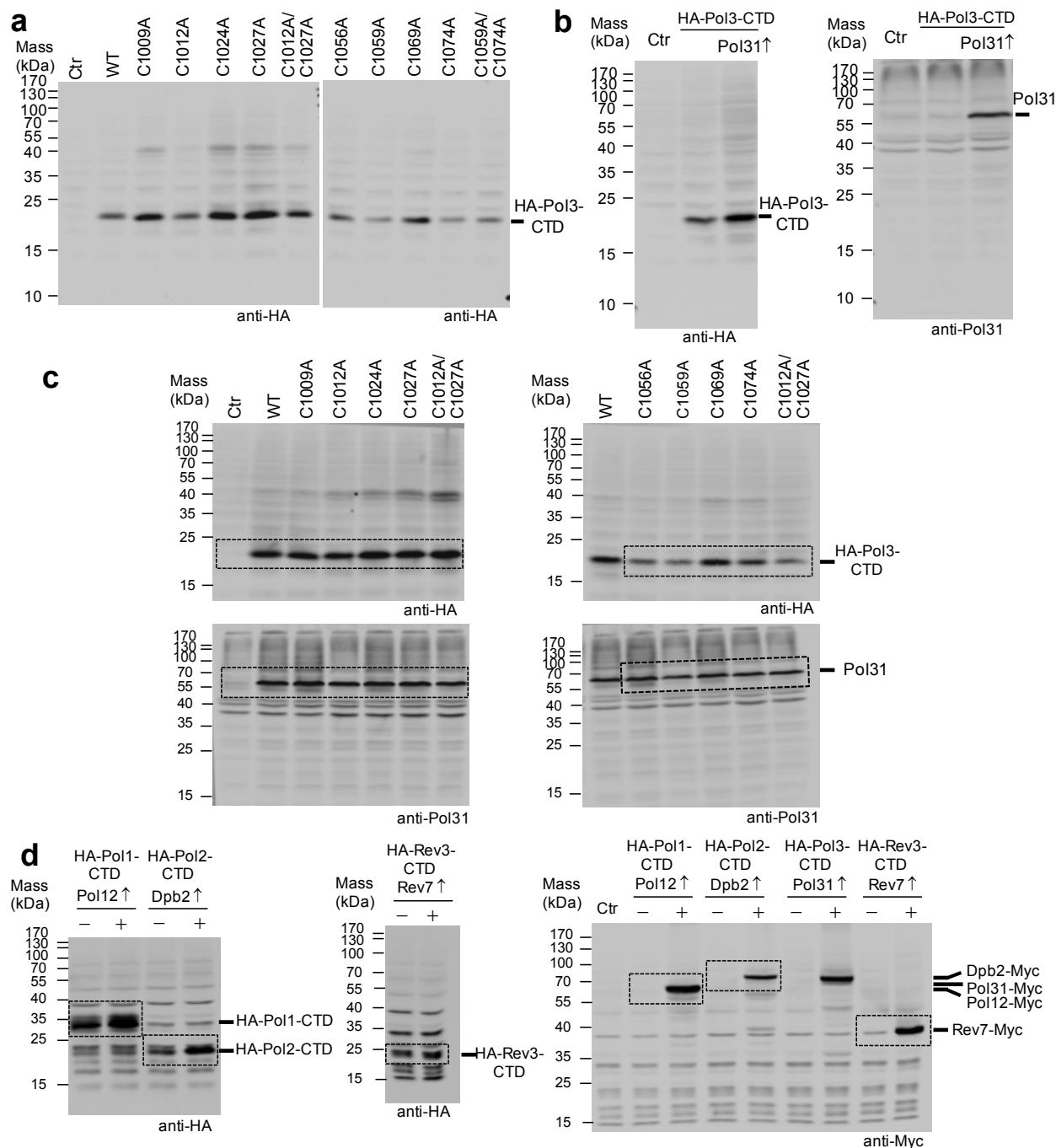
Supplementary Figure 5. Comparison of ⁵⁵Fe associated with endogenous levels of Pol1 and the [4Fe-4S] cluster-containing primase subunit Pri2. **a**, ⁵⁵Fe radiolabelling and immunoprecipitation was performed as in Fig. 1 using wild-type cells (Ctr) or a yeast strain with genomically integrated Pol1-Myc/HA-Pri2. Cells were grown in iron-free SC medium supplemented with galactose. **b**, Co-immunoprecipitation of HA-Pri2 and Pol1-Myc with anti-HA or anti-Myc beads. The strains described in **a** were grown on regular SC medium supplemented with galactose and lysates were prepared with glass beads (Input). After centrifugation, the obtained supernatants were separated into two aliquots and incubated with anti-HA or anti-Myc agarose beads. The beads were washed (IP-HA and IP-Myc) and analyzed by SDS-PAGE and immunoblotting using the indicated monoclonal antibodies. Bands labeled heavy and light chain are cross-reactive IgG subunits released from beads. The intensity of the HA-Pri2 band in the Myc beads was 20% of the same band in the HA beads (boxed bands in left blot) as quantified from the chemiluminescence recording of the CCD camera. Error bars, s.d. (n ≥ 3).



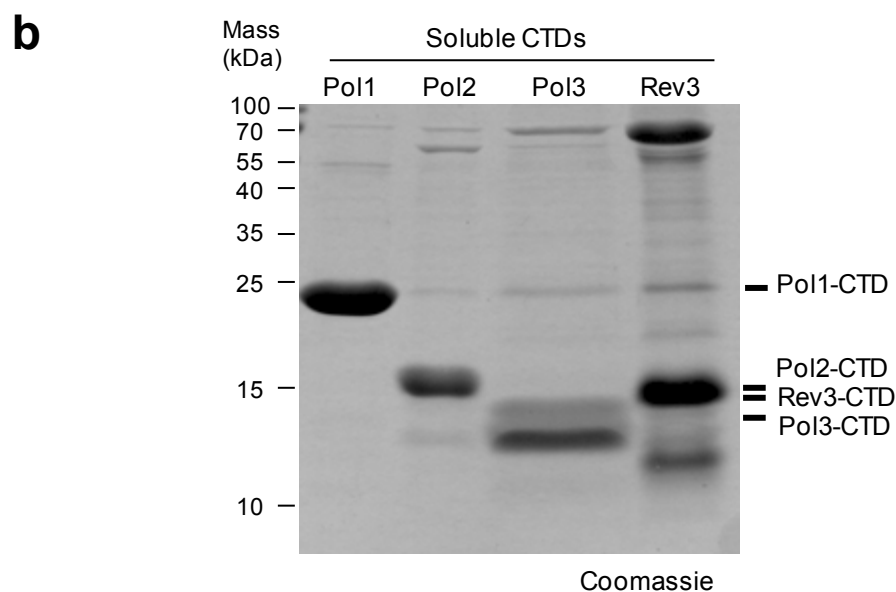
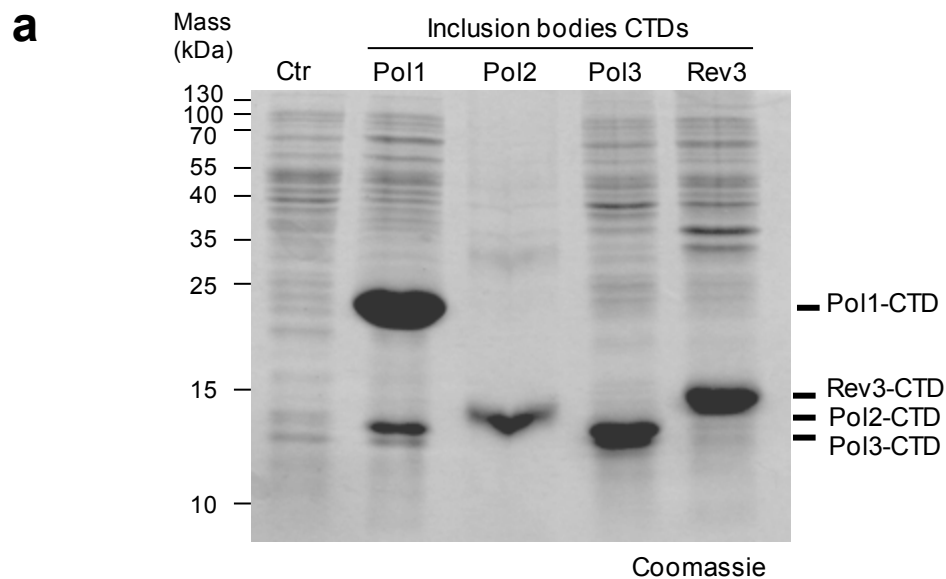
Supplementary Figure 6. Immunoblots for the indicated (tagged) proteins in the cell extracts subjected to ^{55}Fe incorporation in Figure 1b. Proteins were visualized by immunostaining using specific antibodies and chemiluminescence detection by a CCD camera. Hatched boxes denote areas of particular interest (target of immunoprecipitation or protein depleted). The positions of molecular mass markers are indicated.



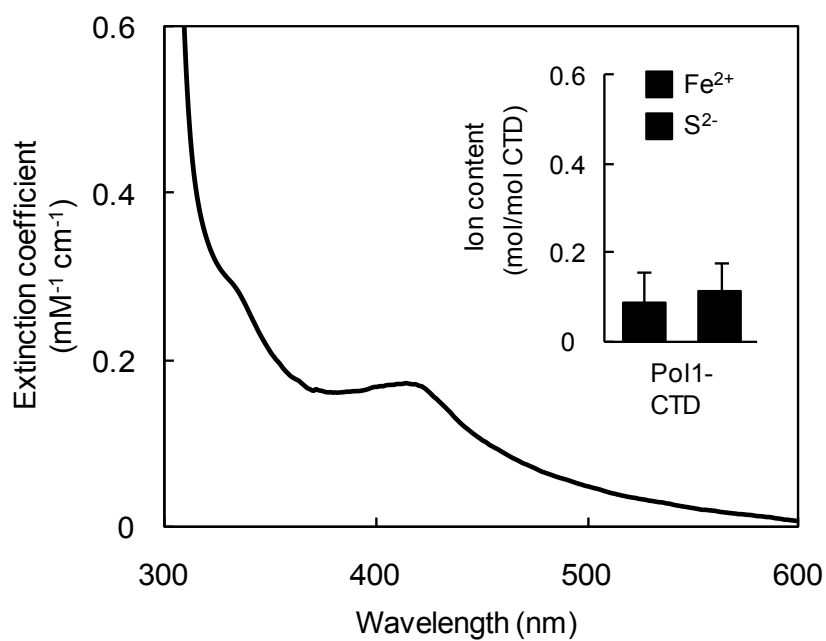
Supplementary Figure 7. Comparison of the expression levels of yeast B-family DNA polymerases shows that Rev3 has a low abundance. **a**, Wild-type yeast cells (Ctr) and cells carrying genomically Myc-tagged polymerases were grown in Fe-free galactose-containing SC medium. Cell extracts were prepared and an immunoprecipitation of the Myc-tagged, indicated polymerases was performed. Co-immunoprecipitated ⁵⁵Fe was analyzed by scintillation counting. Data for Ctr, Pol1, Pol2 and Pol3 correspond to the Ctr and the WT bars of Fig. 1a in the main text. **b**, The indicated (tagged) proteins in cell extracts from **a** were visualized by immunostaining using specific antibodies and chemiluminescence detection by a CCD camera. The summed intensities (bottom) of discrete bands with molecular mass above 120 kDa were normalized to the intensity of a cross-reactive band at ~60 kDa. The positions of molecular mass markers are indicated. Error bars, s.d. (n ≥ 3).



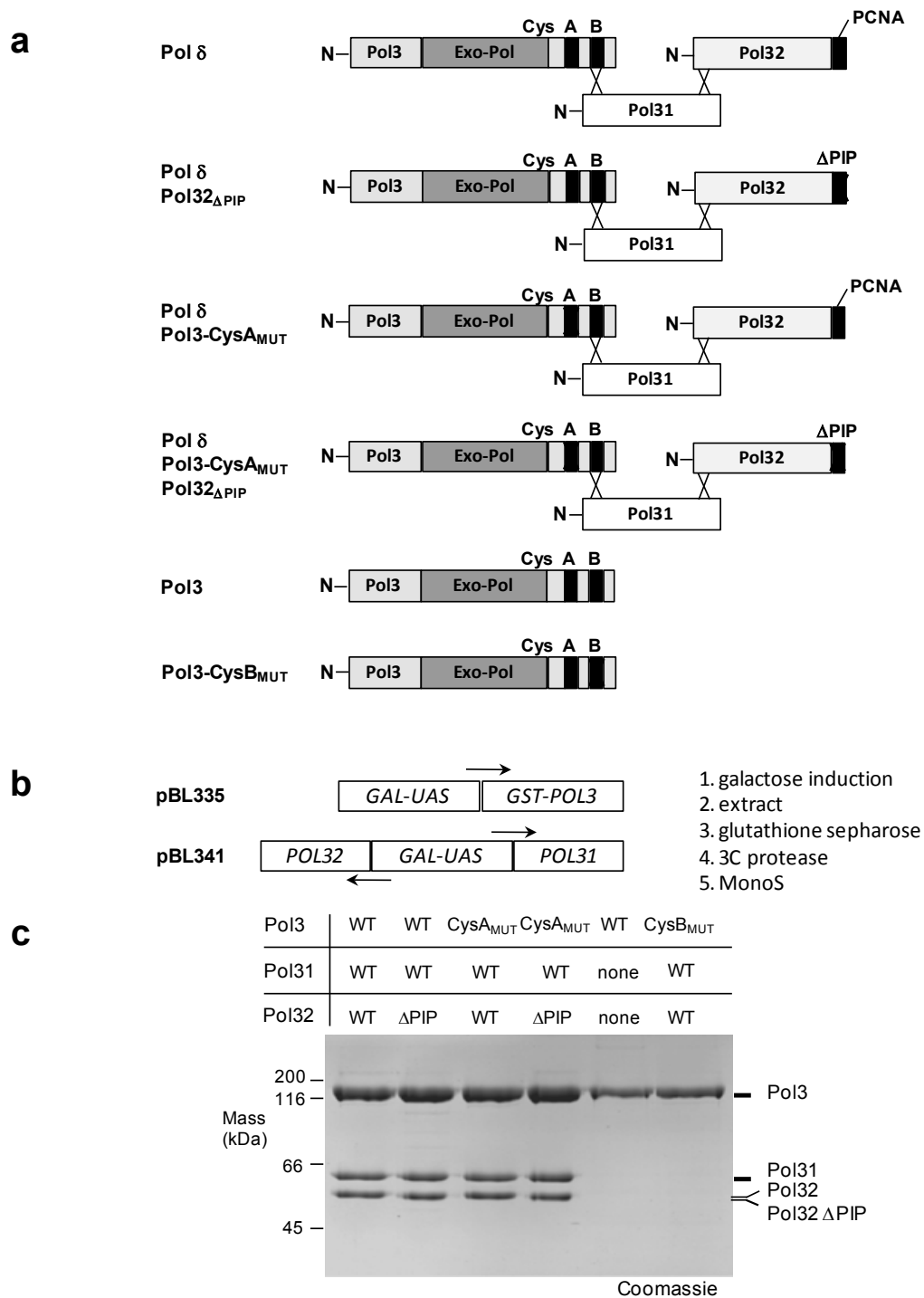
Supplementary Figure 8. Immunostaining for the Pol3-CTD ^{55}Fe incorporation experiment at endogenous Pol31 level and comparison of CTD and accessory subunit levels after over-expression. **a**, HA-Pol3-CTDs in cell extracts were visualized by immunostaining using specific antibodies and chemiluminescence detection by a CCD camera. Nomenclature corresponds to Fig. 2, samples are from the light olive-green bars in Fig. 2. **b**, Idem, but with comparison of HA-Pol3-CTD and Pol31 upon Pol31 over-expression (Pol31[↑]), **c**, **d** Full-size immunoblots corresponding to the cropped data (hatched boxes) shown in Figure 2a and 2b, respectively. The positions of molecular mass markers are indicated.



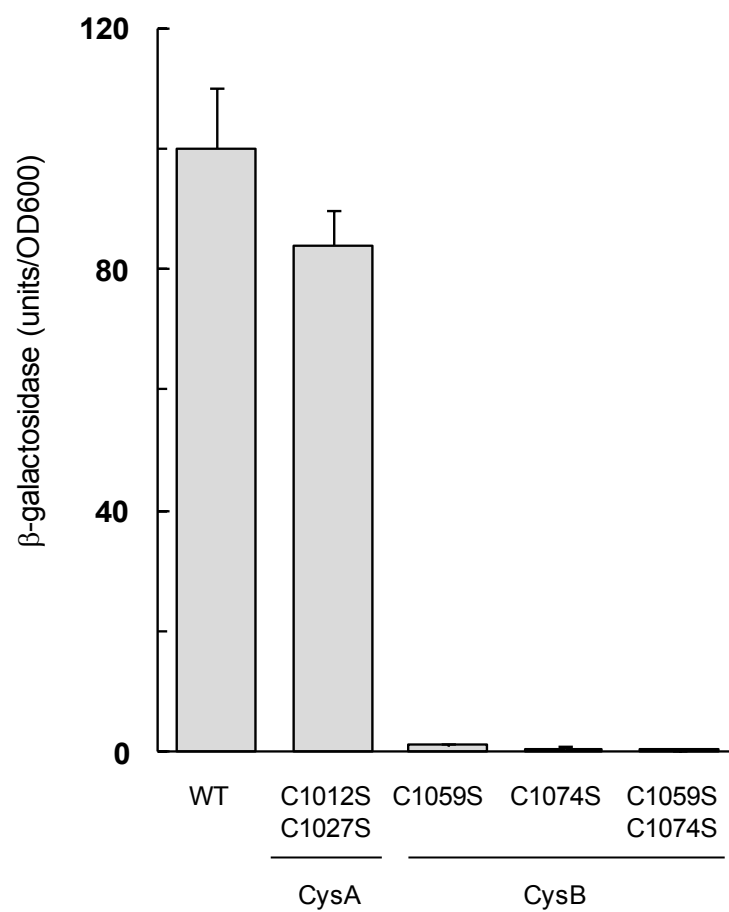
Supplementary Figure 9. Purification of DNA polymerase CTDs after expression in *E. coli*. **a**, Inclusion bodies solubilized with chaotropic agents (shown in Fig. 3a) were analyzed by SDS-PAGE and Coomassie staining. **b**, As in **a** but for soluble purified Pol1-, Pol2-, Pol3- and Rev3-CTDs used in Fig. 3 b,c and Supplementary Fig. 10.



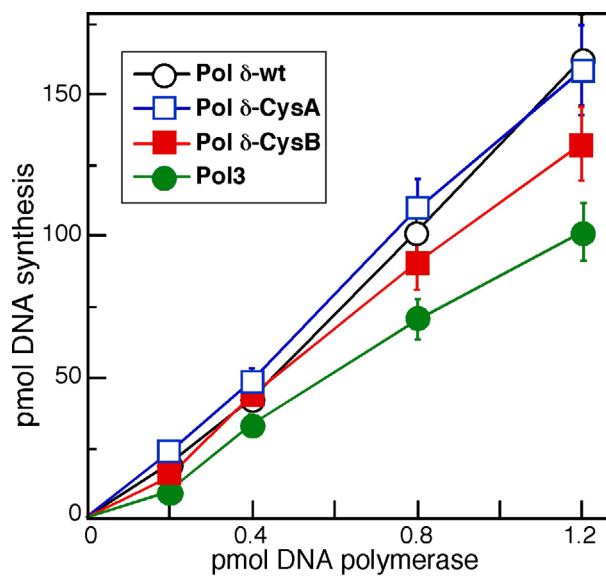
Supplementary Figure 10. UV-Vis spectrum of soluble purified Pol1-CTD. Pol1-CTD was purified as described in Methods. The inset shows the average non-heme iron and acid-labile sulfide content for three soluble Pol1-CTD preparations. Error bars, s.d. ($n \geq 3$).



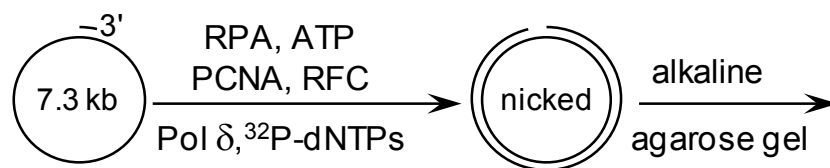
Supplementary Figure 11. Pol δ and Pol3 protein preparations used in this study. **a**, Overview of (mutant) Pol δ complexes used in Figs. 4 and 5. **b**, Scheme for overexpression (arrows indicate orientation of transcription) and protein purification. **c**, Photograph of the full length gel (SDS-PAGE) of purified proteins visualized by colloidal Coomassie staining. Fig. 4a in the main article contains cropped areas from the first, third and sixth lane of this gel image.



Supplementary Figure 12. Pol3-CysB mutants are defective in binding Pol31. Yeast two-hybrid interactions were measured employing plasmids with LexA_{DBD}-POL3 (WT) or the indicated CysA and CysB mutants and with GAL4_{AD}-POL31. Averages of β -galactosidase activities are shown. Error bars, s.d. (n \geq 3).



Supplementary Figure 13. Basal DNA polymerase activity of Pol δ is unaffected by CTD mutations. The assay measures incorporation of dNTPs into activated salmon sperm DNA as described². Note that the activity of the single Pol3 enzyme (lacking Pol31 and Pol32) is somewhat lower. We ascribe this to its tendency to aggregation. Error bars, s.d. ($n \geq 3$).



Supplementary Figure 14. Outline of the assay for processive DNA replication. The black circle represents single-stranded M13mp18 DNA primed with a 36 bp oligonucleotide (short red line) which is complementary to nucleotides 6330–6295. Polymerase replicates the single strand by extension of the primer with ^{32}P -dNTPs to form double-stranded DNA with a single nick. Formation of the radioactive strand (red) is subsequently detected by alkaline agarose gel electrophoresis and phosphorimaging (see Fig. 5 a and b).

Supplementary Table 1. Yeast strains used in this study.

Strain name	Background strain	Template for PCR (marker)	Tag and/or promoter introduced into genome	Source
Gal-NFS1	W303	pFA (His)	<i>GALI-10</i> promoter	³
Gal-NBP35	W303	pFA (His)	<i>GALI-10</i> promoter	⁴
Gal-NAR1	W303	pFA (His)	<i>GALI-10</i> promoter	⁵
Pol1-Myc	W303	pYM19 (His)	C-terminal 9xMyc	this study
Pol2-Myc	W303	pYM19 (His)	C-terminal 9xMyc	this study
Pol3-Myc	W303	pYM21 (Nat)	C-terminal 9xMyc	this study
Rev3-Myc	W303	pYM19 (His)	C-terminal 9xMyc	this study
TFIIIA-Myc	Gal-NFS1	pYM21 (Nat)	C-terminal 9xMyc	this study
Gal-NFS1 Pol1-Myc	Pol1-Myc	pYM-N23 (Nat)	<i>GALI-10</i> promoter	this study
Gal-NBP35 Pol1-Myc	Pol1-Myc	pYM-N23 (Nat)	<i>GALI-10</i> promoter	this study
Gal-NFS1 Pol2-Myc	Pol2-Myc	pYM-N23 (Nat)	<i>GALI-10</i> promoter	this study
Gal-NBP35 Pol2-Myc	Pol2-Myc	pYM-N23 (Nat)	<i>GALI-10</i> promoter	this study
Gal-NFS1 Pol3-Myc	Gal-NFS1	pYM21 (Nat)	<i>GALI-10</i> promoter	this study
Gal-NBP35 Pol3-Myc	Gal-NBP35	pYM21 (Nat)	<i>GALI-10</i> promoter	this study
Gal-NAR1 Pol3-Myc	Gal-NAR1	pYM21 (Nat)	<i>GALI-10</i> promoter	this study
GalL-HA-Pri2	W303	pYM-N28 (Nat)	<i>GALL</i> promoter & N-terminal 3xHA	this study
HA-Pri2	GalL-HA-Pri2	See text	Loss of <i>GALL</i> promoter	this study
HA-Pri2 Pol1-Myc	HA-Pri2	pYM21 (Nat)	C-terminal 9xMyc	this study

Abbreviations: pFA, pFA6a-HIS3MX6-Gal1-10; His, *Kluyveromyces lactis* His3; for pYM plasmids see⁶; Nat, nourseothricin acetyl transferase. TFIIIA is Transcription Factor IIIA (systematic name Pzf1).

Supplementary Table 2. Plasmids used in this study.

Plasmid (promoter)	Encoding protein	Tag and position	Use
416 (<i>MET25</i>)	Pol3-CTD	3HA N	⁵⁵ Fe incorporation
	Rev3-CTD	3HA N	⁵⁵ Fe incorporation
	Pol1-CTD	3HA N	⁵⁵ Fe incorporation
	Pol2-CTD	3HA N	⁵⁵ Fe incorporation
	Pol3-CTD C1009A	3HA N	⁵⁵ Fe incorporation
	Pol3-CTD C1012A	3HA N	⁵⁵ Fe incorporation
	Pol3-CTD C1024A	3HA N	⁵⁵ Fe incorporation
	Pol3-CTD C1027A	3HA N	⁵⁵ Fe incorporation
	Pol3-CTD C1012A/C1027A	3HA N	⁵⁵ Fe incorporation
	Pol3-CTD C1056A	3HA N	⁵⁵ Fe incorporation
	Pol3-CTD C1059A	3HA N	⁵⁵ Fe incorporation
	Pol3-CTD C1069A	3HA N	⁵⁵ Fe incorporation
	Pol3-CTD C1074A	3HA N	⁵⁵ Fe incorporation
	Pol3-CTD C1059A/C1074A	3HA N	⁵⁵ Fe incorporation
ΔMTS-Nfs1	none		⁵⁵ Fe incorporation
424 (<i>TDH</i>)	Pol12	3Myc C	Co-expression with Pol1-CTD
	Dpb2	3Myc C	Co-expression with Pol2-CTD
	Pol31	none	Co-expression with Pol3-CTD
	Rev7	3Myc C	Co-expression with Rev3-CTD
pASK-IBA43plus (<i>TET</i>)	Pol1-CTD	Strep C	Protein expression in <i>E.coli</i>
	Pol2-CTD	Strep C	Protein expression in <i>E.coli</i>
	Pol3-CTD	Strep C	Protein expression in <i>E.coli</i>
	Rev3-CTD	Strep C	Protein expression in <i>E.coli</i>
pBL335 (<i>Gal1-10</i>)	GST-Pol3	GST N	Protein expression in yeast
pBL341 (<i>Gal1-10</i>)	Pol31 and Pol32	none	Protein expression in yeast
pBL322 (<i>ADH</i>)	Pol3 (mutants)	LexA _{DBD} N	Two-hybrid analysis
pBL364 (<i>ADH</i>)	Pol31	<i>GAL4</i> _{AD} N	Two-hybrid analysis

Abbreviations: N, N-terminal; C, C-terminal; LexA_{DBD}, bacterial LexA DNA-binding domain; *GAL4*_{AD}, yeast *GAL4* activating domain. ΔMTS-Nfs1 is Nfs1 lacking amino acids 1-94¹.

Supplementary Methods

Yeast strains and genetic manipulation. Cassettes for the introduction of promoter sequences were amplified from pFA6a-HIS3MX6-Gal1-10⁷, pYM-N23 or pYM-N27 templates⁶. pYM19 or pYM21 were used as template for C-terminal fusion of polymerase proteins with a nona-Myc tag sequence⁶. For these strains constructs the endogenous promoters remained unchanged. Exchange of the endogenous promoter for the *Gall* promoter with concomitant introduction of an N-terminal triple HA epitope tag for the construction of the Gall-HA-Pri2 strain was achieved with the pYM-N28 template⁶. Primers contained 20 nucleotides of the template plasmid and 50 nucleotides corresponding to the relevant genomic region used for homologous recombination. Gall-HA-Pri2 was converted to a strain with N-terminally tagged Pri2 under control of its natural promoter by homologous recombination and selection on glucose supplemented medium⁸. The fragment for recombination was obtained by PCR amplification of wild-type DNA with a promoter primer and the reverse complement of the 20 nucleotides directly 5' of the start ATG and 50 nucleotides encoding the HA tag. A complete list of strains and plasmids is presented in Supplementary Tables 1 and 2, respectively. Cells were grown in rich (YP) or minimal (SC) media at 30°C, containing the required carbon sources at a concentration of 2 % (w/v) and appropriate auxotrophic markers⁹.

Cloning and cysteine mutagenesis of polymerase CTDs. A PCR fragment from pYM-N28⁶ encoding an N-terminal triple HA tag was amplified with primers which added XbaI and SpeI restriction sites. The cut fragment was cloned into an XbaI-digested p416 plasmid with *Met25* promoter. Sequencing identified a clone with the correct orientation (p416-Met25-3HA). The coding regions of the CTDs of Pol3 (amino acids 982-1097), Rev3 (amino acids 1374-1504) Pol1, (amino acids 1262-1468) and Pol2 (amino acids 2084-2222) were PCR amplified from yeast chromosomal DNA with primers adding SpeI

(all) and EcoRI (Pol3 and Rev3) or HindIII (Pol1 and Pol2) restriction sites. After digestion, these fragments were cloned into the corresponding sites of p416-Met25-3HA. Pol3-CTD cysteine mutagenesis (see Supplementary Table 2 for plasmids) was carried out in p416-Met25-3HA-Pol3-CTD as template with primer design as described by Zheng et al.¹⁰. The Watcut tool (<http://watcut.uwaterloo.ca/>) from Michael Palmer (University of Waterloo, Canada) was used to introduce restriction sites with silent mutations. The coding regions of Pol31, Pol12, Dpb2 and Rev7 were PCR amplified from yeast chromosomal DNA with primers adding SpeI (all) and EcoRI (Pol31) or Sall (all other) restriction sites. After digestion, these fragments were cloned into the corresponding sites of p424-TDH (Pol31) or p424-TDH-3Myc (all other). The latter vector was prepared by cloning a fragment which was obtained by PCR amplification with primers adding Sall and XhoI restriction sites to the C-terminal 3Myc encoding region of pYM19⁶ into p424-TDH.

Regions coding for the natural C terminus of the B-family polymerases were cloned into the NheI and NcoI restriction sites of pASK-IBA43-plus after amplification from yeast chromosomal DNA. This vector supplies a C-terminal Strep-tag. The constructs encompassed the following amino acids: Pol1, 1262-1468; Pol2, 2084-2222; Pol3, 982-1097 and Rev3, 1374-1504. All constructs and mutations were confirmed by DNA sequencing.

⁵⁵Fe incorporation into yeast proteins. The yeast strains listed in Supplementary Table 1 were grown in regular SC medium for 24 h, followed by growth in iron-free SC medium for 16 h. Depletion in glucose-containing medium led to less than 11 % decrease in cellular growth (wet cell mass) compared to wild-type cells. After washing with de-ionized water, cells (~0.5 g) were incubated for 2 h with ⁵⁵FeCl₃ in iron-free SC medium. From this point onwards all steps were carried out below 4°C. Cells were collected by centrifugation and resuspended in an equal volume of TNETG buffer [10 mM Tris-

HCl pH 7.4, 150 mM NaCl, 2.5 mM EDTA, 0.5 % (v/v) Triton X-100, 10% (v/v) glycerol] with 2 mM PMSF and complete protease inhibitor tablets (Roche). Disruption of the cells was achieved by vortexing with glass beads in three one-min bursts, alternated with cooling on ice for 1 min. Cell debris were removed by centrifugation (1,500×g, 5 min), followed by clarification of the supernatant by centrifugation at 13,000×g for 12 min. Aliquots of 200 µl were incubated in 1.5 ml vials for 1 h with 20 µl suspension of agarose beads with coupled anti-Myc or anti-HA antibodies (Santa Cruz). After three washes with 0.5 ml TNTEG buffer, the beads were dispersed in 1 ml scintillation fluid and the amount of protein-associated ⁵⁵Fe was measured by scintillation counting (LS 6500, Beckman Coulter Inc.). Presence of tagged proteins and/or depletion of proteins in the cell extracts were confirmed by SDS-PAGE and immunostaining analysis of aliquots taken before immunoprecipitation. Monoclonal antibodies against Myc or HA epitopes were from Santa Cruz. Polyclonal antibodies against yeast Nfs1, Nbp35, Nar1, Porin, Pol31 and Pol32 proteins were raised in rabbits in our laboratories.

Yeast two-hybrid analysis. The interaction of the Pol3-CysB mutants with Pol31 was analyzed by yeast two-hybrid assays carried out in strain L40 (*MATa*, *his3-Δ200*, *trp1-901*, *leu2-3,112*, *ade2*, *LYS2::(lexAop)₄-HIS3*, *URA3::(lexAop)₈-lacZ*) as described before². Pol3-Pol31 interactions were measured using plasmid pBL322 (*LexA_{DBD}-POL3* in 2µ vector pBTM116 with *TRP1* marker) or its corresponding CysA (C1012S, C1027S) or CysB (C1059S, C1074S) mutants, and plasmid pBL364 (*GAL4_{AD}-POL31* in 2µ vector pACT2 with *LEU2* marker). Quantitative β-galactosidase assays were carried out in triplicate and were corrected for the background obtained in absence of the pBL364 plasmid.

Chemical analysis. Non-heme iron bound to protein was determined by colorimetry with the iron chelator Ferene¹¹. Iron in (mutant) yeast Pol δ preparations was determined with the chelator 2-(5-nitro-2-pyridylazo)-5-(*N*-propyl-*N*-sulfopropylamine)phenol (nitro-PAPS)¹². Quantitative release of iron ions from polymerase (25 μ l) was effected by addition of 125 μ l of 7 M guanidine hydrochloride, 0.4 M sodium acetate, 100 mM sodium thioglycolate at pH 4.3. After denaturation 75 μ l water and 25 μ l 1 mM nitro-PAPS were added. Spectra of the samples (200 μ l) were recorded in flat bottom Greiner 96 well microtiter plates. The low pH value, wavelength (690 nm minus background at 900 nm) and presence of thioglycolate eliminated interference of other metal ions.

Acid-labile sulfide content was measured¹¹ by formation of methylene blue (absorbing at 670 nm) from the reaction of *N,N'*-dimethyl-*p*-phenylenediamine with H₂S and excess FeCl₃. Standardization was carried out with freshly purchased Li₂S. This method is highly specific for acid-labile sulfide and does not give a response with commonly encountered sulfur compounds including protein-bound cysteine or methionine¹³. The same method was downscaled 4-fold for determination of S²⁻ in microtiter plates (200 μ l sample volume) and to confirm by visible spectroscopy that methylene blue was produced.

Protein concentrations for assays, Fe/S analysis and calculation of extinction coefficients were determined by the Bradford method, using bovine serum albumin as standard. The protein quantities were insufficient for extensive quantification with quantitative amino acid analysis or the biuret method. Metal and sulfide contents could therefore be influenced by small differences [\sim 20 %]¹⁴ in the relative extent of color development of Pol δ and CTDs in comparison to the bovine serum albumin standard.

Statistical analysis. All quoted values have standard deviations (error bars in figures) calculated for at least three independent experiments. Significant means that values differ from the control or blank according to non-paired Student's t-test ($P < 0.05$).

References

1. Kispal, G., Csere, P., Prohl, C. & Lill, R. The mitochondrial proteins Atm1p and Nfs1p are required for biogenesis of cytosolic Fe/S proteins. *EMBO J.* **18**, 3981-3989 (1999).
2. Gerik, K. J., Li, X., Pautz, A. & Burgers, P. M. Characterization of the two small subunits of *Saccharomyces cerevisiae* DNA polymerase δ . *J. Biol. Chem.* **273**, 19747-19755 (1998).
3. Mühlhoff, U. *et al.* Functional characterization of the eukaryotic cysteine desulfurase Nfs1p from *Saccharomyces cerevisiae*. *J. Biol. Chem.* **279**, 36906-36915 (2004).
4. Hausmann, A. *et al.* The eukaryotic P-loop NTPase Nbp35: An essential component of the cytosolic and nuclear iron-sulfur protein assembly machinery. *Proc. Natl. Acad. Sci. U.S.A.* **102**, 3266-3271 (2005).
5. Balk, J., Pierik, A. J., Netz, D. J. A., Mühlhoff, U. & Lill, R. The hydrogenase-like Nar1p is essential for maturation of cytosolic and nuclear iron-sulphur proteins. *EMBO J.* **23**, 2105-2115 (2004).
6. Janke, C. *et al.* A versatile toolbox for PCR-based tagging of yeast genes: new fluorescent proteins, more markers and promoter substitution cassettes. *Yeast* **21**, 947-962 (2004).
7. Mühlhoff, U., Richhardt, N., Ristow, M., Kispal, G. & Lill, R. The yeast frataxin homologue Yfh1p plays a specific role in the maturation of cellular Fe/S proteins. *Hum. Mol. Genet.* **11**, 2025-2036 (2002).
8. Booher, K. R. & Kaiser, P. A PCR-based strategy to generate yeast strains expressing endogenous levels of amino-terminal epitope-tagged proteins. *Biotechnol. J.* **3**, 524-529 (2008).
9. Sherman, F. Getting started with yeast. *Methods Enzymol.* **350**, 3-41 (2002).
10. Zheng, L., Baumann, U. & Reymond, J. L. An efficient one-step site-directed and site-saturation mutagenesis protocol. *Nucleic Acids Res.* **32**, e115 (2004).
11. Pierik, A. J. *et al.* Redox properties of the iron-sulfur clusters in activated Fe-hydrogenase from *Desulfovibrio vulgaris* (Hildenborough). *Eur. J. Biochem.* **209**, 63-72. (1992).
12. Makino, T., Kiyonaga, M. & Kina, K. A sensitive, direct colorimetric assay of serum iron using the chromogen, nitro-PAPS. *Clin. Chim. Acta* **171**, 19-27 (1988).
13. Rabinowitz, J. C. Analysis of acid-labile sulfide and sulfhydryl groups. *Methods Enzymol.* **53**, 275-277 (1978).
14. Peterson, G. L. Determination of total protein. *Methods Enzymol.* **91**, 95-119 (1983).

CHAPTER IIB

Identification and characterization of PCNA mutants that suppress Pol δ -CysA lethality

**Identification and characterization of PCNA mutants that suppress
Pol δ -CysA lethality**

Joseph L. Stodola, Carrie M. Stith and Peter M. Burgers

Department of Biochemistry and Molecular Biophysics, Washington University School of Medicine,
St. Louis, Missouri 63110, USA

ABSTRACT

In budding yeast, DNA polymerase delta (Pol δ) is responsible for elongation and maturation of Okazaki fragments on the lagging strand of the replication fork. The C-terminal domain of Pol3, the catalytic subunit of Pol δ , contains two metal ion centers necessary for interaction with the Pol δ accessory subunits and the processivity clamp PCNA. One of these, the CysA Zn-ribbon motif, is required for PCNA-dependent processivity. A *pol3-cysA* mutation is lethal in budding yeast. We have identified two PCNA mutants that suppress *-cysA* lethality. Following is a characterization of the genetic and biochemical activities of these two suppressor mutants.

INTRODUCTION

In eukaryotes, each of the replicative DNA polymerases are members of the B-family polymerases, classified as such according to the structure of their catalytic domain¹. These polymerases are necessary for replicating the genome during each cell cycle, faithfully transmitting genomic information from the parent to daughter cells. The three B-family DNA polymerases that participate in eukaryotic DNA replication are Pol α , Pol δ , and Pol ϵ ². Current genetic and biochemical evidence supports the following model: the Pol α -primase complex initiates replication on both the leading and lagging strand, in the latter case initiating each of the many Okazaki fragments that are extended on the lagging strand. The majority of the DNA synthesis is performed by Pol ϵ and Pol δ , replicating on the leading and lagging strands, respectively^{3,4}.

B-family DNA polymerases are found in bacteria, archaea, and in both bacterial and eukaryotic DNA-based viruses, in addition to eukaryotes^{1,5,6}. All B-family enzymes contain three large domains, the classical polymerase domain, the 3'-5' exonuclease domain (which is present but not active in all members), and an N-terminal domain (NTD) of currently unknown function. What separates the eukaryotic B-family polymerases from others is their formation of multi-subunit polymerase complexes, consisting of a single polymerase subunit and additional accessory subunits. The eukaryotic B-family polymerases contain an additional, small C-terminal domain (CTD) within the polymerase subunit that mediates interactions with these accessory subunits.

The CTDs of the eukaryotic enzymes are highly conserved in sequence, suggesting a common structure. The crystal structure of the CTD from Pol α shows an elongated, bilobal form, in which the two lobes are connected by a three-helix bundle⁷. Each lobe contains four conserved cysteines. In all four polymerases, the N-terminal 4-cysteine lobe binds zinc, while the C-terminal 4-cysteine lobe has been proposed to ligand an iron-sulfur cluster in the $[4\text{Fe-4S}]^{2+}$ coordination state. The CTDs are responsible for binding the accessory subunits of the multi-subunit DNA polymerase.

How the metal-ion binding motifs in the CTDs affect polymerase function is best understood in the case of the *S. cerevisiae* DNA polymerase δ . In this polymerase, the N-terminal 4-cysteine lobe (binding zinc) has been termed the CysA motif, and the C-terminal 4-cysteine lobe (binding an iron-sulfur cluster) has been termed the CysB motif. This polymerase complex consists of the catalytic subunit Pol3 and the accessory subunits Pol31 and Pol32. Interactions between Pol3 and the second subunit Pol31 occur through the Pol3 CTD and require an intact iron-sulfur cluster in the CysB position. Pol31 then binds the third subunit, Pol32, to form the complete heterotrimeric polymerase complex⁸.

The second, zinc-containing, CysA influences the processivity of the Pol δ holoenzyme. Pol δ alone is a low-processivity enzyme, replicating only a few nucleotides before dissociating from DNA. This is overcome through interactions between Pol δ and the replication clamp proliferating cell nuclear antigen (PCNA). This donut-shaped, homotrimeric protein is loaded onto DNA primer-termini by the ATP-dependent Replication Factor C (RFC) complex^{9,10}. When loaded, PCNA localizes Pol δ to DNA and increases the processivity of the enzyme so that it can replicate hundreds of nucleotides in a single DNA-binding event. Pol δ contains PCNA-binding motifs in each of its three subunits^{8,11,12}. Within Pol3, functional interaction with PCNA is dependent on an intact zinc-binding motif within the Pol3-CTD, in the CysA position. Inability to coordinate metal binding in this position is synthetically lethal in yeast, and this polymerase exhibits defects in PCNA-mediated replication *in vitro*⁸. Taken together, we hypothesize that the CysA mutant defect in processive DNA replication leads to incomplete replication on the lagging strand to a degree that cannot be tolerated by the cell.

This work provided a link between the integrity of the CysA zinc-ribbon motif and the ability of Pol δ to processively replicate. We wanted to use this observation to better understand the complex interactions that exist between Pol δ and PCNA. With this aim, we sought to identify PCNA mutants that suppress the synthetic lethality of *pol3-CysA*. We hypothesized that such mutants may directly modulate the biochemical activity of Pol δ -CysA. In a genetic screen, we identified two PCNA mutants capable of suppressing CysA mutation lethality. However, these mutants do not appear to act via the mechanism originally hypothesized. While the detailed mechanism concerning how these mutants work to suppress CysA lethality still remains unknown, these mutants could provide a tool to investigate how PCNA coordinates the general response to inefficient replication and replication stress.

RESULTS

Identification and characterization of PCNA suppressors of Pol δ -Cys A lethality

The Zn-ribbon functional group located in the CysA motif of the Pol3 C-terminal domain (CTD) is required for functional interactions between the Pol δ holoenzyme and the PCNA sliding clamp. When Pol3 contains mutations in just two of the four cysteines that make up the CysA motif, C1012S and C1027S, an *in vitro* PCNA-dependent processivity defect is observed⁸. Additionally, these mutations are synthetically lethal in *Saccharomyces cerevisiae*, presumably due to difficulties in completing DNA replication mediated by PCNA. The polymerase complex containing these two mutations will be referred to as Pol δ -CysA. We predict that these two mutations abrogate zinc binding, although this has not been shown directly.

As the Pol δ -CysA complex exhibits defects in PCNA-mediated replication likely due to disrupted interactions between polymerase and PCNA, we hypothesized that these interactions could possibly be restored with specific mutations within PCNA. We therefore tested whether mutations in *POL30*, encoding PCNA, might result in amelioration of the binding defect, suppressing *pol3-CysA* lethality. A yeast strain heterozygous for *POL3/pol3-CysA* was transformed with a heavily mutagenized *POL30* library. Transformants were plated onto media containing 5-FOA, which evicted the wild-type *POL3* plasmid, enforcing viability of the *pol3-CysA* mutant for cell growth. All colonies containing potential suppressors were also screened for sensitivity to the replication stress-inducing reagent hydroxyurea; we hypothesized that even with a PCNA suppressor, CysA-containing cells would still be sensitive to replication stress. From this screen we identified two PCNA suppressor mutants that showed equally robust growth, termed *pol30-sup1* and *pol30-sup2*.

The *-sup1* and *-sup2* genes contain three and five mutations, respectively (**Fig. 1a**). They do not share any mutations, and do not cluster in a specific region of the PCNA structure. We first sought to determine which of the mutations in each suppressor were necessary, and which combinations were sufficient for the phenotype. The same 5-FOA plasmid eviction technique was used to assay different combinations of suppressor mutations; cells were plated in serial dilutions to visualize growth differences. To determine which residue changes were required for the suppression phenotype, each mutation position was changed from the isolated suppressor sequence to that of wild-type PCNA, which we term reversion mutations (**Fig. 1b**). In a reciprocal experiment, we added the suppressor mutations individually to wild-type PCNA to identify combinations that were sufficient for suppression (**Fig. 1c**).

We started with an investigation of *pol30-sup1*, which contains three deviations from the wild-type sequence, F28L, M119I, and D240A. We observe that only the M119I mutation is absolutely required for suppression. Reversion of D240A and F28L exhibit partially suppression phenotypes (**Fig. 1b**). Interestingly, adding only the M119I mutation to PCNA yields only slight suppression. Consistent with the reversion mutation data, the M119I/D240A double mutant suppresses almost to *-sup1* levels, while the F28L/M119I still shows weak growth (**Fig. 1c**). From these data, we infer that the hierarchy of mutations in *pol30-sup1* is M119I>D240A>F28L.

The situation with *pol30-sup2* is somewhat more complex, stemming from the presence of two additional suppressor mutations. The five *-sup2* mutations are V40I, F57I, E165G, K196E, and F207I. As with *-sup1*, the reversion mutations show that one residue change in *-sup2* is absolutely required, in this case V40I. All other single reversions yield intermediate suppression, with the F207I reversion

showing less cell growth than the three remaining mutations (**Fig. 1b**). However, neither of these mutations individually or even the V40I/F207I double mutant shows suppression near that of *-sup2* containing all five mutations. It appears that at least one more mutation is needed to gain appreciable, if not full, suppression of CysA lethality; introduction of F57I, E165G, or K196E to the V40I/F207I pair yields equivalent, intermediate levels of cell growth (**Fig. 1c**). Due to the sheer number of combinations that could be constructed between the five mutations, we did not extend our analysis beyond the combination of mutations shown, but it appears to a first approximation that the F57I, E165G, and K196E mutations carry equivalent importance to the suppression phenotype. Thus, the hierarchy of mutations in *pol30-sup2* is V40I>F207I>F57I=E165G=K196E.

***In vitro* characterization of PCNA suppressors**

We hypothesized that *in vivo* suppressors of Pol δ -CysA would restore interactions between the polymerase and PCNA, thereby increasing the efficiency of PCNA-mediated replication. To evaluate this hypothesis, we introduced the suppressor mutations into purified PCNA to perform *in vitro* replication experiments. First, we tested the ability of both wild-type Pol δ and Pol δ -CysA to replicate around a singly-primed, single-stranded DNA circle (**Fig. 2a**). Prior to reaction initiation with polymerase, the DNA was coated with the single-stranded DNA binding protein RPA, and PCNA, PCNA-sup1, or PCNA-sup2 was loaded onto the DNA with RFC and ATP. With wild-type Pol δ replicating with wild-type PCNA, we observe complete replication around the circular DNA even at short time points (lanes 1-3). Replication by wild-type Pol δ is not impaired with *-sup1*, but was slightly impaired with *-sup2* (data not shown). Pol δ -CysA exhibits a PCNA-dependent replication defect, and at low PCNA levels no full-length product is formed in the 8 min assay (lanes 4-6). This defect is partially rescued by increasing the PCNA concentration (50 nM, lanes 7-9). Contrary to our initial hypothesis, neither PCNA-*sup1* nor *-sup2* stimulated Pol δ -CysA to a level greater than that of wild-type PCNA. In fact, even less DNA synthesis was observed when the suppressor mutants were used. This was more pronounced in *-sup2* than with *-sup1*. These *in vitro* results suggest that the PCNA suppressors identified *in vivo* do not act by directly stimulating Pol δ -CysA activity.

With some evidence that the PCNA suppressors do not directly stimulate Pol δ -CysA activity, we used a different assay to further test this conclusion. Nick translation is the process by which Pol δ and FEN1 cooperate to remove the initiator RNA that is found at the 5'-end of each Okazaki fragment. When it reaches a preceding Okazaki fragment, Pol δ displaces the 5'-end of that strand and continues replicating, producing a short flap. This flap is cut by FEN1, removing 1-2 nucleotides and moving the

nick position. The reiterative action of Pol δ performing strand displacement and FEN1 cutting removes all of the initiator RNA so that the resulting DNA nick can be sealed by DNA ligase I. The ability of Pol δ to complete this process is dependent on PCNA, as it stabilizes the polymerase while it performs strand displacement synthesis.

This process can be reconstituted *in vitro* using short oligonucleotide DNA substrates (**Fig. 2b**). In this assay, a 5'-labeled primer is annealed to a template strand to create a template-primer junction to be extended by Pol δ . A second, downstream blocking oligonucleotide is also annealed to the template to simulate the 5'-end of a preceding Okazaki fragment. Biotin-streptavidin linkages are added to both the 5'- and 3'-ends of the template strand in order to facilitate PCNA loading. Prior to reaction initiation with Pol δ , PCNA is loaded onto the template with RFC and ATP, and RPA is added to coat the single-stranded DNA gap between the primer terminus and the blocking oligonucleotide. Following reaction initiation with polymerase, dNTPs, and FEN1, extension of the primer through the gap and up to the block occurs rapidly, with further extension of the primer through the blocking oligonucleotide evidence of coordinated Pol δ -FEN1 action.

Control reactions showed that with each Pol δ /PCNA pair, extension of the primer through the gap and initial flap formation occurred with similar efficiency (-FEN lanes). Even though the Pol δ -CysA enzyme exhibits a processivity defect, this is not a factor on such a short gap (20 nucleotides). When FEN1 was added to reactions containing both wild-type Pol δ and PCNA, full-length product corresponding to full nick translation to the end of the template was observed after 15 seconds. Consistent with the PCNA-dependent processivity defect, the Pol δ -CysA enzyme did not perform nick translation as efficiently as the wild-type polymerase; an appreciable amount of full-length product was observed only after 120 seconds. Consistent with the data in **Fig. 2a**, we observe that nick translation synthesis is still impaired when Pol δ -CysA is paired with *pcna*-*sup1* and *-sup2*. This provides further evidence that the PCNA suppressors identified *in vivo* do not suppress by stimulating Pol δ -CysA activity directly. Different than the replication assay above, measuring replication over kilobases of DNA, we do not observe a defect with *-sup1* or *-sup2* when paired with wild-type Pol δ . This is likely because the length of DNA that needs to be replicated to observe full product formation in the short oligo assay is much shorter than in **Fig. 2a**.

Finally, as a control, we tested whether the defects observed with Pol δ -CysA were indeed a result of compromised interactions with PCNA, rather than any intrinsic defect of the mutant polymerase. We had previously shown this to be the case for nucleotide incorporation in the absence of PCNA⁸, but wanted to show this in the context of strand displacement synthesis and nick translation.

Strand displacement and nick translation assays were performed on the short oligonucleotide DNA substrate as described above (**Fig. 2b**), but now in the absence of PCNA (**Fig. 2c**). As Pol δ dissociates frequently from DNA intermediates under these conditions, these processes occur on a much slower timescale. However, for both strand displacement synthesis and nick translation, we observe no difference in the activities of wild-type Pol δ and Pol δ -CysA, showing that indeed the source of the *in vitro* Pol δ -CysA defects is diminished interactions with PCNA and not an intrinsic polymerase defect.

PCNA suppressors can act as sole source of PCNA *in vivo*

Due to the unexpected results from the *in vitro* studies, we returned to genetic studies to learn more about how these mutants work *in vivo* (**Fig. 3**). Due to the difficulty in constructing yeast strains that contain chromosomal deletions for two essential genes, like *POL3* and *POL30* here, strains in the previously described genetic studies were heterozygous for *POL30*, with the wild-type gene on the chromosome and the various mutant constructs on a plasmid. Because of this, the previous experiments did not indicate whether cells could tolerate the suppressor mutants as the sole source of PCNA. A heterozygous *POL30/pol30-suppressor* strain was plated onto 5-FOA containing media to evict the plasmid containing *POL30*. It is important to note that this experiment does not involve any polymerase mutations; the strain contained only wild-type *POL3*. Both suppressors (and various subsets of the suppressor mutations) were able to serve as the sole source of PCNA, and grew at wild-type levels on rich media.

Next, the cells expressing only the suppressor PCNAs were irradiated with DNA-damaging UV light or treated with the replication inhibitor hydroxyurea (HU). As a control, *pcna-79* was included; this gene contains two mutations (L126A, I128A) within the inter-domain connection loop (IDCL) of PCNA, which significantly diminishes binding of proteins containing a consensus PCNA-binding motif. These mutations are known to confer UV and HU sensitivity. The *pol30-sup1* and *-sup2* alleles showed only slight sensitivity over wild-type *POL30* to HU. This sensitivity was less than observed with *pol30-79*, from which we conclude that the presence of the suppressor mutations do not substantially alter the cellular response to replication stress.

The response to UV-irradiation differs from that to HU. Both suppressors are highly sensitive to UV as compared to wild-type *POL30*, and are also more sensitive than the *pol30-79* mutant. Interestingly, we observe different amounts of growth in cells expressing different subsets of the PCNA suppressor mutations. The *-sup1* and *-sup2* mutants containing the full complement of mutations, three and five, respectively, are the most sensitive to irradiation. The sensitivity of the other

mutants appears to be inversely related to how well a given mutant suppresses *-CysA* lethality (**Fig. 1**). For example, with *-sup1*, the *-F28L,M119I* mutant that barely suppresses *-CysA* is not sensitive to UV as compared to wild-type. The *-M119I,D240A* mutant that shows an intermediate suppression phenotype shows an intermediate sensitivity to UV. Comparing the data in **Fig. 1** and **Fig. 3** for *-sup2*, we observe the same phenomenon; mutants that suppress *-CysA* lethality more extensively are more sensitive to UV when serving as sole source of PCNA. The implications of this result will be discussed below.

Discussion and Future Directions

Using a genetic screen, we identified two independent PCNA mutants that suppressed the inviability of cells solely expressing *pol3-CysA*. Both suppressor mutants contained multiple mutations spread across the PCNA structure. Analysis of the individual mutations revealed that each suppressor required multiple mutations for the phenotype, and that intermediate phenotypes are observed if only a subset of the identified mutations were present.

We sought to identify genetic suppressors of *pol3-CysA* because we hypothesized that such mutants would provide a greater understanding of how PCNA interacts with the CysA motif region in Pol3, under wild-type circumstances. However, such a hypothesis was based on the assumption that any isolated PCNA suppressor mutants would directly stimulate the activity of Pol δ -CysA to a greater degree than wild-type PCNA. However, this is not what we observe in several *in vitro* replication assays (**Fig. 2**), and the mechanism of suppression used by *pol30-sup1* and *-sup2* remains unresolved.

Given that the suppressors do not directly stimulate Pol δ -CysA activity, we now hypothesize that they suppress *pol3-CysA* lethality by modulating some unidentified pathway that enables a greater tolerance of replication stress. We believe that *-sup1* and *-sup2* are gain-of-function mutants, with suppressor mutations possibly conferring greater affinity for a specific binding partner. We come to this view because we originally identified the suppressors in a strain that is heterozygous for wild-type *POL30* and suppressor *pol30*. If the mutations were loss-of-function mutants, the wild-type PCNA still present would likely substitute for any potential lost activity.

But what specific PCNA client-protein interaction could lead to the suppression phenotype? Several possibilities will be discussed here. Post-translational modifications have been shown to be important in the response to replication stress. PCNA can be modified with both ubiquitin and the related protein SUMO, and both modifications modulate the cellular response to replication stress. I will first consider ubiquitination. The major PCNA residue modified with ubiquitin is K164.

Monoubiquitination of this residue leads to polymerase switching from a replicative polymerase to a translesion polymerase when the replisome encounters a DNA lesion. This mechanism of bypass is error-prone because the translesion polymerases have a low fidelity. Polyubiquitination of the same lysine is linked to error-free bypass mechanisms. Specifically how this occurs remains unresolved; it is hypothesized that polyubiquitination disrupts the replisome in some manner, allowing for either template switching or replication restart following re-priming on the blocked strand^{13,14}.

These pathways are good candidates for future study because of the modification site, K164. In *-sup2* most notably, residues involved in suppression (like E165G and K196E) are located adjacent to the ubiquitination site. Since Pol δ -CysA exhibits a processivity defect, it could lead to fork stalling and incomplete replication *in vivo*, requiring fork restoration mechanisms. Thus, it may be more likely that the PCNA suppressors modulate the polyubiquitination pathway, up-regulating the template-switching or replication restart mechanism. This could be addressed by directly examining the type of PCNA modifications present in cells expressing the PCNA suppressors, and their levels. Additionally, if modulation of PCNA modification were indeed linked to the suppression phenotype, we would hypothesize that particular enzymes required for PCNA modification would also be required for suppression. The group of enzymes involved in PCNA ubiquitination is collectively known as the *RAD6* pathway. Deleting genes from this pathway may prevent suppression if these modifications are indeed required. Additionally, this hypothesis may be consistent with the increased UV sensitivity observed with the PCNA suppressors (**Fig. 3**). If the suppressor mutations lead to an accumulation of a particular PCNA modification (like polyubiquitination), this may come with the consequence that other pathways are down-regulated, like the PCNA monoubiquitination that would aid in bypass of UV-induced lesions.

PCNA can also be modified with SUMO, on both K164 and K127. Sumoylation of PCNA recruits the anti-recombination helicase Srs2. Reviving stalled replication forks by recombination can be disadvantageous for cells because it leads to deleterious gross chromosomal rearrangements in some circumstances. By resolving recombination structures before the process is complete, Srs2 prevents these potentially dangerous rearrangements from occurring. Once again, it is likely that Pol δ -CysA causes replication stalling, and these collapsed forks could lead to ill-advised recombination. If such events cause the lethality of *-CysA* cells, up-regulation of PCNA sumoylation and subsequent Srs2 recruitment could yield the suppression phenotype.

Because of the sheer number of PCNA interacting proteins, it is possible that the pathways discussed above are not involved in the *-cysA* suppression mechanism. A more wide-ranging approach

to the problem would be to generally examine what is occurring in the cells growing in the presence of Pol δ -CysA and the PCNA suppressors. Possible avenues for examination include: levels of activation of the replication stress checkpoint, examining the rate of spontaneous mutagenesis (would indicate whether translesion polymerases are implicated), or measuring the rate of recombination and/or genomic rearrangements. Such assays may provide a better indication of which genome maintenance pathway is involved in suppression, thus allowing a more informed view of which specific PCNA-binding protein(s) lead to this phenotype.

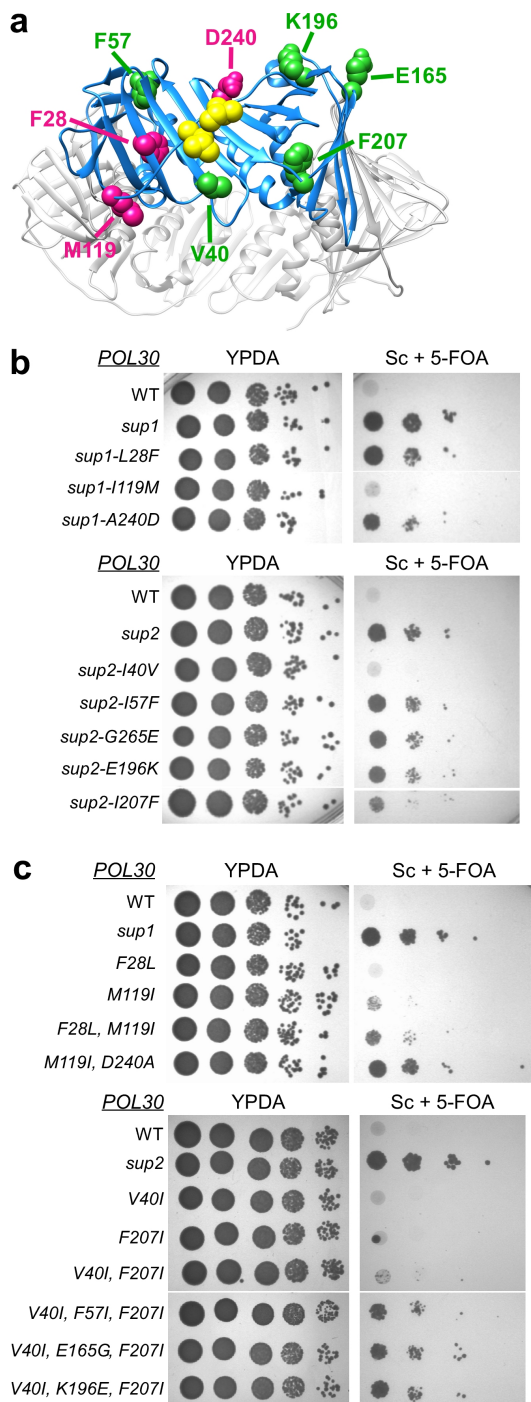


Figure 1. Identification and characterization of PCNA suppressors. (a) Positions of suppressor mutations on PCNA structure (PDB ID:1PLR)⁹. Residues colored magenta belong to *pcna-sup1*, and those in green belong to *pcna-sup2*. For reference, two residues within the Inter-domain connection loop are colored yellow (L126A, I128A); this is where PIP-box containing proteins bind PCNA. (b,c) Serial ten-fold dilutions of a *pol3Δ* strain containing three plasmids: 1, pBL304 (*URA3, POL3*); 2, pBL309-CysA (*TRP1, pol3-cysA*); 3, pBL249 (*LEU2, POL30, pol30-sup1, pol30-sup2* or subsets of mutations). Growth on FOA indicates that *pol3-cysA* supports growth, but only when appropriate *POL30* suppressors are present. In b, reversion mutations are shown, starting with the full complement of mutations and reverting them to wild-type individually. In c, forward mutations in *POL30* are shown.

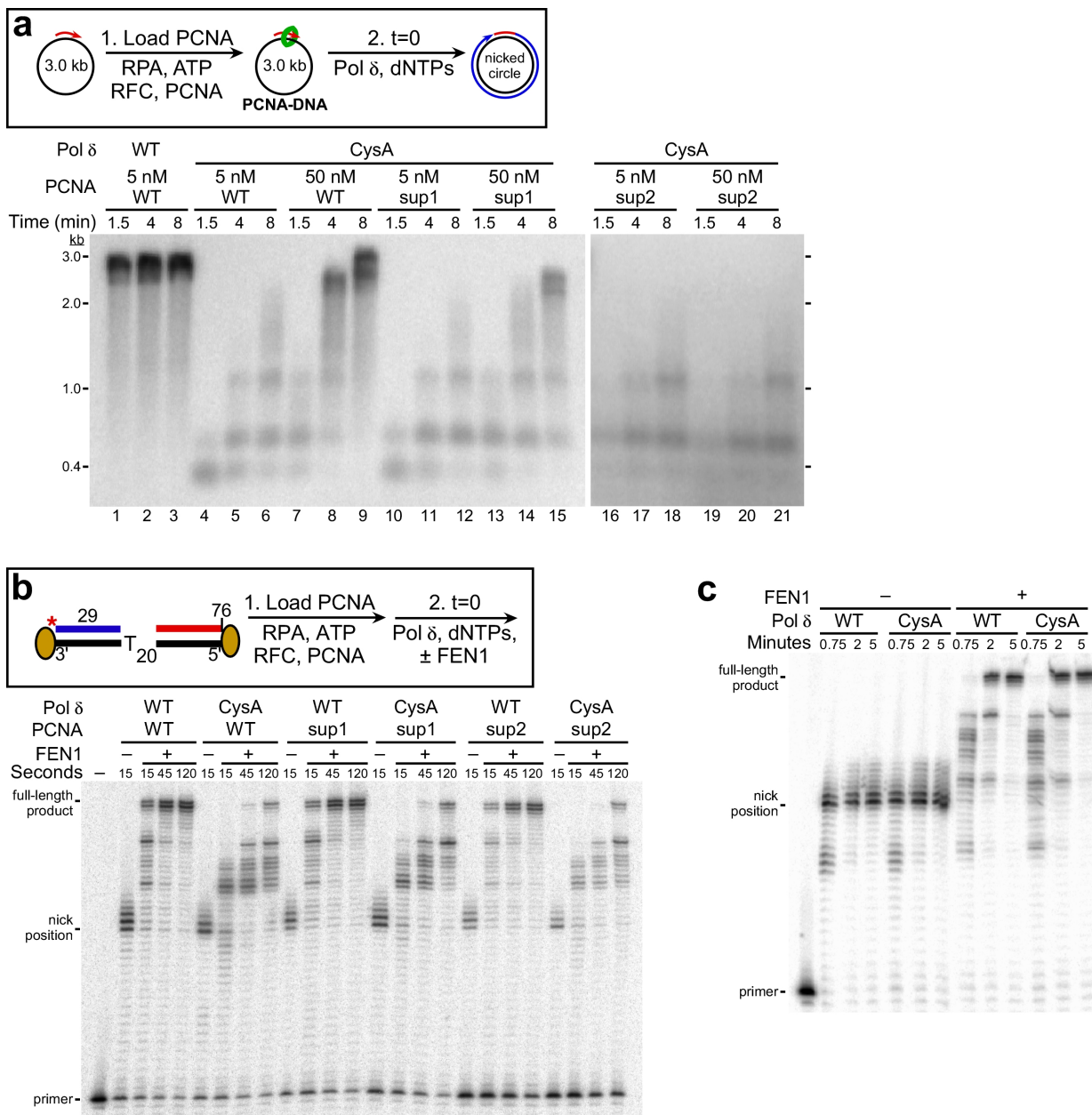


Fig. 2. Biochemical characterization of PCNA suppressors. (a) Alkaline agarose gel electrophoresis of replication products generated with purified proteins as indicated. Single primed mp18 DNA was coated with RPA; 5 or 50 nM PCNA, pcna-sup1, or pcna-sup2 was loaded with RFC and ATP. Reactions were initiated by addition of 12 nM Pol δ or Pol δ -CysA together with dNTPs. Size markers are indicated on left. (b) Urea-PAGE analysis of nick translation assays performed on an oligonucleotide substrate. A 5'-labeled primer and blocking oligonucleotide simulating an Okazaki fragment were annealed to a template oligo, leaving a 20 nucleotide gap. The template was coated with RPA and PCNA was loaded with RFC and ATP. Reactions were initiated with Pol δ or Pol δ -CysA with or without FEN1. The unextended primer, nick position (showing extension through the gap), and fully extended product to the end of the template are denoted on left. (c) Urea-PAGE analysis of strand displacement and nick translation products. Reactions were performed as in b but in the absence of PCNA, RFC, and ATP.

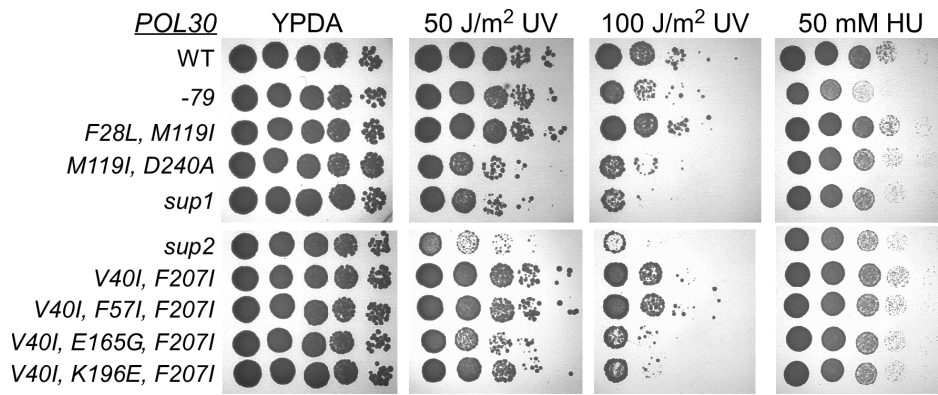


Fig. 3. PCNA suppressor mutants can serve as sole source of PCNA. Serial ten-fold dilutions of a *pol30Δ* strain containing pBL249 (*LEU2*, *POL30*, *pol30-sup1*, or *pol30-sup2*, or a subset of mutations). Cells were plated after treatment with 5-FOA to evict a plasmid encoding wild-type *POL30*. They were either plated on rich media (YPDA) with or without UV irradiation, or onto YPDA containing 50 mM HU.

EXPERIMENTAL PROCEDURES

Proteins: RPA¹⁵, PCNA and suppressor mutants¹⁶, RFC¹⁷, and FEN1¹⁸ were purified from *E. coli* overexpression systems, while Pol δ and Pol δ -CysA were purified from yeast overexpression systems¹⁹.

Single-stranded DNA replication assays: Assays contained 20 mM Tris-HCl pH 7.8, 1 mM DTT, 100 mg/ml bovine serum albumin, 8 mM magnesium acetate, 0.5 mM ATP, 100 mM each of dCTP, dATP, and dTTP, 10 mM of [α -³²P]dGTP, 100 mM NaCl, 1.5 nM singly-primed SKII DNA, 150 nM RPA, and 5 or 50 nM of PCNA or suppressor PCNA. PCNA was loaded onto the primed DNA by incubation with 5 nM RFC at 30 °C for 1.5 min prior to reaction initiation. Reactions were initiated by addition of 12 nM Pol δ or Pol δ -CysA. Aliquots were taken at various time points and stopped with 50 mM EDTA and 0.2% SDS, final concentration. Reactions were resolved on a 0.8% alkaline agarose gel. Gels were dried and documented by PhosphorImager analysis (GE Healthcare).

Oligonucleotide DNA templates: All oligos were ordered from Integrated DNA Technologies, either HPLC or PAGE purified. Template for biochemical experiments was made by annealing primer and block to template in 0.9:1:3, primer:template:block ratio. Annealing was performed in 100 mM NaCl by heating oligonucleotides to 80 °C and cooling slowly to room temperature. Primer was labeled at the 5'-end with ³²P- γ -ATP by Polynucleotide Kinase (New England Biolabs) for visualization. After hybridization, streptavidin was added in 2-fold molar excess to template- primer substrates. DNA concentrations in replication assays were calculated according to the labeled oligonucleotide concentration. Template strands contained 5'- and 3'-biotins so that there were biotin- streptavidin linkages at both ends of the template.

2BioV25-Template	5'-Biotin-TTC CTT CAA CCA GCT TAC CTT CTT CCT TTT TTT TTT TTT TTT TTT TGG TTA CCT TCA ATG TCA TGC TCG CGC TGA-Biotin-3'
PriC25-Primer	5'-TCA GCG CGA GCA TGA CAT TGA AGG TAA CC-3'
BloC25-Block	5'-Phos-rGrGrA rArGrA rArGG TAA GCT GGT TGA AGG A-3'

Strand displacement and nick translation assays: Replication experiments were performed in a buffer containing 20 mM Tris-HCl pH 7.8, 1 mM Dithiothreitol, 200 μ g/ml bovine serum albumin, 8 mM Mg(OAc)₂, and 100 mM NaCl. Reaction conditions were: 5 nM DNA template, 12.5 nM PCNA or suppressor mutant, 10 nM RPA, 5 nM RFC, 500 μ M ATP, 25 nM Pol δ or Pol δ -CysA, 40 nM FEN1, and 100 μ M each dNTP. Templates were loaded with PCNA by RFC and ATP for 60 second prior to reaction initiation with polymerase, dNTPs, and FEN1 (where applicable). Reactions were quenched with an equal volume of 50 mM EDTA and 0.2% SDS, final concentration. DNA products were resolved with 12% denaturing acrylamide gels. Gels were dried after running and subjected to PhosphorImager analysis.

Suppressor Screen: To create the library of random PCNA mutants, the coding region of pBL249 (*LEU2 POL30*) was amplified under mutagenic conditions, as previously described²⁰. The resulting mixture of mutants was ligated back into pBL249. The resulting library was transformed into py227 [*a, arg4-17, his3D-1, leu2-3,112, trp1, ura3-52, pol3D::KANMX4, +pBL304 (POL3 URA3)*], also containing pBL335-CysA (*TRP1 pol3-cysA*). Approximately 5x10⁸ cells were transformed with 15-20 mg of plasmid DNA; cells were divided over approximately ten plates (sc-Leu +5-FOA) to evict the pBL304 plasmid and enforce viability with *pol3-cysA* and *pol30* suppressors. Cells were replica-plated again onto sc-Leu +5-FOA to screen for false positives. Positive colonies were plated onto YPDA+150mM hydroxyurea (HU) and compared to wild-type cells. Only colonies sensitive to HU were used for further analysis. Following validation, pBL249 from suppressor colonies was extracted and sequenced to determine suppressor mutations.

REFERENCES

1. Doublié, S. & Zahn, K. E. Structural insights into eukaryotic DNA replication. *Front Microbiol* **5**, 444 (2014).
2. Johansson, E. & Dixon, N. Replicative DNA polymerases. *Cold Spring Harb Perspect Biol* **5**, a012799–a012799 (2013).
3. Burgers, P. M. J. Polymerase dynamics at the eukaryotic DNA replication fork. *J. Biol. Chem.* **284**, 4041–4045 (2009).
4. Nick McElhinny, S. A., Gordenin, D. A., Stith, C. M., Burgers, P. M. J. & Kunkel, T. A. Division of labor at the eukaryotic replication fork. *Mol. Cell* **30**, 137–144 (2008).
5. Filée, J., Forterre, P., Sen-Lin, T. & Laurent, J. Evolution of DNA polymerase families: evidences for multiple gene exchange between cellular and viral proteins. *J. Mol. Evol.* **54**, 763–773 (2002).
6. Ito, J. & Braithwaite, D. K. Compilation and alignment of DNA polymerase sequences. *Nucleic Acids Res.* **19**, 4045–4057 (1991).
7. Klinge, S., Núñez-Ramírez, R., Llorca, O. & Pellegrini, L. 3D architecture of DNA Pol alpha reveals the functional core of multi-subunit replicative polymerases. *EMBO J.* **28**, 1978–1987 (2009).
8. Netz, D. J. A. *et al.* Eukaryotic DNA polymerases require an iron-sulfur cluster for the formation of active complexes. *Nat. Chem. Biol.* **8**, 125–132 (2012).
9. Krishna, T. S., Kong, X. P., Gary, S., Burgers, P. M. & Kuriyan, J. Crystal structure of the eukaryotic DNA polymerase processivity factor PCNA. *Cell* **79**, 1233–1243 (1994).
10. Majka, J. & Burgers, P. M. J. The PCNA-RFC families of DNA clamps and clamp loaders. *Prog. Nucleic Acid Res. Mol. Biol.* **78**, 227–260 (2004).
11. Acharya, N., Klassen, R., Johnson, R. E., Prakash, L. & Prakash, S. PCNA binding domains in all three subunits of yeast DNA polymerase δ modulate its function in DNA replication. *Proc. Natl. Acad. Sci. U.S.A.* **108**, 17927–17932 (2011).
12. Gerik, K. J., Li, X., Pautz, A. & Burgers, P. M. Characterization of the two small subunits of *Saccharomyces cerevisiae* DNA polymerase delta. *J. Biol. Chem.* **273**, 19747–19755 (1998).
13. Moldovan, G.-L., Pfander, B. & Jentsch, S. PCNA, the maestro of the replication fork. *Cell* **129**, 665–679 (2007).
14. Ulrich, H. D. & Takahashi, T. Readers of PCNA modifications. *Chromosoma* **122**, 259–274 (2013).
15. Henriksen, L. A., Umbricht, C. B. & Wold, M. S. Recombinant replication protein A: expression, complex formation, and functional characterization. *J. Biol. Chem.* **269**, 11121–11132 (1994).
16. Eissenberg, J. C., Ayyagari, R., Gomes, X. V. & Burgers, P. M. Mutations in yeast proliferating cell nuclear antigen define distinct sites for interaction with DNA polymerase delta and DNA polymerase epsilon. *Mol. Cell. Biol.* **17**, 6367–6378 (1997).
17. Gomes, X. V., Gary, S. L. & Burgers, P. M. Overproduction in *Escherichia coli* and characterization of yeast replication factor C lacking the ligase homology domain. *J. Biol. Chem.* **275**, 14541–14549 (2000).
18. Gomes, X. V. & Burgers, P. M. Two modes of FEN1 binding to PCNA regulated by DNA. *EMBO J.* **19**, 3811–3821 (2000).
19. Fortune, J. M., Stith, C. M., Kissling, G. E., Burgers, P. M. J. & Kunkel, T. A. RPA and PCNA suppress formation of large deletion errors by yeast DNA polymerase delta. *Nucleic Acids Res.* **34**, 4335–4341 (2006).
20. Cadwell, R. C. & Joyce, G. F. Mutagenic PCR. *PCR Methods Appl.* **3**, S136–40 (1994).

CHAPTER III

A four-subunit DNA polymerase ζ complex containing Pol δ accessory subunits is essential for PCNA-mediated mutagenesis

PREFACE TO THE CHAPTER

This chapter describes the characterization and functional role of metal binding motifs within the catalytic subunit of the translesion polymerase Pol ζ . Prior to the work described in this chapter, Pol ζ was thought to be a heterodimeric enzyme consisting of a catalytic subunit Rev3 and an accessory subunit Rev7. Rev3 is a B-family polymerase, and contains a metal binding domain like the replicative polymerases Pol δ , ϵ , and α . In these polymerases, the metal binding domain was shown to be involved in subunit-subunit interactions. In Pol ζ , however, the known accessory subunit Rev7 does not interact with the metal binding domain, and it was unclear whether Pol ζ contained additional subunits *in vivo*.

First, we showed that Pol ζ does indeed contain additional constitutive subunits, and exists as a 4-subunit complex. The two previously unrecognized subunits are Pol31 and Pol32, also the accessory subunits of Pol δ . As with Pol δ , Pol ζ contains an Fe-S cluster, required for interactions between Rev3 and Pol31/Pol32. The recognition that the Pol δ accessory subunits were a part of Pol ζ suggested that this enzyme may be stimulated by PCNA in a manner analogous to Pol δ . Indeed, PCNA greatly stimulated the translesion synthesis activity of Pol ζ . Interestingly, this analysis showed that the Zn-binding motif, required for PCNA stimulation in Pol δ , is largely dispensable for PCNA-stimulation of Pol ζ activity, highlighting a difference between the two polymerases.

This chapter was largely the work of a postdoc in the lab, Alena Makarova. My role in this work was to perform *in vitro* DNA replication assays examining the differences between different forms of the Pol ζ enzyme, and investigating PCNA-dependent synthesis by Pol ζ .

A four-subunit DNA polymerase ζ complex containing Pol δ accessory subunits is essential for PCNA-mediated mutagenesis

Alena V. Makarova, Joseph L. Stodola and Peter M. Burgers*

Department of Biochemistry and Molecular Biophysics, Washington University School of Medicine, St. Louis, MO 63110, USA

Received August 30, 2012; Revised and Accepted September 19, 2012

ABSTRACT

DNA polymerase ζ (Pol ζ) plays a key role in DNA translesion synthesis (TLS) and mutagenesis in eukaryotes. Previously, a two-subunit Rev3–Rev7 complex had been identified as the minimal assembly required for catalytic activity *in vitro*. Herein, we show that *Saccharomyces cerevisiae* Pol ζ binds to the Pol31 and Pol32 subunits of Pol δ , forming a four-subunit Pol ζ_4 complex (Rev3–Rev7–Pol31–Pol32). A [4Fe-4S] cluster in Rev3 is essential for the formation of Pol ζ_4 and damage-induced mutagenesis. Pol32 is indispensable for complex formation, providing an explanation for the long-standing observation that *pol32 Δ* strains are defective for mutagenesis. The Pol31 and Pol32 subunits are also required for proliferating cell nuclear antigen (PCNA)-dependent TLS by Pol ζ as Pol ζ_2 lacks functional interactions with PCNA. Mutation of the C-terminal PCNA-interaction motif in Pol32 attenuates PCNA-dependent TLS *in vitro* and mutagenesis *in vivo*. Furthermore, a mutant form of PCNA, encoded by the mutagenesis-defective *pol30-113* mutant, fails to stimulate Pol ζ_4 activity, providing an explanation for the observed mutagenesis phenotype. A stable Pol ζ_4 complex can be identified in all phases of the cell cycle suggesting that this complex is not regulated at the level of protein interactions between Rev3–Rev7 and Pol31–Pol32.

INTRODUCTION

DNA polymerase ζ (Pol ζ) is a B-family DNA polymerase participating in DNA translesion synthesis (TLS) and plays a predominant role in both spontaneous and damage-induced mutagenesis in all eukaryotes (1–3). Pol ζ bypasses a variety of DNA lesions and readily extends

mismatched primer-template termini (4,5). Pol ζ was initially identified as a heterodimeric complex of the catalytic Rev3 subunit with the accessory Rev7 subunit that is also required for DNA polymerase activity (6). Mutations in *REV3* or *REV7* result in a severe decrease of induced mutagenesis. The *rev3 Δ* and *rev7 Δ* strains are also spontaneous antimutators, suggesting that Pol ζ acts to bypass naturally occurring damage or other structural blocks (7–9). Deficiency in the Rev3 catalytic subunit leads to embryonic lethality in mice (10). In humans, alterations in Pol ζ expression are associated with cancer, chromosome instability and cisplatin resistance (11).

All four eukaryotic B-family DNA polymerases, Pol α , δ , ϵ , and ζ , contain two conserved cysteine-rich metal-binding motifs, CysA and CysB, in the C-terminal domain (CTD) of their catalytic subunits [reviewed in (12,13)]. The four cysteine residues of CysA form a classical zinc ribbon motif. In the case of Pol δ , where the role of both CysA and CysB in metal binding has been studied most extensively, the four-cysteine motif of CysB coordinates a [4Fe-4S]²⁺ cluster (14). However, the other catalytic subunits have also been shown to bind [4Fe-4S] clusters. Indeed, expression of the CTD of Rev3 in *Escherichia coli* also indicated the presence of a [4Fe-4S] cluster in this domain (14). In Pol δ , the [Fe-S] cluster is required for stable binding of Pol3 to its second subunit Pol31 (14,15), which in turn binds to Pol32 (16–18). The CysB motif of the catalytic subunit of Pol α also coordinates interactions with its second subunit (19,20). Therefore, an arrangement analogous to that determined for Pol δ may also hold for Pol α and for Pol ϵ .

In contrast to the three replicative DNA polymerases, interactions between the Rev7 subunit of Pol ζ with the catalytic subunit Rev3 have been mapped to the N-terminal region of human Rev3 rather than its CTD (6,21). The possibility then exists that the [4Fe-4S]-containing CTD of Rev3 might provide interactions with other factors that function in mutagenesis. Indeed, two recent articles report on the interaction between Rev3 and Pol31. One interaction study was carried out in

*To whom correspondence should be addressed. Tel: +1 314 362 3872; Fax: +1 314 362 7183; Email: burgers@biochem.wustl.edu

E. coli with the critical CTD of Rev3 (22), whereas the second study reported the purification of a four-subunit Pol ζ complex from yeast (23). Herein, we also report on the isolation and functional characterization of a four-subunit Pol ζ enzyme (Pol ζ_4) and extend these previous studies by showing that the novel interactions with Pol31 and Pol32 are essential for proliferating cell nuclear antigen (PCNA)-mediated TLS. Mutation of the PCNA-binding domain (PIP) of Pol32 attenuates TLS, in accordance with a decrease in mutagenesis in the *pol32- Δ PIP* mutant (24). Furthermore, deletion of the non-essential *POL32* gene results in a failure to form a complex of Pol31 with Rev3–Rev7, suggesting a logical explanation for the mutagenesis defect of *pol32 Δ* mutants (16). Altogether our data suggest that the formation of Pol ζ_4 complex is critical for the TLS function of Pol ζ *in vitro* and *in vivo*.

MATERIALS AND METHODS

Strains and plasmids

All yeast strains are listed in Supplementary Data. Plasmids are listed in Supplementary Table S1.

Enzymes

Saccharomyces cerevisiae Pol δ was expressed in yeast and purified as described previously (25). The replication protein A (RPA), replication factor C (RFC), PCNA and pcna-113 of *Saccharomyces cerevisiae* were expressed and purified from *E. coli* (26,27). Pol ζ_4 (Rev3–Rev7–Pol31–Pol32), Pol ζ_2 (Rev3–Rev7) and their mutant forms were produced in protease-defective strain FM113 or in *pol32 Δ* derivative strain PY117, or in *rev1 Δ* strain PY201, and purified as described previously with several modifications (28). The detailed protocol is described in Supplementary Data.

Yeast two-hybrid analysis

Indicator strain PJ69-4A was co-transformed with plasmids containing *REV3-GAL4* DNA BD fusion genes (pBL816, pBL816A and pBL816B), and plasmids encoding for *REV7* (pBL817), *POL31* (pBL364) and *POL32* (pBL391) fused to *GAL4* activation domain (AD) or with empty vector pACT2. Transformants were grown on -His plates for 5 days to score protein–protein interactions as growth.

GST-pull down

Yeast cells transformed by plasmids encoding for *GST-REV3*, *REV7*, *POL31* and *POL32*, all under control of the *GAL1-10* promoter, were grown in 125 ml of selective medium containing 2% raffinose to O.D₆₆₀ = 0.5. Protein expression was induced by 2% galactose, and cells were grown for another 8 hours. Cells were collected, resuspended in lysis buffer (50 mM Hepes (pH 7.4), 200 mM NaCl, 5% glycerol, 1 mM DTT, 0.1% Tween 20, 0.01% NP40, 10 μ M pepstatin A, 10 μ M leupeptin, 2.5 mM benzamidine, 0.5 mM PMSF) and lysed by vortexing with glass beads on ice. Cell lysates

were clarified by centrifugation, and 0.8 ml of yeast extract containing 1 mg of protein was incubated with 40 μ l of glutathione sepharose beads (GE Healthcare) for 1 h. Beads were washed six times with wash buffer (50 mM Hepes (pH 7.4), 800 mM NaCl, 5% glycerol, 1 mM DTT, 0.1% Tween 20, 0.01% NP40, 1 μ M pepstatin A, 0.5 mM PMSF) and boiled for 2 min in 80 μ l of 2 \times sodium dodecyl sulfate (SDS) sample buffer.

Cell cycle analysis and exposure to DNA-damaging agents

Cells containing *GST-REV3* on plasmid pBL813 were grown in 125 ml of selective medium with 2% raffinose to O.D₆₆₀ = 0.5 without galactose induction. They were arrested in G1 phase by α -factor (20 μ g/ml for 2 h), in G2/M phase with nocodazole (15 μ g/ml for 2 h) and in S phase by hydroxyurea (200 mM for 90 min). Then cells were treated with 4NQO (1 μ g/ml) or methylmethane sulfonate (0.05%) for 30 min at 30°C. The cells from 200 μ l of culture were fixed, stained with propidium iodide and DNA content was measured by flow cytometry. The remaining cultures were harvested, and extract preparation and GST-pull down were performed as described earlier.

Western blot and antibodies

Western blot analysis was performed to detect the presence of GST-Rev3, Rev7, Pol3, Pol31, Pol32 and Rev1 proteins in purified Pol ζ preparations and after pull-down experiments. To detect the Rev1, Rev3 and Rev7 proteins, rabbit polyclonal antisera were raised against purified yeast Rev1 and Pol ζ_2 . GST-Rev3 was detected with anti-GST antibody (ab9085, Abcam). Rabbit anti-Pol3, -Pol31 and -Pol32 antibodies were immunopurified. Detection was carried using alkaline phosphatase-conjugated secondary antibody (Sigma) and a BCIP/TNBT chromogenic substrate (Sigma).

DNA polymerase and translesion synthesis assays

Three different assays were used. (i) Measurement of basal DNA polymerase activity: This measures polymerase activity on activated calf thymus DNA, for 45 min at 30°C, as described (29). (ii) DNA replication assay on circular ssDNA: The assay on primed ssDNA (pSKII) was performed as described previously (24). The reactions containing 5 nM of 3 kb circular ssDNA, 500 nM RPA, 3 nM RFC and 10 nM of Pol ζ were incubated at 30°C for 50 min with increasing PCNA as shown in legends to figures. (iii) *In vitro* DNA translesion bypass assay: Sequences of the 107-nt template (with or without a model abasic site) and the primer are given in Supplementary Data. The standard 20 μ l reaction contained 40 mM Tris–HCl, pH 7.8, 0.2 mg/ml bovine serum albumin, 8 mM Mg acetate, 120 mM NaCl, 100 μ M each dNTPs, 0.5 mM ATP, 10 nM DNA, 15 nM RPA, 30 nM PCNA, 3 nM RFC and 10 nM Pol ζ . The DNA was preincubated with RPA, RFC and PCNA for 30 sec at 30°C, and the reaction was started by addition of Pol ζ and incubated at 30°C. Reactions were stopped with 15 mM ethylenediaminetetraacetic acid and 0.5% SDS and analyzed on a 12% polyacrylamide 7 M urea gel.

Table 1. Damage-induced mutagenesis efficiency of *REV3* mutants

<i>REV3</i>	Spontaneous (10^{-6})	Survival (%)	Induced (10^{-6})
WT	3.1 ± 0.2	56 ± 10	183 ± 30
Δ	2.5 ± 0.5	23 ± 3	1.5 ± 1
<i>cysA</i>	4.7 ± 2	58 ± 4	168 ± 10
<i>cysB</i>	2.0 ± 0.3	12 ± 4	6 ± 2

See 'Materials and Methods' section for details.

Quantification was done by either phosphorimaging of the dried gel (^{32}P) or fluorescence imaging on a Typhoon system.

Damage-induced mutagenesis assays

The *rev3 Δ* strain BY4741 (*rev3::KanMX4*) contained empty vector or plasmid pBL811 (*GST-REV3*) or mutants of *REV3* as shown in Table 1. Strains were grown for 2 days to saturation in selective minimal media. The cells were washed with sterile water and 2×10^7 cells plated on selective plates, with or without 80 $\mu\text{g}/\text{ml}$ canavanine and either irradiated or not irradiated with 30 J/m^2 of UV light. The plating efficiencies and the percent of UV survival were measured on plates without canavanine. Spontaneous frequencies to canavanine resistance were measured on unirradiated canavanine plates, and UV-induced frequencies to canavanine resistance were measured on irradiated canavanine plates. Colonies appearing after 3 days of growth at 30°C were counted. Frequencies of mutation to canavanine resistance were corrected for the UV survival percentage. The experiments were carried out on three independent cultures, and in duplicate, and the results are presented in Table 1.

RESULTS

The [4Fe-4S] cluster is required for the interaction of Rev3 with the Pol31 subunit of Pol δ

The CTD of Pol3 shows strong sequence homology with that of Rev3, particularly in a region C-terminal of the CysB motif (Figure 1A), suggesting the possibility of an interaction between Rev3 and the Pol31–Pol32 subunits of Pol δ . To test this, we performed a yeast two-hybrid analysis using full-length Rev3 as bait (Figure 1B). We co-expressed *REV3*, fused to the *GAL4* DNA BD, together with either *REV7*, as positive control, or with *POL31* or *POL32* fused to the *GAL4* AD, or empty vector. Significant interaction signals were obtained between Rev3 and Rev7 and between Rev3 and Pol31. No interaction between Rev3 and Pol32 was detected by this assay. Importantly, double mutations from cysteine to serine in the CysB motif (*rev3-CC1449,1473SS*), which ligands the [4Fe-4S] cluster, abrogated the Rev3–Pol31 interactions without affecting the Rev3–Rev7 signal. In contrast, double mutations from cysteine to serine in the CysA motif (*rev3-CC1401,1417SS*), did not significantly decrease the Rev3–Pol31 signal (Figure 1B). These data suggest that Pol31 binds to Rev3 through the CysB region, and an intact iron–sulfur cluster is required

for interaction. This is the same binding specificity as observed between Pol3 and Pol31 (14).

We next analyzed these interactions by pull-down experiments using GST–Rev3 trapping. We overexpressed *GST-REV3* and *REV7* and assayed for Rev3–Rev7-associated factors by glutathione chromatography (Figure 1C). Significant levels of Pol31 and Pol32 were detected, when compared with controls (Figure 1D, lane 3 vs. 1 and 2). When *POL31* and *POL32* were also overexpressed, a strong interaction signal was detected (lane 4). However, when the same experiment was carried out in a *pol32 Δ* strain, Pol31 was undetectable after affinity co-purification (lane 7 vs. lane 3). This defect was rescued by providing back overexpressed *POL32* (lane 8). These data strongly suggest the existence of a four-subunit Rev3–Rev7–Pol31–Pol32 complex called Pol ζ_4 . Importantly, unlike Pol δ , in which a Pol3–Pol31 complex is a stable assembly (30), Pol32 is required to stabilize the interactions between Rev3 and Pol31. These important differences in polymerase complex stabilities between Pol δ and Pol ζ explain why *pol32 Δ* mutants are viable, but defective for mutagenesis (16).

In agreement with the yeast two-hybrid experiments, we found that Pol31 and Pol32 fail to bind the CysB mutant of GST–Rev3, independent of overexpression (Figure 1E, lanes 5 and 8). In contrast, the CysA mutant of GST–Rev3 pulled down Pol31–Pol32 with the same efficiency as wild-type (compare lane 3 with 4 and 6 with 7).

Rev3-cysB mutant is defective for mutagenesis

Our model suggests that the four-subunit form of Pol ζ is involved in mutagenesis and predicts that mutations disrupting this complex result in a defect in mutagenesis. We measured UV damage-induced mutagenesis in the CysA and CysB mutants of *REV3*, using a forward mutation assay to canavanine resistance (Table 1). Mutations in the CysB motif that are predicted to disrupt iron–sulfur cluster binding disrupt Rev3–Pol31 interactions (Figure 1B and E), which are almost completely defective for damage-induced mutagenesis, although the observed residual signal is higher than that of a *rev3 Δ* mutant. However, double *cys->ser*, or double *cys->ala* mutations in the CysA motif that should disrupt metal binding to the zinc-ribbon motif show no damage-induced mutagenesis phenotype. Our genetic analysis of the CysA and CysB mutants is in complete agreement with a similar analysis reported recently by Baranovskiy *et al.* (22).

Purification and characterization of two forms of Pol ζ : Pol ζ_2 and Pol ζ_4

To obtain a Pol ζ_4 complex containing an intact [4Fe-4S] cluster, we overexpressed all four genes from galactose-inducible promoters (Figure 1C) and modified the purification protocol of Pol ζ that was described previously (28). Overexpression was carried out in a *rev1 Δ* strain to eliminate trace contamination of the purified preparation with Rev1 (see below). The modified procedure made use of two affinity purification tags, an N-terminal GST tag on Rev3 and an N-terminal His₇

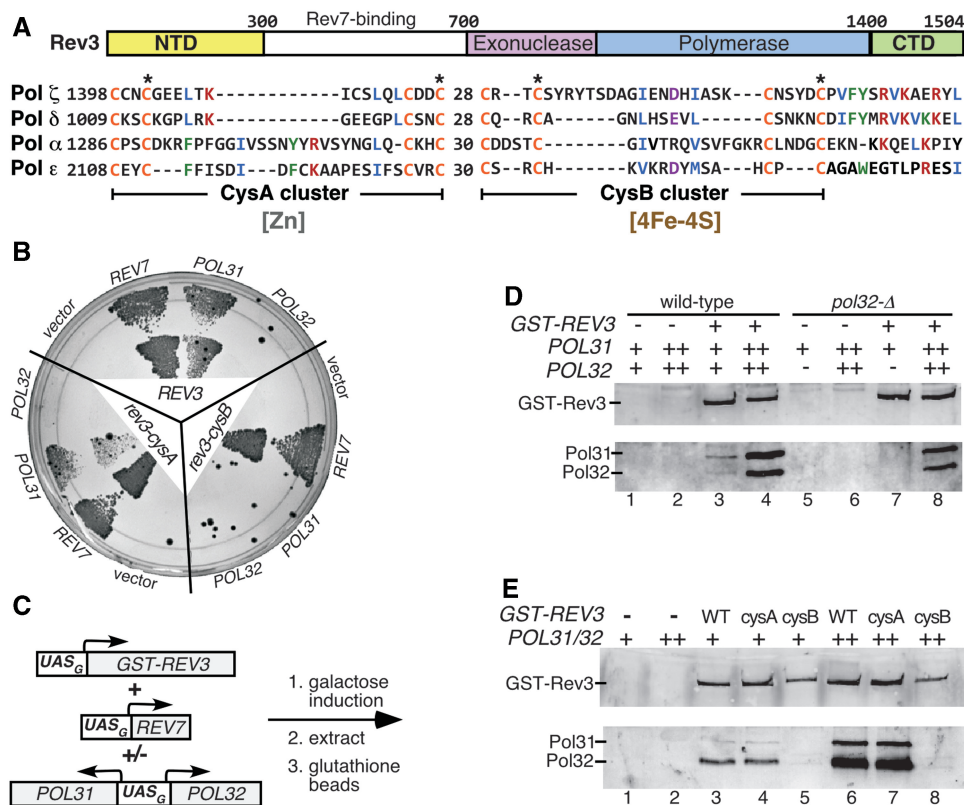


Figure 1. Interaction of Pol ζ catalytic subunit Rev3 with Pol31 and Pol32. (A) Domain organization of *S. cerevisiae* Rev3 and alignment of the CTDs of B-family DNA polymerases. The second and fourth residues of each cysteine-rich cluster were mutated in *REV3* to create the CysA (CC1401,1417SS or CC1401,1417AA) and CysB (CC1449,1473SS) mutants. (B) Yeast two-hybrid analysis. *REV3*, *rev3-cysA* or *rev3-cysB* was fused to the *GAL4* DNA-binding domain. *REV7*, *POL31* or *POL32* was fused to the *GAL4* AD; empty vector pACT2 was the negative control. Analysis was in two-hybrid indicator strain PJ69-4A. Cells were grown on His-selective medium. (C) Scheme for overexpression of *GST-REV3*, *REV7*, *POL31* and *POL32*, and affinity pull down of complexes. (D) Pull down of Pol31 and Pol32 with GST-Rev3. GST-Rev3-Rev7 complex was overexpressed alone or together with Pol31–Pol32 subunits in either wild-type or Δ *pol32* yeast. Cell extracts were incubated with glutathione sepharose beads and washed extensively. GST-Rev3 and Pol31 and Pol32 were detected by western analysis. -, gene deleted; +, native level; ++, overexpression. (E) Analysis of the interaction between Pol31–Pol32 and GST-Rev3 mutants by GST-pull down. Details are as in (D).

tag on Pol32. First, the extract, after an ammonium sulfate precipitation step, was subjected to glutathione-affinity chromatography. The resistance of the Pol ζ_4 complex to ammonium sulfate precipitation indicates that the interaction between Rev3–Rev7 and Pol31–Pol32 is very strong and specific. This procedure yielded a preparation that was slightly substoichiometric for Pol31–Pol32 (~80–90% in three purifications). Next, after cleavage of the GST-tag by rhinoviral 3C protease, the complex was further purified by Ni-chelate affinity chromatography with ~100% stoichiometry (Figure 2A). The Pol32-His₇ tag did not influence the activity of the Pol ζ_4 complex (data not shown).

In agreement with the yeast two-hybrid analysis and pull-down experiments, Pol31 and Pol32 were present in affinity-purified preparations of Pol ζ with mutations in the CysA cluster (Rev3-CC1401,1407SS or Rev3-CC1401,1407AA) but not in the purified preparation of Pol ζ sample with mutations in the CysB cluster (Rev3-CC1449S,1473SS) (Supplementary Figure S1A). The Pol ζ_2 complex was purified from a *pol32 Δ* strain, and in agreement with the pull-down data in Figure 1D, this two-subunit complex lacks any detectable level of

Pol31 by Coomassie staining after sodium dodecyl sulfate polyacrylamide gel electrophoresis (SDS-PAGE) and by western analysis (Figure 2A).

Overexpression of *REV3* and *REV7* in wild-type yeast without concomitant overexpression of *POL31* and *POL32* yielded affinity-purified preparations that were severely substoichiometric for Pol31 and Pol32, with abundances ranging from 3 to 15% (Figure 2A). We had previously noted that different Pol ζ preparations were quite variable in activity, but because of the extreme difficulty in purifying the enzyme and the very low yields, it had not been feasible to investigate those issues further at that time (28). We now think that the variations in activity were due to the variable presence of low levels of Pol31–Pol32 that escaped detection. With improved expression and purification methodologies and increased yields, we re-investigated the protein composition of our purified preparations. First, because Rev1 is known to interact with Pol ζ through Rev7 (31), we probed Pol ζ preparations for the presence of Rev1 by western analysis. Both Pol ζ_2 and Pol ζ_4 complexes, as well as all preparations of Pol ζ mutants, contain similar levels of Rev1 (~1–2% compared with Rev3,

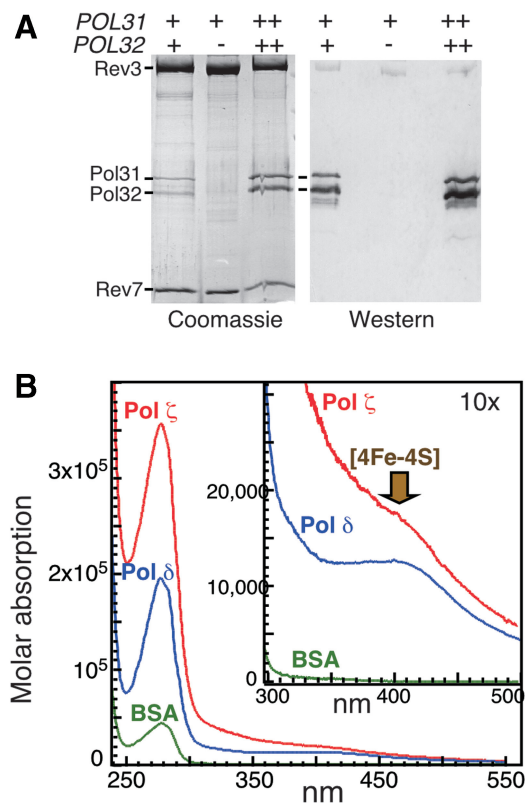


Figure 2. Purification of Pol ζ_2 and Pol ζ_4 . (A) Subunit composition of substoichiometric Pol ζ_4 , Pol ζ_2 and stoichiometric Pol ζ_4 complex. Pol ζ preparations were analyzed by Coomassie blue staining following SDS-PAGE and by western analysis, probed with a mixture of Pol31 and Pol32 antibodies, as indicated. *POL31* and *POL32* were expressed at endogenous levels (+), overexpressed (++) or absent from cells (-). (B) UV-VIS spectra of Pol ζ_4 , Pol δ and bovine serum albumin. Spectra were collected at ~ 0.3 to 1 mg/ml protein and recalculated to molar absorptions. Absorption maximum due to the presence of [4Fe-4S] cluster in proteins is indicated.

Supplementary Figure S1B). Therefore, we have purified Pol ζ_2 and Pol ζ_4 from a *rev1A* mutant strain without loss of complex stability, indicating that Rev1 is not required for the formation of the Pol ζ_4 complex (data not shown). Second, because Pol31 interacts with the catalytic subunit of Pol δ , we investigated the possibility of the presence of Pol3 by western analysis. However, none of the Pol ζ preparations contained Pol3 at detectable levels (detection limit is $\sim 0.1\%$), suggesting that Pol31 binds either Pol3 or Rev3, but not both catalytic subunits (Supplementary Figure S1C). Therefore, we conclude that our current forms of Pol ζ_4 and Pol ζ_2 contain the expected subunits without contamination by other proteins that may function in TLS and mutagenesis.

Expression in *E. coli* of the entire CTD of Rev3, containing both CysA and CysB motifs, yielded a yellow-brown preparation that after reduction by dithionite was converted into an electron spin resonance (EPR) active form with the spin signal of that of a [4Fe-4S]¹⁺ cluster (14). This suggests that, like Pol3, Rev3 has a [4Fe-4S]²⁺ cluster. Indeed, similar to Pol δ , purified Pol ζ_4 has a UV-spectral signature that is indicative of the presence of an iron-sulfur cluster (Figure 2B). Unfortunately, we

were unable to obtain sufficiently high quantities of the CysB mutant form to query whether the iron-sulfur cluster was eliminated in the mutant, but on the basis of the strong sequence homology between Pol3 and Rev3 CTD, we accept this as a likely explanation.

Pol31 and Pol32 are essential for functional interactions between PCNA and Pol ζ

The presence of Rev7 is required for DNA polymerase activity of Rev3 (6). We measured basal DNA polymerase activity of Pol ζ preparations on activated DNA in the absence of PCNA. The presence of the Pol31 and Pol32 subunits in Pol ζ_4 enhanced the activity 5- to 10-fold compared with the Pol ζ_2 preparations, which were either obtained by purification from a *pol32A* strain or by mutation of the CysB motif in *REV3* (Supplementary Figure S2A).

To determine the role of PCNA in TLS by Pol ζ , we used an oligonucleotide-based replication system with defined template damage. The substrate is incubated with RPA to coat the ssDNA regions, and PCNA is loaded by RFC and ATP. To prevent sliding of PCNA off the DNA, biotin-streptavidin bumpers are added to the 5'- and 3'-termini of the template (Figure 3A). We first assayed the replication by Pol ζ_2 on an undamaged template-primer. Pol ζ_2 activity on this template was much less efficient compared with the Pol ζ_4 complex (Figure 3B). In addition, the presence of PCNA had no detectable effect on DNA replication by Pol ζ_2 . Because of the robust activity of Pol ζ_4 on this DNA substrate, PCNA stimulation could not be detected under these conditions. However, PCNA stimulation of Pol ζ_4 on undamaged DNA was readily detected using primed single-stranded plasmid DNA substrates (Supplementary Figure S2C).

To study the role of PCNA in DNA damage TLS, we used the oligonucleotide assay system with a model abasic site at the +2 position after the primer terminus. We observed that Pol ζ_2 readily extended the primer by one nucleotide but did not insert a nucleotide opposite the abasic site, and PCNA did not enhance this activity (Figure 3C). In contrast, the Pol ζ_4 complex bypassed the abasic site damage even in the absence of PCNA. Remarkably, a dramatic stimulation of damage bypass synthesis was detected in the presence of PCNA. These data indicate that formation of the Pol ζ_4 complex is essential for both efficient damage bypass in the absence of PCNA and stimulation of Pol ζ -mediated TLS in the presence of PCNA. Therefore, we conclude that functional interactions between Pol ζ and PCNA require its Pol31 and Pol32 subunits. However, ubiquitination of PCNA did not significantly enhance TLS by Pol ζ_4 (Supplementary Figure S2B). This is consistent with a model in which ubiquitination of PCNA exerts its TLS-promoting activity through Rev1 (32).

The observation that interactions with Pol31–Pol32 enhanced the PCNA-dependent activity of Pol ζ raised the possibility that the PCNA-binding motif is localized in the Pol31 or Pol32 subunit. Previously, we have identified a C-terminal PCNA-binding motif in Pol32

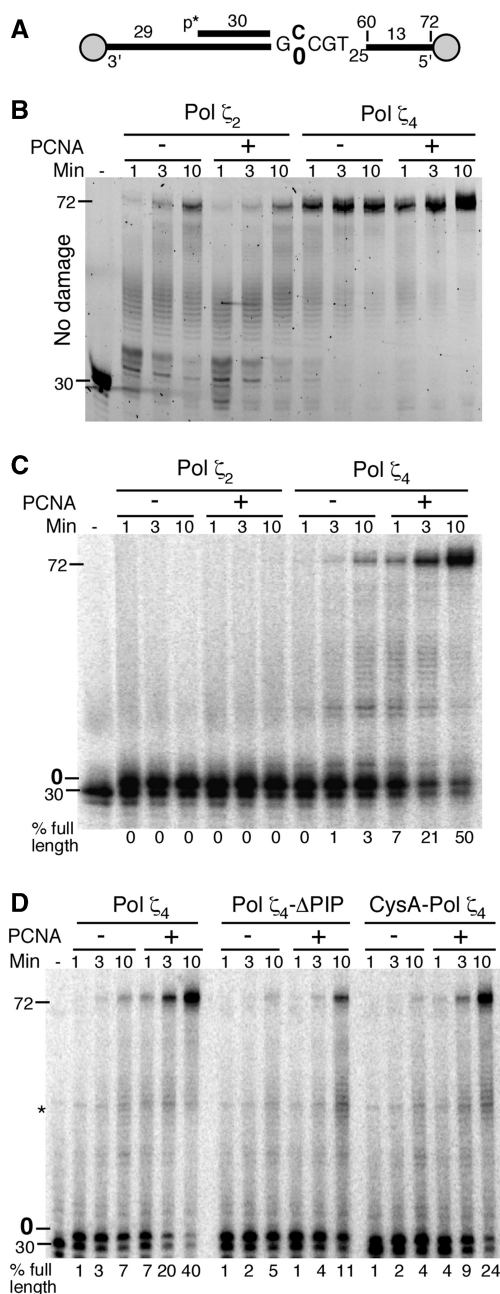


Figure 3. PCNA-mediated translesion activity of Pol ζ_2 and Pol ζ_4 . (A) A schematic diagram of the oligonucleotide substrate. The template is a 102-mer with streptavidin-biotin blocks at the 5' and 3' ends. The template at the +2 position is either a C (in (B)) or an abasic site, indicated as a '0' (in (C) and (D)). The 72-mer products represent full extension of the 30-mer primer to the end of the template. PCNA (30 nM) was added where indicated in (B–D). See Materials and Methods for details. (B) Time course of reactions of Pol ζ_2 and Pol ζ_4 on undamaged template DNA. (C) Time course of translesion synthesis by Pol ζ_2 and Pol ζ_4 on an abasic site (0) template. (D) Stimulation by PCNA of the DNA polymerase activity of Pol ζ_4 , Pol ζ_4 - Δ PIP and Pol ζ_4 -CysA on template DNA with an abasic site. Asterisk indicates an impurity in the radiolabeled primer.

(24). Deletion of this motif only marginally affected processive DNA replication by Pol δ ; however, the *pol32- Δ PIP* mutant showed a substantial reduction in the efficiency of damage-induced mutagenesis, particularly

at higher loads of DNA damage. We purified a mutant Pol ζ_4 containing a truncated form of Pol32 that lacks its PCNA-binding motif (Pol ζ_4 - Δ PIP). Although the basal activities of Pol ζ_4 and Pol ζ_4 - Δ PIP were comparable, PCNA stimulation of the mutant complex was substantially reduced (Figure 3D and Supplementary Figure S2A and S2C). We conclude that the PCNA BD of Pol32 contributes to the functional interaction between Pol ζ_4 and PCNA.

DNA replication by Pol δ requires an intact CysA motif, as CysA mutants are severely compromised for PCNA-dependent replication (14). In contrast, the CysA mutant form of Pol ζ_4 demonstrated close to wild-type basal DNA polymerase activity (Supplementary Figure S2A). Although its TLS activity was slightly reduced (~60% of wild-type), PCNA stimulated this TLS activity to the same degree as it did wild-type Pol ζ_4 (Figure 3D). This lack of a strong *in vitro* phenotype is consistent with the lack of a damage-induced mutagenesis phenotype of the same CysA mutations in yeast (Table 1).

The *pol30-113* mutant of PCNA shows severe defects in damage-induced mutagenesis, without affecting the efficiency of a proper DNA damage response through PCNA ubiquitination at Lys164 (27,33). *Pol30-113* has mutations at Glu113 and Leu151 near the monomer-monomer interface of PCNA. Previously, we showed that this mutant form of PCNA was defective for PCNA-mediated TLS *in vitro* (27). With our increased knowledge of the assembly state of Pol ζ , we assume that the previous preparations of Pol ζ contained low levels of Pol31–Pol32 that drove the observed PCNA stimulation. Indeed, the stoichiometrical Pol ζ_4 complex was unable to perform processive replication with *pca-113* (Supplementary Figure S2C).

The Pol ζ_4 complex is stable throughout the cell cycle

To test whether the formation of the Pol ζ_4 complex is subject to either cell cycle or DNA damage control, we prepared synchronized cell populations and determined co-purification of Pol31 and Pol32 with GST-Rev3 on glutathione sepharose beads. For this experiment, we used the *GST-REV3* expression plasmid, however, omitted galactose induction to maintain Rev3 at low levels. Under the same growth conditions, this construct fully complemented the mutagenesis defect of a *rev3 Δ* mutant (data not shown). *POL31* and *POL32* were not overexpressed in these experiments. Cells were arrested in G1 phase with α -factor, in S phase with hydroxyurea and in G2/M phase with nocodazole. About 80–95% of cells were arrested in the appropriate phase of the cell cycle in our experiments (Figure 4A). Synchronized cells were also treated with MMS or 4NQO to induce the DNA damage response. After affinity purification on glutathione beads, the presence of Rev7, Pol32 and Rev1 was monitored by western analysis (Figure 4B). The data indicate that Pol ζ can exist as a four-subunit complex in all phases of the cell cycle. Furthermore, treatment with DNA-damaging agents did not alter the formation or stability of the complex. Interestingly, Rev1 association with Pol ζ is highest in G2 phase. This study addressed the question

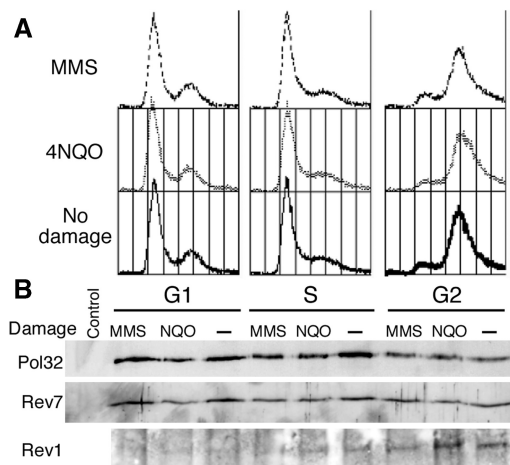


Figure 4. Stability of Pol ζ_4 during the cell cycle. (A) Fluorescence-activated cell sorting analysis of the DNA content of cells. Cells expressing low levels of *GST-REV3* and *REV7*, and *POL31* and *POL32* at native levels, were arrested in G1, S, or G2 phase, followed by treatment with MMS or 4NQO. (B) Extracts were prepared from arrested cells, and Pol32, Rev7 and Rev1 were detected by western analysis after GST-Rev3 pull down with glutathione sepharose beads. Control: Western analysis of extracts made from cells lacking GST-Rev3 and subjected to glutathione affinity purification.

whether the four-subunit complex, or its stability, is regulated at the level of posttranslational modification, and we found it is not, but we cannot exclude the possibility of cell cycle-specific transcriptional regulation of Rev3.

DISCUSSION

Pol ζ is a low-fidelity, B-family DNA polymerase and the sixth eukaryotic DNA polymerase to be described (6). The original article described a form of Pol ζ that was overexpressed in yeast, and all subsequent studies, including those from our laboratory, used forms that were also purified from yeast overexpression systems (5, 28,30). Therefore, it is likely that these forms contained low, variable levels of Pol31 and Pol32 in the preparations. Our previous observations that TLS by Pol ζ is stimulated by PCNA likely originated from the use of preparations that contained such low levels of Pol31–Pol32, which we now know varied from 3 to 15% over the years. Coupled with the fact that Pol ζ_2 has much lower basal polymerase activity than Pol ζ_4 (Supplementary Figure S2A and Figure S3), the latter species would have contributed more to the observed activity than considerations of abundance suggest. This also explains the variability in activity of different Pol ζ preparations that we remarked on several years ago (28).

Previously, we have shown that the catalytic subunits of the yeast B-family DNA polymerases contain an $[4\text{Fe-4S}]^{2+}$ cluster, coordinated by the CysB motif in their CTDs, and we and others have suggested that all B-family polymerases are similarly organized (14,20). However, a comparison between the architecture of Pol δ and Pol ζ reveals some interesting differences that may

underlie their different functions in the cell. Both Pol3 and Rev3 bind Pol31 through their CysB motif as mutations in this motif abrogate binding, while mutations in the CysA motif do not. However, Pol3 forms a stable complex with Pol31 alone (34), but Rev3 does not (Figure 1D). As a result, *pol32Δ* mutants are viable, but they are defective for damage-induced mutagenesis (16,35). Furthermore, transformation studies with plasmids containing specific DNA damage show that *pol32Δ* is defective for the bypass of abasic site damage similar to *rev3Δ*, but proficient for the bypass of thymine dimers, which is Pol η dependent (36). This is consistent with Pol32 functioning as an integral part of the Pol ζ complex.

CysA mutations in *POL3* are lethal, most likely because the mutant form of Pol δ is severely defective for PCNA-mediated processive replication (14). However, the analogous mutations in the CysA motif of *REV3* show no defect in mutagenesis [Table 1, (22)] nor is the mutant polymerase defective for PCNA-mediated processive replication (Figure 3D). Functional interactions of Pol δ with PCNA is imparted by multiple potential PCNA-binding motifs in the various subunits of Pol δ (14,24,37–40). In Pol ζ_4 , PCNA interacts through the consensus PIP box in the extreme C-terminus of Pol32 as deletion of this motif reduces TLS *in vitro* (Figure 3D). This *POL32* mutant also has a reduced efficiency in damage-induced mutagenesis (24). The residual PCNA stimulation observed *in vitro* and mutagenesis *in vivo* suggests that Pol ζ_4 contains additional PCNA interaction motif(s). The striking difference in CysA phenotype between Pol δ and Pol ζ_4 suggests a different positioning of the PCNA clamp in relation to this motif in these enzymes. Consistent with this, mutations in PCNA differentially affect its interactions with Pol δ versus Pol ζ . A *pcna-113* mutant functions as a processivity clamp for Pol δ , although its activity is somewhat reduced (27); however it is defective with Pol ζ_4 (Supplementary Figure S2C). This provides a rational explanation for the mutagenesis defect in this mutant.

The formation and stability of the Pol ζ_4 complex was unaffected by the cell cycle or by exposure to DNA-damaged agents (Figure 4). This result suggests that Pol ζ -mediated mutagenesis can occur throughout the cell cycle. However, other factors, for example, Rev1 and PCNA, show cell cycle and/or DNA damage control, and overall pathway control is likely mediated through those factors. Ubiquitination of PCNA is a key switch in this pathway, and both damage-induced mutagenesis as well as spontaneous mutagenesis in response to replisome dysfunction is dependent on ubiquitination of PCNA (27,41,42). The Rev1 protein, considered to be the scaffold onto which the mutasome assembles through binding of ubiquitinated PCNA on one hand and Pol ζ on the other hand, is most highly expressed in G2 phase (43). Indeed, it has been shown that PCNA ubiquitination and mutagenesis can be restricted to the G2 phase of the cell cycle (44,45). We found that Rev1 association with Pol ζ_4 is also highest during G2 phase (Figure 4). Therefore we suggest that the regulation of Pol ζ_4 -dependent mutagenesis is likely mediated by the formation of multisubunit complexes of higher order, for example

with Rev1 and ubiquitinated PCNA, but not through the assembly of the Pol ζ_4 complex. Finally, the cell cycle kinase *CDC7/DBF4* promotes the efficiency of UV mutagenesis (46).

As stated before, two other groups have recently reported that Rev3 interacts with Pol31 and Pol32. The article by Baranovskiy *et al.* reported the co-purification from *E. coli* of the CTD of human Rev3 together with human Pol31 and Pol32 (22). Although this approach did not permit functional polymerase studies, it allowed these authors to probe the relevance of the CysA and CysB motifs for complex formation. In agreement with our results in Figure 1E, CysB mutations, but not CysA mutations, abrogated complex formation. Similarly, their genetic studies of the CysA and B motifs in yeast yielded analogous results to ours (Table 1). The second article by Johnson *et al.* reported the isolation of a Pol ζ_4 complex from a yeast overexpression system and is in accord with ours when all four genes are overexpressed (23). However, our conclusion that Pol32 is required for stable complex formation between Rev3 and Pol31 is at variance with their study. These authors reported the purification of a three-subunit Rev3-Rev7-Pol31 complex from a strain that overexpressed just the *REV3*, *REV7*, and *POL31* genes, and based on this purification concluded that Pol32 was not required for complex formation. However, this three-subunit preparation was purified from a wild-type yeast strain rather than a *pol32Δ* strain and was highly non-stoichiometric containing predominantly the Pol31 polypeptide, to which the purification tag was fused. Given the low levels of Rev3 in this preparation, and the close migration of Pol31 and Pol32 by SDS-PAGE, low levels of Pol32 may have escaped detection. Unfortunately, a more sensitive western analysis with Pol32 antibodies was not used as a detection method in this study. We think that these are important considerations, because our study indicates that Pol32 is absolutely required for complex formation and thereby provides a logical explanation for the long-standing observation that *pol32Δ* strains are defective for damage-induced mutagenesis.

SUPPLEMENTARY DATA

Supplementary Data are available at NAR Online: Supplementary Text, Supplementary Table 1, Supplementary Figures 1 and 2 and Supplementary Reference [47].

ACKNOWLEDGEMENTS

The authors thank Carrie Stith and Bonnie Yoder for strain and plasmid construction and for help with protein purification, Sandeep Kumar for help with fluorescence-activated cell sorting analysis, and Sara Binz for advice during the course of this study.

FUNDING

Funding for open access charge: National Institutes of Health [GM032431 to P.B.].

Conflict of interest statement. None declared.

REFERENCES

- Morrison,A., Christensen,R.B., Alley,J., Beck,A.K., Bernstine,E.G., Lemontt,J.F. and Lawrence,C.W. (1989) REV3, a *Saccharomyces cerevisiae* gene whose function is required for induced mutagenesis, is predicted to encode a nonessential DNA polymerase. *J. Bacteriol.*, **171**, 5659–5667.
- Lawrence,C.W. and Maher,V.M. (2001) Eukaryotic mutagenesis and translesion replication dependent on DNA polymerase zeta and Rev1 protein. *Biochem. Soc. Trans.*, **29**, 187–191.
- Gibbs,P.E., McGregor,W.G., Maher,V.M., Nisson,P. and Lawrence,C.W. (1998) A human homolog of the *Saccharomyces cerevisiae* REV3 gene, which encodes the catalytic subunit of DNA polymerase zeta. *Proc. Natl Acad. Sci. USA*, **95**, 6876–6880.
- Guo,D., Wu,X., Rajpal,D.K., Taylor,J.S. and Wang,Z. (2001) Translesion synthesis by yeast DNA polymerase zeta from templates containing lesions of ultraviolet radiation and acetylaminofluorene. *Nucleic Acids Res.*, **29**, 2875–2883.
- Haracska,L., Prakash,S. and Prakash,L. (2003) Yeast DNA polymerase zeta is an efficient extender of primer ends opposite from 7,8-dihydro-8-Oxoguanine and O6-methylguanine. *Mol. Cell Biol.*, **23**, 1453–1459.
- Nelson,J.R., Lawrence,C.W. and Hinkle,D.C. (1996) Thymine-thymine dimer bypass by yeast DNA polymerase zeta. *Science*, **272**, 1646–1649.
- Lemontt,J.F. (1971) Mutants of yeast defective in mutation induced by ultraviolet light. *Genetics*, **68**, 21–33.
- Lawrence,C.W., Das,G. and Christensen,R.B. (1985) REV7, a new gene concerned with UV mutagenesis in yeast. *Mol. Gen. Genet.*, **200**, 80–85.
- Larimer,F.W., Perry,J.R. and Hardigree,A.A. (1989) The REV1 gene of *Saccharomyces cerevisiae*: isolation, sequence, and functional analysis. *J. Bacteriol.*, **171**, 230–237.
- Wittschieben,J., Shivji,M.K., Lalani,E., Jacobs,M.A., Marini,F., Gearhart,P.J., Rosewell,I., Stamp,G. and Wood,R.D. (2000) Disruption of the developmentally regulated Rev3 gene causes embryonic lethality. *Curr. Biol.*, **10**, 1217–1220.
- Lin,X., Trang,J., Okuda,T. and Howell,S.B. (2006) DNA polymerase zeta accounts for the reduced cytotoxicity and enhanced mutagenicity of cisplatin in human colon carcinoma cells that have lost DNA mismatch repair. *Clin. Cancer Res.*, **12**, 563–568.
- Tahirov,T.H., Makarova,K.S., Rogozin,I.B., Pavlov,Y.I. and Koonin,E.V. (2009) Evolution of DNA polymerases: an inactivated polymerase-exonuclease module in Pol epsilon and a chimeric origin of eukaryotic polymerases from two classes of archaeal ancestors. *Biol. Direct*, **4**, 11.
- Johansson,E. and Macneill,S.A. (2010) The eukaryotic replicative DNA polymerases take shape. *Trends Biochem. Sci.*, **35**, 339–347.
- Netz,D.J., Stith,C.M., Stumpfig,M., Kopf,G., Vogel,D., Genau,H.M., Stodola,J.L., Lill,R., Burgers,P.M. and Pierik,A.J. (2011) Eukaryotic DNA polymerases require an iron-sulfur cluster for the formation of active complexes. *Nat. Chem. Biol.*, **8**, 125–132.
- MacNeill,S.A., Moreno,S., Reynolds,N., Nurse,P. and Fantes,P.A. (1996) The fission yeast Cdc1 protein, a homologue of the small subunit of DNA polymerase delta, binds to Pol3 and Cdc27. *EMBO J.*, **15**, 4613–4628.
- Gerik,K.J., Li,X., Pautz,A. and Burgers,P.M. (1998) Characterization of the two small subunits of *Saccharomyces cerevisiae* DNA polymerase delta. *J. Biol. Chem.*, **273**, 19747–19755.
- Sanchez Garcia,J., Ciuffo,L.F., Yang,X., Kearsley,S.E. and MacNeill,S.A. (2004) The C-terminal zinc finger of the catalytic subunit of DNA polymerase delta is responsible for direct interaction with the B-subunit. *Nucleic Acids Res.*, **32**, 3005–3016.
- Baranovskiy,A.G., Babayeva,N.D., Liston,V.G., Rogozin,I.B., Koonin,E.V., Pavlov,Y.I., Vassilyev,D.G. and Tahirov,T.H. (2008) X-ray structure of the complex of regulatory subunits of human DNA polymerase delta. *Cell Cycle*, **7**, 3026–3036.

19. Mizuno, T., Yamagishi, K., Miyazawa, H. and Hanaoka, F. (1999) Molecular architecture of the mouse DNA polymerase alpha-primase complex. *Mol. Cell. Biol.*, **19**, 7886–7896.
20. Klinge, S., Nunez-Ramirez, R., Llorca, O. and Pellegrini, L. (2009) 3D architecture of DNA Pol alpha reveals the functional core of multi-subunit replicative polymerases. *EMBO J.*, **28**, 1978–1987.
21. Hara, K., Hashimoto, H., Murakumo, Y., Kobayashi, S., Kogame, T., Unzai, S., Akashi, S., Takeda, S., Shimizu, T. and Sato, M. (2010) Crystal structure of human REV7 in complex with a human REV3 fragment and structural implication of the interaction between DNA polymerase zeta and REV1. *J. Biol. Chem.*, **285**, 12299–12307.
22. Baranovskiy, A.G., Lada, A.G., Siebler, H.M., Zhang, Y., Pavlov, Y.I. and Tahirov, T.H. (2012) DNA polymerase delta and zeta switch by sharing accessory subunits of DNA polymerase delta. *J. Biol. Chem.*, **287**, 17281–17287.
23. Johnson, R.E., Prakash, L. and Prakash, S. (2012) Pol31 and Pol32 subunits of yeast DNA polymerase delta are also essential subunits of DNA polymerase zeta. *Proc. Natl Acad. Sci. USA*, **109**, 12455–12460.
24. Johansson, E., Garg, P. and Burgers, P.M. (2004) The Pol32 subunit of DNA polymerase delta contains separable domains for processive replication and proliferating cell nuclear antigen (PCNA) binding. *J. Biol. Chem.*, **279**, 1907–1915.
25. Fortune, J.M., Stith, C.M., Kissling, G.E., Burgers, P.M. and Kunkel, T.A. (2006) RPA and PCNA suppress formation of large deletion errors by yeast DNA polymerase delta. *Nucleic Acids Res.*, **34**, 4335–4341.
26. Henriksen, L.A., Umbricht, C.B. and Wold, M.S. (1994) Recombinant replication protein A: expression, complex formation, and functional characterization. *J. Biol. Chem.*, **269**, 11121–11132.
27. Northam, M.R., Garg, P., Baitin, D.M., Burgers, P.M. and Shcherbakova, P.V. (2006) A novel function of DNA polymerase zeta regulated by PCNA. *EMBO J.*, **25**, 4316–4325.
28. Garg, P., Stith, C.M., Majka, J. and Burgers, P.M. (2005) Proliferating Cell Nuclear Antigen Promotes Translesion Synthesis by DNA Polymerase zeta. *J. Biol. Chem.*, **280**, 23446–23450.
29. Bauer, G.A., Heller, H.M. and Burgers, P.M.J. (1988) DNA polymerase III from *Saccharomyces cerevisiae*. I. Purification and characterization. *J. Biol. Chem.*, **263**, 917–924.
30. Murakumo, Y., Ogura, Y., Ishii, H., Numata, S., Ichihara, M., Croce, C.M., Fishel, R. and Takahashi, M. (2001) Interactions in the error-prone postreplication repair proteins hREV1, hREV3, and hREV7. *J. Biol. Chem.*, **276**, 35644–35651.
31. Wood, A., Garg, P. and Burgers, P.M. (2007) A ubiquitin-binding motif in the translesion DNA polymerase Rev1 mediates its essential functional interaction with ubiquitinated proliferating cell nuclear antigen in response to DNA damage. *J. Biol. Chem.*, **282**, 20256–20263.
32. Amin, N.S. and Holm, C. (1996) In vivo analysis reveals that the interdomain region of the yeast proliferating cell nuclear antigen is important for DNA replication and DNA repair. *Genetics*, **144**, 479–493.
33. Murakumo, Y. (2002) The property of DNA polymerase zeta: REV7 is a putative protein involved in translesion DNA synthesis and cell cycle control. *Mutat. Res.*, **510**, 37–44.
34. Burgers, P.M. and Gerik, K.J. (1998) Structure and processivity of two forms of *Saccharomyces cerevisiae* DNA polymerase delta. *J. Biol. Chem.*, **273**, 19756–19762.
35. Huang, M.E., Rio, A.G., Galibert, M.D. and Galibert, F. (2002) Pol32, a subunit of *Saccharomyces cerevisiae* DNA polymerase delta, suppresses genomic deletions and is involved in the mutagenic bypass pathway. *Genetics*, **160**, 1409–1422.
36. Gibbs, P.E., McDonald, J., Woodgate, R. and Lawrence, C.W. (2005) The relative roles in vivo of *Saccharomyces cerevisiae* Pol eta, Pol zeta, Rev1 Protein and Pol32 in the bypass and mutation induction of an abasic site, T-T (6-4) photoadduct and T-T cis-syn cyclobutane dimer. *Genetics*, **169**, 575–582.
37. Zhou, J.Q., He, H., Tan, C.K., Downey, K.M. and So, A.G. (1997) The small subunit is required for functional interaction of DNA polymerase delta with the proliferating cell nuclear antigen. *Nucleic Acids Res.*, **25**, 1094–1099.
38. Zhang, P., Mo, J.Y., Perez, A., Leon, A., Liu, L., Mazloum, N., Xu, H. and Lee, M.Y. (1999) Direct interaction of proliferating cell nuclear antigen with the p125 catalytic subunit of mammalian DNA polymerase delta. *J. Biol. Chem.*, **274**, 26647–26653.
39. Reynolds, N., Warbrick, E., Fantes, P.A. and MacNeill, S.A. (2000) Essential interaction between the fission yeast DNA polymerase delta subunit Cdc27 and Pcn1 (PCNA) mediated through a C-terminal p21(Cip1)-like PCNA binding motif. *EMBO J.*, **19**, 1108–1118.
40. Acharya, N., Klassen, R., Johnson, R.E., Prakash, L. and Prakash, S. (2011) PCNA binding domains in all three subunits of yeast DNA polymerase delta modulate its function in DNA replication. *Proc. Natl Acad. Sci. USA*, **108**, 17927–17932.
41. Hoege, C., Pfander, B., Moldovan, G.L., Pyrowolakis, G. and Jentsch, S. (2002) RAD6-dependent DNA repair is linked to modification of PCNA by ubiquitin and SUMO. *Nature*, **419**, 135–141.
42. Stelter, P. and Ulrich, H.D. (2003) Control of spontaneous and damage-induced mutagenesis by SUMO and ubiquitin conjugation. *Nature*, **425**, 188–191.
43. Waters, L.S. and Walker, G.C. (2006) The critical mutagenic translesion DNA polymerase Rev1 is highly expressed during G(2)/M phase rather than S phase. *Proc. Natl Acad. Sci. USA*, **103**, 8971–8976.
44. Daigaku, Y., Davies, A.A. and Ulrich, H.D. (2010) Ubiquitin-dependent DNA damage bypass is separable from genome replication. *Nature*, **465**, 951–955.
45. Karras, G.I. and Jentsch, S. (2010) The RAD6 DNA damage tolerance pathway operates uncoupled from the replication fork and is functional beyond S phase. *Cell*, **141**, 255–267.
46. Pessoa-Brandao, L. and Sclafani, R.A. (2004) CDC7/DBF4 functions in the translesion synthesis branch of the RAD6 epistasis group in *Saccharomyces cerevisiae*. *Genetics*, **167**, 1597–1610.
47. Freudenthal, B.D., Gakhar, L., Ramaswamy, S. and Washington, M.T. (2010) Structure of monoubiquitinated PCNA and implications for translesion synthesis and DNA polymerase exchange. *Nat. Struct. Mol. Biol.*, **17**, 479–484.

SUPPLEMENTARY DATA TO:

A four-subunit DNA polymerase ζ complex containing Pol δ accessory subunits is essential for PCNA-mediated mutagenesis

Alena V. Makarova, Joseph L. Stodola, and Peter M. Burgers*

Department of Biochemistry and Molecular Biophysics, Washington University School of Medicine,
St. Louis, MO 63110, USA

Running Title: A four-subunit Pol ζ complex in mutagenesis

*corresponding author:

TEL: (314) 362-3872

FAX: (314) 362-71831

E-mail:

Materials and Methods

Strains.

The protease deficient yeast strain FM113 (a haploid version of BJ2168; *MATa*: *leu2-3,112*, *pep4-3*, *prb1-1122*, *prc1-407*, *trp1-289*, *ura3-52*), Pol32 deficient strain PY117 (*MATa*: *his3-11, 15*, *leu2-3,112*, *nuc1 Δ ::LEU2*, *pep4-3*, *pol32 Δ ::HIS3*, *prb1-1122*, *trp1- Δ* , *ura3-52*) and Rev1 deficient strain PY201 (*MATa*: *arg4-17*, *his3 Δ -1*, *leu2-3, 112*, *trp1*, *ura3-52*, *rev1::HISG*) were used for overexpression of Pol ζ_4 and Pol ζ_2 complexes. Strain PJ69-4A (*MATa*: *gal4- Δ* , *gal80- Δ* , *his3- Δ 200*, *leu2-3, 112*, *LYS2::GAL1-HIS3*, *GAL2-ADE2*, *met2::GAL7-lacZ*, *trp1-901*, *ura3-52*) was used for two-hybrid analysis.

Plasmids

The plasmids used in this study are listed in Supplementary Table 1. The pBL813 plasmid encodes *REV3* and *REV7* genes optimized to yeast codon usage. *REV3opt* and *REV7opt* genes were chemically synthesized by GenScript (NJ). Mutations in *REV3* gene were obtained by site-directed mutagenesis using the Quick Change mutagenesis kit (Stratagene). Plasmids and sequences are available upon request.

Supplementary Table 1. Plasmids

name	plasmid	description	reference
pBL346	pRS425-GAL-POL31-POL32	expression of Pol31 and Pol32 under GAL1-10	this work
pBL347	pRS425-GAL-HIS-POL31-POL32	expression of 7xHIS-Pol31 and Pol32 under GAL1-10	this work
pBL348	pRS425-GAL-HIS-POL31-POL32 ^{ΔPIP}	expression of 7xHIS-Pol31 and Pol32 under GAL1-10	this work
pBL811	pRS426-GAL-GST-REV3	expression of wild type GST-Rev3 under GAL1-10	(28)
pBL811-A1	pRS426-GAL-GST-REV3 ^{C1401S, C1417S}	expression of cysA-GST-Rev3 under GAL1-10	this work
pBL811-A2	pRS426-GAL-GST-REV3 ^{C1401A, C1417A}	expression of cysA'-GST-Rev3 under GAL1-10	this work
pBL811-B	pRS426-GAL-GST-REV3 ^{C1449S, C1473S}	expression of cysB-GST-Rev3 under GAL1-10	this work
pBL812	pRS424-GAL-REV7	expression of Rev7 under GAL1-10	this work
pBL813	pRS426-GAL-GST-REV3opt-REV7opt	expression of wild type GST-Rev3 and Rev7 under GAL1-10 using codon-optimized genes	this work
pBL816	pGBT8-BD-REV3	yeast two hybrid plasmid encoding for wild type Rev3 in a frame with GAL4 DNA binding domain	this work
pBL816-A	pGBT8-BD-REV3 ^{C1401S, C1417S}	yeast two hybrid plasmid encoding for cysA-Rev3 in a frame with GAL4 DNA binding domain	this work
pBL816-B	pGBT8-BD-REV3 ^{C1449S, C1473S}	yeast two hybrid plasmid encoding for cysB-Rev3 in a frame with GAL4 DNA binding domain	this work
pBL817	pACT2-AD-REV7	yeast two hybrid plasmid encoding for Rev7 in a frame with GAL4 activation domain	this work
pBL364	pACT2-AD-POL31	yeast two hybrid plasmid encoding for Pol31 in a frame with GAL4 activation domain	(16)
pBL391	pACT2-AD-POL32	yeast two hybrid plasmid encoding for Pol32 in a frame with GAL4 activation domain	(16)

Expression and purification of four and two subunit Pol ζ complexes

Stoichiometric and nonstoichiometric Pol ζ₄ and Pol ζ₂ complexes were produced in strains BJ2168, PY117 or PY201 and purified as described previously with modifications (26). Galactose induction was performed at OD₆₆₀ ≥ 3 and cells were grown for another 10-12 h. 500 - 800 g of cells were resuspended in 3x lysis buffer (150 mM Hepes (pH 7.8), 900 mM KCl, 90 mM K₂HPO₄/KH₂PO₄ (pH 7.8), 6% glycerol, 7.5 mM sucrose, 0.15% Tween 20, 0.03% Nonidet P40, 6 mM DTT, 30 μM pepstatin A, 30 μM leupeptin, 7.5 mM benzamidine) and disrupted in a blender with dry ice. All further steps were carried out at 0–4 °C. When the powder was dissolved, PMSF was added to the suspension to 0.5 mM and glycerol was adjusted to final 8%. To precipitate nucleic acids 45 ml of 10% Polymin P was added per one liter of lysate and the mixture was stirred for 20 min. After preclearing of lysate at 18,000 rpm for 25 min, 0.31 g/ml ammonium sulfate was added to the supernatant and the mixture was stirred for another 20-30 min. The pellet was collected at 18,000 for 20 min and dissolved in 750-1200 ml of buffer A1 (50 mM Hepes (pH 7.4), 300 mM KCl, 30 mM K₂HPO₄/KH₂PO₄ (pH 7.4), 8% glycerol, 2.5 mM sucrose, 0.05% Tween 20, 0.01% Nonidet P-40, 2 mM DTT, 8 μM pepstatin A, 8 μM leupeptin, 2 mM benzamidine, 0.5 mM PMSF) and gently agitated with 2.5 ml of glutathione sepharose

beads (GE Healthcare) for 2 hours. The beads were packed into a disposable BioRad column and washed with 200 ml of buffer A1, followed by 200 ml of A2 (30 mM Hepes (pH 7.8), 200 mM KCl, 30 mM K₂HPO₄/KH₂PO₄ (pH 7.8), 8% glycerol, 2.5 mM sucrose, 0.05% Tween 20, 0.01% Nonidet P-40, 1 mM DTT, 5 mM MgCl₂, 1 mM ATP, 2 μM pepstatin A, 0.5 mM PMSF), and buffer A3 (30 mM Hepes (pH 8), 100 mM KCl, 30 mM K₂HPO₄/KH₂PO₄ (pH 8), 8% glycerol, 2.5 mM sucrose, 0.05% Tween 20, 0.01% Nonidet P-40, 1 mM DTT, 2 μM pepstatin A, 0.5 mM PMSF). Proteins were eluted by 4-5 stepwise washes with 2 ml of buffer A3 containing 30 mM of reduced glutathione. Fractions were combined and digested overnight at 4 °C with PreScission protease. The proteins were diluted 2-fold with buffer B0 (30 mM Hepes (pH 7.4), 5% glycerol, 2.5 mM sucrose, 1 mM DTT, 0.01% E10-C12 detergent) and loaded onto a 1-ml heparin agarose column. After washing the column with buffer B1 (30 mM Hepes (pH 7.4), 150 mM KCl, 10 mM K₂HPO₄/KH₂PO₄ (pH 7.4), 5% glycerol, 2.5 mM sucrose, 1 mM DTT, 0.01% E10-C12), the proteins were eluted by step-gradient with buffer B2 (30 mM Hepes (pH 7.4), 750 mM KCl, 20 mM K₂HPO₄/KH₂PO₄ (pH 7.4), 5% glycerol, 2.5 mM sucrose, 1 mM DTT, 0.01% E10-C12). Full stoichiometric Pol ζ₄ was purified as described above, except that a metal-chelate affinity chromatography was performed instead of heparin column step. Fractions with PreScission protease-digested protein were diluted 2-fold with buffer E (30 mM Hepes (pH 7.4), 200 mM KCL, 20 mM K₂HPO₄/KH₂PO₄ (pH 7.4) 5% glycerol, 2.5 mM sucrose, 1 mM DTT, 0.01% E10-C12, 0.5 mM PMSF) containing 10mM imidazole and incubated with 2 ml of Ni-NTA agarose beads (Qiagen) for 45 min. The beads were packed into a column, washed with 400 ml of buffer E with 20 mM imidazole and eluted with buffer E containing 200 mM imidazole. All final preparations were dialyzed against buffer D (30 mM Hepes (pH 7.4), 200 mM NaCl, 8% glycerol, 1 mM DTT).

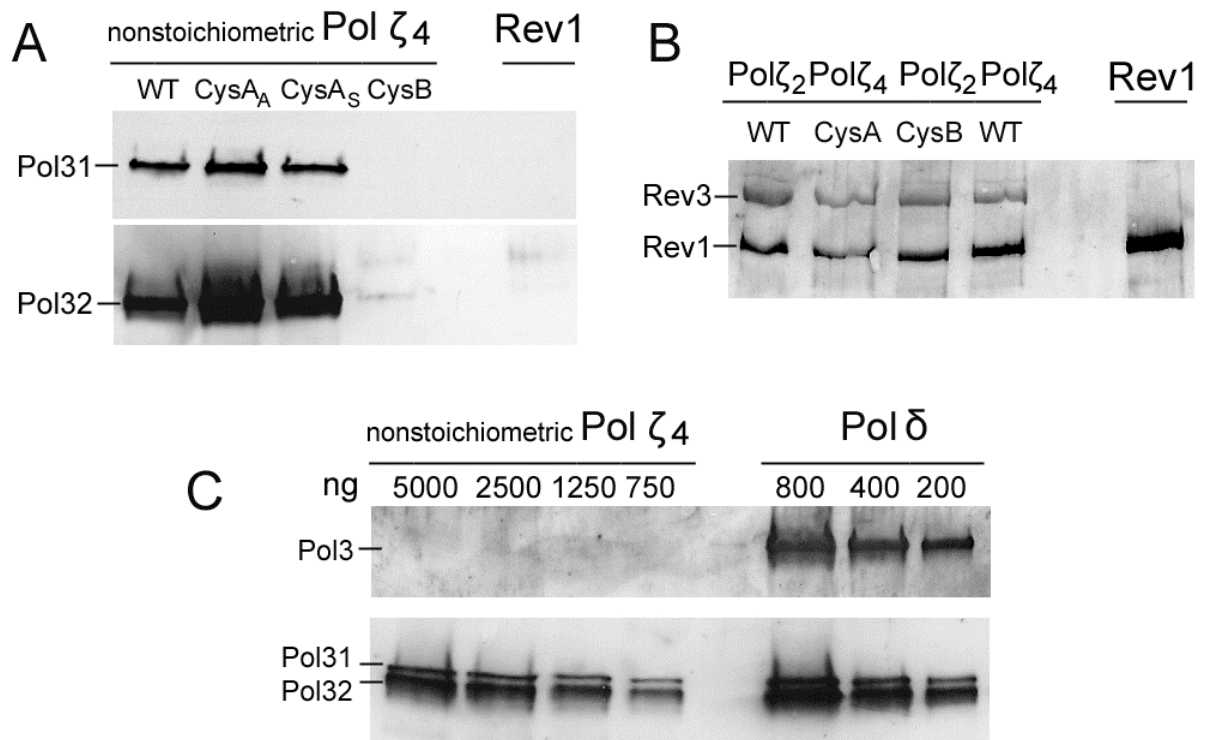


Figure S1: Characterization of composition of stoichiometric and nonstoichiometric Pol ζ_4 and Pol ζ_2 complexes preparations by Western analysis. **(A)** Detection of Pol31 and Pol32 in nonstoichiometric Pol ζ_4 complexes purified from cells without Pol31-Pol32 overexpression. 5 μ g of each protein was loaded per lane. CysA_A-Pol ζ_4 contains a double mutation in CysA motif (CC1401,1417AA), CysA_S-Pol ζ_4 variant harbours a CysA mutation (CC1401,1417SS). The right lane had 5 μ g of purified Rev1, and shows the lack of Pol31 and Pol32 in the preparation. **(B)** Detection of Rev1 in purified preparations of Pol ζ_4 and Pol ζ_2 complexes. The Western blots contained ~600 ng of the indicated complexes, and the right lane contained 80 ng of Rev1 as control. The observed Rev3 signal is due to crossreactivity of Rev3 with the anti-Rev1 antibodies. **(C)** Detection and estimation of amount of Pol3 and Pol31-Pol32 subunits in purified preparation of nonstoichiometric Pol ζ_4 . (left lanes) and in Pol δ (right lanes).

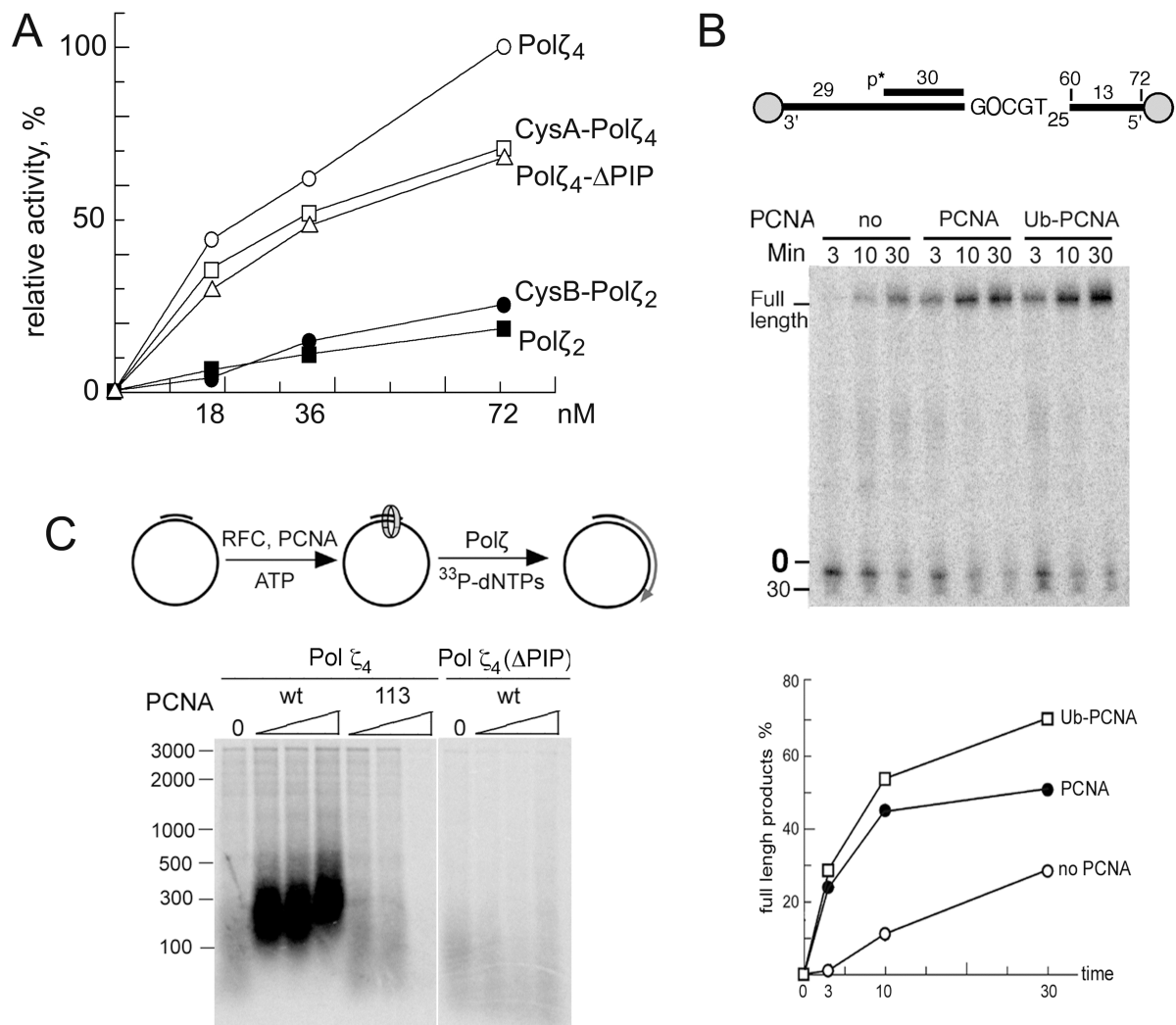


Figure S2: DNA polymerase activity of Pol ζ_4 and Pol ζ_2 complexes. **(A)** Basal DNA polymerase activity of Pol ζ_4 , Pol ζ_2 , CysA-Pol ζ_4 , CysB-Pol ζ_2 and Pol ζ_4 - Δ PIP on activated calf thymus DNA. **(B)** Stimulation of translesion bypass activity of Pol ζ_4 by ubiquitinated and nonubiquitinated PCNA on oligonucleotide substrate with an abasic site. For these experiments we used a split version of PCNA, that is fully functional in vivo, but allows for the facile addition of ubiquitination at position 164 (1). **(C)** Stimulation of DNA polymerase activity of Pol ζ_4 - Δ PIP and Pol ζ_4 by wild type PCNA and by mutant pcna-113 on primed circular bluescript SKII DNA.

Supplementary Reference

47. Freudenthal, B.D., Gakhar, L., Ramaswamy, S. and Washington, M.T. (2010) Structure of monoubiquitinated PCNA and implications for translesion synthesis and DNA polymerase exchange. *Nat Struct Mol Biol*, 17, 479-484.

CHAPTER IV

Proficient Replication of the Yeast Genome by a Viral DNA Polymerase

PREFACE TO THE CHAPTER

The following chapter extends my interest in how the metal binding motifs within Pol δ contribute to the structure and function of the polymerase complex. From the work described in Chapter II, we developed the hypothesis that the two crucial, eukaryotic-specific characteristics of Pol δ were the ability to bind its accessory subunits and the ability to bind the replication clamp PCNA. If this were the case, then we thought that one could replace the entire polymerase domain of Pol δ with an analogous polymerase, provided it synthesized DNA with a high enough efficiency and contained a proofreading exonuclease. To test this, we created a chimeric Pol δ catalytic subunit, containing the majority of the bacteriophage RB69 DNA polymerase fused to the metal binding domain of the Pol δ catalytic subunit Pol3.

We found that this chimeric subunit could proficiently bind the Pol δ accessory subunits Pol31 and Pol32, and could perform processive DNA replication in complex with PCNA. The chimeric polymerase complex, termed RbPol δ , did not support DNA replication *in vivo*. However, introduction of two PCNA mutations, identified in a screen, did allow RbPol δ to substitute for Pol δ *in vivo*. The suppressor PCNA mutant stimulated processive synthesis by RbPol δ to a greater extent than wild-type PCNA, providing insight into the suppression mechanism *in vivo*. Since any yeast specific protein-protein interactions involving the Pol3 polymerase domain are lost in our chimeric polymerase, these observations suggest that there are no essential protein-protein interactions mediated by this domain. This supports our hypothesis that all protein interactions necessary for replication occur through the metal binding domain of Pol3 and the Pol δ accessory subunits.

This work was a collaboration between myself and Carrie Stith. Carrie and I both performed protein purification and genetic experiments. I performed all *in vitro* biochemical assays. Peter and I worked together to write the manuscript.

Proficient Replication of the Yeast Genome by a Viral DNA PolymeraseJoseph L. Stodola, Carrie M. Stith and Peter M. Burgers¹

From the Department of Biochemistry and Molecular Biophysics, Washington University School of Medicine, St. Louis, Missouri 63110, USA

To whom correspondence should be addressed: Peter M. Burgers, 314-362-3872:

Running title: *Rb69 DNA polymerase replicates the yeast genome***Keywords:** DNA replication, gene fusion, Okazaki fragment maturation, PCNA, replication fidelity, mutagenesis**ABSTRACT**

DNA replication in eukaryotic cells requires minimally three B-family DNA polymerases: Pol α , Pol δ and Pol ϵ . Pol δ replicates and matures Okazaki fragments on the lagging strand of the replication fork. *Saccharomyces cerevisiae* Pol δ is a three-subunit enzyme (Pol3-Pol31-Pol32). A small C-terminal domain of the catalytic subunit Pol3 carries both iron-sulfur cluster and zinc binding motifs, which mediate interactions with Pol31, and processive replication with the replication clamp PCNA, respectively. We show that the entire N-terminal domain of Pol3, containing polymerase and proofreading activities, could be effectively replaced by those from bacteriophage RB69, and carry out chromosomal DNA replication in yeast with remarkable high fidelity, provided adaptive mutations in the replication clamp PCNA were introduced. This result is consistent with the model that all essential interactions for DNA replication in yeast are mediated through the small C-terminal domain of Pol3. The chimeric polymerase carries out processive replication with PCNA *in vitro*, however, in yeast, it requires an increased involvement of the mutagenic translesion DNA polymerase ζ during DNA replication.

Replication of genomic DNA during each cell cycle requires the action of replicative DNA polymerases. To ensure faithful transmission of genomic information from the parent to the daughter cells, these polymerases must work efficiently and with very high fidelity (1). The eukaryotic replicative DNA polymerases are members of the B-family polymerases, which are classified as such according to the structure of their catalytic domains (2-5). Three B-family DNA polymerases participate in DNA replication. The current model states that Pol

ϵ^2 replicates the leading strand of the replication fork, whereas Pol α -primase initiates Okazaki fragments on the lagging strand that are elongated and matured by Pol δ (6). This simple “division of labor” model is still a matter of debate (7-9). Furthermore, under certain conditions, such as those of replication restart following DNA recombination, Pol δ carries out substantial DNA synthesis of both strands (10). The fourth B-family enzyme, Pol ζ , is required for translesion synthesis in response to DNA damage, which results in the bulk of damage-induced mutagenesis in eukaryotes (11). Pol ζ also participates in replication past structural blocks when normal replication forks stall (12).

B-family DNA polymerases are ubiquitous; they are found in eukaryotes, bacteria, archaea, and in both bacterial and eukaryotic DNA-based viruses (13). All B-family enzymes contain three conserved domains: a structural N-terminal domain (NTD), a 3'-5' exonuclease domain, and the polymerase domain containing the palm, finger, and thumb subdomains. The NTD is highly conserved, but a specific function for this domain has only been assigned to some archaeal enzymes, in which the NTD recognizes template uracil residues and inhibits continued replication by the DNA polymerase (14,15). The exonuclease domain serves to carry out proofreading of polymerase errors in most enzymes. However, eukaryotic Pol α and Pol ζ , while maintaining this structural domain, lack exonuclease activity. The polymerase domain carries out high-fidelity DNA synthesis, with the notable exception of the translesion synthesis enzyme Pol ζ (16-18).

The cellular eukaryotic members of the B-family are structurally more complex in that they are multi-subunit enzymes, and secondly, they uniquely contain an additional, small C-terminal domain (CTD) in the polymerase subunit, which mediates

interactions with these accessory subunits (13,19). The CTD sequences of the four eukaryotic enzymes are highly conserved suggesting a common 3D structure of the CTD. Only the structure of the CTD of Pol α has been determined (19,20). It shows an elongated, bilobal form, in which the two lobes are connected by a three-helical bundle. Each lobe contains four conserved cysteines (Figure 1A). In the Pol α CTD structures, both 4-cysteine lobes bind zinc. However, biochemical studies of Pol δ and Pol ζ have shown that the C-terminal 4-cysteine lobe ligands an iron-sulfur cluster in the $[4\text{Fe-4S}]^{2+}$ coordination state (21,22). The CTDs of Pol α , Pol δ , and Pol ϵ each bind a distinct B subunit, called Pol12, Pol31, and Dpb2, respectively, in budding yeast (19,21,23), and these B subunits show both sequence and structural conservation (19,20,24,25). Pol ζ has appropriated the B subunit from Pol δ to elaborate its own 4-subunit assembly (Rev3-Rev7-Pol31-Pol32) (22,26-28).

In order to better understand how the multi-subunit structures of eukaryotic replicative DNA polymerases are intricately tied to their function, we have used the lagging strand polymerase Pol δ as a model. Budding yeast Pol δ consists of the catalytic subunit Pol3 and the accessory subunits Pol31 and Pol32 (29). Interactions between Pol3 and Pol31 occur through the Pol3 CTD and require an intact iron-sulfur cluster (21). Pol31 binds the third subunit Pol32 to form the complete heterotrimeric polymerase complex (29). This architecture of Pol δ is conserved in other organisms (25,30), except for the presence of an additional, small regulatory subunit in fission yeast and in mammals (31,32). Pol δ alone is a low-processivity enzyme, replicating only a few nucleotides before dissociating from DNA. This problem is overcome through interactions with the replication clamp proliferating cell nuclear antigen (PCNA) (33). PCNA is a donut-shaped homotrimeric protein that is loaded onto DNA template-primer termini by Replication Factor C (RFC) in an ATP-dependent manner (34,35). DNA-bound PCNA then recruits Pol δ and increases both the catalytic activity and the processivity of the enzyme, so that it can rapidly replicate hundreds of nucleotides in a single DNA-binding event (36-38). PCNA-dependent polymerase processivity is vital to efficient genomic DNA replication. Pol δ mutants that are compromised for interactions with PCNA, exhibit *in vitro* processivity defects that, if severe, are associated with lethality in yeast (21,39,40).

We were interested in understanding what structural domains of Pol δ are required for efficient replication of the budding yeast genome. While mutations that inactivate polymerase activity cause lethality in yeast (41), mutations that abrogate exonuclease activity are viable but cause fidelity defects (42). However, it is possible that structural determinants in the NTD, or in the two catalytic domains may be essential for replisome activity. The overall structure of these three domains is conserved in B-family DNA polymerases, as shown by the superimposition of the structure of bacteriophage Rb69 DNA polymerase with that of the same domains of Pol3 (Figure 1A). Lacking from the Pol3 structure is its CTD, which mediates interactions with the accessory subunits and, both directly and indirectly, with PCNA. We hypothesized that the essential factors enabling Pol δ to act in a eukaryotic setting are the ability to bind its accessory subunits and PCNA. In order to test this hypothesis, we created a chimeric polymerase subunit by replacing the Pol3 NTD and catalytic core domains with those from the structurally homologous bacteriophage RB69 DNA polymerase. Rb69 and T4 are closely related bacteriophages that use a polymerase processivity model similar to Pol δ , containing a homotrimeric clamp and an ATP-dependent clamp loader (gp45 and gp44/62, respectively) (43).

We found that fusing the 104 kDa RB69 DNA polymerase to the 13 kDa CTD of Pol3 was sufficient to form a three-subunit polymerase complex with Pol31 and Pol32 in yeast. The processivity of this polymerase complex was stimulated by PCNA, but processivity was compromised as compared to Pol δ . We obtained more robust stimulation of this engineered form of Pol δ when we introduced two adaptive mutations in PCNA, and this genetic arrangement conferred growth in yeast that contained the fusion polymerase as only source of Pol δ . Remarkably, when we eliminated fidelity-lowering contributions made by the mutagenic Pol ζ , the fidelity of the engineered Pol δ approximated that of the native enzyme.

EXPERIMENTAL PROCEDURES

Yeast strains and proteins – Strains were derived from PY227 by integration of the appropriate gene deletion cassettes. PY227 (*MAT α his3 Δ -1 leu2-3,112 trp1- Δ ura3-52 pol3 Δ ::KANMX4 + pBL304 (POL3 URA3)*); PY236 (PY227 but *leu2::pBL248-rb2 (LEU2, pol30-rb2 (pol30-Q29H,K31R))*); PY237 (PY236 but *rev3 Δ ::NATMX4*), PY238

(PY236 but *rad30Δ::HIS3*), PY239 (PY236 but *rev3Δ::NATMX4 rad30Δ::HIS3*), and PY343 (PY236 but *pol32Δ::HIS3*).

The plasmids used were pBL248 (*LEU2, POL30*); pBL248-rb2 (as pBL248 but *pol30-rb2 (pol30-Q29H,K31R)*); pBL249 (*POL30* in pRS315 (*CEN ARS LEU2*)); pBL249-rb2 (as pBL249 but *pol30-rb2 (pol30-Q29H,K31R)*); pBL304 (*POL3* in yCP50 (*CEN ARS URA3*)); pBL309 (*POL3* in pRS314 (*CEN6 ARSHI TRP1*)); pBL325 (2 μ m ori *TRP1 GAL1-[GST-3C-RbPol-POL3CTD]*), containing a fusion of the glutathione-S-transferase gene (*GST*) to a rhinoviral 3C protease recognition site, followed by the RbPol(1-896)-*POL3*(981-1097) fusion gene; pBL326 (RbPol(1-896)-*POL3*(981-1097) fusion under control of the attenuated *ADHI* promoter, in pRS424 (*TRP1* 2 μ m ori)); pBL341 (2 μ m ori *URA3 GAL1-POL31 GAL10-POL32*). All strains and plasmids and their sequences are available from the corresponding author upon request.

Pol δ , Rb69 DNA polymerase (RbPol), PCNA, RFC, RPA, FEN1, and DNA ligase I were purified as described (2,44,45). In order to obtain RbPol δ , yeast strain BJ2168 (*MATa ura3-52 trp1-289 leu2-3,112 prb1-1122 prc1-407 pep4-3*) was transformed with plasmids pBL341 and pBL325. Growth and galactose induction and extract preparation was as described, and RbPol δ was purified by glutathione-affinity purification and, following removal of the GST tag with rhinoviral 3C protease, by MonoS chromatography analogously to described for Pol δ (45).

Genetic techniques – In order to make yeast strains containing a chromosomal copy of the *pol30-rb2* allele, integrating plasmid pBL248-rb2, and pBL248 as control was cut with *HpaI*, which cuts once in the *LEU2* gene, and transformed into the appropriate *leu2-3,112* strains to leucine prototrophy. To determine phenotypes of the *pol3-69* allele, the appropriate *pol3Δ* strains, containing pBL304 as complementing plasmid, were transformed with pBL326, or pBL309 as positive control, with Trp selection, and transformants were passed over 5-fluoroorotic acid-containing media (5-FOA) to evict complementing plasmid pBL304 (*POL3 URA3*).

DNA damage sensitivity assays were carried using standard protocols. Fluctuation analyses to determine spontaneous mutation rates were carried out in triplicate with 15-20 independent cultures, and analyzed by the median (46).

Identification of PCNA suppressor mutants – The *POL30* gene in pBL249 was PCR-mutagenized as described (47). The library was transformed into PY227 containing both pBL304 and pBL326, and plated onto SC-Leu media, and after 2 days of growth, replica-plated onto SC-Leu plates containing 5-FOA, to evict the pBL304 plasmid. Plasmid DNA was isolated from positive colonies and re-applied to the same screen. The pBL249 isolates from the second screen that allowed yeast growth without pBL304 were sequenced. The most robust suppressor *pol30-rb1* carried six non-synonymous mutations (F12Y, D17A, Q29H, K31R, I52M, I100T). Each mutation was separately reverted back to wild-type and loss of suppression assessed. From this analysis, we determined that the Q29H mutation was essential for suppression, and K31R increased suppression. Therefore, *pol30-rb2* contains only the Q29H and K31R mutations.

DNA replication assays – Assays contained 20 mM Tris-HCl pH 7.8, 1 mM DTT, 100 μ g/ml bovine serum albumin, 8 mM magnesium acetate, 0.5 mM ATP, 100 μ M each of dCTP, dGTP, and dTTP, 10 mM of [α -³²P]dATP, 100 mM NaCl, 3.5 nM single-stranded bluescript DNA, singly primed at positions 592-621, either with a 30-mer DNA primer or 5'-RNA₈DNA₂₂ primer, 400 nM RPA, and PCNA or *pca-rb2* as indicated. PCNA was loaded onto the primed DNA by incubation with 7 nM RFC at 30 °C for 1 min prior to reaction initiation. Reactions were initiated by addition of 7 nM Pol δ or RbPol δ . In the assays in Figure 2D, 7 nM FEN1 and 14 nM DNA ligase I were added together with the polymerase. Aliquots were taken at various time points and stopped with 50 mM EDTA and 0.2% SDS, final concentration. Reactions were either resolved on a 1% alkaline agarose gel (Figure 2B) or a 1% neutral agarose gel containing 0.5 μ g/ml ethidium bromide. Gels were dried and documented by PhosphorImager analysis (GE Healthcare). Alternatively, 1 ml of 10% trichloroacetic acid was added to stopped replication samples. After 10 min on ice, the mixture was filtered over a GF/C filter, The filter was washed twice with 2 ml of 1M HCl and 0.05 M sodium pyrophosphate, rinsed with ethanol, dried, and counted in counting fluid in a liquid scintillation counter. All assays were carried out in duplicate or triplicate, and either representative gels are presented or standard errors are shown (Figure 2C).

RESULTS AND DISCUSSION

Designing the Rb69-Pol3 polymerase fusion gene – Bacteriophage T4 expresses a replication elongation apparatus consisting of a B-family DNA polymerase, a homotrimeric replication clamp gp45, which is the ortholog of eukaryotic PCNA, and an ATP-dependent clamp loader. While extensive biochemical and genetic DNA replication studies are available for the T4 system (48,49), we focused our attention on the highly related bacteriophage Rb69, because its DNA polymerase has been the subject of detailed structural characterization (3,50). Rb69 DNA polymerase can efficiently substitute for T4 DNA polymerase in faithfully replicating the T4 genome (51). The closest eukaryotic homologue to these bacteriophage enzymes is Pol3, the catalytic subunit of Pol δ . T4 and Rb69 DNA polymerase (Rb-Pol) not only carry out high-fidelity DNA replication, but are also responsible for the proper maturation of Okazaki fragments during phage DNA replication. The latter activity is allocated solely to Pol δ in eukaryotic cells (52). Figure 1A shows a structural comparison between Rb69-Pol and aa95-985 of the 1097aa yeast Pol3 (3,53). The structures of both enzymes were solved in a complex with template-primer and a base-paired dNTP. The Pol3 structure comprises the structured NTD and the exonuclease and polymerase domains, but lacks the unstructured N-terminal tail and its CTD. The CTD of Pol α serves as a structural model for this domain in the other B-family DNA polymerases (19,20).

We decided to fuse Rb69-Pol (1-896), which lacks only the C-terminal 7aa that mediate interactions with its gp45 clamp (54), to the CTD (981-1097) of Pol3 (Figures 1A and 2A). This CTD contains a putative PCNA-binding motif (996-1005) (40), and the two 4-cysteine cluster metal binding sites, starting at aa1009 (21). The fusion gene is designated as *pol3-69* and the resulting three-subunit variant of Pol δ as RbPol δ . First, we established that the fusion polypeptide contained the necessary determinants for expressing a stable 3-subunit enzyme in yeast, which it does (Figure 2A). Preliminary biochemical studies showed that the replication activity by the fusion enzyme was stimulated by PCNA, but much less so than wild-type Pol δ (see below). Therefore, it was not surprising that the *pol3-69* fusion gene failed to complement the lethality of a *pol3 Δ* mutant (Figure 1B). Among the potential reasons for this failure to complement could be: (i) that the fusion protein lacked essential interactions with other replication proteins, e.g. though its NTD; (ii) that either the

fidelity or rate of replication by the RB69 catalytic domains was incompatible with yeast genome replication; (iii) that, for structural reasons, the fusion protein failed to properly present its PCNA-binding domains to PCNA for highly processive DNA replication. We pursued the latter possibility, particularly because we noted that the PCNA binding motifs on the CTD of the catalytic subunit are located close to the fusion point. We therefore tested whether we could select for PCNA mutations that might ameliorate the processivity defect and thereby allow growth of *pol3-69*. A yeast *pol3 Δ* strain containing both *POL3* and *pol3-69* on separate plasmids was transformed with a heavily mutagenized *POL30* library, encoding PCNA. Transformants were replica-plated onto 5-fluoroorotic acid-containing media (5-FOA), which evicted the wild-type *POL3* plasmid, enforcing viability of the *pol3-69* mutant for cell growth. We isolated two PCNA suppressor mutants of which only one, designated *pol30-rb1*, showed robust growth. The *pcna-rb1* mutant carried six amino acid changes. By subsequent elimination analysis, we determined that the Q29H mutation was essential for suppression of lethality, while the additional K31R mutation increased the efficiency of suppression to that of the *pol30-rb1* suppressor containing all six mutations (Figure 1B and data not shown). These two mutations are localized adjacent to each other on the outer rim of the PCNA donut, close to the interaction pocket of many PCNA-interacting proteins (Figure 1C). All further studies were carried with this double mutant, which we designate as *pol30-rb2*.

Biochemical activities of RbPol δ – We next investigated the replication properties of RbPol δ with either wild-type PCNA or the double mutant *pcna-rb2* (Figure 2B). While wild-type PCNA stimulated the replication activity of RbPol δ (Figure 2B, compare lanes 6,7 with 5), it did not replicate as efficiently as Pol δ . The defect was somewhat suppressed at higher concentrations of PCNA (lanes 8,9; Figure 2C), consistent with an impaired stability of the the DNA-PCNA-RbPol δ complex. Significantly, the mutant *pcna-rb2* clamp largely suppressed this processivity defect, allowing more rapid DNA synthesis at lower concentrations than wild-type PCNA did (Figure 2B,C). Rb69 DNA polymerase itself showed no processive DNA synthesis with either wild-type PCNA or *pcna-rb2*.

In addition to the elongation of Okazaki fragments, another essential function of Pol δ is the maturation of these fragments (55). During this process, Pol δ coordinates with the flap endonuclease FEN1 to remove a 7-10 nt RNA primer and replace it with DNA during a process called nick translation, in order to generate a DNA-DNA nick that can be sealed by DNA ligase I. In our biochemical assay, the polymerizing complex encounters an 8 nt RNA primer when it has completely replicated around the 3 kb DNA circle as shown in Figure 1D. The RNA is degraded by iterative steps of Pol δ -mediated strand displacement synthesis of 1-2 ribonucleotides, followed by FEN1 cutting of the emerging 5'-flap (56). Finally, after all RNA has been degraded, DNA ligation is mediated by DNA ligase I. With wild-type Pol δ and PCNA, this reaction is essentially complete after 3 min, and substituting *pcna-rb2* did not affect the kinetics (Figure 2D). In contrast, Rb-Pol δ only completed replication and subsequent Okazaki fragment maturation when the suppressor *pcna-rb2* was present, and not with wild-type PCNA. These data suggest that the lethality of the *pol3-69* fusion mutant may result not just from inefficient elongation of replication, but perhaps even more from the inability to perform efficient Okazaki fragment maturation, with the suppressor mutant *pol30-rb2* largely overcoming these deficiencies.

Fidelity defects associated with Rb69 polymerase activity – Having established that the suppressor *pcna-rb2* largely restored processive functionality to RbPol δ *in vitro*, we next asked which potential defects were associated with the genome being replicated by RbPol δ . All genetic studies were carried out in a *POL30/pol30-rb2* heterozygous background, comparing the phenotypes of *pol3-69* with that of *POL3*. While the *pol3-69* fusion allele showed robust growth at 30 °C, it was cold-sensitive for growth at 15 °C (Figure 3B). Secondly, the Pol32 subunit is non-essential in yeast, even though many phenotypic defects are associated with *pol32Δ* mutants (29,56-58). However, *pol32Δ* showed synthetic lethality with *pol3-69*, suggesting that the activity of RbPol δ lacking Pol32 was unacceptably compromised (Figure 3A). The *pol30-69* mutant was sensitive to the replication inhibitor hydroxyurea (Figure 3B), but not to the topoisomerase inhibitor camptothecin, which induces double stranded breaks (data not shown). However, the mutant was significantly more sensitive to UV irradiation than wild-type *POL3*.

We combined the *pol3-69* allele with a deletion of *REV3*, the catalytic subunit of Pol ζ , and/or with a deletion of *RAD30*, which encodes Pol η . Pol ζ is responsible for the bulk of damage-induced mutagenesis in the cell (11,59), and Pol η mediates mostly error-free bypass of pyrimidine dimers (60). While defects in these damage-response mechanisms showed a slight increase in damage sensitivity, it was not profound, suggesting that no specific pathway was inactivated in *pol3-69* (Figure 3B).

Despite being responsible for the replication of a relatively small genome, Rb69 DNA polymerase shows a remarkably high replication fidelity (61). We determined whether this high fidelity phenotype was preserved in yeast, using the *CAN1* gene as a target for forward mutagenesis. In the *pol3-69* mutant, canavanine-resistant mutations occurred at an 8-fold increased rate compared to wild-type (Figure 3C). However, defects in the stability of replication complexes can induce the recruitment of Pol ζ , which results in an increased accumulation of mutations (12,62-64). This process is called DRIM (defective replisome-induced mutagenesis). DRIM is under analogous genetic control as damage-induced mutagenesis (62,65). Therefore, we repeated the fluctuation analysis in a *rev3Δ* strain, defective for Pol ζ . Indeed, the *pol3-69 rev3Δ* mutant showed a strongly reduced mutator phenotype, being only ~3-fold higher than that of *POL3 rev3Δ*. An analysis of the spectrum of mutations obtained showed that by far the largest class of mutations in the *pol3-69* single mutant are GC→CG transversion mutations that are a classical signature of Pol ζ - and Rev1-dependent activity (Table 1)(17,41,66). Indeed, they are not observed in the *pol3-69 rev3Δ* double mutant. Other types of mutations that are substantially enhanced in *pol3-69* compared to *pol3-69 rev3Δ* are AT→TA transversions and complex mutations, also consistent with Pol ζ - and Rev1-dependent activity (62,66). When the mutation spectrum of the *pol3-69 rev3Δ* strain is compared to that of *POL3 rev3Δ* (63,64,67), substitution mutations in all classes are somewhat enhanced, but the largest increase attributable to RbPol δ are in deletion formation.

Half of the mutants in *pol3-69 rev3Δ* are due to intermediate size deletions (11-64 nt) between direct repeats, 4-8 nt in length (Table I). These deletions are caused by primer misalignment during lagging strand replication by RbPol δ . When Pol ζ is functional, the rate of formation of these deletions is

not significantly altered, suggesting that the misaligned primer does not provoke a TLS response by Pol ζ . Interestingly, the same 4-8 nt direct repeats that cause deletion formation in *pol3-69*, induce duplications in a *rad27 Δ* strain that is defective for FEN1 flap endonuclease, and therefore compromised in Okazaki fragment maturation (68).

Our analysis has shown that the catalytic polymerase and domains of Pol δ can be substituted

with those from a bacteriophage DNA polymerase, provided adaptive mutations are made in PCNA. The N-terminal domain is structurally conserved in all B-family DNA polymerases, and in archaea serves a specific function in the recognition of template uracil residues (15). The function of the NTD in other organisms remains to be determined, but our analysis shows that this NTD does not specify organism-specific essential functions.

Acknowledgments: The authors thank John Majors and Roberto Galletto for critical discussions during the progress of this work.

Conflict of interest: The authors declare no competing financial interests.

Author contributions: J.S., C.S. and P.B. designed experiments and analyzed data. C.S. carried out sequence analyses. J.S. and C.S. performed genetic experiments. J.S. and P.B. carried out biochemical experiments. Manuscript was written by J.S. and P.B.

REFERENCES

1. Drake, J. W. (1991) A constant rate of spontaneous mutation in DNA-based microbes. *Proc Natl Acad Sci USA* **88**, 7160-7164
2. Wang, J., Sattar, A. K., Wang, C. C., Karam, J. D., Konigsberg, W. H., and Steitz, T. A. (1997) Crystal structure of a pol alpha family replication DNA polymerase from bacteriophage RB69. *Cell* **89**, 1087-1099
3. Franklin, M. C., Wang, J., and Steitz, T. A. (2001) Structure of the replicating complex of a pol alpha family DNA polymerase. *Cell* **105**, 657-667
4. Hopfner, K. P., Eichinger, A., Engh, R. A., Laue, F., Ankenbauer, W., Huber, R., and Angerer, B. (1999) Crystal structure of a thermostable type B DNA polymerase from *Thermococcus gorgonarius*. *Proc Natl Acad Sci USA* **96**, 3600-3605
5. Burgers, P. M., Koonin, E. V., Bruford, E., Blanco, L., Burtis, K. C., Christman, M. F., Copeland, W. C., Friedberg, E. C., Hanaoka, F., Hinkle, D. C., Lawrence, C. W., Nakanishi, M., Ohmori, H., Prakash, L., Prakash, S., Reynaud, C. A., Sugino, A., Todo, T., Wang, Z., Weill, J. C., and Woodgate, R. (2001) Eukaryotic DNA polymerases: proposal for a revised nomenclature. *J. Biol. Chem.* **276**, 43487-43490
6. Kunkel, T. A., and Burgers, P. M. (2008) Dividing the workload at a eukaryotic replication fork. *Trends Cell Biol* **18**, 521-527
7. Johnson, R. E., Klassen, R., Prakash, L., and Prakash, S. (2015) A Major Role of DNA Polymerase delta in Replication of Both the Leading and Lagging DNA Strands. *Mol Cell* **59**, 163-175
8. Burgers, P. M., Gordenin, D., and Kunkel, T. A. (2016) Who Is Leading the Replication Fork, Pol epsilon or Pol delta? *Mol Cell* **61**, 492-493
9. Daigaku, Y., Keszthelyi, A., Muller, C. A., Miyabe, I., Brooks, T., Retkute, R., Hubank, M., Nieduszynski, C. A., and Carr, A. M. (2015) A global profile of replicative polymerase usage. *Nat Struct Mol Biol* **22**, 192-198
10. Miyabe, I., Mizuno, K., Keszthelyi, A., Daigaku, Y., Skouteri, M., Mohebi, S., Kunkel, T. A., Murray, J. M., and Carr, A. M. (2015) Polymerase delta replicates both strands after homologous recombination-dependent fork restart. *Nat Struct Mol Biol* **22**, 932-938
11. Nelson, J. R., Lawrence, C. W., and Hinkle, D. C. (1996) Thymine-thymine dimer bypass by yeast dna polymerase zeta. *Science* **272**, 1646-1649
12. Northam, M. R., Garg, P., Baitin, D. M., Burgers, P. M., and Shcherbakova, P. V. (2006) A novel function of DNA polymerase zeta regulated by PCNA. *EMBO J* **25**, 4316-4325
13. Johansson, E., and Dixon, N. (2013) Replicative DNA polymerases. *Cold Spring Harb Perspect Biol* **5**, 1-14

14. Fogg, M. J., Pearl, L. H., and Connolly, B. A. (2002) Structural basis for uracil recognition by archaeal family B DNA polymerases. *Nat Struct Biol* **9**, 922-927
15. Wardle, J., Burgers, P. M., Cann, I. K., Darley, K., Heslop, P., Johansson, E., Lin, L. J., McGlynn, P., Sanvoisin, J., Stith, C. M., and Connolly, B. A. (2008) Uracil recognition by replicative DNA polymerases is limited to the archaea, not occurring with bacteria and eukarya. *Nucleic Acids Res* **36**, 705-711
16. Haracska, L., Prakash, S., and Prakash, L. (2003) Yeast DNA polymerase zeta is an efficient extender of primer ends opposite from 7,8-dihydro-8-Oxoguanine and O6-methylguanine. *Mol Cell Biol* **23**, 1453-1459
17. Zhong, X., Garg, P., Stith, C. M., McElhinny, S. A., Kissling, G. E., Burgers, P. M., and Kunkel, T. A. (2006) The fidelity of DNA synthesis by yeast DNA polymerase zeta alone and with accessory proteins. *Nucleic Acids Res* **34**, 4731-4742
18. McCulloch, S. D., and Kunkel, T. A. (2008) The fidelity of DNA synthesis by eukaryotic replicative and translesion synthesis polymerases. *Cell Res* **18**, 148-161
19. Klinge, S., Nunez-Ramirez, R., Llorca, O., and Pellegrini, L. (2009) 3D architecture of DNA Pol alpha reveals the functional core of multi-subunit replicative polymerases. *EMBO J* **28**, 1978-1987
20. Baranovskiy, A. G., Babayeva, N. D., Zhang, Y., Gu, J., Suwa, Y., Pavlov, Y. I., and Tahirov, T. H. (2016) Mechanism of Concerted RNA-DNA Primer Synthesis by the Human Primosome. *J Biol Chem*, in press.
21. Netz, D. J., Stith, C. M., Stumpfig, M., Kopf, G., Vogel, D., Genau, H. M., Stodola, J. L., Lill, R., Burgers, P. M., and Pierik, A. J. (2011) Eukaryotic DNA polymerases require an iron-sulfur cluster for the formation of active complexes. *Nat Chem Biol* **8**, 125-132
22. Makarova, A. V., Stodola, J. L., and Burgers, P. M. (2012) A four-subunit DNA polymerase zeta complex containing Pol delta accessory subunits is essential for PCNA-mediated mutagenesis. *Nucleic Acids Res* **40**, 11618-11626
23. Kilkenny, M. L., De Piccoli, G., Perera, R. L., Labib, K., and Pellegrini, L. (2012) A conserved motif in the C-terminal tail of DNA polymerase alpha tethers primase to the eukaryotic replisome. *J Biol Chem* **287**, 23740-23747
24. Makiniemi, M., Pospiech, H., Kilpelainen, S., Jokela, M., Vihinen, M., and Syvaioja, J. E. (1999) A novel family of DNA-polymerase-associated B subunits. *Trends Biochem Sci* **24**, 14-16
25. Baranovskiy, A. G., Babayeva, N. D., Liston, V. G., Rogozin, I. B., Koonin, E. V., Pavlov, Y. I., Vassilyev, D. G., and Tahirov, T. H. (2008) X-ray structure of the complex of regulatory subunits of human DNA polymerase delta. *Cell Cycle* **7**, 3026-3036
26. Baranovskiy, A. G., Lada, A. G., Siebler, H. M., Zhang, Y., Pavlov, Y. I., and Tahirov, T. H. (2012) DNA polymerase delta and zeta switch by sharing accessory subunits of DNA polymerase delta. *J Biol Chem* **287**, 17281-17287
27. Johnson, R. E., Prakash, L., and Prakash, S. (2012) Pol31 and Pol32 subunits of yeast DNA polymerase delta are also essential subunits of DNA polymerase zeta. *Proc Natl Acad Sci U S A* **109**, 12455-12460
28. Lee, Y. S., Gregory, M. T., and Yang, W. (2014) Human Pol zeta purified with accessory subunits is active in translesion DNA synthesis and complements Pol eta in cisplatin bypass. *Proc Natl Acad Sci USA* **111**, 2954-2959
29. Gerik, K. J., Li, X., Pautz, A., and Burgers, P. M. (1998) Characterization of the two small subunits of *Saccharomyces cerevisiae* DNA polymerase delta. *J Biol Chem* **273**, 19747-19755
30. Sanchez Garcia, J., Ciufu, L. F., Yang, X., Kearsley, S. E., and MacNeill, S. A. (2004) The C-terminal zinc finger of the catalytic subunit of DNA polymerase delta is responsible for direct interaction with the B-subunit. *Nucleic Acids Res* **32**, 3005-3016
31. Reynolds, N., Watt, A., Fantes, P. A., and MacNeill, S. A. (1998) Cdm1, the smallest subunit of DNA polymerase delta in the fission yeast *Schizosaccharomyces pombe*, is non-essential for growth and division. *Curr Genet* **34**, 250-258
32. Liu, L., Mo, J., Rodriguez-Belmonte, E. M., and Lee, M. Y. (2000) Identification of a fourth subunit of mammalian DNA polymerase delta. *J Biol Chem* **275**, 18739-18744
33. Tan, C. K., Castillo, C., So, A. G., and Downey, K. M. (1986) An auxiliary protein for DNA polymerase delta from fetal calf thymus. *J. Biol. Chem.* **261**, 12310-12316

34. Majka, J., and Burgers, P. M. (2004) The PCNA-RFC families of DNA clamps and clamp loaders. *Prog Nucleic Acid Res Mol Biol* **78**, 227-260
35. Moldovan, G. L., Pfander, B., and Jentsch, S. (2007) PCNA, the maestro of the replication fork. *Cell* **129**, 665-679
36. Chilkova, O., Stenlund, P., Isoz, I., Stith, C. M., Grabowski, P., Lundstrom, E. B., Burgers, P. M., and Johansson, E. (2007) The eukaryotic leading and lagging strand DNA polymerases are loaded onto primer-ends via separate mechanisms but have comparable processivity in the presence of PCNA. *Nucleic Acids Res* **35**, 6588-6597
37. Hedglin, M., Pandey, B., and Benkovic, S. J. (2016) Stability of the human polymerase delta holoenzyme and its implications in lagging strand DNA synthesis. *Proc Natl Acad Sci USA* **113**, 1777-1786
38. Stodola, J. L., and Burgers, P. M. (2016) Resolving individual steps of Okazaki fragment maturation at a msec time-scale. *Nat Struct Mol Biol* in press
39. Johansson, E., Garg, P., and Burgers, P. M. (2004) The Pol32 subunit of DNA polymerase delta contains separable domains for processive replication and proliferating cell nuclear antigen (PCNA) binding. *J Biol Chem* **279**, 1907-1915
40. Acharya, N., Klassen, R., Johnson, R. E., Prakash, L., and Prakash, S. (2011) PCNA binding domains in all three subunits of yeast DNA polymerase delta modulate its function in DNA replication. *Proc Natl Acad Sci U S A* **108**, 17927-17932
41. Pavlov, Y. I., Shcherbakova, P. V., and Kunkel, T. A. (2001) In vivo consequences of putative active site mutations in yeast DNA polymerases alpha, epsilon, delta, and zeta. *Genetics*. **159**, 47-64
42. Simon, M., Giot, L., and Faye, G. (1991) The 3' to 5' exonuclease activity located in the DNA polymerase delta subunit of *Saccharomyces cerevisiae* is required for accurate replication. *EMBO J.* **10**, 2165-2170
43. Moarefi, I., Jeruzalmi, D., Turner, J., O'Donnell, M., and Kuriyan, J. (2000) Crystal structure of the DNA polymerase processivity factor of T4 bacteriophage. *J Mol Biol.* **296**, 1215-1223
44. Ayyagari, R., Gomes, X. V., Gordenin, D. A., and Burgers, P. M. (2003) Okazaki fragment maturation in yeast. I. Distribution of functions between FEN1 AND DNA2. *J Biol Chem.* **278**, 1618-1625
45. Fortune, J. M., Pavlov, Y. I., Welch, C. M., Johansson, E., Burgers, P. M., and Kunkel, T. A. (2005) *Saccharomyces cerevisiae* DNA polymerase delta: high fidelity for base substitutions but lower fidelity for single- and multi-base deletions. *J Biol Chem* **280**, 29980-29987
46. Lea, D. E., and Coulson, C. A. (1948) The distribution of the number of mutants in bacterial populations. *J. Genet.* **49**, 264-285
47. Cadwell, R. C., and Joyce, G. F. (1992) Randomization of genes by PCR mutagenesis. *PCR Meth. Appl.* **2**, 28-33
48. Kreuzer, K. N., and Brister, J. R. (2010) Initiation of bacteriophage T4 DNA replication and replication fork dynamics: a review in the Virology Journal series on bacteriophage T4 and its relatives. *Virology J* **7**, 358
49. Noble, E., Spiering, M. M., and Benkovic, S. J. (2015) Coordinated DNA Replication by the Bacteriophage T4 Replisome. *Viruses* **7**, 3186-3200
50. Karam, J. D., and Konigsberg, W. H. (2000) DNA polymerase of the T4-related bacteriophages. *Prog Nucleic Acid Res Mol Biol* **64**, 65-96
51. Dressman, H. K., Wang, C. C., Karam, J. D., and Drake, J. W. (1997) Retention of replication fidelity by a DNA polymerase functioning in a distantly related environment. *Proc Natl Acad Sci U S A* **94**, 8042-8046
52. Nick McElhinny, S. A., Gordenin, D. A., Stith, C. M., Burgers, P. M., and Kunkel, T. A. (2008) Division of labor at the eukaryotic replication fork. *Mol Cell* **30**, 137-144
53. Swan, M. K., Johnson, R. E., Prakash, L., Prakash, S., and Aggarwal, A. K. (2009) Structural basis of high-fidelity DNA synthesis by yeast DNA polymerase delta. *Nat Struct Mol Biol* **16**, 979-986
54. Shamoo, Y., and Steitz, T. A. (1999) Building a replisome from interacting pieces: sliding clamp complexed to a peptide from DNA polymerase and a polymerase editing complex. *Cell.* **99**, 155-166
55. Burgers, P. M. (2009) Polymerase dynamics at the eukaryotic DNA replication fork. *J Biol Chem* **284**, 4041-4045

56. Stith, C. M., Sterling, J., Resnick, M. A., Gordenin, D. A., and Burgers, P. M. (2008) Flexibility of eukaryotic Okazaki fragment maturation through regulated strand displacement synthesis. *J Biol Chem* **283**, 34129-34140
57. Lydeard, J. R., Jain, S., Yamaguchi, M., and Haber, J. E. (2007) Break-induced replication and telomerase-independent telomere maintenance require Pol32. *Nature* **448**, 820-823
58. Hanna, M., Ball, L. G., Tong, A. H., Boone, C., and Xiao, W. (2007) Pol32 is required for Pol zeta-dependent translesion synthesis and prevents double-strand breaks at the replication fork. *Mutat Res* **625**, 164-176
59. Morrison, A., Christensen, R. B., Alley, J., Beck, A. K., Bernstine, E. G., Lemontt, J. F., and Lawrence, C. W. (1989) REV3, a *Saccharomyces cerevisiae* gene whose function is required for induced mutagenesis, is predicted to encode a nonessential DNA polymerase. *J Bacteriol* **171**, 5659-5667
60. Johnson, R. E., Prakash, S., and Prakash, L. (1999) Efficient bypass of a thymine-thymine dimer by yeast DNA polymerase, Poleta. *Science* **283**, 1001-1004
61. Bebenek, A., Dressman, H. K., Carver, G. T., Ng, S., Petrov, V., Yang, G., Konigsberg, W. H., Karam, J. D., and Drake, J. W. (2001) Interacting fidelity defects in the replicative DNA polymerase of bacteriophage RB69. *J Biol Chem* **276**, 10387-10397
62. Northam, M. R., Robinson, H. A., Kochenova, O. V., and Shcherbakova, P. V. (2010) Participation of DNA polymerase zeta in replication of undamaged DNA in *Saccharomyces cerevisiae*. *Genetics* **184**, 27-42
63. Aksenova, A., Volkov, K., Maceluch, J., Pursell, Z. F., Rogozin, I. B., Kunkel, T. A., Pavlov, Y. I., and Johansson, E. (2010) Mismatch repair-independent increase in spontaneous mutagenesis in yeast lacking non-essential subunits of DNA polymerase epsilon. *PLoS Genet* **6**, e1001209
64. Garbacz, M., Araki, H., Flis, K., Bebenek, A., Zawada, A. E., Jonczyk, P., Makiela-Dzbenska, K., and Fijalkowska, I. J. (2015) Fidelity consequences of the impaired interaction between DNA polymerase epsilon and the GINS complex. *DNA Repair (Amst)* **29**, 23-35
65. Wojtaszek, J., Lee, C. J., D'Souza, S., Minesinger, B., Kim, H., D'Andrea, A. D., Walker, G. C., and Zhou, P. (2012) Structural basis of Rev1-mediated assembly of a quaternary vertebrate translesion polymerase complex consisting of Rev1, heterodimeric polymerase (Pol) zeta, and Pol kappa. *J Biol Chem* **287**, 33836-33846
66. Northam, M. R., Moore, E. A., Mertz, T. M., Binz, S. K., Stith, C. M., Stepchenkova, E. I., Wendt, K. L., Burgers, P. M., and Shcherbakova, P. V. (2014) DNA polymerases zeta and Rev1 mediate error-prone bypass of non-B DNA structures. *Nucleic Acids Res* **42**, 290-306
67. Huang, M. E., Rio, A. G., Galibert, M. D., and Galibert, F. (2002) Pol32, a subunit of *Saccharomyces cerevisiae* DNA polymerase delta, suppresses genomic deletions and is involved in the mutagenic bypass pathway. *Genetics* **160**, 1409-1422
68. Tishkoff, D. X., Filosi, N., Gaida, G. M., and Kolodner, R. D. (1997) A novel mutation avoidance mechanism dependent on *S. cerevisiae* RAD27 is distinct from DNA mismatch repair. *Cell* **88**, 253-263
69. Krishna, T. S., Kong, X.-P., Gary, S., Burgers, P. M., and Kuriyan, J. (1994) Crystal structure of the eukaryotic DNA polymerase processivity factor PCNA. *Cell* **79**, 1233-1243
70. Bruning, J. B., and Shamoo, Y. (2004) Structural and thermodynamic analysis of human PCNA with peptides derived from DNA polymerase-delta p66 subunit and flap endonuclease-1. *Structure* **12**, 2209-2219

FOOTNOTES

¹ This work was supported in part by Grants GM032431 from the National Institutes of Health and 2013358 from the U.S.-Israel Binational Science Foundation.

² The abbreviations used are: Pol, DNA polymerase; PCNA, proliferating cell nuclear antigen; RFC, Replication Factor C; RbPol δ , the three subunit Pol δ complex containing the RB69-Pol3CTD fusion subunit; NTD, N-terminal domain; CTD, C-terminal domain; 5-FOA, 5-fluoroorotic acid;

FIGURE LEGENDS

Figure 1. Creating RbPol δ . (A) Structural alignment of yeast Pol3 (PDB: 3IAY, purple) and Rb69 (PDB: 1RG9, green), both in a ternary complex with DNA (template in red, primer in orange; only the DNA bound to Pol3 is shown) and dNTP (3,53). The three main domains are the N-terminal domain (NTD), the exonuclease domain (Exo) and the polymerase domain (Pol). Also shown is the portion of the CTD of yeast Pol1 (PDB: 3FLO) that is conserved with the Pol3 CTD (~1005-1080) (19). The proposed localization of the Zn and [4Fe-4S] metal centers within Pol3 is indicated, although in the Pol α -CTD structure both centers contain Zn. RB69-Pol(1-896) was fused to Pol3(981-1097). No structural model exists for the ~20 aa of Pol3 (dashed line) separating the two structural domains. (B) Serial ten-fold dilutions of *pol3 Δ* strain PY227 containing three plasmids: pBL304 (*URA3, POL3*), pBL309 (*TRP1, POL3*) or pBL326 (*TRP1, pol3-69*), and pBL249 (*LEU2, POL30* or *pol30-rb1 [F12Y,D17A,Q29H,K31R,I52M,I100T]* or *pol30-rb2 [Q29H,K31R]*). Growth on 5-FOA media versus selective complete media indicates that the *pol3-69* fusion allele supports growth, but only when the *POL30* suppressors are present. (C) Location of the *pol30-rb2* suppressor mutations (in red) within PCNA (PDB: 1PLQ) (69). Amino acids in the inter-domain connector loop (IDCL) and C-terminus that interact with a human Pol32 peptide are shown in black (70).

Figure 2. Replication activity of RbPol δ . (A) Top panel, schematic of interactions within RbPol δ . RbPol3 subunit interacts with Pol31 through its [4Fe-4S] cluster. Pol31 interacts with Pol32. Interaction with PCNA is supported through motifs in the Zn-ribbon of RbPol3 and at the C-terminus of Pol32. Lower panel, SDS-PAGE analysis of purified polymerase complexes. RbPol3 co-purifies with stoichiometric levels of Pol31 and Pol32. (B) Alkaline agarose gel electrophoresis of replication products with purified proteins as indicated. Schematic is shown and described in Experimental Procedures. (C) PCNA titration; replication assays were performed with the indicated proteins, as in B, for 60 sec. Incorporation of [α - 32 P] dNTPs was determined by scintillation counting. Activity is represented relative to that of Pol δ with saturating PCNA. Rb69-Pol, RB69 DNA polymerase (D) Okazaki fragment maturation assay; replication products were resolved on an agarose gel containing 0.5 μ g/ml ethidium bromide. Replication assays were performed as in B, except for the addition of both FEN1 and DNA ligase I along with polymerase and dNTPs upon reaction initiation (see Experimental Procedures). Labels at left indicate positions of nicked double-stranded DNA and closed circular double-stranded DNA. The latter has a high mobility in an ethidium bromide-containing gel.

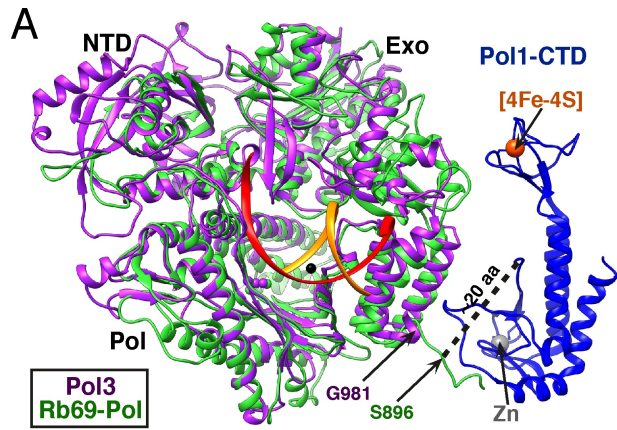
Figure 3. Damage-sensitivity and fidelity phenotypes of the *pol3-69* mutant. (A) The *pol3-69* mutation shows synthetic lethality with *pol32 Δ* . Growth of either *POL3* or *pol3-69* in PY236 (*POL30/pol30-rb2*) and PY243 (*POL30/pol30-rb2 pol32 Δ*) on 5-FOA media, which evicts complementing plasmid pBL304 (*POL3 URA3*), was monitored. (B) Sensitivity of the *pol3-69 POL30/pol30-rb2* strain to low-temperature growth and to DNA damaging agents. Serial ten-fold dilutions of strains PY236 (*REV3 RAD30*), PY237 (*rev3 Δ*), PY238 (*rad30 Δ*), or PY239 (*rev3 Δ rad30 Δ*), containing either *POL3* or *pol3-69*. All strains contain *pol30-rb2* integrated into the chromosomal *LEU2* locus. HU, hydroxyurea. (C) Spontaneous forward mutation rates (with 95% confidence intervals) to canavanine resistance, of PY236 and PY237, containing either *POL3* or *pol3-69*.

TABLE I. Spectra of spontaneous mutations in *pol3-69* mutants

Mutations	<i>WT</i>	<i>rev3Δ</i>	<i>pol3-69</i>		<i>pol3-69 rev3Δ</i>	
	rate	rate	No	rate	No.	rate
Base Substitutions						
GC→AT	4.4	3.3	5	15	11	8
AT→GC	2.1	1.4	1	3	2	1.4
GC→TA	4	1.3	2	6	4	2.7
GC→CG	3	0.5	24	74	0	<0.7
AT→CG	0.8	<0.5	2	6	0	<0.7
AT→TA	0.5	<0.5	9	28	6	4
Indels						
+1	0.7	0.3	0	<3	1	0.7
-1	2.6	1	3	9	3	2.1
-2	1.0	2.0	1	3	3	2.1
Deletions between short direct	<0.5	<0.5	5	15	24	16
	1.5	<0.5	6	18	0	<0.7
Complex ^b	-	-	1	3	0	<0.7
Other ^c						
Total ^a	20.5	11	58	179	54	37
95% C.I.	17-24	9-17		148-217		36-49

^aRates and Confidence intervals (C.I.) are from Figure 3C; ^bspectra from WT and *rev3Δ* are composite from references 63,64,67. ^cComplex mutations are defined as multiple changes within 10 nt. ^cOne duplication between direct repeats.

Figure 1



B

<i>POL3</i>	<i>POL30</i>	Sc media	Sc + 5-FOA media
wt	wt/wt	● ● ● ● ●	● ● ● ● ●
-69	wt/wt	● ● ● ● ●	● ● ● ● ●
wt	wt/-rb1	● ● ● ● ●	● ● ● ● ●
-69	wt/-rb1	● ● ● ● ●	● ● ● ● ●
wt	wt/-rb2	● ● ● ● ●	● ● ● ● ●
-69	wt/-rb2	● ● ● ● ●	● ● ● ● ●

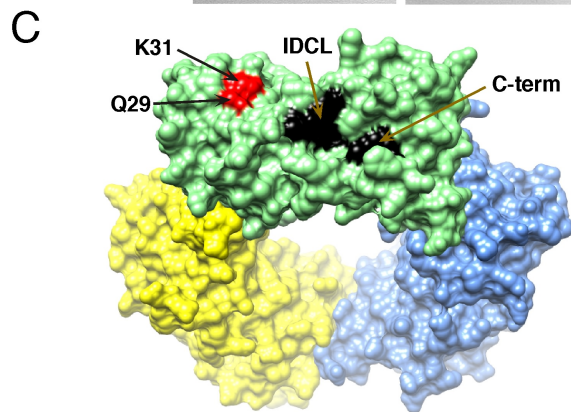


Figure 2

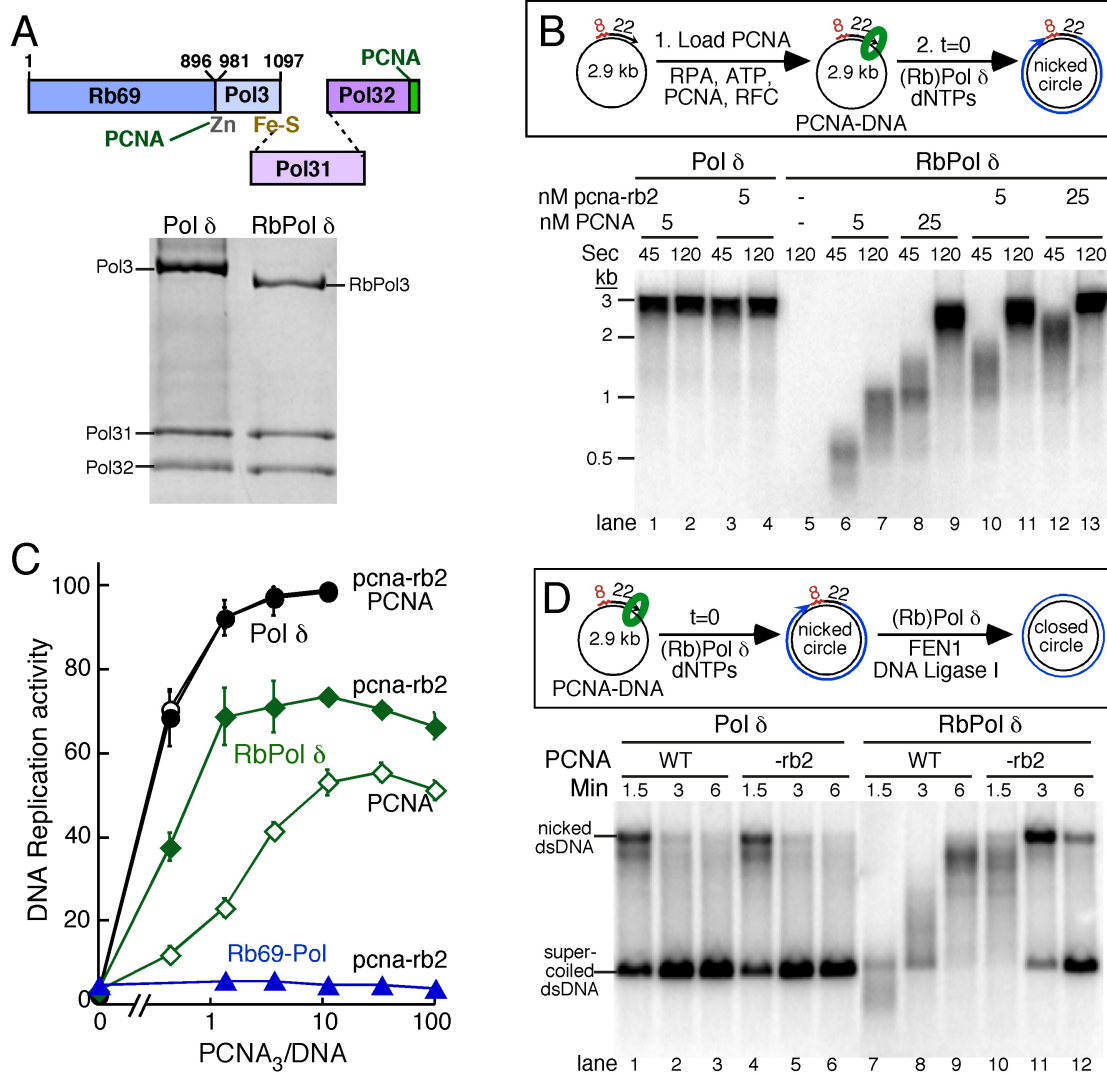
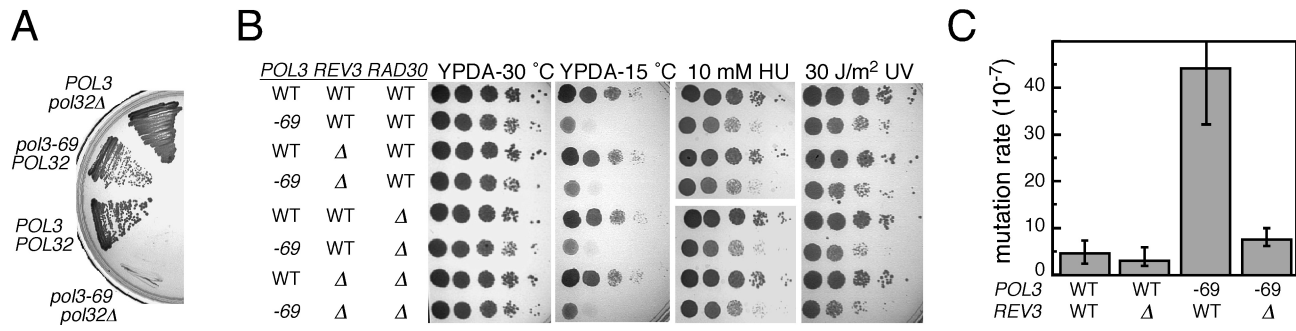


Figure 3



CHAPTER V

Resolving individual steps of Okazaki-fragment maturation at a millisecond timescale

PREFACE TO THE CHAPTER

Chapter V describes my analysis of DNA synthesis, strand displacement synthesis, and nick translation synthesis at high kinetic resolution using a rapid-quench flow apparatus. These lagging strand activities, performed by the PCNA–Pol δ replicase, have been studied *in vitro* by the Burgers lab and other groups for many years. However, the traditional biochemical techniques were limited in their kinetic resolution, and many details concerning how PCNA–Pol δ performs lagging strand synthesis and Okazaki fragment maturation remained unresolved. The studies described in this chapter represent the first pre-steady state analysis of Pol δ in complex with the replication clamp PCNA. These experiments revealed many important details about Pol δ 's activities on the lagging strand, and provided further insight into the multiple controls placed on the replication machinery that serve to limit the production of potentially damaging, long 5'-flaps.

Also included in this study is our continuing interest in evaluating the toolbelt model of PCNA action, which hypothesizes that PCNA can bind multiple enzymes simultaneously (further work in this area is presented in the next chapter). Different from the approach taken in Chapter VI, I used forced single turnover experiments to determine what activities during Okazaki fragment maturation could be performed processively. This technique provided evidence that Pol δ remains stably bound to PCNA while performing strand displacement synthesis and also that FEN1 can remain bound to PCNA through multiple cycles of nick translation. These data taken together provide support for the toolbelt model.

I performed all the experiments presented in this chapter; Peter and I worked together to write the resulting manuscript.

Resolving individual steps of Okazaki-fragment maturation at a millisecond timescale

Joseph L Stodola & Peter M Burgers

DNA polymerase delta (Pol δ) is responsible for elongation and maturation of Okazaki fragments. Pol δ and the flap endonuclease FEN1, coordinated by the PCNA clamp, remove RNA primers and produce ligatable nicks. We studied this process in the *Saccharomyces cerevisiae* machinery at millisecond resolution. During elongation, PCNA increased the Pol δ catalytic rate by >30-fold. When Pol δ invaded double-stranded RNA–DNA representing unmaturing Okazaki fragments, the incorporation rate of each nucleotide decreased successively to 10–20% that of the preceding nucleotide. Thus, the nascent flap acts as a progressive molecular brake on the polymerase, and consequently FEN1 cuts predominantly single-nucleotide flaps. Kinetic and enzyme-trapping experiments support a model in which a stable PCNA–DNA–Pol δ –FEN1 complex moves processively through iterative steps of nick translation, ultimately completely removing primer RNA. Finally, whereas elongation rates are under dynamic dNTP control, maturation rates are buffered against changes in dNTP concentrations.

In eukaryotes, Okazaki-fragment synthesis is initiated by DNA polymerase (Pol) α -primase, which creates a 20- to 30-base primer initiated by approximately 7–10 nt of RNA¹. A conserved and highly regulated process synthesizes lagging-strand DNA from these primers and removes the Pol α -primase-synthesized RNA from each of the ~50 million Okazaki fragments synthesized in mammalian cells, forming continuous double-stranded DNA upon nick ligation². Many different DNA structures are formed during Okazaki-fragment synthesis and maturation, and improper processing of these intermediates is a major cause of genome instability. Moreover, mutations can arise from the incomplete removal of Pol α -synthesized DNA³.

Pol δ performs the bulk of lagging-strand DNA synthesis, extending Pol α primers until reaching the 5' terminus of the preceding Okazaki fragment. In *S. cerevisiae*, Pol δ is a three-subunit complex consisting of Pol3, Pol31, and Pol32 (ref. 4). The catalytic subunit, Pol3, contains both the polymerase and the proofreading 3'–5' exonuclease activities. Each subunit contains motifs that bind to the sliding clamp proliferating cell nuclear antigen (PCNA)^{4–8}. When loaded onto primer termini by replication factor C (RFC) in an ATP-dependent reaction⁹, PCNA increases the intrinsic processivity of Pol δ , allowing it to replicate hundreds of nucleotides in a single DNA binding event¹⁰.

Because Okazaki fragments are initiated with Pol α -synthesized RNA, ligation cannot occur until initiator RNA is removed. This removal requires the joint activity of Pol δ and the structure-specific flap endonuclease I (FEN1). When Pol δ reaches the 5' end of the previous Okazaki fragment, it continues replicating by limited displacement of the RNA primer, forming a 5' flap, which is cut by FEN1. To completely remove the RNA primer, it has been proposed that iterative Pol δ strand displacement and FEN1 cleavage is required,

a process termed nick translation^{11,12}. The forward movement of Pol δ that results in strand displacement is countered by exonucleolytic activity of Pol δ , which reverses this action; repetition of this cycle is known as idling. Idling supports maintenance of the nick position in the absence of other processing activities¹³. Without idling, unregulated strand-displacement synthesis generates problematic long flaps that require alternative processing mechanisms¹⁴ and can cause lethality when FEN1 activity is also compromised¹⁵.

Okazaki-fragment maturation, involving the action of Pol δ , FEN1, and DNA ligase I, is the best-studied example of a sequential multi-enzyme process coordinated by PCNA. For maturation to occur efficiently, cooperation with PCNA must be tightly regulated, and enzymes exchange access for DNA intermediates in a prescribed sequence. Debate remains concerning the mechanism of this cooperation. Because of PCNA's homotrimeric structure, it has been suggested that multiple enzymes may simultaneously bind to PCNA, each occupying a separate monomer; this is called the tool-belt model¹⁶. Biochemical evidence in support of tool-belt models has been reported in bacterial systems^{16,17} and in archaea¹⁸. The alternative model presupposes dynamic binding to and dissociation from PCNA, thus resulting in sequential switching of partners. Use of engineered yeast PCNA heterotrimers has provided biochemical evidence that nick translation does not absolutely require simultaneous binding of Pol δ and FEN1 (ref. 19), but the methodology has not allowed for evaluation of whether this switching actually occurs.

Although the general pathway of Okazaki-fragment maturation has been well established, several critical mechanistic steps have remained unresolved because of the low kinetic resolution of existing studies. With the goal of better understanding how PCNA coordinates multiple enzymes during Okazaki-fragment synthesis and maturation, we

Department of Biochemistry and Molecular Biophysics, Washington University School of Medicine, Saint Louis, Missouri, USA. Correspondence should be addressed to P.M.B. (burgers@biochem.wustl.edu).

Received 18 December 2015; accepted 18 March 2016; published online 11 April 2016; doi:10.1038/nsmb.3207

performed millisecond-resolution kinetic studies with a quench-flow apparatus. This analysis reveals new and unexpected insights into the regulation of 5'-flap generation and processing. Furthermore, our analysis provides evidence for the proposed tool-belt model of the Okazaki-fragment maturation machinery.

RESULTS

PCNA increases the catalytic rate of Pol δ

The experimental design of our studies in the quench-flow apparatus is described in Online Methods. Unless otherwise noted, the exonuclease-deficient Pol δ -DV was used in all experiments to prevent degradation of DNA substrates¹⁵. We started by measuring the rate of incorporation of a single nucleotide by a preformed DNA–Pol δ complex (Fig. 1a); this rate constant is $9 \pm 1 \text{ s}^{-1}$ (Fig. 1b,c). Under our standard assay conditions, binding of the polymerase to DNA was saturated, and the dTTP concentration (250 μM) was near saturation (Supplementary Fig. 1a,b). This rate constant was higher than that observed in a previous analysis of Pol δ (ref. 20) but much slower than previously determined rates of replication by PCNA–Pol δ on RPA-coated single-stranded DNA²¹. We first investigated whether inclusion of RPA enhanced the catalytic rate of Pol δ alone, and we found instead that RPA strongly inhibited incorporation (Supplementary Fig. 1e).

In contrast, when PCNA was loaded onto DNA, we observed that PCNA–Pol δ incorporated a single nucleotide at a rate too fast to be accurately determined in our apparatus ($>300 \text{ s}^{-1}$) (Fig. 1b,c). Because polymerase was prebound to DNA in both experiments, the increase in the rate constant was probably caused by intrinsic stimulation of the nucleotide incorporation rate by PCNA. Whether PCNA enhances the rate of the conformational change of the ternary polymerase–DNA–dNTP complex or the chemical step cannot be distinguished here²². Nevertheless, these data provide evidence that PCNA can actively influence the catalytic activity of a bound enzyme in addition to stabilizing it on DNA.

To determine how RPA influenced the rate of nucleotide incorporation by PCNA–Pol δ , we initiated reactions with dTTP and dATP, allowing the polymerase to incorporate 21 nt (Fig. 1a,d and Supplementary Fig. 1d). For graphical representation, we plotted the median extension product as a function of time (Fig. 1e and description of analysis in Online Methods). At saturating dNTP concentrations (Supplementary Fig. 1c), PCNA–Pol δ synthesized at a rate of $\sim 340 \text{ nt/s}$, with or without RPA (Fig. 1e), thus indicating that RPA does not affect replication of homopolymeric templates. On mixed-sequence DNAs, RPA aids in processivity by resolving secondary structures; however, this stimulation can also be accomplished by heterologous single-stranded binding proteins^{23,24}.

In yeast, dNTP concentrations are only 12–30 μM (ref. 25). When we performed extension reactions with physiological levels of the four dNTPs, replication rates were reduced substantially, to 66 nt/s, thus indicating that these rates are not maximized at normal cellular dNTP levels (Supplementary Fig. 1f,g). These submaximal rates are advantageous for fidelity purposes because proofreading of errors is more efficient at subsaturating dNTP concentrations²⁶. Furthermore, rNTPs, which are present at much higher concentrations than dNTPs, represent a discrimination challenge to DNA polymerases^{25,27}. When we included both dNTPs and rNTPs at physiological concentrations, DNA synthesis by PCNA–Pol δ proceeded at a rate of 51 nt/s (Supplementary Fig. 1f,g), a rate compatible with rates of fork movement in yeast²⁸.

Strand-displacement synthesis by Pol δ

We next observed Pol δ approaching the 5' terminus of a model Okazaki fragment and initiating strand-displacement synthesis. Previous experiments have lacked the kinetic resolution to determine what occurs when Pol δ reaches the double-stranded block and which features of the 5' block determine the kinetics of this process^{21,29}. We annealed the primer and a downstream oligonucleotide block to their

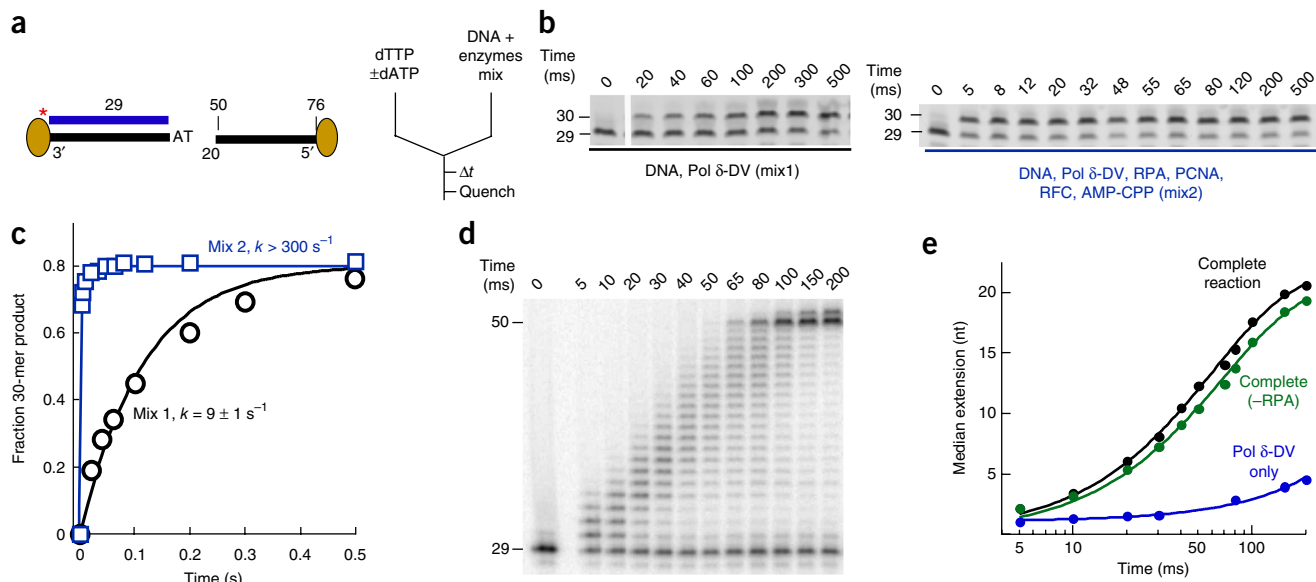


Figure 1 PCNA stimulates the catalytic rate of Pol δ . (a) DNA substrate and rapid-quench experimental setup. Asterisk indicates position of label. (b) Time courses of single-nucleotide incorporation by Pol δ -DV. Reactions contained standard DNA and enzyme concentrations, as described in Online Methods, with or without accessory proteins as defined in ‘mixes’. Reactions were initiated with 250 μM dTTP. (c) Quantification of data in b. Time courses were fit to single exponentials, representative of first-order kinetics (mean \pm s.d.). (d) Replication of a homopolymeric DNA by PCNA–Pol δ . Reactions contained all accessory proteins and were initiated with 250 μM of each dTTP and dATP, allowing extension of 29-mer to a 50-mer product. (e) Quantification of data in d and of Supplementary Figure 1d. Median extension was determined as described in detail in Online Methods. Black, complete reaction containing DNA and Pol δ -DV, RPA, PCNA, RFC, and AMP-CPP; green, reaction containing all components except RPA; blue, reaction containing only DNA and Pol δ -DV.

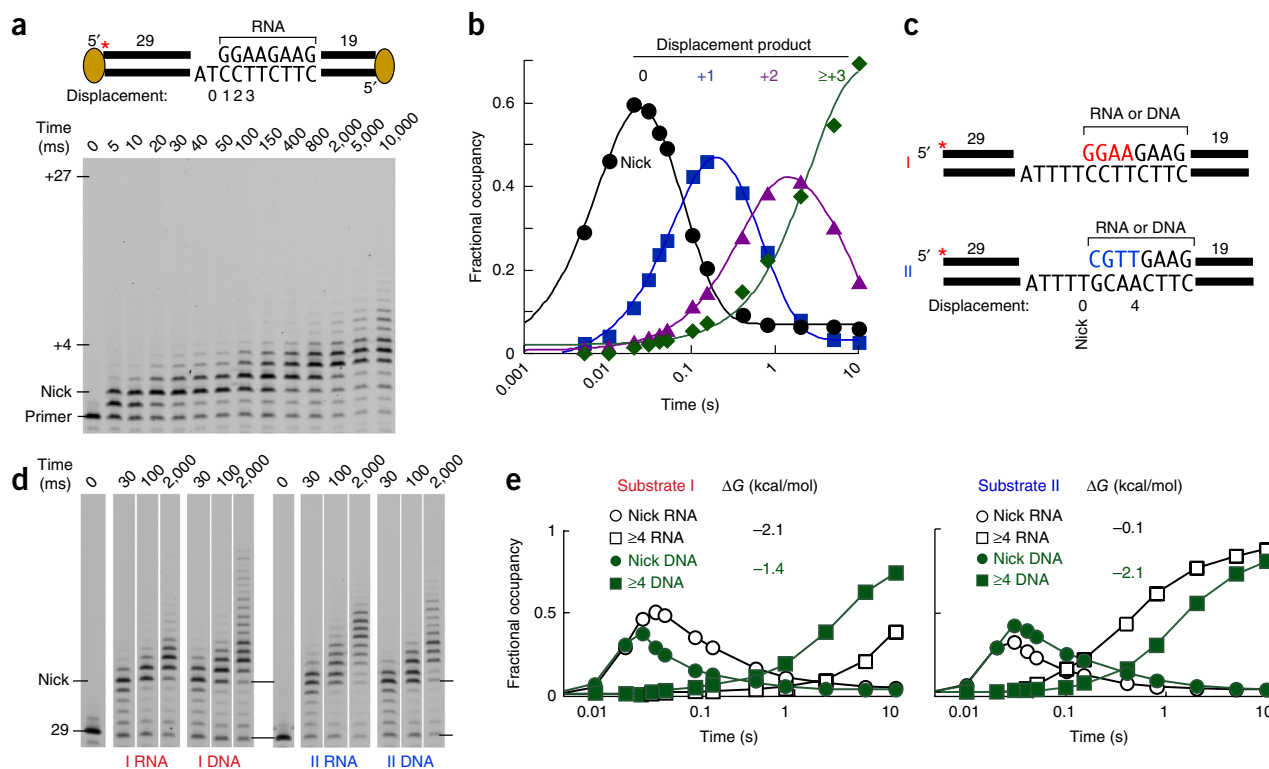


Figure 2 Strand-displacement synthesis by PCNA–Pol δ . **(a)** Top, model of DNA substrate. Strand-displacement positions (nick = 0) are indicated. Block was initiated with RNA₈. Bottom, gel of replication products. Asterisk indicates position of label. **(b)** Quantification of data in **a**. Fractional occupancy of strand-displacement intermediates. Nick position (circles), and strand-displacement products of one (squares), two (triangles), and three or more (diamonds) nucleotides are shown. Time courses were fit to the sum of two exponentials, to model formation and decay of intermediates, with the exception of the $\geq+3$ (green) curve, which was fit to a single exponential. **(c)** Strand-displacement substrates used in **d**, containing a 5-nt gap. Substrate I (red) and substrate II (blue) differ in four nucleotides at the 5' end of the blocking oligonucleotide. Blocks were initiated with either RNA₈ or DNA₈ as indicated. Asterisks indicate position of label. **(d)** Select time points of strand-displacement time courses; full time courses are shown in **Supplementary Figure 2c,d**. **(e)** Fractional occupancy of select replication products from **d**. Nick position (circles) and intermediates four nucleotides or more past the nick (squares) are plotted. Free-energy (ΔG) values of the 5'-terminal 4-bp duplexes were calculated as previously described³⁰.

corresponding templates (**Fig. 2a,c**), leaving either a 2-nt or a 5-nt gap between the primer terminus and block.

We first focused on the substrate with a 2-nt gap and a RNA₈DNA₁₉ block (**Fig. 2a**). We performed rapid-quench kinetic experiments with the complete system (RPA, PCNA, RFC, Pol δ -DV, and α,β -methyleneadenosine 5'-triphosphate (AMP-CPP), as described in **Fig. 1a**) but in the presence of all four dNTPs at saturation. After reaction initiation with dNTPs, Pol δ rapidly extended the primer at 200–300 nt/s. We plotted the fractional occupancy of the nick product and of each strand-displacement product over time (**Fig. 2b**). The final nucleotide closing the gap into a nick was inserted at a rate $\sim 50\%$ that of the normal synthesis rate, thus indicating that the presence of the block is sensed by the polymerase. Pol δ stalled substantially at the nick position (designated as 0), thus indicating that it cannot seamlessly initiate strand displacement. Furthermore, the observed rate of nucleotide incorporation, in which the polymerase invaded the duplex DNA, slowed to 10–20% that of the previous step, from $11.3 \pm 1.0 \text{ s}^{-1}$ for the first nucleotide displaced, to $1.4 \pm 0.2 \text{ s}^{-1}$ for the second, to $0.38 \pm 0.06 \text{ s}^{-1}$ for the third nucleotide. Thus, the nascent flap acts as a progressive molecular brake on the DNA polymerase, limiting formation of longer flaps. Furthermore, this progressive slowdown was not the result of specific DNA or RNA sequences but instead was a consequence of the increasing length of the flap (**Supplementary Fig. 2e–g**). To extend the model-free fitting in **Figure 2b**, we performed global kinetic fitting of these data to two different models. These models are discussed

in detail in **Supplementary Fig. 2a,b** and their implications are considered further in the Discussion.

Given its function in Okazaki-fragment maturation, Pol δ may have evolved the ability to displace RNA–DNA duplexes more readily than DNA–DNA duplexes. We investigated whether either the duplex stability or the sugar identity (RNA versus DNA) is the main determining factor for strand-displacement capacity. We focused on the relative duplex stabilities of the 5'-proximal 4 bp that initially block invasion by Pol δ (**Fig. 2c**). RNA–DNA and DNA–DNA duplex stabilities have been determined by nearest-neighbor analysis³⁰. The RNA–DNA duplex of substrate I was more stable than the DNA–DNA duplex by 0.7 kcal/mol. Pol δ reached the nick at the same rate for both substrates (**Fig. 2d,e** and **Supplementary Fig. 2c**). However, the rate of release from the nick position and strand-displacement synthesis proceeded faster for the DNA–DNA duplex than for the more stable RNA–DNA duplex. When we reversed the duplex stabilities, with the DNA–DNA substrate being more stable, the RNA block was displaced more rapidly than the DNA block (**Fig. 2c–e** and **Supplementary Fig. 2d**). These data suggest that strand-displacement rates are governed primarily by duplex stability rather than by RNA versus DNA identity.

Pol δ idling at a nick

We carried out the studies above with exonuclease-deficient Pol δ -DV, so that calculations of forward polymerization rates were uncomplicated by exonucleolytic degradation. After limited strand displacement,

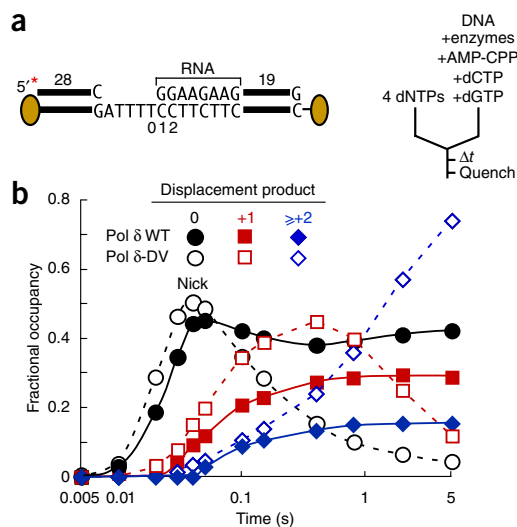
Figure 3 Strand-displacement synthesis and idling by wild-type Pol δ . (a) DNA substrate I. RNA block was preincubated with RPA, PCNA, RFC, AMP-CPP, and Pol δ under standard assay conditions, with 150 μ M dCTP and dGTP to prevent degradation of oligonucleotides by wild-type Pol δ . Asterisk indicates position of label. (b) Distribution of strand-displacement products of Pol δ -DV and wild-type (WT) Pol δ . Quantification of data in **Supplementary Figures 3a** (wild type) and **2c** (DV). Fractional occupancies of the nick position, +1 product, and +2 or more products past the nick are plotted.

wild-type Pol δ degrades DNA back to the nick position, using its exonuclease in a process called idling¹³. To perform experiments with wild-type Pol δ , we assembled replication-competent complexes in the presence of dCTP and dGTP to prevent substrate degradation, and we initiated replication by addition of the four dNTPs (**Fig. 3a**). We compared fractional occupancies of select replication intermediates with those measured with Pol δ -DV (**Fig. 3b** and **Supplementary Fig. 3a**). Replication up to the nick position was comparable for both forms of Pol δ . However, as the wild-type enzyme invaded the nick, it reversed, using its exonuclease activity. As a result, the fraction of nick products did not decay, and in comparison with the results for Pol δ -DV, flap products did not accumulate (**Fig. 3b**). An equilibrium distribution of products maintained by idling was reached within 500 ms. At equilibrium, the fractional occupancy of nick product was comparable to that of all flap products combined, thus suggesting that the rate of degradation was comparable to that of strand displacement of the first nucleotide (~ 10 s⁻¹). Rates of strand displacement by wild-type Pol δ were also governed by the stability of the block. A more stable block yielded an equilibrium distribution of extension products favoring the nick product and shorter flaps (**Supplementary Fig. 3b–d**).

FEN1 processes single-nucleotide flaps

We next reconstituted nick-translation synthesis, which requires coordinated action of Pol δ and FEN1. Structural and mechanistic studies have shown that FEN1 does not simply cut 5' flaps at their base, as generally depicted, but binds a single 3' extrahelical nucleotide into a specificity pocket, then cuts the 5' strand one nucleotide into the double-stranded DNA, which itself has become partially unpaired³¹. For a single-nucleotide 5' flap, which can equilibrate into a 3' flap, the proposed cleavage mechanism is depicted in **Figure 4a**. Previous studies have shown that the major product produced by FEN1 during nick translation is a mononucleotide¹², which is presumably the result of cleavage following formation of a 1-nt flap by Pol δ . However, many studies have shown that the 1-nt flap is not the preferred substrate for FEN1; instead, FEN1 cuts double-flap structures with a single-nucleotide 3' flap and a variable-length 5' flap much more avidly^{31–33}. Indeed, in our sequence context, double-flap substrates were cut faster than the single nucleotide flap (**Supplementary Fig. 4i**). Given the temporal resolution of our system, we were able to determine which strand-displacement products provide substrates for FEN1. We labeled DNA substrates in various positions (**Fig. 4b**) to monitor different enzyme activities. Then we initiated reactions with dNTPs together with FEN1 (**Fig. 4b**). Addition of FEN1 did not alter the rate at which Pol δ reached the nick position or the rate of +1 extension-product formation (**Fig. 4b** and **Supplementary Fig. 4a,b**). However, the addition of FEN1 led to a very rapid decay of the +1 extension product, thus suggesting that FEN1 acted on this substrate (**Fig. 4c**).

We also monitored the production of FEN1-digestion products. The mononucleotide product predominated, but dinucleotides and trinucleotides were also formed (**Supplementary Fig. 4c**). The 1-nt cleavage product formed with kinetics that lagged behind the formation of the +1 displacement product but preceded formation of



the +2 displacement product (**Fig. 4c**), thus indicating that the 1-nt cleavage product resulted from the displacement of a single nucleotide. If reequilibration of the single-nucleotide 5' flap into a 3' flap is a prerequisite for FEN1 activity, reequilibration must occur at a timescale faster than cutting (>5 s⁻¹). Products of 2 nt and 3 nt resulted from processing of longer flaps that accumulated at later times (**Supplementary Fig. 4d**). Efficient flap cleavage relied on the interaction between PCNA and FEN1. The PCNA-defective mutant FEN1-p³⁴ was strongly compromised in cutting flaps generated by PCNA–Pol δ (**Fig. 4d** and **Supplementary Fig. 5e**).

The prediction from these studies is that relative rates of strand-displacement synthesis through sequences with different stabilities determine the distribution of FEN1 products. This is indeed what we observed; on our most stable substrate (substrate III), strand-displacement synthesis proceeded much more slowly than on the standard substrate (**Supplementary Fig. 2f,g**), and FEN1 products longer than the mononucleotide were negligible (**Supplementary Fig. 4e–g**). From these data sets, we conclude that the major FEN1 substrate during nick translation is a single-nucleotide flap and not the double flap that is more active in FEN1 cutting.

Coupling strand displacement to FEN1 action

A central proposal in the current view of nick translation is its coupled, reiterative nature, i.e., that multiple cycles of strand displacement and FEN1 cutting of predominantly 1-nt flaps removes the initiator RNA. As such, we predict that first, FEN1 cuts iteratively at every position in the downstream oligonucleotide, in effect producing a ladder of products, and second, the degradation of the downstream oligonucleotide should match the extension of the primer oligonucleotide. To visualize all intermediates of FEN1 cutting, we labeled the 3' end of the blocking oligonucleotide (**Fig. 4b**). Indeed, we observed a ladder of downstream oligonucleotides resulting from regular and reiterative FEN1 cutting. To examine polymerase–FEN1 coupling, we compared the median primer length of products replicated past the nick position with the median length of 3'-labeled oligonucleotides cut by FEN1 (**Fig. 4b,e**). When plotted, the slopes were nearly equivalent, with the median primer length increasing at ~ 5 nt/s and the median downstream oligonucleotide degrading at ~ 4 nt/s. This inverse relationship suggests a tight coupling of strand displacement and FEN1 nuclease activity during nick translation.

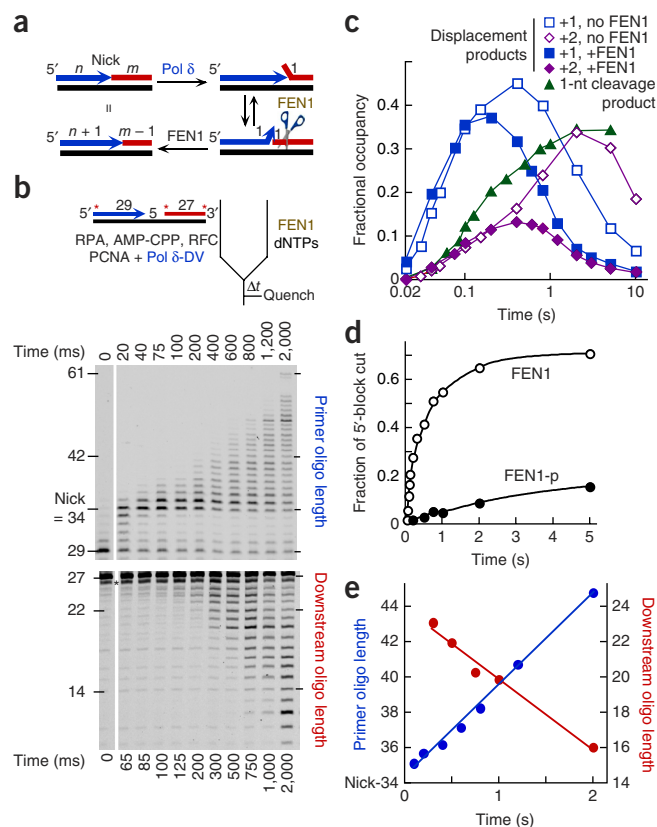
If polymerization during nick translation were rate limiting, a decrease in dNTP concentrations from saturating to physiological

Figure 4 Nick translation by Pol δ and FEN1. (a) Model for the FEN1 mechanism in nick translation n and m are arbitrary DNA lengths. (b) Top, design of the nick translation assay. DNA templates (substrate I RNA block) contained a 5'-primer label, a 5'-block label, or a 3'-block label. 5'-primer labeling reports extension by Pol δ . 5'-block labeling measures the first product released by FEN1. 3'-block labeling measures how far FEN1 has cut into the block. The PCNA–Pol δ complex was preformed, and reactions were initiated with dNTPs plus 40 nM FEN1. Top gel, primer extension (5'-labeled primer); bottom gel, FEN1 cleavage of block (3'-labeled block). Asterisk, nonspecific band; oligo, oligonucleotide. (c) Quantification of data in b (top gel, +FEN1), **Supplementary Figure 2c** (substrate I RNA, no FEN1), and **Supplementary Figure 4c** (fraction of 1-nt product). (d) 5'-labeled-block products cut by FEN1 or FEN1-p (40 nM). Fraction cut is the sum of 1-, 2-, and 3-nt products. (e) Quantification of data in b. Blue, median extension product past the nick position (left y axis) derived from the top gel; red, median cleavage product (right y axis) derived from the bottom gel. Analysis of the FEN1-generated products (bottom gel) was started at the 300-ms time point, at which substantial FEN1-mediated degradation had occurred. Asterisk denotes the presence of contaminants in the oligonucleotide, which precluded accurate quantification of products at earlier time points.

levels should decrease the nick-translation rate to ~25%, as observed with unimpeded elongation (**Supplementary Fig. 1g**). We performed nick translation assays at physiological dNTP concentrations. Primer-elongation rates during the linear range of nick translation were comparable at both saturating and physiological dNTP concentrations (**Supplementary Fig. 4h**), thus indicating that other steps during nick translation are likely to be rate limiting.

Experimental evaluation of the PCNA tool-belt model

Interaction with PCNA allows Pol δ to replicate single-stranded DNA processively, but the extent to which PCNA–Pol δ can perform processive strand-displacement synthesis, and whether a stable PCNA–Pol δ –FEN1 complex exists that performs processive nick translation, remains unresolved. To determine whether PCNA–Pol δ can processively replicate through a typical Okazaki-fragment primer (~7–10 nt), we used heparin to trap free Pol δ that had dissociated from DNA (**Fig. 5a**). In the absence of PCNA, 10 $\mu\text{g/ml}$ heparin completely inhibited Pol δ even when the polymerase was prebound to DNA (**Fig. 5a**, lanes 1 and 2). A second control experiment showed that pretrapped Pol δ could not bind PCNA–DNA, and replication was inhibited (lanes 9 and 10). However, when Pol δ was prebound to PCNA–DNA, challenge with heparin upon initiation with dNTPs did not cause a decrease in strand-displacement products after 5 s, and we observed only a partial decrease after 20 s (lanes 3–6), thus indicating



that the complex is processive at the timescale during which nick translation normally occurs. Processive strand-displacement synthesis occurred through either DNA or RNA blocks, and at saturating or physiological dNTP levels (**Fig. 5a** and **Supplementary Fig. 5a,b**).

Second, we asked whether FEN1 also acted processively during nick translation. Because heparin inhibited FEN1 under all conditions (data not shown), we used an oligonucleotide-trap substrate with a structure representing the optimal substrate for FEN1 (**Supplementary Fig. 5e**). This trap did not inhibit strand-displacement synthesis by Pol δ (**Fig. 5b**, lanes 1–4). In a control experiment, when FEN1 was prebound to the oligonucleotide trap before reaction initiation with dNTPs, we observed no products longer than the expected strand-displacement products (lanes 3 and 4 and 9 and 10), thus indicating that the trap did not inhibit strand-displacement synthesis but did inhibit FEN1. In addition, preincubation of FEN1 with the trap blocked cleavage of a preformed flap-containing DNA (**Supplementary Fig. 5e**). However, when FEN1 was allowed to assemble onto the DNA–PCNA–Pol δ complex before addition of dNTPs with the DNA trap, very long extension products were formed, consistently with FEN1 acting processively during multiple cycles of nick translation (**Fig. 5b**, lanes 5 and 6 and 7 and 8). The processivity of nick translation was not absolute, because more efficient nick translation was observed in the absence of the trap, which allowed reloading of dissociated FEN1. One caveat of this experiment is that,

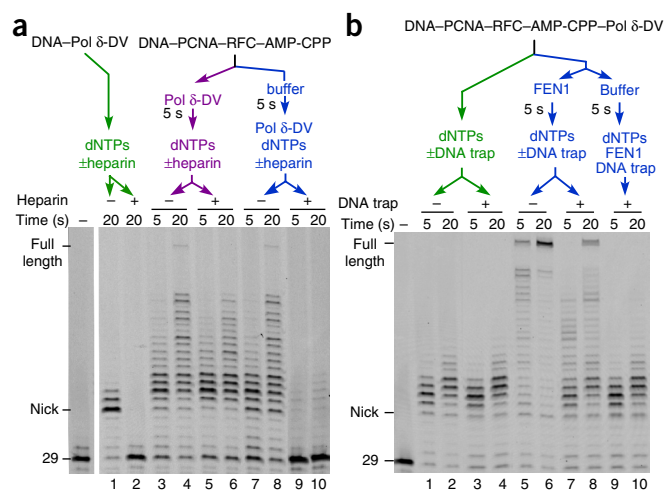


Figure 5 Processivity of the nick-translation machinery. (a) Strand-displacement synthesis by PCNA–Pol δ on the substrate I DNA block. Reactions were initiated with 250 μM dNTPs with or without 10 $\mu\text{g/ml}$ heparin. (b) Nick translation assay; forced single turnover of 40 nM FEN1. The DNA template was substrate I RNA block. Reactions were initiated with 250 μM dNTPs, with or without 6 μM oligonucleotide FEN1 trap (**Supplementary Fig. 4i**, bottom DNA).

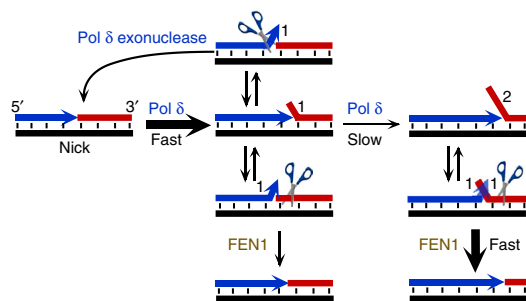


Figure 6 Model for short-flap maintenance and nick translation. Details are in main text.

because the DNA trap does not trap Pol δ , we formally cannot exclude the possibility that some polymerase dissociated and rebound during nick translation, even while FEN1 remained bound. However, because FEN1 remained processive, a DNA–PCNA–Pol δ –FEN1 complex that advances nick translation must exist.

These processive activities are completely dependent on the interaction of FEN1 with PCNA, because they were abrogated when we used the PCNA-interaction-defective mutant FEN1-p (Supplementary Fig. 5c). Stable FEN1 binding to PCNA during nick translation did not depend on the form of polymerase used, because both exonuclease-deficient Pol δ -DV and wild-type Pol δ showed processive nick translation (Fig. 5b and Supplementary Fig. 5d). In sum, these data provide evidence that the quaternary DNA–PCNA–Pol δ –FEN1 complex performs efficient and processive nick translation.

DISCUSSION

Our high-resolution kinetic analysis has illuminated new aspects of the basic steps of Okazaki-fragment synthesis and maturation. Analysis of the DNA–Pol δ complex yielded the unexpected result that the presence of PCNA greatly accelerated the observed incorporation rate of Pol δ (Fig. 1). This finding was surprising because the leading-strand Pol ϵ shows a high rate of incorporation in the absence of PCNA (~200–300 nt/s), which is comparable to that of PCNA–Pol δ (ref. 35). Furthermore, the orthologous bacteriophage T4 DNA polymerase shows a full catalytic rate of ~400 s⁻¹ in the absence of its PCNA-like replication clamp³⁶. Thus, Pol δ shows two unique PCNA-stimulated activities: catalysis and processivity.

Our analysis focused on strand-displacement synthesis by Pol δ and on nick translation, to determine which activities could act in synergy to restrict flap sizes. When the polymerase enters an RNA–DNA or DNA–DNA block and initiates strand-displacement synthesis, a progressive molecular brake is applied to the polymerase. Reduction of base-pairing energetics at the block alleviates the severity of the molecular brake. We show here that this alleviation can be accomplished by introducing less stable sequences at the block site (Fig. 2), but it can also be accomplished by reducing the salt concentration or raising the assay temperature²¹, or even by mechanically pulling on the displaced strand, as shown by single-molecule techniques³⁷.

Our modeling of the kinetics of strand-displacement synthesis does not currently allow us to conclusively provide a specific molecular mechanism explaining the progressive slowing of the polymerase. We considered two different models in Supplementary Figure 2a,b. It is possible that nucleotide insertion by Pol δ is progressively inhibited by the growing flap (model 1), or that during strand-displacement synthesis, the enzyme equilibrates between an extension-competent form and an extension-incompetent form (model 2), or that a combination of both models occurs. Model 1 does not sufficiently describe

our data because it does not contain steps in which Pol δ switches from its polymerase to its exonuclease domain (idling, Fig. 3) or steps in which the primer terminus is released, thus allowing FEN1 to act (nick translation, Fig. 4). Even though several rates in model 2 remain poorly defined, we believe that this model has merit because it incorporates these additional steps necessary for nick translation.

Several studies, including ours (Supplementary Fig. 4i), have indicated that the 1-nt flap is not the optimal FEN1 substrate^{31,33}. Yet this structure is cut most frequently because it is the substrate presented to FEN1 during nick translation; the rate with which the 2-nt flap is produced from the 1-nt flap is generally lower than that of FEN1 cutting (Fig. 4c). However, if 2-nt or longer flaps are made, albeit infrequently, the increased rate with which they are cut by FEN1 should ensure that flaps generally do not grow to a dangerously long size (Fig. 6).

PCNA's homotrimeric structure has the potential to serve as a binding platform for multiple enzymes simultaneously (the tool-belt model). Previous studies have shown that two functional PCNA monomers are sufficient for full Pol δ activity¹⁹. Because FEN1 binds only a single PCNA monomer³⁸, Pol δ and FEN1 have the potential to remain simultaneously bound to a single PCNA during nick translation. Our data support the model in which a quaternary DNA–PCNA–Pol δ –FEN1 complex performs processive nick-translation synthesis. Evaluating the PCNA tool-belt model *in vivo* remains a challenge. The PCNA interaction defect in FEN1-p not only reduced nuclease recruitment to the emerging flap but also prevented processive action by FEN1 during nick translation (Supplementary Fig. 5c). The latter defect prevents the tool-belt mechanism from operating. Remarkably, despite these defects, FEN1-p (*rad27-p*) mutants show only marginal genetic instability phenotypes in yeast^{34,39}. However, when redundant controls on excessive strand-displacement synthesis are eliminated, such as in a Pol δ exonuclease-defective mutant, the *rad27-p* mutation can cause synthetic lethality⁴⁰. At this point, we are unable to attribute the genetic defect of the *rad27-p* mutant to either the recruitment or processivity defect of FEN1-p.

We show that Pol δ processively performs strand displacement on a timescale relevant for Okazaki-fragment maturation (Fig. 5a); nick translation proceeds at a rate of ~5 nt/s (Fig. 4e), thus suggesting that removal of RNA should generally be accomplished within 2 s. A previous report has determined that Pol δ collision with the 5' end of an Okazaki fragment decreases the affinity of the polymerase for DNA, designated 'collision release'²⁴. Because we found that the whole process should be complete within just a few seconds, our data do not disagree with those from that study, which was carried out on a time scale of minutes. Therefore, although the collision release model may be important under some circumstances, appreciable dissociation of Pol δ occurs too slowly to substantially affect nick translation. It could be argued that at lower, physiological dNTP concentrations, nick translation might occur at a reduced rate. However, we found this not to be the case (Supplementary Fig. 4h). These data suggest that steps other than primer elongation are rate limiting; these steps are likely to involve the consecutive steps of polymerase release, flap reequilibration, FEN1 flap engagement, and cutting. Nucleotide levels in yeast are under dynamic control, for example, during the stress response⁴¹. Our data suggest that, whereas elongation rates are under strict dNTP control, maturation rates are buffered against changes in dNTP concentrations.

The focus of our study has been on Pol δ and FEN1, and their DNA-bound complex with PCNA. DNA ligase I, which completes the process, was not included in this study. In archaeal replication studies, a processive complex of polymerase, FEN1, and ligase with the heterotrimeric PCNA has been observed^{18,42}. It is likely that the eukaryotic machinery works in a slightly different manner. Eukaryotic

DNA ligase I also contains a PCNA-binding domain⁴³, one function of which is recruiting ligase to replication foci⁴⁴. However, previous studies have shown that ligase acts distributively, and the position of ligation after RNA removal is largely dependent on ligase concentrations²¹. In yeast, acute depletion of DNA ligase allows nick translation to proceed up to the dyad of the nucleosome that has been assembled on the completed lagging strand⁴⁵. The analysis of these small fragments has provided valuable information regarding the limits that the cellular environment sets to nick translation by the PCNA–Pol δ –FEN1 complex.

METHODS

Methods and any associated references are available in the [online version of the paper](#).

Note: Any Supplementary Information and Source Data files are available in the [online version of the paper](#).

ACKNOWLEDGMENTS

The authors thank J. Majors, R. Galletto, and T. Lohman for critical discussions during the progress of this work, and C. Stith for protein purification. This work was supported in part by the US National Institutes of Health (GM032431 to P.B.) and from the US-Israel Binational Science Foundation (2013358 to P.B.).

AUTHOR CONTRIBUTIONS

J.L.S. and P.M.B. designed experiments and analyzed data. J.L.S. performed all experiments. J.L.S. and P.M.B. wrote the manuscript.

COMPETING FINANCIAL INTERESTS

The authors declare no competing financial interests.

Reprints and permissions information is available online at <http://www.nature.com/reprints/index.html>.

- Perera, R.L. *et al.* Mechanism for priming DNA synthesis by yeast DNA polymerase α . *eLife* **2**, e00482 (2013).
- Balakrishnan, L. & Bambara, R.A. Eukaryotic lagging strand DNA replication employs a multi-pathway mechanism that protects genome integrity. *J. Biol. Chem.* **286**, 6865–6870 (2011).
- Reijns, M.A. *et al.* Lagging-strand replication shapes the mutational landscape of the genome. *Nature* **518**, 502–506 (2015).
- Gerik, K.J., Li, X., Pautz, A. & Burgers, P.M. Characterization of the two small subunits of *Saccharomyces cerevisiae* DNA polymerase delta. *J. Biol. Chem.* **273**, 19747–19755 (1998).
- Bermudez, V.P., MacNeill, S.A., Tappin, I. & Hurwitz, J. The influence of the Cdc27 subunit on the properties of the *Schizosaccharomyces pombe* DNA polymerase delta. *J. Biol. Chem.* **277**, 36853–36862 (2002).
- Lu, X. *et al.* Direct interaction of proliferating cell nuclear antigen with the small subunit of DNA polymerase delta. *J. Biol. Chem.* **277**, 24340–24345 (2002).
- Netz, D.J. *et al.* Eukaryotic DNA polymerases require an iron-sulfur cluster for the formation of active complexes. *Nat. Chem. Biol.* **8**, 125–132 (2012).
- Acharya, N., Klassen, R., Johnson, R.E., Prakash, L. & Prakash, S. PCNA binding domains in all three subunits of yeast DNA polymerase δ modulate its function in DNA replication. *Proc. Natl. Acad. Sci. USA* **108**, 17927–17932 (2011).
- Tsurimoto, T. & Stillman, B. Functions of replication factor C and proliferating-cell nuclear antigen: functional similarity of DNA polymerase accessory proteins from human cells and bacteriophage T4. *Proc. Natl. Acad. Sci. USA* **87**, 1023–1027 (1990).
- Chilkova, O. *et al.* The eukaryotic leading and lagging strand DNA polymerases are loaded onto primer-ends via separate mechanisms but have comparable processivity in the presence of PCNA. *Nucleic Acids Res.* **35**, 6588–6597 (2007).
- Bhagwat, M. & Nossal, N.G. Bacteriophage T4 RNase H removes both RNA primers and adjacent DNA from the 5' end of lagging strand fragments. *J. Biol. Chem.* **276**, 28516–28524 (2001).
- Stith, C.M., Sterling, J., Resnick, M.A., Gordenin, D.A. & Burgers, P.M. Flexibility of eukaryotic Okazaki fragment maturation through regulated strand displacement synthesis. *J. Biol. Chem.* **283**, 34129–34140 (2008).
- Garg, P., Stith, C.M., Sabouri, N., Johansson, E. & Burgers, P.M. Idling by DNA polymerase delta maintains a ligatable nick during lagging-strand DNA replication. *Genes Dev.* **18**, 2764–2773 (2004).
- Kang, Y.H., Lee, C.H. & Seo, Y.S. Dna2 on the road to Okazaki fragment processing and genome stability in eukaryotes. *Crit. Rev. Biochem. Mol. Biol.* **45**, 71–96 (2010).
- Jin, Y.H. *et al.* The 3'→5' exonuclease of DNA polymerase delta can substitute for the 5' flap endonuclease Rad27/Fen1 in processing Okazaki fragments and preventing genome instability. *Proc. Natl. Acad. Sci. USA* **98**, 5122–5127 (2001).
- Indiani, C., McInerney, P., Georgescu, R., Goodman, M.F. & O'Donnell, M. A sliding-clamp toolbelt binds high- and low-fidelity DNA polymerases simultaneously. *Mol. Cell* **19**, 805–815 (2005).
- Kath, J.E. *et al.* Polymerase exchange on single DNA molecules reveals processivity clamp control of translesion synthesis. *Proc. Natl. Acad. Sci. USA* **111**, 7647–7652 (2014).
- Beattie, T.R. & Bell, S.D. Coordination of multiple enzyme activities by a single PCNA in archaeal Okazaki fragment maturation. *EMBO J.* **31**, 1556–1567 (2012).
- Dovrat, D., Stodola, J.L., Burgers, P.M. & Aharoni, A. Sequential switching of binding partners on PCNA during *in vitro* Okazaki fragment maturation. *Proc. Natl. Acad. Sci. USA* **111**, 14118–14123 (2014).
- Dieckman, L.M., Johnson, R.E., Prakash, S. & Washington, M.T. Pre-steady state kinetic studies of the fidelity of nucleotide incorporation by yeast DNA polymerase delta. *Biochemistry* **49**, 7344–7350 (2010).
- Ayyagari, R., Gomes, X.V., Gordenin, D.A. & Burgers, P.M. Okazaki fragment maturation in yeast. I. Distribution of functions between FEN1 AND Dna2. *J. Biol. Chem.* **278**, 1618–1625 (2003).
- Johnson, K.A. Role of induced fit in enzyme specificity: a molecular forward/reverse switch. *J. Biol. Chem.* **283**, 26297–26301 (2008).
- Burgers, P.M.J. *Saccharomyces cerevisiae* replication factor C. II. Formation and activity of complexes with the proliferating cell nuclear antigen and with DNA polymerases delta and epsilon. *J. Biol. Chem.* **266**, 22698–22706 (1991).
- Langston, L.D. & O'Donnell, M. DNA polymerase delta is highly processive with proliferating cell nuclear antigen and undergoes collision release upon completing DNA. *J. Biol. Chem.* **283**, 29522–29531 (2008).
- Nick McElhinny, S.A. *et al.* Abundant ribonucleotide incorporation into DNA by yeast replicative polymerases. *Proc. Natl. Acad. Sci. USA* **107**, 4949–4954 (2010).
- Kunkel, T.A., Sabatino, R.D. & Bambara, R.A. Exonucleolytic proofreading by calf thymus DNA polymerase delta. *Proc. Natl. Acad. Sci. USA* **84**, 4865–4869 (1987).
- Sparks, J.L. *et al.* RNase H2-initiated ribonucleotide excision repair. *Mol. Cell* **47**, 980–986 (2012).
- Raghuraman, M.K. *et al.* Replication dynamics of the yeast genome. *Science* **294**, 115–121 (2001).
- Podust, V.N., Podust, L.M., Müller, F. & Hübscher, U. DNA polymerase delta holoenzyme: action on single-stranded DNA and on double-stranded DNA in the presence of replicative DNA helicases. *Biochemistry* **34**, 5003–5010 (1995).
- Sugimoto, N., Nakano, S., Yoneyama, M. & Honda, K. Improved thermodynamic parameters and helix initiation factor to predict stability of DNA duplexes. *Nucleic Acids Res.* **24**, 4501–4505 (1996).
- Tsutakawa, S.E. *et al.* Human flap endonuclease structures, DNA double-base flipping, and a unified understanding of the FEN1 superfamily. *Cell* **145**, 198–211 (2011).
- Kaiser, M.W. *et al.* A comparison of eubacterial and archaeal structure-specific 5'-exonucleases. *J. Biol. Chem.* **274**, 21387–21394 (1999).
- Kao, H.I., Henriksen, L.A., Liu, Y. & Bambara, R.A. Cleavage specificity of *Saccharomyces cerevisiae* flap endonuclease 1 suggests a double-flap structure as the cellular substrate. *J. Biol. Chem.* **277**, 14379–14389 (2002).
- Gomes, X.V. & Burgers, P.M.J. Two modes of FEN1 binding to PCNA regulated by DNA. *EMBO J.* **19**, 3811–3821 (2000).
- Ganai, R.A., Osterman, P. & Johansson, E. Yeast DNA polymerase catalytic core and holoenzyme have comparable catalytic rates. *J. Biol. Chem.* **290**, 3825–3835 (2015).
- Capson, T.L. *et al.* Kinetic characterization of the polymerase and exonuclease activities of the gene 43 protein of bacteriophage T4. *Biochemistry* **31**, 10984–10994 (1992).
- Manosas, M. *et al.* Mechanism of strand displacement synthesis by DNA replicative polymerases. *Nucleic Acids Res.* **40**, 6174–6186 (2012).
- Chapados, B.R. *et al.* Structural basis for FEN-1 substrate specificity and PCNA-mediated activation in DNA replication and repair. *Cell* **116**, 39–50 (2004).
- Gary, R. *et al.* A novel role in DNA metabolism for the binding of Fen1/Rad27 to PCNA and implications for genetic risk. *Mol. Cell. Biol.* **19**, 5373–5382 (1999).
- Jin, Y.H. *et al.* The multiple biological roles for the 3'→5' exonuclease of *Saccharomyces cerevisiae* DNA polymerase delta require switching between the polymerase and exonuclease domains. *Mol. Cell. Biol.* **25**, 461–471 (2005).
- Chabes, A. *et al.* Survival of DNA damage in yeast directly depends on increased dNTP levels allowed by relaxed feedback inhibition of ribonucleotide reductase. *Cell* **112**, 391–401 (2003).
- Cannone, G., Xu, Y., Beattie, T.R., Bell, S.D. & Spagnolo, L. The architecture of an Okazaki fragment-processing holoenzyme from the archaeon *Sulfolobus solfataricus*. *Biochem. J.* **465**, 239–245 (2015).
- Vijayakumar, S. *et al.* The C-terminal domain of yeast PCNA is required for physical and functional interactions with Cdc9 DNA ligase. *Nucleic Acids Res.* **35**, 1624–1637 (2007).
- Montecucco, A. *et al.* DNA ligase I is recruited to sites of DNA replication by an interaction with proliferating cell nuclear antigen: identification of a common targeting mechanism for the assembly of replication factories. *EMBO J.* **17**, 3786–3795 (1998).
- Smith, D.J. & Whitehouse, I. Intrinsic coupling of lagging-strand synthesis to chromatin assembly. *Nature* **483**, 434–438 (2012).



ONLINE METHODS

Proteins. RPA⁴⁶, PCNA⁴⁷, RFC⁴⁸, FEN1, and the PCNA-interaction-defective FEN1-p (F346G F347A)³⁴ were purified from *Escherichia coli* overexpression systems, whereas Pol δ and the exonuclease-defective Pol δ -DV (D520V) were purified from yeast overexpression systems⁴⁹.

DNA substrates. All oligonucleotides were obtained from Integrated DNA Technologies and were purified by either polyacrylamide gel electrophoresis or high-pressure liquid chromatography before use. Sequences of oligonucleotides are listed in **Supplementary Table 1**. Primer29, used in all studies, was either 5'-³²P-labeled with T4 polynucleotide kinase (New England BioLabs) and [γ -³²P]ATP, or was ordered with a 5'-Cy3 fluorophore. No difference in primer-extension activity was observed between the different labeling methods. Primer-extension DNA templates were generated by annealing labeled primer and blocking oligonucleotides to the template in a 0.8:2:1 ratio. 3'-labeled block templates were generated by annealing primer and labeled block to the template in a 1.4:0.8:1 ratio, respectively. 5'-labeled block templates were generated by annealing primer and labeled block to the template in a 0.8:1.4:1 ratio, respectively. To hybridize, oligonucleotides were heated to 75 °C in 100 mM NaCl and cooled slowly to room temperature. After hybridization, streptavidin was added in a two-fold molar excess to template-primer substrates. All substrates, except those in **Supplementary Figure 4i**, contain 3'- and 5'-biotin-streptavidin bumpers to support stable PCNA loading by RFC²¹. DNA concentrations in replication assays were calculated according to the labeled oligonucleotide concentration. In strand-displacement templates, the gap between the primer terminus and the 5'-block was limited to either two or five nucleotides to maximize the synchrony of replicating complexes initiating strand-displacement synthesis.

Replication reactions. All replication experiments were performed in a buffer containing 20 mM Tris-HCl, pH 7.8, 1 mM dithiothreitol, 200 μ g/ml bovine serum albumin, 8 mM Mg(OAc)₂, and 100 mM NaCl. Unless otherwise noted, standard reaction conditions were 10 nM DNA template, 40 nM Pol δ (DV or wild type), 30 nM PCNA, 15 nM RFC, 100 μ M α,β -methyleneadenosine 5'-triphosphate (AMP-CPP) for RFC-catalyzed loading of PCNA, and 50 nM RPA for studies in **Figure 1** or 25 nM RPA for all other studies. PCNA loading by RFC is an ATP-dependent process⁹. However, because ATP is also a substrate for Pol δ (ref. 25), it could not be used in our system. Therefore, we replaced ATP with AMP-CPP, which acts efficiently in PCNA loading but cannot be incorporated by the DNA polymerase. The Pol δ -DV (D520V) mutant was used in most reactions, unless otherwise noted. This exonuclease-deficient mutant prevents degradation of oligonucleotide substrates before reaction initiation¹⁵.

Reactions were initiated with 250 μ M of each dNTP, unless otherwise noted. In select experiments, physiological concentrations of the four dNTPs and rNTPs

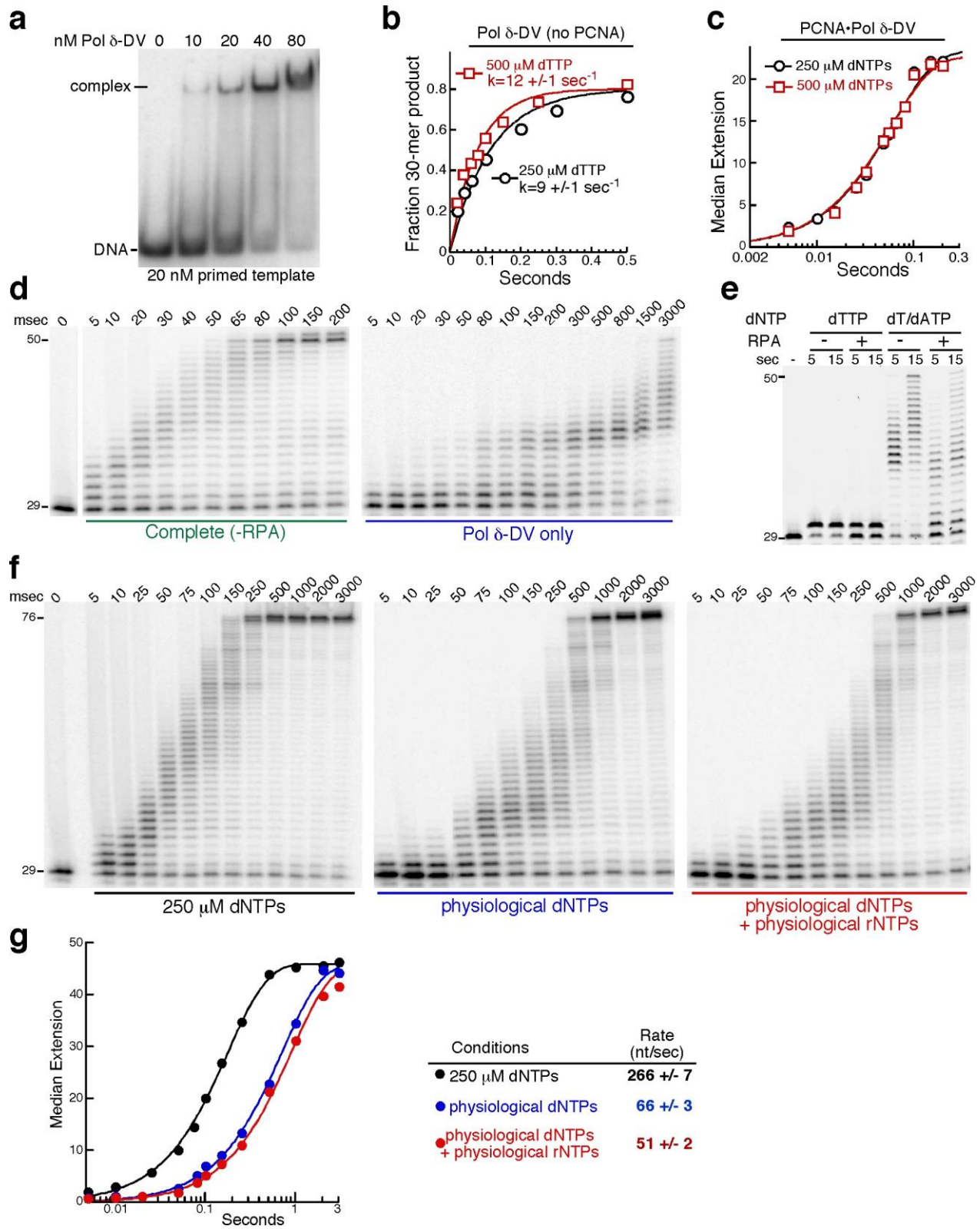
were used; physiological dNTP concentrations in *S. cerevisiae* were 16 μ M dATP, 14 μ M dCTP, 12 μ M dGTP, and 30 μ M dTTP, and the rNTP concentrations were 3 mM ATP, 0.5 mM CTP, 0.7 mM GTP, and 1.7 mM UTP²⁵.

All reactions except those in **Figure 5** and **Supplementary Figure 5** were performed in a quenched-flow apparatus (KinTek RQF-3) maintained at 30 °C with a circulating water bath. DNA templates were preincubated with Pol δ , with or without other protein factors (PCNA, RFC, and RPA) and AMP-CPP as indicated. The preassembled complexes were loaded into one loop of the quenched-flow apparatus. The second loop contained initiating nucleotides (and FEN1 when present) in reaction buffer. Reactions were initiated by mixture of equal volumes and quenched with 200 mM EDTA and 0.2% SDS. DNA products were ethanol-precipitated in the presence of 10 μ g/ml glycogen and resolved on 12–20% denaturing polyacrylamide gels. Gels containing ³²P-labeled DNAs were dried and subjected to PhosphorImager analysis. Gels containing Cy3-labeled DNAs were visualized by detection of Cy3 fluorescence with a Typhoon-Trio (GE Healthcare). All quantifications were carried out with ImageQuant software (GE Healthcare).

Each reaction was performed at least twice under identical conditions. For exact repeats of strand-displacement reactions, variations in the fractional occupancy of specific products did not exceed 0.1, even at the shortest time points. At time points exceeding 50 ms, curves from identical replicates were indistinguishable. Observed rates in all figures are reported to highlight qualitative differences between reaction conditions, with standard errors reported for the fits of individual time courses.

Median analysis. The median analysis method was used to generate the data presented in **Figures 1e** and **4e** and **Supplementary Figures 1c,g** and **4h**. This methodology takes into consideration that complexes do not move with perfect synchrony through the available template, and it is described in detail in the legend to **Supplementary Figure 6**.

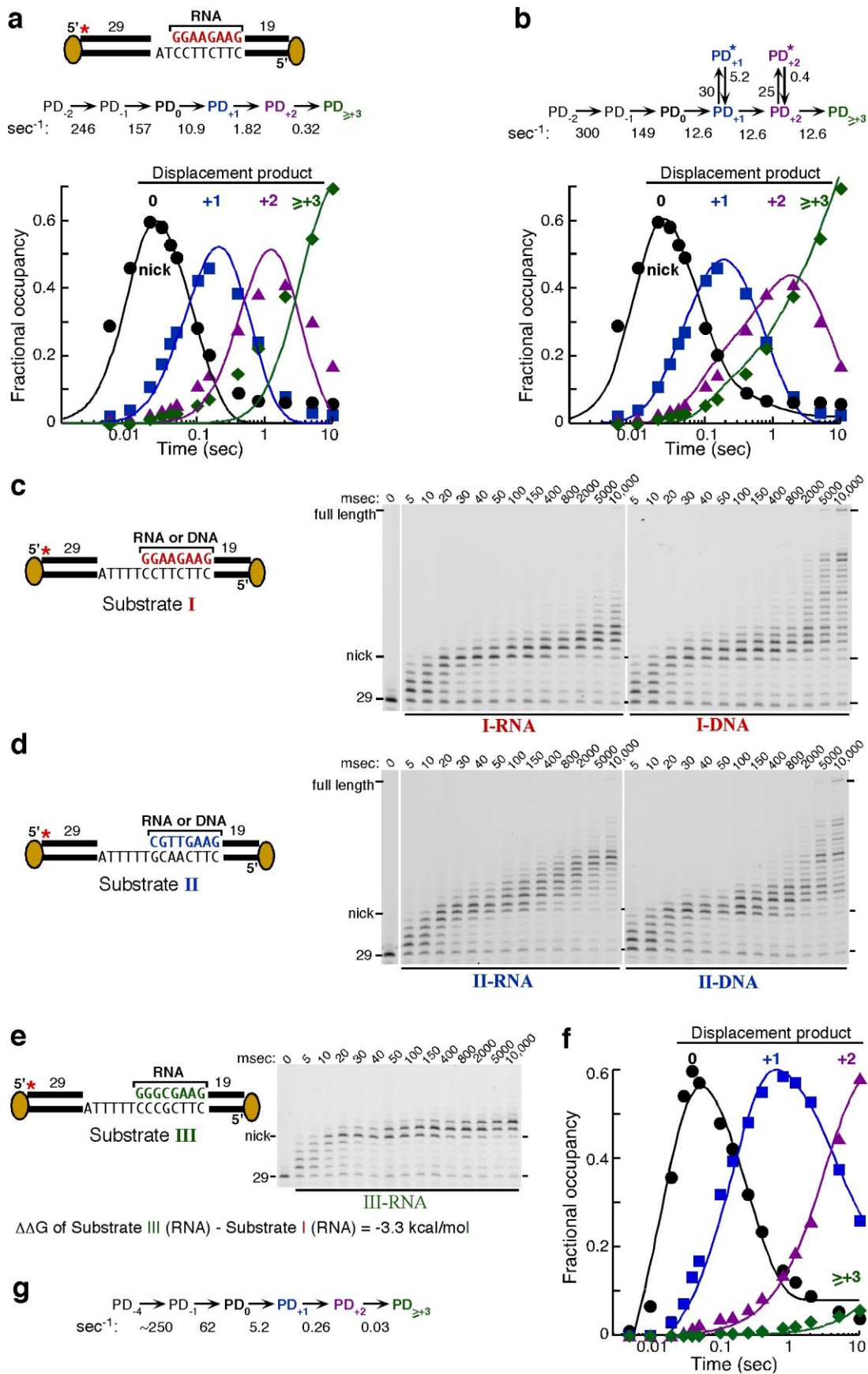
- Henricksen, L.A., Umbricht, C.B. & Wold, M.S. Recombinant replication protein A: expression, complex formation, and functional characterization. *J. Biol. Chem.* **269**, 11121–11132 (1994).
- Eissenberg, J.C., Ayyagari, R., Gomes, X.V. & Burgers, P.M. Mutations in yeast proliferating cell nuclear antigen define distinct sites for interaction with DNA polymerase delta and DNA polymerase epsilon. *Mol. Cell. Biol.* **17**, 6367–6378 (1997).
- Gomes, X.V., Gary, S.L. & Burgers, P.M. Overproduction in *Escherichia coli* and characterization of yeast replication factor C lacking the ligase homology domain. *J. Biol. Chem.* **275**, 14541–14549 (2000).
- Fortune, J.M., Stith, C.M., Kissling, G.E., Burgers, P.M. & Kunkel, T.A. RPA and PCNA suppress formation of large deletion errors by yeast DNA polymerase delta. *Nucleic Acids Res.* **34**, 4335–4341 (2006).



Supplementary Figure 1

Analysis of replication rates by Pol δ .

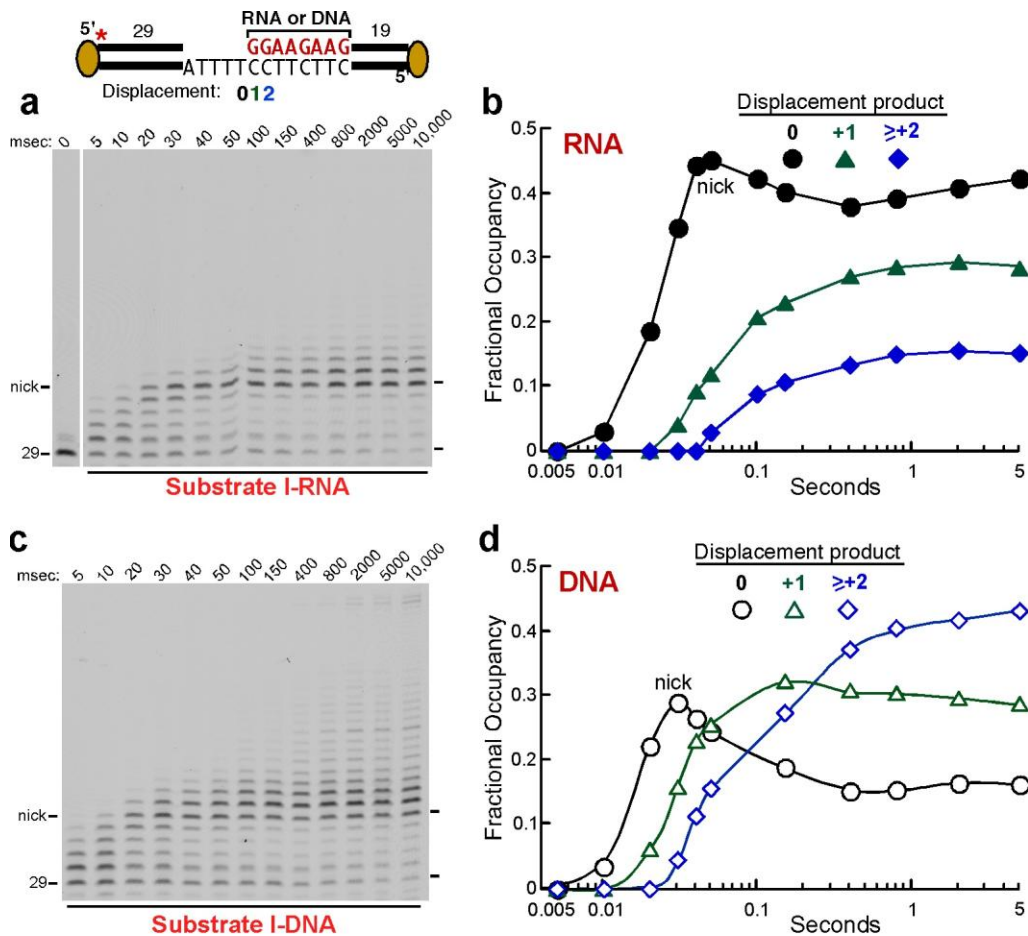
(a) Electrophoretic Mobility Shift Assay (EMSA) of Pol δ -DV binding to template-primer DNA (Fried, M. & Crothers, D.M. Equilibria and kinetics of lac repressor-operator interactions by polyacrylamide gel electrophoresis. *Nucleic Acids Res.* **9**, 6505-6518 (1981)). 20 nM DNA was incubated with increasing concentrations of Pol δ -DV. Complexes were resolved on a 5%, 1X TBE native polyacrylamide gel. Analysis was carried out with 20 nM template as this was the pre-incubation concentration of DNA prior to mixing with an equal volume of dNTP solution in the rapid-quench apparatus. **(b)** Single nucleotide incorporation by Pol δ -DV alone (no PCNA), identical to described in **Fig. 1 b,c**, with either 250 μ M or 500 μ M dTTP. Time courses were fit to single exponentials, representative of first-order kinetics. **(c)** Quantification of replication time courses of a homopolymeric DNA by PCNA-Pol δ . Experiments were performed identically to that in **Fig. 1d**, but with either 250 μ M or 500 μ M each of dTTP and dATP. Median analysis is described in detail in "Supplementary Experimental Procedures". **(d)** Replication through a homopolymeric stretch of DNA by PCNA-Pol δ ; images of gels quantified in **Fig. 1e**. DNA template was pre-incubated with subsets of an enzyme mix containing Pol δ -DV, RPA, PCNA, RFC, and AMP-CPP. Omissions from this standard reaction mix are noted. Reactions were initiated with 250 μ M dTTP and dATP each to allow extension of the 29-mer primer to a 50-mer product. **(e)** Effect of RPA on Pol δ -DV extension in the absence of PCNA. Primer extension reactions were performed on substrate described in **Fig. 1a**, with and without 50 nM RPA pre-bound to the single-stranded DNA template. Reactions were initiated with either 250 μ M dATP or 250 μ M each dATP and dTTP as noted. **(f)** Primer extension reactions by PCNA-Pol δ . Standard replication reactions on the template shown in **Fig. 1a** containing all components were initiated with either 250 μ M each of all four dNTPs, all four dNTPs at *S. cerevisiae* physiological concentrations (16 μ M dATP, 14 μ M dCTP, 12 μ M dGTP, 30 μ M dTTP), or all four dNTPs and rNTPs at *S. cerevisiae* physiological concentrations (dNTPs as before plus 3 mM ATP, 0.5 mM CTP, 0.7 mM GTP, 1.7 mM UTP). **(g)** Quantification of data from **f**. The median extension product at each time point was determined and plotted as a function of time. Each curve was fit to a single exponential.



Supplementary Figure 2

Strand-displacement synthesis by exonuclease-deficient Pol δ .

(a, b) Global kinetic modeling of data from **Fig. 2a** to the respective kinetic models shown. KinTek Explorer software was used to perform fits (Johnson, K.A., Simpson, Z.B. & Blom, T. Global kinetic explorer: a new computer program for dynamic simulation and fitting of kinetic data. *Anal Biochem* **387**, 20-9 (2009)) The fitting shown in **Fig. 2b** was performed in a model-free manner, providing information concerning the observed macroscopic rates of strand displacement synthesis, but not about the molecular mechanism of the observed slow-down. In an attempt to better define this molecular mechanism, we performed global kinetic fitting of the data in **Fig. 2a** to two different models. First, we globally fit the data to the simplest model, in which the flap inhibits the actual rate of extension by Pol δ and a longer flap inhibits more effectively in **(a)**. This model yielded a poor fit, especially for the +2 and +3-nt displacement products. The rates obtained from this global fit were comparable to those generated by fitting each product curve to the sum of two exponentials individually (compare **(a)** with **Fig. 2b**). A second, more complex mechanism was considered, in which Pol δ equilibrates between two states during strand displacement, one that is competent for further extension and one incompetent for extension **(b)**. Fitting to such a model provided a better fit to the data, as is expected by the inclusion of more variables. Our modeling indicates that the incompetent state is not significantly populated during polymerization of single-strand DNA templates, but becomes increasingly more populated as strand displacement synthesis progresses. While several rates were not well defined by this model, we believe that its principle has merit because it provides a mechanistic explanation for Pol δ carrying out activities on flap substrates other than polymerization, such as idling and hand-off to FEN1. **(c, d)** Strand displacement time courses performed on the indicated Substrates I and II with either RNA or DNA-initiating blocking oligonucleotides. Select time points from these gels are shown in **Fig. 2b**. **(e)** Strand displacement time course performed on DNA Substrate III-RNA block. The reaction was performed identically to those in **(c)** and **(d)**. **(f)** Quantitation of data from **(e)**; Displacement products (0) and (+1) were fit to two exponentials, and (+2) and (\geq +3) to single exponentials. **(g)** Global KinTek modeling using the simple model in **(a)**. The experiments in **(e-g)** were carried out to show that the progressive slowdown observed during strand displacement synthesis in Substrates I and II was not the result of the specific DNA or RNA sequence used, but a consequence of the increasing length of the flap. In Substrate III, the dinucleotide stability for each pair of nucleotides within the four, 5'-proximal nucleotides was constant (5'-rGrGrC), yet the strand displacement time-course shows that rate of strand displacement synthesis progressively decreases as the nascent flap grows longer.

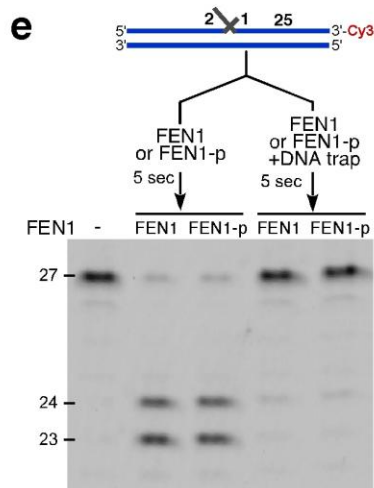
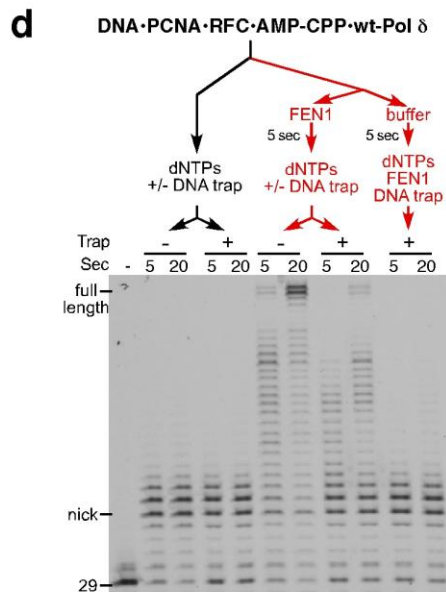
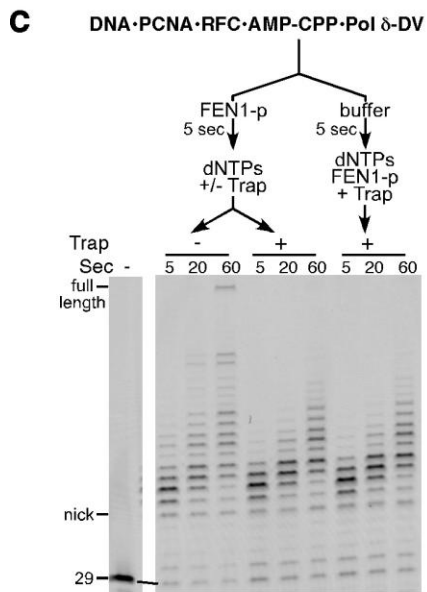
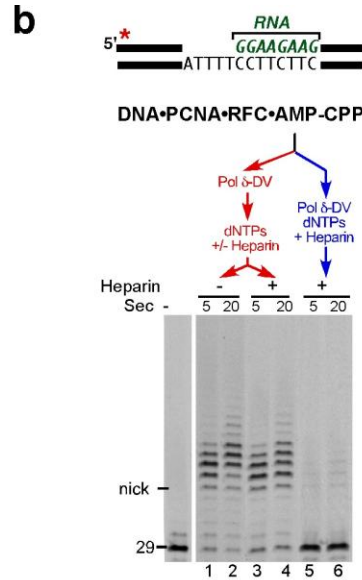
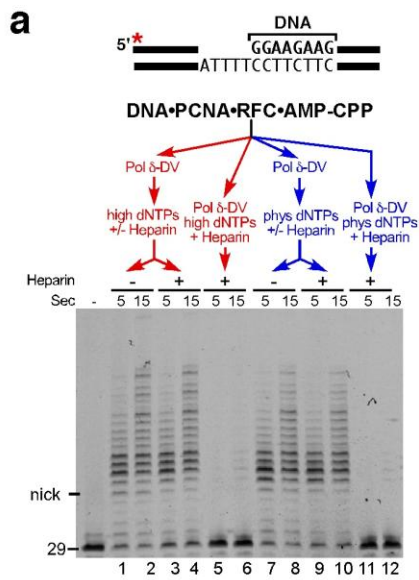


Supplementary Figure 3

Strand-displacement synthesis and idling by wild-type Pol δ .

(a,c) Strand displacement time courses performed with Pol δ -wt as described in Fig. 3a. The substrate and enzymes were pre-incubated in the presence of dCTP and dGTP to prevent polymerase degradation of the primer and blocking oligonucleotide. (b,d) Quantification of products in a,c. Fractional occupancy was determined and select products are plotted. The nick position product (0), +1 position past nick, and the +2 and greater position were plotted for both the RNA-initiating block (a,b) and the DNA block (c,d) of Substrate I. The c plot is also in Figure 3, but is shown again for easier comparison.

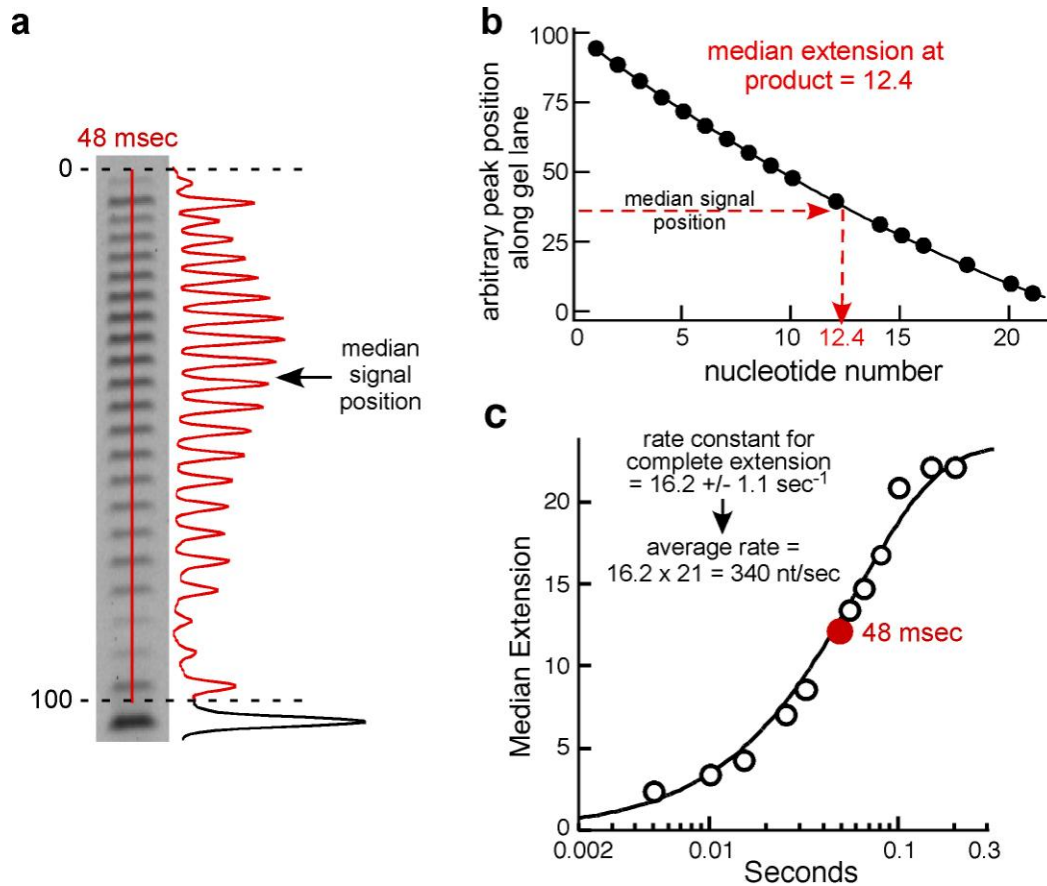
showing nick position and +1 displacement product. (c) FEN1-cut products from Substrate I-RNA with 5'-labeled blocking oligonucleotide. The fraction of each product size is shown. The total of cut products and substrate remaining equals 1. (d) The ratio of (2-nt + 3-nt)/1-nt product formed during each subsequent 0.2 sec interval was plotted against assay time. The plot shows that at the start the 1-nt product predominated (ratio =0.3), while after 2 sec, the larger products predominated (ratio =4.5). (e) Nick translation assay on Substrate III-RNA block, as diagramed in a. (f) Quantification of e (+FEN1) and **Supplementary Fig. 2e** (no FEN1). Nick position (0), and +1 and +2 displacement products were plotted. (g) FEN1-cut products from Substrate III-RNA with 5'-labeled blocking oligonucleotide. The fraction of each product size is shown. The total of cut products and substrate remaining equals 1. (h) Median extension analysis of nick translation assays performed at 250 μ M each dNTP (blue), and at physiological dNTP levels (red, concentrations listed in legend to **Supplementary Fig. 1f**). Data for saturating dNTPs are the same as in **Fig. 4e**. Data collected with low dNTP levels shows a lag in nick translation at early time points, which we attribute to slower gap filling and formation of the +1 flap at the lower, physiological dNTPs. Comparison of the two slopes in the linear range indicates that iterative nick translation proceeds at approximately the same rate at physiological as at saturating nucleotide concentrations. (i) Quench-flow assay with FEN1 and various flap-containing DNAs. Reactions were initiated by mixing FEN1 with DNA template. Other than the nick-containing template (green), DNAs contained a single extrahelical 3'-nucleotide complementary to the template. Templates then contained either 0 (blue), 1 (black), or 2 (purple) extrahelical 5'-rU bases, not complementary to the template. All templates were labeled with a 5'-³²P on the strand cut by FEN1. The fraction of flap cut is plotted. These assays were carried out without PCNA since it was not efficiently loaded on the flap substrates.



Supplementary Figure 5

Processivity of the nick-translation machinery.

(a) Similar to **Fig. 5a**; strand displacement time-course by PCNA-Pol δ on Substrate I-DNA block. Standard reaction conditions were used, initiated with either 250 μ M of each dNTP (high) or physiological levels of each dNTP (phys, concentrations listed in legend to **Supplementary Fig. 1f**). 10 μ g/ml heparin was used as trap for free Pol δ -DV in noted lanes. (b) Similar to **Supplementary Fig. 5a**, lanes 1-6 (250 μ M each dNTP), except Substrate I-RNA block was used instead of a DNA-block. (c) Companion to **Fig. 5b**; nick translation assay with forced single turnover of 40 nM FEN1-p, containing mutations in the FEN1 PIP-motif. DNA template was Substrate I-RNA block. Reactions were initiated with 250 μ M each dNTP with or without 6 μ M oligonucleotide FEN1 trap to trap free FEN1-p. The data show that the trap completely blocked FEN1-p action, even when it was pre-bound to the DNA-PCNA- Pol δ complex, indicating that it is not stably associated with this complex. (d) Nick translation assay with forced single turnover of 40 nM FEN1, with wild-type Pol δ . Reactions were initiated with 250 μ M each dNTP with or without 6 μ M oligonucleotide FEN1 trap to trap free FEN1. The data show that FEN1 is able to remain associated with the PCNA-wild-type Pol δ complex throughout nick translation (e) Testing the efficiency of the FEN1 oligonucleotide trap; FEN1 and FEN1-p cutting of labeled substrate containing a stable flap. Labeled DNA contained a single nucleotide 3'-flap and a two-nucleotide 5'-flap (both non-complementary to template), with a 3'-Cy3 label on the strand cut by FEN1. Reactions were initiated by mixing the enzyme with DNA template. To test the effectiveness of the oligonucleotide trap, FEN1 and FEN1-p were pre-incubated with excess trap template prior to incubation with labeled template. The structure of the trap substrate was identical to that of the labeled substrate.



Supplementary Figure 6

Median analysis of replication rates.

This analysis method was used to generate the data presented in **Fig. 1e, 4e, and Supplementary Fig. 1c,g, 4h**. **(a)** Plot profiles of all products, except starting material, were produced using ImageQuant (GE Healthcare). These profiles plotted the intensity signal in the gel against an arbitrary y-coordinate. Following background subtraction, we determined the position on the y-coordinate at which the median of the total lane signal was. This was defined as the point along the lane coordinate in which 50% of the signal lay above and below. **(b)** Next, for each gel, a standard curve was produced, fit to a quadratic function, in order to convert the arbitrary y-coordinate values to a value represented in nucleotides. **(c)** After determining the median product for many points throughout an entire time-course, the plots were assembled.

Supplementary Table. Oligonucleotides used in this study

Primer29	5'-TCA GCG CGA GCA TGA CAT TGA AGG TAA CC-3'
Primer29-Cy3	5'-Cy3-TCA GCG CGA GCA TGA CAT TGA AGG TAA CC-3'
Template-AT ₂₀	5'-BiotinTEG-TTC CTT CAA CCA GCT TAC CTT CTT CCT TTT TTT TTT TTT TTT TAG GTT ACC TTC AAT GTC ATG CTC GCG CTG A-BiotinTEG-3'
Template-Sub I	5'-BiotinTEG-TCT TCC TTC AAC CAG CTT ACC TTC TTC CTT TTA GGT TAC CTT CAA TGT CAT GCT CGC GCT GA-BiotinTEG-3'
Block-Sub I-pRNA	5'-Phos-GGA AGA AGG TAA GCT GGT TGA AGG AAG-3'
Block-Sub I-pDNA	5'-Phos-rGrGrA rArGrA rArGG TAA GCT GGT TGA AGG AAG-3'
Template-Sub II	5'-BiotinTEG-TCT TCC TTC AAC CAG CTT ACC TTC AAC GTT TTA GGT TAC CTT CAA TGT CAT GCT CGC GCT GA-BiotinTEG-3'
Block-Sub II-pDNA	5'-Phos-CGT TGA AGG TAA GCT GGT TGA AGG AAG-3'
Block-Sub II-pRNA	5'-Phos-rCrGrU rUrGrA rArGG TAA GCT GGT TGA AGG AAG-3'
Template-Sub III	5'-BiotinTEG-TCT TCC TTC AAC CAG CTT ACC TTC GCC CTT TTA GGT TAC CTT CAA TGT CAT GCT CGC GCT GA-BiotinTEG-3'
Block-Sub III-pRNA	5'-Phos-rGrGrG rCrGrA rArGG TAA GCT GGT TGA AGG AAG-3'
Block-Sub I-pRNA-3'Cy3	5'-Phos-rGrGrA rArGrA rArGG TAA GCT GGT TGA AGG AAG-Cy3-3'
Block-Sub I-RNA	5'-rGrGrA rArGrA rArGG TAA GCT GGT TGA AGG AAG-3'
Block-Sub III-RNA	5'-rGrGrG rCrGrA rArGG TAA GCT GGT TGA AGG AAG-3'
FEN1 trap template	5'-TCT TCC TTC AAC CAG CTT ACC TTC TTC CTT TTA GGT TAC CTT CAA TGT CAT GCT CGC GCT GA-3'
FEN1 trap 3'-flap	5'-TCA GCG CGA GCA TGA CAT TGA AGG TAA CCT AAA AT-3'
FEN1 trap 5'-flap	5'-TT GGA AGA AGG TAA GCT GGT TGA AGG AAG-3'
FEN1 template-nick primer	5'-TCA GCG CGA GCA TGA CAT TGA AGG TAA CCT AAA A-3'
FEN1 template-3'G primer	5'-TCA GCG CGA GCA TGA CAT TGA AGG TAA CCT AAA AG-3'
FEN1-template-U1 block	5'-rU rGrGrA rArGrA rArGG TAA GCT GGT TGA AGG AAG-3'
FEN1-template-U2 block	5'-rUrU rGrGrA rArGrA rArGG TAA GCT GGT TGA AGG AAG-3'

CHAPTER VI

Sequential switching of binding partners on PCNA during *in vitro* Okazaki fragment maturation

PREFACE TO THE CHAPTER

This chapter describes the development and biochemical characterization of engineered PCNA heterotrimers. Since eukaryotic PCNA exists as a homotrimer, it has proved difficult to address how many monomers of PCNA are required to bind client proteins during replication processes. One solution to this problem is through the production of the PCNA heterotrimers described in this chapter. In these proteins, the residues primarily responsible for binding Pol δ and FEN1 have been mutated in zero, one, two, or all three PCNA subunits. Amir Aharoni and his student Daniel Dovrat at Ben-Gurion University of the Negev in Israel initiated this work, and the work described here is a collaboration with them. This chapter describes the development and purification of the PCNA heterotrimers, and their use in assays isolating the various steps of Okazaki fragment maturation. Our primary question was whether the tool-belt model of PCNA action, whereby multiple enzymes bind a single PCNA simultaneously, was absolutely required for *in vitro* Okazaki fragment maturation. We found that while having fewer than three wild-type PCNA monomers delayed various steps of Okazaki fragment maturation, simultaneous binding of multiple enzymes to a single PCNA was not absolutely required. This work provided important insights to the work described in Chapter V, in which I further addressed the PCNA toolbelt model. My contribution to this work was in purifying replication enzymes, providing technical assistance for the *in vitro* assays, and helping prepare the manuscript.

Sequential switching of binding partners on PCNA during in vitro Okazaki fragment maturation

Daniel Dovrat^{a,b}, Joseph L. Stodola^c, Peter M. J. Burgers^c, and Amir Aharoni^{a,b,1}

^aDepartment of Life Sciences and ^bNational Institute for Biotechnology in the Negev, Ben-Gurion University of the Negev, Be'er Sheva 84105, Israel; and ^cDepartment of Biochemistry and Molecular Biophysics, Washington University School of Medicine, St. Louis, MO 63110

Edited by Mark D. Sutton, University at Buffalo, The State University of New York, Buffalo, NY, and accepted by the Editorial Board August 20, 2014 (received for review November 15, 2013)

The homotrimeric sliding clamp proliferating cell nuclear antigen (PCNA) mediates Okazaki fragment maturation through tight coordination of the activities of DNA polymerase δ (Pol δ), flap endonuclease 1 (FEN1) and DNA ligase I (Lig1). Little is known regarding the mechanism of partner switching on PCNA and the involvement of PCNA's three binding sites in coordinating such processes. To shed new light on PCNA-mediated Okazaki fragment maturation, we developed a novel approach for the generation of PCNA heterotrimers containing one or two mutant monomers that are unable to bind and stimulate partners. These heterotrimers maintain the native oligomeric structure of PCNA and exhibit high stability under various conditions. Unexpectedly, we found that PCNA heterotrimers containing only one functional binding site enable Okazaki fragment maturation by efficiently coordinating the activities of Pol δ , FEN1, and Lig1. The efficiency of switching between partners on PCNA was not significantly impaired by limiting the number of available binding sites on the PCNA ring. Our results provide the first direct evidence, to our knowledge, that simultaneous binding of multiple partners to PCNA is unnecessary, and if it occurs, does not provide significant functional advantages for PCNA-mediated Okazaki fragment maturation in vitro. In contrast to the "toolbelt" model, which was demonstrated for bacterial and archaeal sliding clamps, our results suggest a mechanism of sequential switching of partners on the eukaryotic PCNA trimer during DNA replication and repair.

Proliferating cell nuclear antigen (PCNA) is a central coordinator of genome duplication and maintenance pathways in eukaryotes (1, 2). A member of the conserved sliding clamp family, PCNA is a homotrimeric ring-shaped protein that encircles DNA and serves as a processivity factor for DNA polymerases and a binding platform for many DNA modifying enzymes. PCNA interacts with partners involved in numerous processes, including DNA replication, recombination and repair, chromatin remodeling, and cell-cycle regulation. PCNA recruits these partners to replication forks or other chromosomal locations, enhances their catalytic activities, and orchestrates their cooperation in multistep enzymatic processes. Because most partners interact with the same binding site on PCNA, competition for binding must be tightly regulated during complex PCNA-mediated processes. The switching of partners on the PCNA platform has been shown to be crucial for the proper progression of multiple DNA replication and repair pathways, such as lagging strand replication, translesion synthesis, and mismatch repair (1). In recent years, several regulatory mechanisms, mostly involving posttranslational modifications of PCNA by ubiquitin or small ubiquitin-like modifier, have been shown to affect partner switching on PCNA by favoring the recruitment of specific partners (3–5).

Despite extensive research into the regulation of PCNA-mediated processes, very little is known regarding how PCNA coordinates the activity of several enzymes during sequential processes. Two simple models have been proposed to explain this coordination (1, 2, 6, 7). The first model assumes highly dynamic partner switching on PCNA due to sequential binding and release events on the same or different PCNA monomers (Fig. 1, *Upper*). This

model predicts that a single functional binding site on the PCNA trimer should be sufficient for the coordination of the entire process. In contrast, the second model assumes simultaneous binding of two or three partners to different monomers on the PCNA trimer (Fig. 1, *Lower*). In this case, the partners are stably associated with PCNA, which acts as a "toolbelt" throughout the process. According to this model, only PCNA trimers with two or three functional binding sites would be able to coordinate the process.

One of the best studied examples of such a multipartner PCNA-mediated process is the synthesis and maturation of Okazaki fragments during lagging strand DNA replication. This process involves the sequential activity of three PCNA binding partners—DNA polymerase δ (Pol δ), flap endonuclease 1 (FEN1), and DNA ligase I (Lig1), which mediate DNA synthesis, flap cleavage, and ligation, respectively (7–9). This is a fast and efficient process that is estimated to take place \sim 100,000 times during each yeast cell division with a low tolerance for errors (8). The enzymes involved must cooperate through PCNA in a tightly regulated manner, acting sequentially on the same substrate while repeatedly exchanging access to it (Fig. 1). In particular, removal of the initiator RNA requires several rapid iterative switches between Pol δ and FEN1 (7). This PCNA-dependent cooperation is particularly important to ensure that flaps will not become too long for processing by this short-flap pathway (7, 10, 11).

To directly examine the mechanism of partner switching on PCNA and the functional significance of its homotrimeric structure, we developed a novel approach for the generation of PCNA heterotrimers that contain both wild-type (WT) and mutant

Significance

Proliferating cell nuclear antigen (PCNA) is a homotrimeric DNA sliding clamp that coordinates multiple DNA replication and repair processes by orchestrating the activity of various essential proteins. PCNA can bind up to three partners simultaneously, but despite extensive research, the functional significance of PCNA's trimeric structure remains unclear. We developed a novel approach for the generation of PCNA heterotrimers that contain both wild-type and mutant monomers. Using these heterotrimers, we show that PCNA can efficiently coordinate the activities of the three enzymes involved in Okazaki fragment maturation without binding them simultaneously. In contrast to the previously suggested "toolbelt" model for PCNA function, our results demonstrate sequential binding and release of partners on the PCNA trimer during complex biological processes.

Author contributions: D.D., P.M.J.B., and A.A. designed research; D.D. performed research; J.L.S. and P.M.J.B. contributed new reagents/analytic tools; D.D. analyzed data; and D.D., J.L.S., P.M.J.B., and A.A. wrote the paper.

The authors declare no conflict of interest.

This article is a PNAS Direct Submission. M.D.S. is a Guest Editor invited by the Editorial Board.

¹To whom correspondence should be addressed. Email: aaharoni@bgu.ac.il.

This article contains supporting information online at www.pnas.org/lookup/suppl/doi:10.1073/pnas.1321349111/-DCSupplemental.

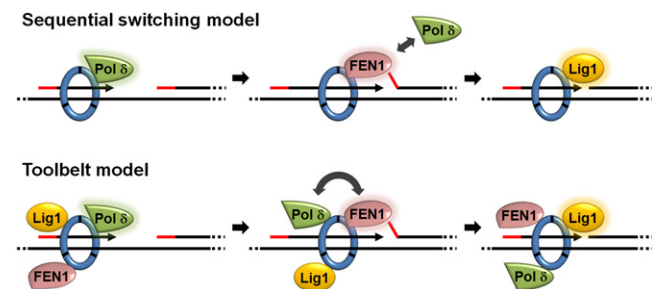


Fig. 1. Two possible models describing PCNA-mediated Okazaki fragment maturation. (Upper) A dynamic model in which Pol δ , FEN1, and Lig1 are bound and released from PCNA in a sequential manner. (Lower) The toolbelt model in which the three enzymes are simultaneously bound to PCNA using all available PCNA binding sites. The red segments represent the RNA primers; glowing circles represent enzymes currently active on the substrate.

monomers that are unable to bind different partners. We used these heterotrimers to determine whether simultaneous binding of more than one partner to a PCNA trimer is necessary to coordinate PCNA-mediated nick translation and Okazaki fragment maturation. Contrary to the toolbelt model, our findings indicate that simultaneous binding is not required, and sequential switching of partners on a single monomer of PCNA is sufficient to coordinate Okazaki fragment maturation. Our findings suggest that PCNA can efficiently orchestrate complex processes by regulating sequential binding and release events of several partners without binding them simultaneously.

Results

Generation of PCNA Heterotrimers. To generate and purify PCNA heterotrimers with native tertiary structure containing both WT and mutant monomers, we coexpressed both monomers in *Escherichia coli* fused to two affinity tags of considerably different sizes (Fig. 2). We used N-terminal His tag (<1 kDa) and maltose binding protein (MBP) tag (~40 kDa) for WT and mutant PCNA, respectively. Due to random trimerization of PCNA during coexpression, four trimer species spontaneously form in vivo (Fig. 2). Tandem affinity purification steps using nickel-nitrilotriacetic acid (Ni-NTA) followed by amylose chromatography enabled the isolation of the two heterotrimeric species, containing at least one His tag and one MBP tag. These species were then separated by size exclusion chromatography, due to a difference of ~40 kDa in their molecular weight (Fig. S1A). Finally, the large MBP tag was removed using site-specific tobacco etch virus (TEV) protease cleavage and the resulting MBP-free heterotrimers were isolated using a second gel filtration step. The contents of these highly purified heterotrimers were verified by SDS/PAGE (Fig. S1B) and MALDI-TOF mass spectrometry (Fig. S1C). The presence of both WT and mutant monomers in the same trimers was further validated by covalent cross-linking of neighboring monomers (Fig. S1D).

We specifically constructed heterotrimers of *Saccharomyces cerevisiae* PCNA, including mutant monomers that are deficient for partner binding while retaining the ability to assemble into stable trimers. Three different mutants were used: the interdomain connector loop (IDCL) mutant pcna-79 (I126A,L128A), which is particularly deficient in stimulation of Pol δ activity (12), the C-terminal mutant pcna-90 (P252A,K253A), which is particularly deficient in stimulation of FEN1 activity (12, 13), and the double mutant, which we designate pcna-7990 (I126A,L128A, P252A,K253A), which we expect to be deficient in stimulation of both Pol δ and FEN1 activities. We denote, for example, a PCNA trimer containing two WT monomers and one monomer of pcna-7990 as WT₂:7990₁. Whereas pcna-79 and pcna-90 are known to be efficiently loaded onto DNA by the clamp loader replication factor C (RFC) (12), we validated that this is also the case for the

combined mutant pcna-7990 and heterotrimers containing this mutant, by measuring the PCNA-dependent ATPase activity of RFC in the presence of a suitable DNA effector (Fig. S2).

Heterotrimer Stability. The PCNA heterotrimers generated using our approach are self-assembled and maintain a native monomer-monomer interface. Consequently, these heterotrimers may dissociate into monomers and randomly reassemble into different trimer species after purification. To assess the kinetics of trimer reassembly, we purified WT₁:7990₂ heterotrimers without removing the MBP tag, incubated them at different temperatures, and examined them by gel filtration chromatography. We found that significant reassembly of the trimers is only observed following prolonged incubations at elevated temperatures (Fig. S3 A and B). Because the in vitro experiments detailed in this report are performed at a maximal temperature of 30 °C for a maximal period of ~15 min, the extent of reassembly is expected to be negligible under the assay conditions. We also verified that the loading of PCNA onto DNA by RFC does not promote reassembly of the heterotrimers (Fig. S3C).

Activities of Pol δ and FEN1 Separately. We first examined how Pol δ activity is stimulated by PCNA heterotrimers. This was measured using an in vitro replication assay, in which PCNA is loaded onto primed single-stranded DNA by RFC and ATP, and the kinetics of processive DNA synthesis by Pol δ are analyzed by resolving replication products using gel electrophoresis (Fig. 3A). We found that heterotrimers of WT₂:7990₁ and WT₁:7990₂ display decreased rates of Pol δ activity relative to the WT homotrimer (Fig. 3B, example gel in Fig. S4A), suggesting that the ability of PCNA to stimulate Pol δ is partially dependent on the number of functional binding sites on the PCNA trimer. Nevertheless, heterotrimers containing even one WT monomer

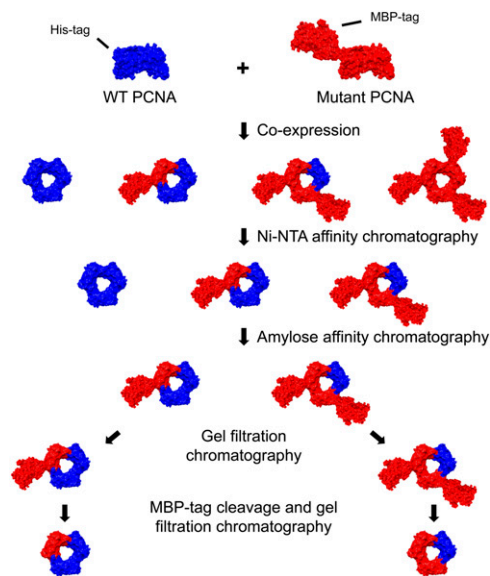


Fig. 2. Scheme describing the PCNA heterotrimer purification strategy. WT and mutant PCNA are coexpressed in *E. coli* fused to 6 \times His- and MBP-fusion tags, respectively, leading to the spontaneous formation of four trimer species. Tandem Ni-NTA and amylose affinity chromatography steps isolate the two heterotrimeric species. These two species are then separated by gel filtration chromatography, owing to the size difference between the two fusion tags (Fig. S1A). Following site-specific cleavage of the MBP tag by TEV protease, a second gel filtration step is used to obtain pure PCNA heterotrimers. Images are schematic models for illustration purposes, created using University of California San Francisco chimera, based on Protein Data Bank entries 1plq and 1anf for PCNA and MBP, respectively.

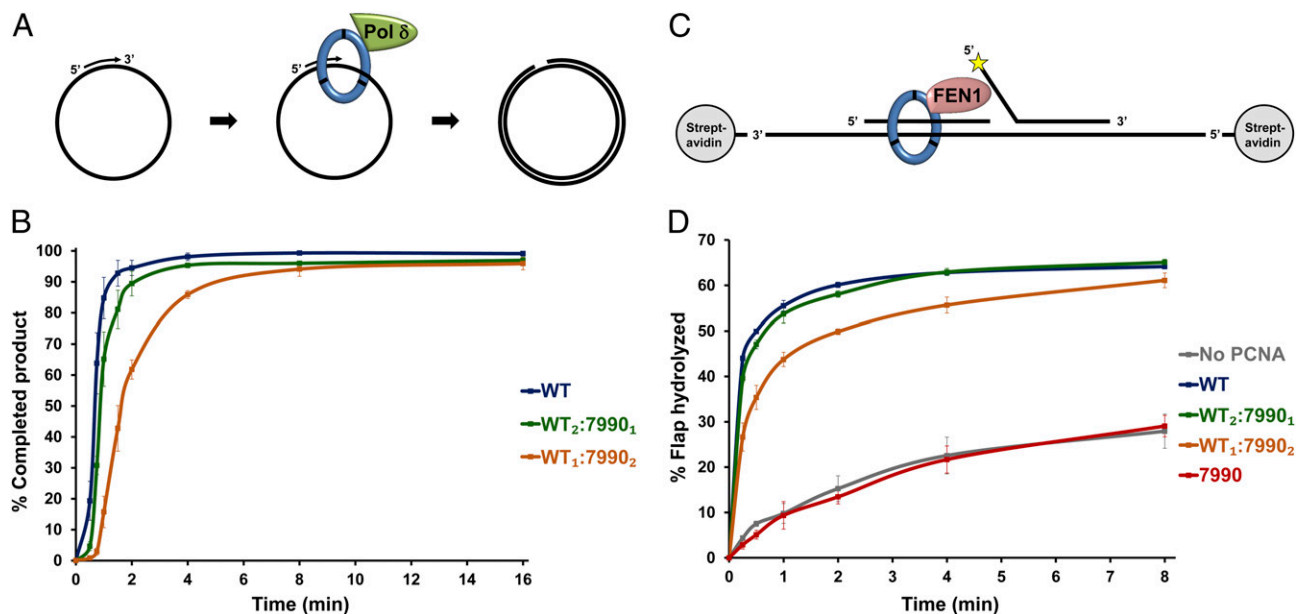


Fig. 3. Stimulation of Pol δ and FEN1 by heterotrimeric PCNA. (A) Schematic illustration of Pol δ assay. PCNA was loaded on a primed single-stranded plasmid by RFC and Pol δ was added to initiate replication. (B) Pol δ activity assays in the presence of three different trimer species, analyzed by agarose gel electrophoresis and autoradiography. The completed 2.9-kb product was quantified as a percentage of the maximum product observed in the assay. Results with pcna-7990 homotrimer are not shown, because no activity was observed. Results shown are averages of four independent assays (see example gel in Fig. S4A); error bars represent SEM. (C) Schematic illustration of FEN1 assay. PCNA was loaded on a radioactively labeled oligonucleotide substrate, FEN1 was added and the reaction was allowed to proceed for the indicated times. FEN1 activity results in cleavage of the 5' flap portion of the oligonucleotide. Yellow star denotes radioactive label at 5' end of the flap. (D) FEN1 activity assays in the absence of PCNA or in the presence of four different PCNA trimer species. Reactions were analyzed by urea-PAGE and autoradiography, and the percentage of substrate cleaved by FEN1 was quantified. Results shown are averages of three independent assays; error bars represent SEM.

significantly stimulate Pol δ activity compared with the pcna-7990 homotrimer, which displays no activity. This indicates that a single functional binding site on the PCNA trimer is sufficient to support processive DNA synthesis by Pol δ .

To further validate that Pol δ stimulation originates from the presence of heterotrimeric PCNA rather than minute quantities of WT homotrimer due to reassembly, we examined Pol δ activity with mixtures of WT and pcna-7990 homotrimers at different ratios (Fig. S3D). Even at a ratio that resembles full reassembly of the WT₁:7990₂ trimer, Pol δ activity was lower than observed with the actual heterotrimer, indicating that a small degree of reassembly into WT homotrimers cannot explain our results.

FEN1 activity is also stimulated by PCNA (13, 14). We measured the kinetics of 5'-flap cleavage by FEN1 on an oligonucleotide-based model substrate (Fig. 3C). Pca-7990 homotrimers did not stimulate FEN1 activity over the background levels, whereas PCNA heterotrimers containing one or two pcna-7990 monomers significantly stimulated FEN1 but with slightly lower efficiency relative to the WT homotrimer (Fig. 3D). These results indicate that FEN1 stimulation by a single functional PCNA binding site occurs, with additional binding sites improving kinetics, as observed with Pol δ . Essentially similar results were obtained in a K⁺-containing as in a Na⁺-containing buffer system (Fig. S5C). We also examined a double-flap rather than a 5'-flap substrate, but in contrast to previous studies performed using archaeal proteins (15, 16), we could not detect any PCNA-dependent stimulation of FEN1 on this substrate (Fig. S5D).

Nick Translation by Pol δ and FEN1. Having observed the activities of Pol δ and FEN1 separately, we next examined whether the cooperation between these two enzymes during Okazaki fragment maturation requires multiple binding sites on the PCNA trimer, as posited by the toolbelt model. Nick translation, the result of iterative, sequential strand displacement synthesis by

Pol δ and flap cleavage by FEN1, requires rapid and efficient cooperation between the enzymes in the presence of PCNA (7, 10, 11). We examined the kinetics of nick translation on an oligonucleotide-based model substrate in the presence of different PCNA trimers. In this assay, PCNA-dependent cooperation of Pol δ and FEN1 will result in rapid progression of replication through a downstream RNA-DNA blocking oligo (9, 10). In the absence of FEN1, Pol δ will stall for a relatively long period and only slowly succeed in completely displacing the blocking oligo (Fig. 4A). Hence, a comparison between Pol δ strand displacement activity in the presence and absence of FEN1 provides a measure of the degree of PCNA-dependent cooperation between the two enzymes.

We found that both heterotrimers allowed FEN1 to significantly stimulate the progression of Pol δ through the blocking oligo (Fig. 4B). These results indicate that Pol δ and FEN1 efficiently cooperate during nick translation even if only one functional binding site is present on the PCNA trimer, suggesting that simultaneous binding of both enzymes to PCNA is not required. To further examine whether simultaneous binding may pose some advantage to this cooperation, we examined the kinetics of nick translation in the presence of heterotrimers containing the pcna-79 and pcna-90 mutants (Fig. S6). As controls, we measured Pol δ and FEN1 activities separately, in the presence of heterotrimers containing pcna-79 and pcna-90 mutants, respectively (Fig. S5A and B). Because pcna-79 is only partially deficient in stimulation of FEN1 (Fig. S5B) (13), we expect that defects in nick translation that may occur in the WT₁:7990₂ trimer would be alleviated in the WT₁:79₂ trimer, as FEN1 should be able to bind the pcna-79 monomers of this trimer. We found that both pcna-79 and pcna-7990 heterotrimers exhibit the same level of cooperation between Pol δ and FEN1 (Fig. S6, compare samples 5 and 11), indicating that in case simultaneous binding of these enzymes to PCNA does

28). This suggests that Pol δ may engage different PCNA monomers simultaneously or consecutively during replication. Using our PCNA heterotrimers, we may have limited the number of PCNA–Pol δ contacts leading to a decrease in Pol δ processivity.

We present here a fast, reproducible approach that allows the simple purification of heterotrimers with a native tertiary and quaternary structure. Our method takes place under native conditions and can be extended to incorporate any mutant into heterotrimers, as long as it does not impede natural trimerization. For example, heterotrimers bearing the K164R mutation (3), combined with in vitro ubiquitylation methods (5, 29), may address several fundamental questions regarding the polymerase switching mechanism during translesion DNA synthesis (30). We believe that this can be an effective approach for the mechanistic study of structure–function relationships in PCNA and can be applied for the study of many other homooligomeric proteins that participate in a variety of complex biological processes.

Materials and Methods

Purification of PCNA Heterotrimers. *S. cerevisiae* PCNA was cloned with an N-terminal His tag into the first multiple cloning site (MCS) of pETDuet-1 (Novagen). Mutant pcna-79, pcna-90, or pcna-7990 was cloned with an N-terminal MBP tag followed by a TEV protease cleavage site into the second MCS of the same vector. This vector allows the simultaneous overexpression of both proteins at similar levels. Overexpression was performed in *E. coli* BL21(DE3) cells. Following cell lysis using a French press (Thermo Scientific), the lysate was purified over a Ni-NTA His-bind column (Novagen), and the eluate was pooled and purified over an amylose column (New England Biolabs). The amylose eluate was concentrated and injected into a Superdex 200 16/60 prep grade gel filtration column (GE Healthcare) using the AKTA purifier FPLC system (GE Healthcare). Next, selected 0.5-mL fractions were collected and examined for purity by performing analytical gel filtration on a Superdex 200 10/300 GL column (GE Healthcare). For each heterotrimer species, fractions that contained the desired heterotrimer without significant contamination were selected and pooled. TEV protease was added at 1:100 (enzyme:substrate) molar ratio and incubated overnight

at 4 °C. Following cleavage, the samples were again purified by gel filtration on a Superdex 200 10/300 GL column.

Heterotrimer stability assays, RFC ATPase assays, cross-linking assays, and purification of other proteins are described in *SI Materials and Methods*.

Pol δ Replication Assays and Okazaki Fragment Maturation Assays. Assays were performed essentially as described previously (9). For consistency, Pol δ assays and Okazaki fragment maturation assays were performed under identical conditions. The template DNA, single-stranded Bluescript SKIII(+) plasmid, was obtained as previously described and hybridized with primer SKrc14 (9). Standard 40- μ L assays contained 20 mM Tris-HCl pH = 7.8, 1 mM DTT, 100 μ g/mL BSA, 7.5 mM MgAc₂, 0.4 mM ATP, 100 μ M each of dCTP, dGTP, and dTTP, 10 μ M dATP, 4 nM (α -³²P)dATP (3,000 Ci/mmol), 100 mM NaCl, 50 fmol of template plasmid, 10 pmol of replication protein A (RPA), 100 fmol of RFC, 100 fmol of PCNA trimers, and 200 fmol of Pol δ . Okazaki fragment maturation assays also contained 200 fmol each of FEN1 and Lig1. The template plasmid was preincubated with RPA, PCNA, and RFC for 1 min at 30 °C for RPA coating and PCNA loading. The other enzymes were then added in a mix, and the reactions were incubated at 30 °C for the indicated times. Products were analyzed by electrophoresis on a 1% agarose gel in the presence of 0.5 μ g/mL ethidium bromide. The gels were dried, exposed to a storage phosphor screen (GE Healthcare), and analyzed on a PhosphorImager (Fuji Film).

Pol δ processivity assays were performed as previously described (26) with slight modifications. Details can be found in *SI Materials and Methods*.

FEN1 Flap Cleavage Assays. Oligonucleotide-based FEN1 assays were performed as previously described (13, 14) with slight modifications. Details can be found in *SI Materials and Methods*.

Nick Translation Assays. Assays were performed essentially as previously described (7, 9, 10). Details can be found in *SI Materials and Methods*.

ACKNOWLEDGMENTS. The authors thank Carrie Stith and Dan Od-Cohen for protein purification and technical assistance, Enav Drori for assistance with graphics, and Ron Milo for assistance with the calculation of cellular protein concentrations. This work was supported in part by Grant GM032431 from the National Institutes of Health (to P.M.J.B.). A.A. was supported by the European Research Council "Ideas Program" (201177).

- Moldovan GL, Pfander B, Jentsch S (2007) PCNA, the maestro of the replication fork. *Cell* 129(4):665–679.
- Maga G, Hubscher U (2003) Proliferating cell nuclear antigen (PCNA): A dancer with many partners. *J Cell Sci* 116(Pt 15):3051–3060.
- Hoegge C, Pfander B, Moldovan GL, Pyrowolakis G, Jentsch S (2002) RAD6-dependent DNA repair is linked to modification of PCNA by ubiquitin and SUMO. *Nature* 419(6903):135–141.
- Stelter P, Ulrich HD (2003) Control of spontaneous and damage-induced mutagenesis by SUMO and ubiquitin conjugation. *Nature* 425(6954):188–191.
- Garg P, Burgers PM (2005) Ubiquitinated proliferating cell nuclear antigen activates translesion DNA polymerases eta and REV1. *Proc Natl Acad Sci USA* 102(51):18361–18366.
- Lehmann AR (2006) Clubbing together on clamps: The key to translesion synthesis. *DNA Repair (Amst)* 5(3):404–407.
- Stith CM, Sterling J, Resnick MA, Gordenin DA, Burgers PM (2008) Flexibility of eukaryotic Okazaki fragment maturation through regulated strand displacement synthesis. *J Biol Chem* 283(49):34129–34140.
- Burgers PMJ (2009) Polymerase dynamics at the eukaryotic DNA replication fork. *J Biol Chem* 284(7):4041–4045.
- Ayyagari R, Gomes XV, Gordenin DA, Burgers PMJ (2003) Okazaki fragment maturation in yeast. I. Distribution of functions between FEN1 AND DNA2. *J Biol Chem* 278(3):1618–1625.
- Garg P, Stith CM, Sabouri N, Johansson E, Burgers PM (2004) Idling by DNA polymerase delta maintains a ligatable nick during lagging-strand DNA replication. *Genes Dev* 18(22):2764–2773.
- Rossi ML, Bambara RA (2006) Reconstituted Okazaki fragment processing indicates two pathways of primer removal. *J Biol Chem* 281(36):26051–26061.
- Eissenberg JC, Ayyagari R, Gomes XV, Burgers PM (1997) Mutations in yeast proliferating cell nuclear antigen define distinct sites for interaction with DNA polymerase delta and DNA polymerase epsilon. *Mol Cell Biol* 17(11):6367–6378.
- Gomes XV, Burgers PM (2000) Two modes of FEN1 binding to PCNA regulated by DNA. *EMBO J* 19(14):3811–3821.
- Li X, Li J, Harrington J, Lieber MR, Burgers PM (1995) Lagging strand DNA synthesis at the eukaryotic replication fork involves binding and stimulation of FEN-1 by proliferating cell nuclear antigen. *J Biol Chem* 270(38):22109–22112.
- Chapados BR, et al. (2004) Structural basis for FEN-1 substrate specificity and PCNA-mediated activation in DNA replication and repair. *Cell* 116(1):39–50.
- Craggs TD, Hutton RD, Brenlla A, White MF, Penedo JC (2014) Single-molecule characterization of Fen1 and Fen1/PCNA complexes acting on flap substrates. *Nucleic Acids Res* 42(3):1857–1872.
- Pascal JM, O'Brien PJ, Tomkinson AE, Ellenberger T (2004) Human DNA ligase I completely encircles and partially unwinds nicked DNA. *Nature* 432(7016):473–478.
- de Godoy LMF, et al. (2008) Comprehensive mass-spectrometry-based proteome quantification of haploid versus diploid yeast. *Nature* 455(7217):1251–1254.
- Hacker KJ, Alberts BM (1994) The rapid dissociation of the T4 DNA polymerase holoenzyme when stopped by a DNA hairpin helix. A model for polymerase release following the termination of each Okazaki fragment. *J Biol Chem* 269(39):24221–24228.
- Subramanian J, Vijayakumar S, Tomkinson AE, Arnheim N (2005) Genetic instability induced by overexpression of DNA ligase I in budding yeast. *Genetics* 171(2):427–441.
- Riva F, et al. (2004) Distinct pools of proliferating cell nuclear antigen associated to DNA replication sites interact with the p125 subunit of DNA polymerase δ or DNA ligase I. *Exp Cell Res* 293(2):357–367.
- Sporbert A, Domaing P, Leonhardt H, Cardoso MC (2005) PCNA acts as a stationary loading platform for transiently interacting Okazaki fragment maturation proteins. *Nucleic Acids Res* 33(11):3521–3528.
- Dionne I, Nookala RK, Jackson SP, Doherty AJ, Bell SD (2003) A heterotrimeric PCNA in the hyperthermophilic archaeon *Sulfolobus solfataricus*. *Mol Cell* 11(1):275–282.
- Beattie TR, Bell SD (2012) Coordination of multiple enzyme activities by a single PCNA in archaeal Okazaki fragment maturation. *EMBO J* 31(6):1556–1567.
- Indiani C, McInerney P, Georgescu R, Goodman MF, O'Donnell M (2005) A sliding-clamp toolbelt binds high- and low-fidelity DNA polymerases simultaneously. *Mol Cell* 19(6):805–815.
- Chilkova O, et al. (2007) The eukaryotic leading and lagging strand DNA polymerases are loaded onto primer-ends via separate mechanisms but have comparable processivity in the presence of PCNA. *Nucleic Acids Res* 35(19):6588–6597.
- Netz DJ, et al. (2011) Eukaryotic DNA polymerases require an iron-sulfur cluster for the formation of active complexes. *Nat Chem Biol* 8:125–132.
- Acharya N, Klassen R, Johnson RE, Prakash L, Prakash S (2011) PCNA binding domains in all three subunits of yeast DNA polymerase δ modulate its function in DNA replication. *Proc Natl Acad Sci USA* 108(44):17927–17932.
- Haracska L, Unk I, Prakash L, Prakash S (2006) Ubiquitylation of yeast proliferating cell nuclear antigen and its implications for translesion DNA synthesis. *Proc Natl Acad Sci USA* 103(17):6477–6482.
- Friedberg EC, Lehmann AR, Fuchs RPP (2005) Trading places: How do DNA polymerases switch during translesion DNA synthesis? *Mol Cell* 18(5):499–505.

Bluescript SKII(+) DNA. The 30- μ L assays contained 20 mM Tris-HCl pH = 7.8, 1 mM DTT, 100 μ g/mL BSA, 8.3 mM MgAc₂, 1 mM ATP, 0.1 mM of each dNTP, 100 mM NaCl, 200 fmol of template plasmid, 40 pmol of RPA, 200 fmol of RFC, 400 fmol of PCNA trimers, and 5 fmol of Pol δ (polymerase to PCNA-loaded primer-template ratio of 1:40, to achieve single-hit criteria). The template plasmid was preincubated with RPA, PCNA, and RFC for 1 min at 30 °C for RPA coating and PCNA loading. Pol δ was then added, and the reactions were incubated

at 30 °C for the indicated times. Products were analyzed by electrophoresis on a 2% (wt/vol) denaturing alkaline agarose gel, in the presence of 0.5 μ g/mL ethidium bromide. A 100-bp ladder was also run on the gel, and photographed under UV illumination. The gel was dried, exposed to a storage phosphor screen and analyzed on a PhosphorImager. Finally, the UV picture and the autoradiograph were overlaid to position the ladder onto the autoradiograph and assess the sizes of the radioactive products.

1. Ayyagari R, Gomes XV, Gordenin DA, Burgers PMJ (2003) Okazaki fragment maturation in yeast. I. Distribution of functions between FEN1 AND DNA2. *J Biol Chem* 278(3):1618–1625.
2. Harrington JJ, Lieber MR (1994) Functional domains within FEN-1 and RAD2 define a family of structure-specific endonucleases: Implications for nucleotide excision repair. *Genes Dev* 8(11):1344–1355.
3. Gomes XV, Gary SL, Burgers PM (2000) Overproduction in Escherichia coli and characterization of yeast replication factor C lacking the ligase homology domain. *J Biol Chem* 275(19):14541–14549.
4. Henricksen LA, Umbricht CB, Wold MS (1994) Recombinant replication protein A: Expression, complex formation, and functional characterization. *J Biol Chem* 269(15):11121–11132.

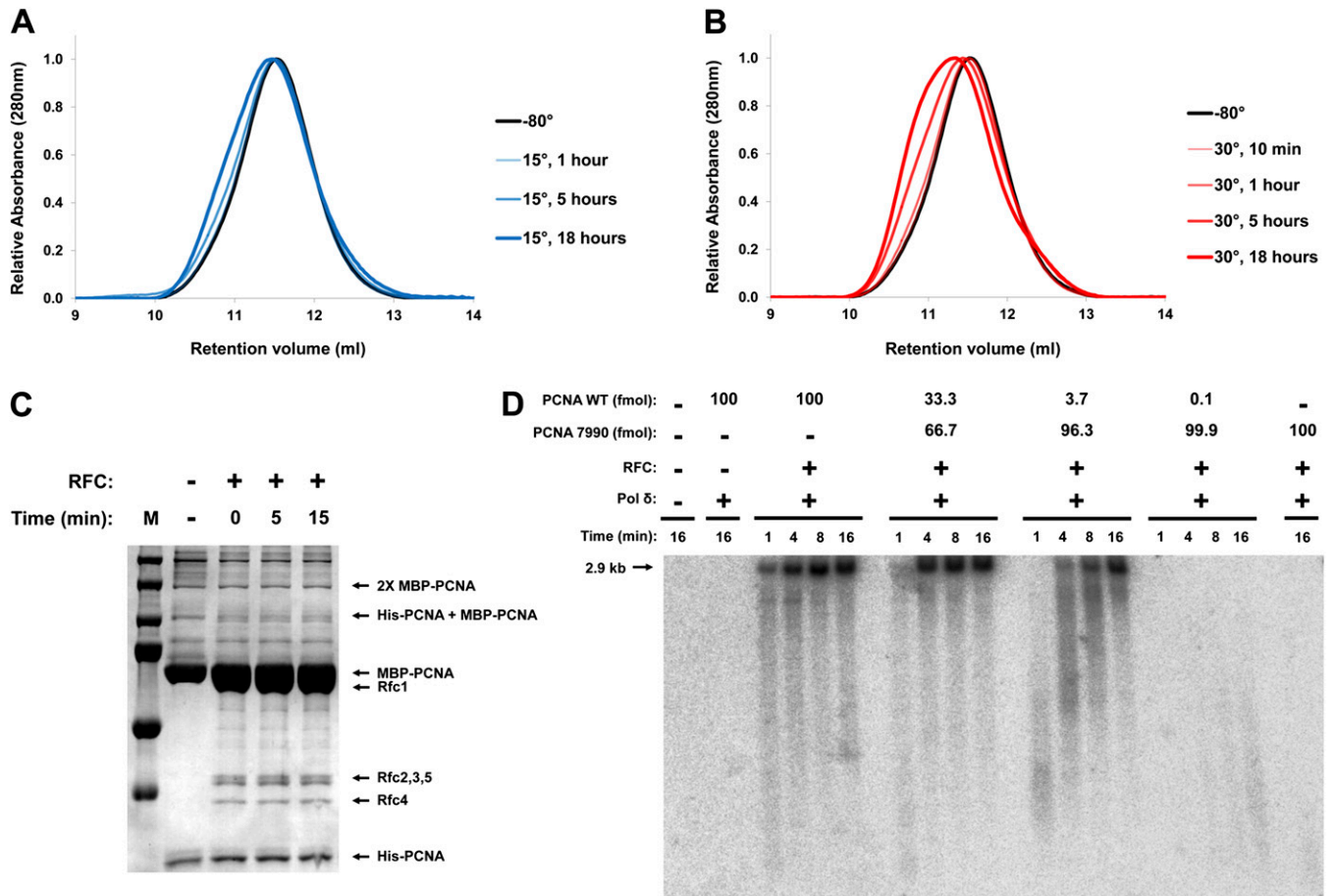


Fig. S3. Stability of PCNA heterotrimers. (A and B) The WT₁:7990₂ heterotrimer was purified as described but without MBP-tag cleavage to allow detection of trimer reassembly. After incubation for various lengths of time (as indicated) at 15 °C (A) or 30 °C (B), the samples were analyzed by gel filtration on a Superdex 200 column. As the initially homogenous population of heterotrimers with two MBP tags undergoes reassembly and gains increasing amounts of trimers with zero, one, or three MBP tags, the chromatogram gains additional peaks on both sides of the central peak and broadens. The maximal peak height has been normalized in all chromatograms, so that peak width represents trimer reassembly. Note that such peak broadening represents only minor reassembly—significant reassembly would lead to the appearance of new peaks at significant distance from the central peak. (C) Cross-linking of PCNA heterotrimers after loading by RFC. WT₁:7990₂ heterotrimer was purified as described but the MBP tags were not cleaved. We separately verified that the presence of MBP tags does not interfere with loading by RFC using an RFC ATPase assay. The heterotrimer was incubated with RFC, an appropriate DNA construct, and ATP, in conditions similar to RFC ATPase assays described above (Fig. S2). The loading reaction was allowed to proceed for the indicated times before it was stopped and disuccinimidyl suberate (DSS) was added. Changes in the pattern of cross-linking products over time may indicate reassembly of the heterotrimer, but no significant change is visible. M, size marker. (D) Functional examination of PCNA stability using Pol δ assay. Assay was performed as described in Fig. 3A, but mixtures of WT and *pcna*-7990 homotrimers were used in different ratios as indicated. Products were analyzed by agarose gel electrophoresis and autoradiography. The arrow denotes the fully replicated, 2.9-kb plasmid. Combinatorially, 3.7% is the maximum expected amount of WT homotrimers in case of full reassembly of the WT₁:7990₂ trimer.

CHAPTER VII

Pif1 removes a Rap1-dependent barrier to the strand displacement activity of DNA polymerase δ

PREFACE TO THE CHAPTER

This chapter describes a potential impediment to efficient lagging strand synthesis *in vivo*. In the cell, the replication machinery must cope with difficult to replicate sequences, collisions with the transcription machinery, and proteins bound to double-stranded DNA ahead of the fork, among other challenges. The work presented in this section uses the yeast transcription factor Rap1 as a potential protein block on the lagging strand, asking whether strand displacement synthesis would be affected if Rap1 were bound to double-stranded DNA to be displaced by Pol δ . This is indeed the case; Rap1 blocks strand displacement synthesis when bound to the upstream duplex.

A potential mechanism for resolving such protein blocks is presented. The helicase Pif1 is able to stimulate strand displacement synthesis by Pol δ , and removes the Rap1 protein block so that it is not an impediment to the polymerase. Interestingly, this cannot be accomplished by the helicase/nuclease Dna2, even though it plays a role long-flap processing. This work is a project in the lab of Roberto Galletto; my role was performing *in vitro* replication assays on the plasmid DNAs.

Pif1 removes a Rap1-dependent barrier to the strand displacement activity of DNA polymerase δ

Katrina N. Koc[†], Saurabh P. Singh[†], Joseph L. Stodola[†], Peter M. Burgers and Roberto Galletto^{*}

Department of Biochemistry and Molecular Biophysics, Washington University School of Medicine, Saint Louis, MO 63110, USA

Received February 12, 2016; Revised March 04, 2016; Accepted March 08, 2016

ABSTRACT

Using an *in vitro* reconstituted system in this work we provide direct evidence that the yeast repressor/activator protein 1 (Rap1), tightly bound to its consensus site, forms a strong non-polar barrier for the strand displacement activity of DNA polymerase δ . We propose that relief of inhibition may be mediated by the activity of an accessory helicase. To this end, we show that Pif1, a 5'–3' helicase, not only stimulates the strand displacement activity of Pol δ but it also allows efficient replication through the block, by removing bound Rap1 in front of the polymerase. This stimulatory activity of Pif1 is not limited to the displacement of a single Rap1 molecule; Pif1 also allows Pol δ to carry out DNA synthesis across an array of bound Rap1 molecules that mimics a telomeric DNA-protein assembly. This activity of Pif1 represents a novel function of this helicase during DNA replication.

INTRODUCTION

During DNA replication the actions of the replicative helicase and nucleosome remodelers/chaperones are thought to lead to destabilization of chromatin, thus facilitating progression of the replication fork (1–5). In addition to the need of dealing with nucleosomes packaged into chromatin, non-histone protein barriers along DNA regulate or hinder the progression of DNA replication (6,7). In this case the sole activity of the replicative helicase and polymerase may not be sufficient for efficient progression of replication across a protein barrier. Indeed, growing experimental evidence points to a role in this process of specialized DNA helicases (8).

In eukaryotes, one example of a non-histone protein barrier regulating DNA replication is the *S. cerevisiae* Fob1 protein (9,10). Fob1 binds to a strong replication fork bar-

rier site and generates a polar protein block that prevents head-on collisions between the replication and transcription forks (10–12). In *S. cerevisiae*, telomeres are one additional example of a non-histone protein barrier to progression of replication. At these sites, replication stalls at the repetitive telomeric DNA tracts, both terminal and internal to the chromosome ends (13–17). These regions contain multiple Rap1 binding sites and bound Rap1, rather than the nature of the repetitive sequence itself, was shown to be the cause of replication stalling (13).

These observations suggest that the replicative helicase and polymerase within the replisome are not sufficient for efficient bypass of non-histone protein barriers, and the activity of accessory motor proteins may be needed. In *S. cerevisiae*, deletion of Rrm3, a 5'–3' helicase that belongs to the Pif1 subfamily of SF1 helicases, increases replication fork pausing at ~1400 sites across the genome (14–17). These sites include rDNA, bound by Fob1, and telomeres, bound by Rap1. This has led to the proposal that Rrm3 helicase activity is important for efficient progression across a protein barrier (i.e. displacement of the protein) and provides an example *in vivo* of an accessory motor protein needed for efficient replication fork progression. Despite the genetic evidence *in vivo*, direct biochemical support *in vitro* for this function of Rrm3 is still missing. It is interesting to note that at difference with initial reports (13,16), recently it has been shown that Pif1 may also have a role in removal of bound proteins, facilitating fork progression at telomeric sites (18). Whether this function originates from Pif1 removing bound Rap1 at telomeres or else remains to be determined.

During lagging strand DNA synthesis, Pol δ extends the short Okazaki fragments generated by Pol α (19–21) and catalyzes strand displacement DNA synthesis through the downstream Okazaki fragment. Genome wide analysis of the distribution of Okazaki fragments showed that the ligation junctions map in close proximity to nucleosome dyads (22,23). The same is true for the tightly bound transcription factors Abf1, Reb1 and Rap1 (22,23). On the lagging

^{*}To whom correspondence should be addressed. Tel: +1 314 362 4368; Fax: +1 314 362 7183; Email: galletto@biochem.wustl.edu

[†]These authors contributed equally to the work as the first authors.

strand, both nucleosomes and tightly bound proteins appear to control the degree of strand displacement of Pol δ , affecting the position of the ligatable nick generated during maturation (23) and the degree to which the DNA synthesized by the error prone Pol α is removed by the strand displacement activity of Pol δ (22). Therefore, it is reasonable to postulate that the degree to which a tightly bound protein (e.g. Rap1) limits Pol δ activity solely relies on the effect that a protein block would have on strand displacement. To the best of our knowledge this has never been examined for Pol δ *in vitro*. Moreover, the amount of strand displacement activity by Pol δ needs to be regulated to avoid generating long 5'-flaps that can bind RPA, thus becoming inhibitory to FEN1 cleavage (24). Indeed, a secondary pathway for flap processing has been proposed and it involves Dna2 helicase/nuclease cleavage of flaps that have been extended by the Pif1 helicase (25,26). The mechanism that regulates the transition from short to long flaps is currently not well understood. Whether proteins bound to the downstream duplex to be displaced also affect the activities of Pif1 and/or Dna2 also remains to be established.

In this work we used model DNA substrates and purified proteins to ask two basic questions. First, we asked whether a Rap1 protein, tightly bound to the downstream duplex DNA, poses a block to an incoming Pol δ , thereby impairing its strand displacement activity. Our data show that in a reconstituted system a single bound Rap1 is sufficient to block the strand displacement activity of Pol δ , even when the enzyme is in a complex with its processivity factor PCNA. Second, we asked whether the helicase activity of Pif1 or the helicase/nuclease activity of Dna2 is sufficient to remove the bound Rap1 from the dsDNA, thus allowing Pol δ to catalyze primer extension past the protein barrier. Pif1 stimulates the apparent strand displacement activity of the polymerase by unwinding the downstream duplex DNA. Moreover, in the presence of Pif1, but not Dna2, Rap1 is no longer a block for Pol δ , indicating that the helicase activity of Pif1 is sufficient to remove a protein block from the dsDNA.

MATERIAL AND METHODS

Reagents and buffers

All chemicals used were reagent grade. All solutions were prepared with distilled and deionized Milli-Q water (18 M Ω at 25°C). Oligonucleotides were purchased from Integrated DNA Technology (IDT, Coralville, IA, USA). Annealed substrates were prepared by mixing the template, primer and strand to be displaced at a ratio of 1:1.2:1.1, respectively, in 10 mM Tris-HCl (pH 8.1), 50 mM NaCl, 5 mM MgCl₂ and heated at 95°C for 3 min, followed by slow cooling to room temperature. The TeloA sequence is 5'-ACACCCACACACC; RPG is 5'-ACACCCATACATT. To generate the pUC19 substrate with a 18 nt gap (pUC19g18), 2 Nt.BbvCI sites spaced by 11 bp were introduced 3' to the BamHI site by Quickchange mutagenesis. pUC19g18 was nicked with Nt.BbvCI for 60 min at 37°C, followed by addition of 20-fold excess of a 18 nt oligonucleotide complementary to the nicked strand at 65°C for 20 min and purification on MicroSpin S-400HR (GE Healthcare). The 336 bp cassette, containing 16 TeloA sites spaced by 21 bp and

flanked by EcoRI/HindIII, was synthesized (Genescript) and cloned in pUC19. The two sites for Nt-BbvCI were then introduced by Quickchange mutagenesis 50 bp from the first TeloA site and the 18 nt gap generated as describe above.

Purification of proteins

DNA polymerase δ wild-type and D520V (Pol δ^{DV}), purified as previously described (27–29). Replication Protein A (RPA), PCNA and Replication Factor C (RFC) were purified from *E. coli* overproduction strains as described (19,30,31). Untagged, full-length Rap1 was overexpressed and purified from *E. coli* as described (32). Full-length Pif1, its shorter variant missing the first 237 amino acids and the K264A mutant were purified with a N-terminus His₆-tag from *E. coli* (33).

Strand displacement and replication assay

Strand displacement DNA synthesis reactions were carried out in Buffer TM (20 mM Tris-HCl pH7.8, 8 mM MgAc₂, 1 mM DTT, 0.1mg/ml BSA) with 75 mM NaCl (or otherwise indicated). For experiments with PCNA a standard loading protocol was followed (20,34). For simplicity the concentrations reported are the final ones after starting the reaction. RFC (25 nM) was allowed to react with a double-biotinylated DNA substrate (25 nM) in presence of neutravidin (600 nM) and ATP (1 mM) for 5 min at 30°C, followed by the addition of Pol δ (25 nM) and dNTP mix (100 μ M). RPA (50 nM) and/or Rap1 (100 nM) were added before Pol δ . Pif1, at the indicated concentrations, was added with Pol δ . The experiments in absence of PCNA a DNA-Pol δ^{DV} complex (25 nM) was pre-forming in the absence or presence of Rap1 (100 nM, sufficient to saturate the single site with Rap1 in a canonical DNA-binding mode (32)) and/or Pif1 (25 nM) and the reaction started by addition of 100 μ M dNTP. At the indicated times the reactions were stopped by the addition of 80 mM EDTA, 0.08% SDS. After addition of formamide (50% final), the samples were heated at 95°C for 2 min and analyzed on a 12% denaturing polyacrylamide gel, pre-run for 2 h in 0.5x TBE. The gels were scanned using a Typhoon 9400 Variable Mode Imager (GE Healthcare), monitoring the Cy3 fluorescence of the labeled primer. Replication assays were performed at 30°C with 10 nM of the indicated plasmid DNA in Buffer TM. PCNA (15 nM) was loaded onto DNA with RFC (15 nM) and 1 mM ATP by incubation at 30°C for 2 min in the presence of RPA (1 μ M) and in the absence or presence of Rap1 (400 nM). The reactions were initiated by addition of Pol δ (15 nM) and 100 μ M each of dATP, dGTP, dTTP and 10 μ M of [α -³²P]-dCTP and Pif1 when indicated. The reactions were stopped with 50 mM EDTA and 0.1% SDS (final concentration) and the products analyzed by electrophoresis on a 1% alkaline agarose gel. The gels were dried and visualized by PhosphorImager analysis (GE Healthcare).

RESULTS

A single Rap1 bound to a high-affinity recognition site is a barrier for DNA polymerase δ

In order to test whether a single Rap1 bound to a downstream duplex is a block to the strand displacement activity

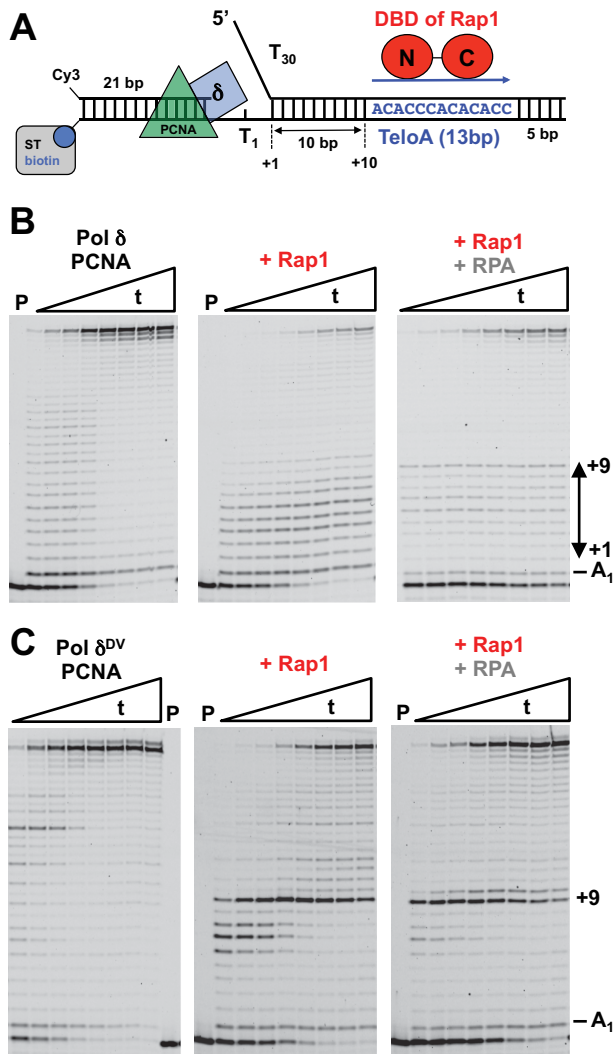


Figure 1. A single bound Rap1 is a barrier to the strand displacement activity of Pol δ . (A) Substrate used in the assays. (B) Primer extension assays by PCNA-loaded Pol δ (25 nM) in the absence or presence of Rap1 (100 nM) or RPA (50 nM) and Rap1 (100 nM). The DNA is 25 nM. (C) Same primer extension assays as in (B) but with Pol δ^{DV} . Times (t) are: 10'', 20'', 30'', 1', 2', 4', 6', 10'.

of Pol δ , we used a DNA substrate that contains a 21 nt primer labeled at the 5'-end with Cy3, followed by a gap of a single thymine and a 28 bp dsDNA region to be displaced (Figure 1A). The downstream dsDNA region contains a dT₃₀ 5'-flap and a high-affinity Rap1 recognition sequence found at telomeres (TeloA) positioned 10 bp from the junction of the 5'-flap. For this orientation of the recognition sequence, Rap1 binds with the N-terminal Myb-like region of its DNA-binding domain (DBD) facing the incoming polymerase and with the majority of the Rap1 contacts with the phosphate backbone of the DNA occurring on the non-template strand (35–38). Finally, the 3'-end of the template strand is biotinylated to allow binding of streptavidin that in combination with the presence of the 5'-flap restricts PCNA binding to the primer region of the substrate.

PCNA was loaded on the substrate with RFC and ATP in the absence (Figure 1B, left panel) or presence (Figure

1B, middle panel) of a 4-fold excess of Rap1 over the DNA, the reaction started by addition of Pol δ and dNTPs and monitored by extension of the Cy3-labeled primer. In the presence of Rap1, the amount of full product generated is decreased, suggesting that Rap1 is a block to the strand displacement activity of Pol δ (see Supplementary Figure S1A). Moreover, there is a concomitant increase of intermediate bands between +1 and +9 generated by strand displacement. These intermediate bands likely originate from the 3'–5' exonuclease activity of Pol δ , which causes the polymerase to idle (reiterative cycles of strand displacement synthesis followed by exonucleolytic degradation) between the nick position and the Rap1 block. Indeed, the presence of a Rap1 block (and disappearance of idling) becomes evident when an exonuclease deficient Pol δ (Pol δ^{DV} , D520V) is used (Figure 1C, Supplementary Figure S1B and S1C). In this case, the +9 extension band becomes very pronounced, indicating that the polymerase is halted 1 bp prior to first position of the Rap1 recognition sequence. Taken together these data indicate that Rap1 is a strong block for Pol δ that is bypassed very slowly.

Next, we asked whether binding of RPA to the 5'-flap would allow bypass of Rap1. In the presence of RPA the amount of full-product generated by wild-type Pol δ is more than in its absence (right panel in Figure 1B, and Supplementary Figure S1A). We note that in this case the fraction of substrate utilized during the reaction is also lower, leading to an apparent lower fraction of extended products. It is possible that on this substrate containing a single nucleotide gap, the loading of the polymerase in the presence of RPA and Rap1 is slightly less efficient. Nevertheless, in the presence of RPA there is a clear accumulation of the +9 band. These data indicate that Rap1 is still a block to the strand displacement activity of the polymerase. Because of the lack of exonuclease activity the presence of a +9 extension band becomes evident when Pol δ^{DV} is used (right panel in Figure 1C, and Supplementary Figure S1B), again indicating that RPA does not allow bypass of the Rap1 block. However, in the presence of RPA the fraction of polymerase that can extend past the Rap1 block is larger than in its absence, consistent with RPA stimulating the strand displacement activity of Pol δ^{DV} .

Next, we tested whether the position, orientation, or nature of the Rap1 recognition sequence would affect the ability of Rap1 to hinder Pol δ . Because of the presence of well-defined extension bands, for these experiments we used Pol δ^{DV} . Rap1 still blocked Pol δ^{DV} when the 13 bp TeloA was moved 5 bp closer to the 5'-flap (Figure 2, lanes 19–24). However, in this case the fraction of Pol δ that can bypass the block is higher than when the TeloA sequence is placed 10 bp downstream. Next, we placed the TeloA sequence in the opposite orientation (Figure 2, lanes 31–36). In this orientation the C-terminal Myb-like region of the DBD of Rap1 faces the incoming polymerase and the majority of the protein contacts with the phosphate backbone of the DNA occur with the template strand (35–38). Rap1 is a block for Pol δ^{DV} also when bound in this opposite orientation. Interestingly, now a +3 rather than a +4 extension band is prominent, suggesting an asymmetrical interaction of Rap1 with its recognition sequence. Finally, we also tested a different Rap1 recognition sequence found at the ribosomal protein

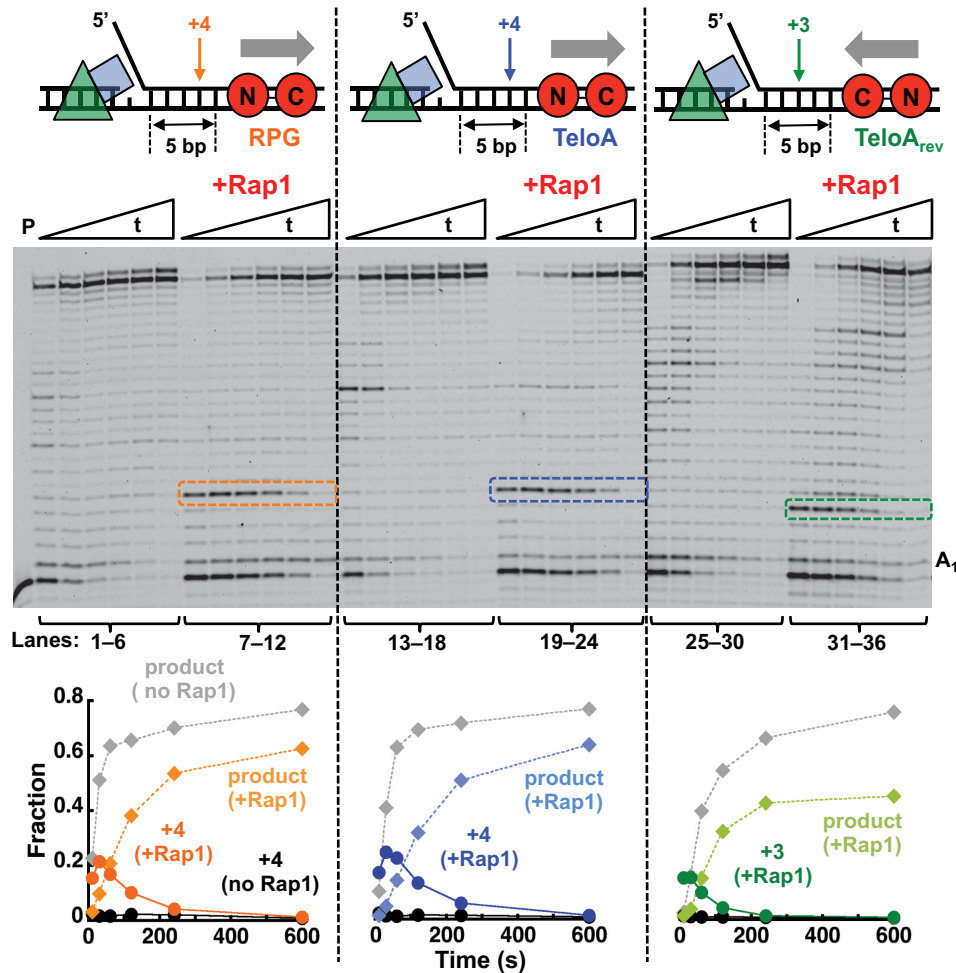


Figure 2. A single bound Rap1 is a non-polar barrier to the strand displacement activity of Pol δ^{DV} . Primer extension assays by PCNA-loaded Pol δ^{DV} (25 nM) in the absence or presence of Rap1 (100 nM) bound to the different recognition sequences indicated in the cartoons. The graphs are the quantitation of full-product and the strong pause band observed in the gel (arrow in the cartoons). For reference the same bands were quantitated also for the experiments in the absence of Rap1.

genes (RPG) (Figure 2, lanes 7–12). Rap1 bound to this alternative recognition sequence is still a block for Pol δ^{DV} .

Pif1 stimulates the activity of Pol δ by unwinding the downstream dsDNA

The data in the previous section provide strong evidence that a single tightly bound Rap1 is a block to an incoming Pol δ and therefore it must be removed for strand displacement to occur. The presence of a pre-formed 5'-ssDNA flap or creation of a flap during strand displacement by the polymerase would generate the proper substrate for the activity of a 5'-3' helicase. Interestingly, it has been shown that Pif1 is involved both in Okazaki fragment maturation and break-induced replication *in vivo*, processes that involve Pol δ and the presence of 5'-ssDNA available either as a flap or within a D-loop (25,26,39–41). Indeed, in reconstituted reactions excess Pif1 stimulates the strand displacement activity of Pol δ bound to PCNA (25,40). However, we showed that in excess enzyme over the DNA, Pif1 undergoes DNA-induced dimerization (42). Therefore, we tested whether at

concentrations where a monomer of Pif1 is favored on the DNA (equimolar to or lower than the DNA), Pif1 would still be able to stimulate Pol δ strand displacement.

We used a substrate that contains a T₇ gap and a longer dsDNA downstream (45 bp) with a T₃₀ 5'-flap. When Pol δ is bound to PCNA on the DNA, addition of a low concentration of Pif1 led to higher primer extension activity (Figure 3A). Stimulation of primer extension activity by Pif1 does not require the presence of the first 237 amino acids, suggesting that the helicase core is sufficient, but it requires an active ATPase (K264A variant is inactive (33)). This indicates that at these concentrations binding of Pif1 to the 5'-flap is not sufficient to stimulate strand displacement. Also, we do not find evidence of direct interaction between the helicase and polymerase, as stimulation of primer extension by Pif1 also occurs with the heterologous phage T7 DNA polymerase (33). The stimulation of the primer extension activity of Pol δ originates from multiple turnovers of Pif1 unwinding, with DNA synthesis by the polymerase preventing re-annealing of the template strand.

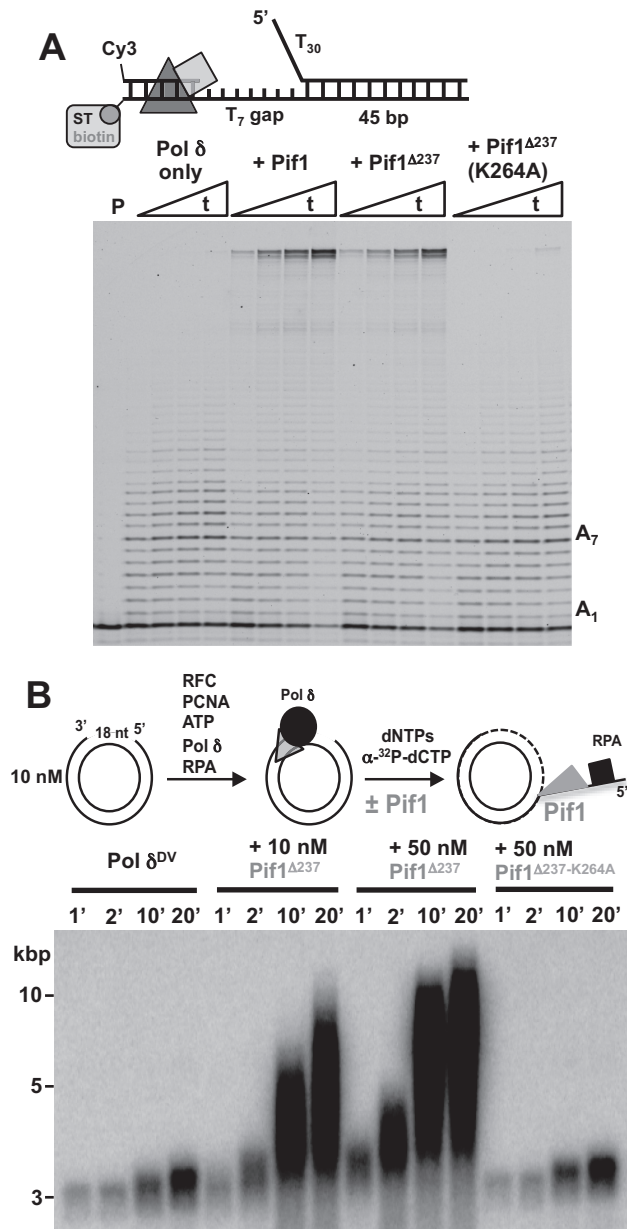


Figure 3. Pif1 stimulates the strand displacement activity of Pol δ . (A) Primer extension assays using the indicated DNA (25 nM) and PCNA-loaded Pol δ (25 nM) performed in the absence and presence of different versions of Pif1 (20 nM). Times (t) are: 5", 15", 30", 60". (B) Replication assays of a 18 nt gapped pUC19 (10 nM) with PCNA-loaded Pol δ^{DV} (15 nM) in the absence or presence of the shorter version of Pif1 (10 or 50 nM) or its ATPase inactive variant (50 nM).

Finally, it has been shown that Pif1 in excess over the DNA can stimulate kbps of DNA synthesis when Pol δ extends a D-loop, and this stimulation has been proposed to generate from the activity of Pif1 either in front of the polymerase or at the backend of the D-loop by removing the newly synthesized DNA (40). In order to test whether Pif1 can stimulate Pol δ DNA synthesis over DNA lengths longer than the oligonucleotides used in the previous section, we performed replication assays with pUC19 containing a 18 nt ssDNA gap. With this substrate, only the effect

of Pif1 in front of the polymerase is monitored. The data in Figure 3B show that addition of Pif1 stimulates DNA synthesis by Pol δ and this requires the ATPase activity of the helicase. In the presence of Pif1 products longer than the length of the plasmids are generated, indicating that the activity of Pif1 in front of Pol δ is sufficient to lead to synthesis of kbps of DNA.

Pif1 but not Dna2 allows Pol δ to bypass a Rap1 block

The data in the previous section indicate that Pif1 stimulates polymerase activity of Pol δ by unwinding the downstream dsDNA and suggest that a monomer of Pif1 is sufficient. Next, we asked whether Pif1 would allow Pol δ to catalyze primer extension even across a bound Rap1, indicating that the block has been removed. Figure 4A shows strand displacement reactions with Pol δ^{DV} in the presence of bound Rap1 and absence or presence of Pif1. With Pif1 in the reaction (lanes 9–16) a larger amount of full product is formed in shorter times, and also the +9 extension band is less prominent and is cleared faster. This indicates that Pif1 unwinding activity leads to displacement of the Rap1 block, independent of the presence of RPA bound to the 5'-flap (Supplementary Figure S3). Moreover, stimulation by Pif1 of the strand displacement activity of Pol δ and bypass of the Rap1 block were observed also with Pol δ that is not in a complex with PCNA (Supplementary Figure S2), indicating that the reported interaction of Pif1 with PCNA (40) is not required.

In yeast, Dna2 is a 5'-3' helicase/nuclease that is involved in maturation of Okazaki fragments by cleaving long 5'-flaps in conjunction with Pif1 (25,26,39). In the presence of nuclease activity, it has been shown that Dna2 will preferentially cleave the substrate rather than unwind it (43). Indeed, Dna2 alone does not relieve the Rap1 block (Figure 4A, lanes 17–24). RPA stimulates the activity of Dna2 (43), but its presence did not allow Dna2 helicase to relieve the Rap1 block (Supplementary Figure S3). When Dna2 and Pif1 were added together (Figure 4A, lanes 25–32) the Rap1 block was still relieved, but to a lesser extent than for Pif1 alone, possibly due to the nuclease activity of Dna2 removing the 5'-flap and thus eliminating the entry point for Pif1. These data suggest that if a Rap1 block needs to be dealt with by Pol δ during Okazaki fragment maturation, the activity of Pif1, and not Dna2, is sufficient.

Next, we used a DNA substrate containing the RPG recognition sequence positioned 5 bp from the 5'-flap and performed the experiment at 21°C rather than 30°C to better visualize blocked intermediates. Pif1 displaces Rap1 also when it is bound to this alternative sequence (Figure 4B). The N-terminus region of Pif1 is not required for Rap1 displacement but the presence of an active ATPase is (Figure 4B). Sub-stoichiometric concentrations of Pif1 are sufficient for removal of Rap1, indicating that a monomer of Pif1 unwinds the dsDNA and displaces Rap1. Similar to what observed with the DNA substrate in Figure 1A, in the presence of RPA the fraction of Pol δ^{DV} that can bypass a Rap1 bound to the RPG sequence is larger, consistent with RPA stimulating the strand displacement activity of the polymerase. Interestingly, in the presence of RPA even at a concentration of Pif1 4-fold lower than the DNA con-

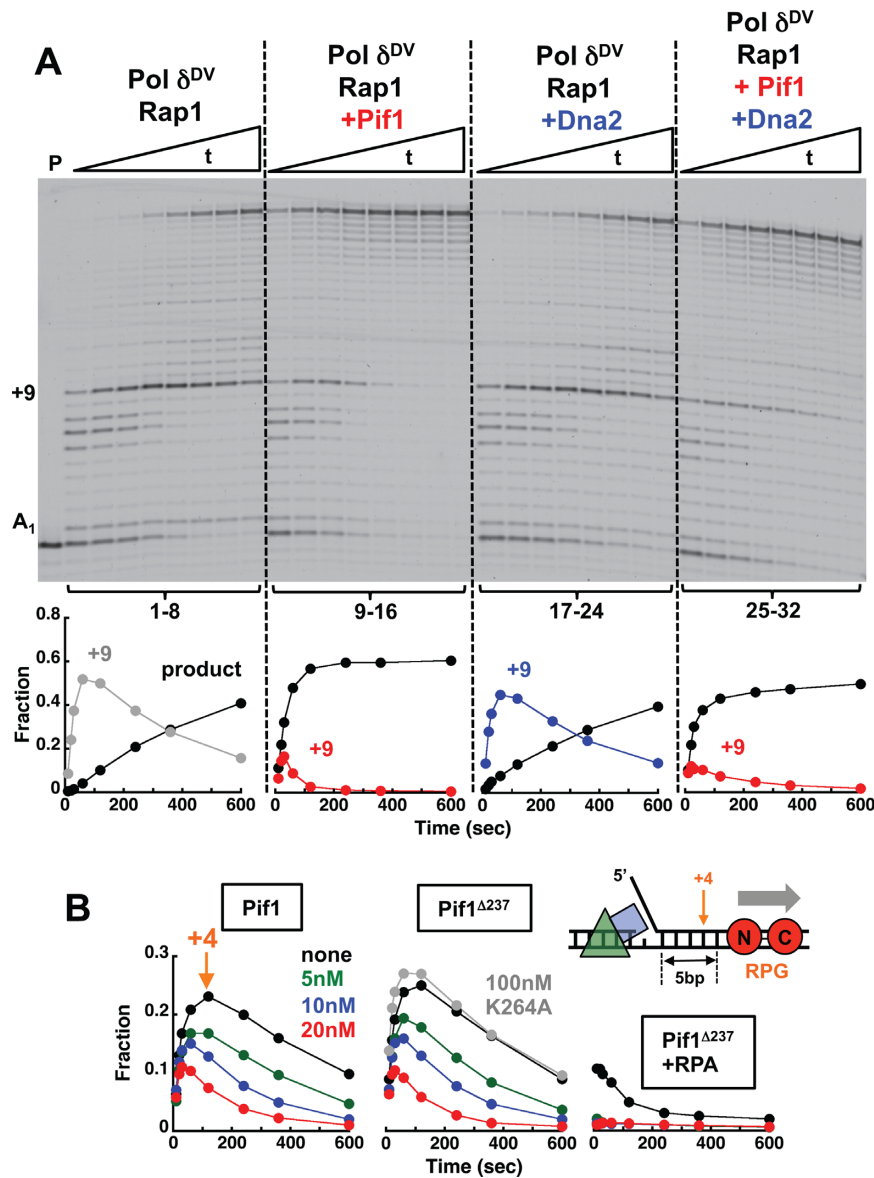


Figure 4. Pif1 allows Pol δ to bypass a Rap1 block. (A) Primer extension assays with PCNA-loaded Pol δ^{DV} (25 nM) using the DNA (25 nM) in Figure 1A bound to Rap1 (100 nM). The experiments were performed in the absence (lanes 1–8) or presence of 20 nM Pif1 (lanes 9–16), 20 nM Dna2 (lanes 17–24) or 20 nM Pif1 and 20 nM Dna2 (lanes 25–32). The graphs show quantitation of the full-product and the +9 position in the downstream duplex. (B) Quantitation of full-product and the +4 position using the indicated DNA (25 nM) bound to Rap1 (100 nM). The primer extension assays were performed with PCNA-loaded Pol δ^{DV} (25 nM) in the absence (black) or presence of 20 nM (red), 10 nM (blue) or 5 nM (green) of either Pif1 (left) or its variant missing the first 237 amino acids and its ATPase inactive form (middle). The experiments in the right panel were performed in the presence of 50 nM RPA.

centration, Rap1 is efficiently displaced, so much so that no +4 extension band is detected.

A 5'-flap generated during strand displacement is sufficient for Pif1-mediated removal of Rap1 even when bound to an array of sites

The DNA substrates used in the previous experiments contained a pre-formed 5'-ssDNA flap, however, during Okazaki fragment maturation flaps are formed only transiently. Therefore, we tested whether Pif1 would be able to displace a bound Rap1 when the flap is generated during strand displacement by the polymerase. For this we used

a DNA substrate with a T₁ gap, the TeloA sequence positioned 10 bp downstream in the dsDNA to be displaced and a doubly biotinylated template bound to streptavidin to prevent PCNA from sliding off the DNA (Figure 5A). Similar to what observed with the same substrate containing a 5'-flap, Rap1 is a block for the incoming Pol δ^{DV} . However, addition of Pif1 stimulates formation of full-extension product and the amount of the +9 extension band is reduced. This indicates that generation of a 5'-flap during strand displacement by the polymerase allows for Pif1 to bind to the substrate and displace Rap1.

Next, we asked whether Pif1 could displace multiple Rap1 proteins and thus stimulate DNA synthesis by Pol δ

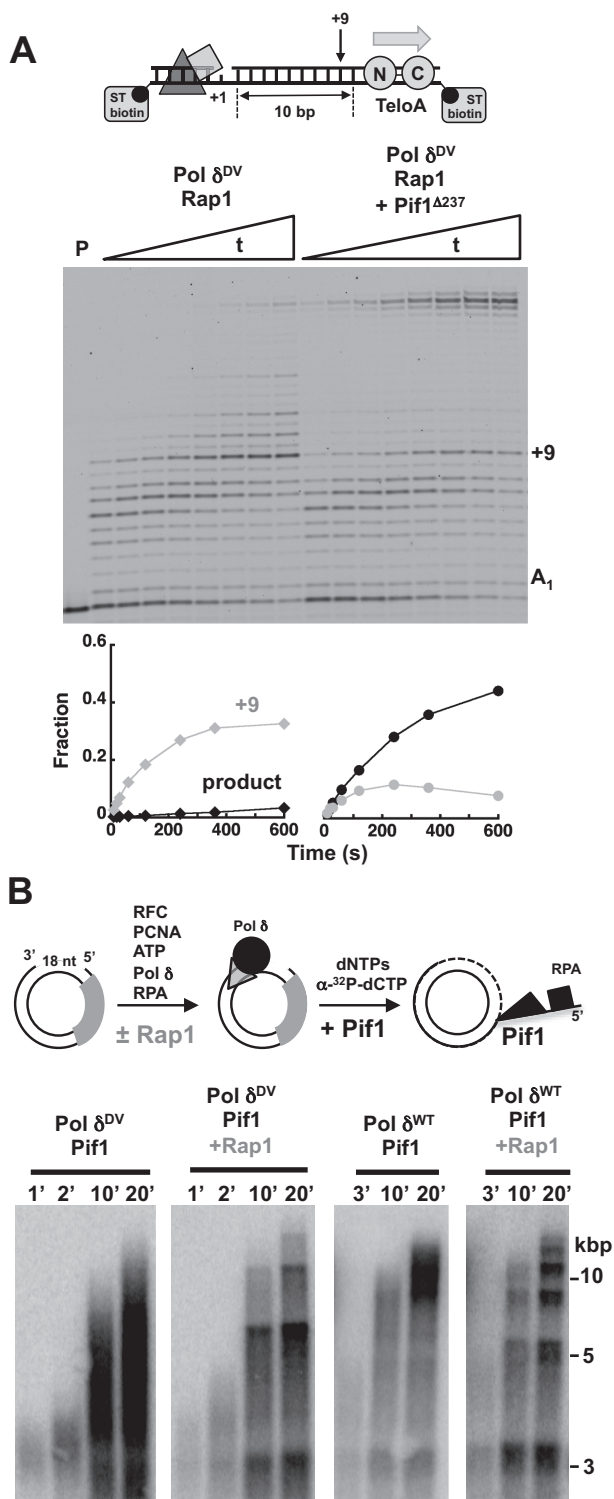


Figure 5. Transient generation of a 5'-flap is sufficient for Pif1 to allow Pol δ to bypass a single or multiple Rap1. (A) Primer extension assays with PCNA loaded Pol δ^{DV} (25 nM) in the absence and presence of Pif1 (20 nM) with Rap1 (100 nM) bound to a DNA (25 nM) without a 5'-flap. The graphs show quantitation of the full product and the +9 position in the downstream duplex. (B) Replication assays by wild-type and exo-nuclease deficient Pol δ (15 nM) in the absence and presence of Pif1 (10 nM), using a 18 nt gapped pUC19 (10 nM) with an array of 16 Rap1 sites positioned 50 bp from the gap and bound by a 2.5-fold excess of Rap1 relative to the concentration of sites (160 nM).

across an array of bound Rap1 that mimics a telomere. Arrays of Rap1 sites with 21 bp spacing are counted *in vivo* as a normal telomere (44). Thus, we used a 336 bp cassette containing 16 identical sites (TeloA) spaced by 21 bp and in the same orientation. The cassette was cloned into pUC19 and the nicking sites used generate the 18 nt ssDNA gap to initiate DNA synthesis by Pol δ were introduced 50 bp upstream of the cassette. In the presence or the absence of Rap1, the DNA synthesis activity of Pol δ^{DV} alone was similar to what observed with pUC19 in Figure 3B (not shown). Similarly, in the absence of Rap1, addition of Pif1 stimulates DNA synthesis by Pol δ and Pol δ^{DV} (Figure 5B). In the presence of a 2.5-fold excess of Rap1 relative to the concentration of sites (sufficient for saturation, not shown) Pif1 is still able to stimulate DNA synthesis by Pol δ , indicating that Pif1 displaces multiple bound Rap1 molecules. Indeed, Pif1 displaces Rap1 over multiple cycles of Rap1 dissociation and re-binding, as indicated by the presence of discrete bands spaced according to the size of the plasmid.

DISCUSSION

Despite evidence *in vivo* of the role of tightly bound proteins in affecting DNA replication, comparatively less is known at the biochemical level using reconstituted proteins. In this work we used *S. cerevisiae* Rap1 as an example of a well-documented natural protein obstacle (13,15,16,22,23) and showed that a single bound Rap1 is a barrier to the strand displacement activity of Pol δ . The presence of RPA stimulates the strand displacement activity of Pol δ but this is not sufficient to allow bypass of a tightly bound Rap1. Interestingly, for wild-type Pol δ the presence of bound Rap1 leads to an increase in the idling of polymerase in the region preceding the recognition site for Rap1. This suggests that the protein block does not induce dissociation of Pol δ , but rather favors the exo-nuclease activity and backtracking. Bound Rap1 is a barrier independent of the orientation of its recognition site, indicating that Rap1 is not a polar block. Our findings using a reconstituted system, showing that a single Rap1 bound to a high affinity site is sufficient to limit the strand displacement activity of Pol δ , provide strong and direct support to the observation that at the genome-wide level Rap1 sites impart a signature for the boundaries of Okazaki fragment junctions (22,23).

During Okazaki fragment maturation, in addition to the processing by FEN1 of short flaps generated by Pol δ (45,46), a second pathway exists in which long flaps generated by Pif1 are substrates for cleavage by Dna2 (25,26,39). *In vitro*, excess Pif1 unwinds substrates that mimic an Okazaki fragment (26), thus stimulating the incorporation activity of Pol δ . However, in excess enzyme over the DNA, Pif1 undergoes DNA-induced dimerization (42). The data in this work show that at concentrations that favor binding of a monomer to the DNA, Pif1 stimulates the replication activity of Pol δ (alone or in a complex with PCNA). A monomer of Pif1 binds to the 5'-flap and unwinds the downstream dsDNA, with DNA synthesis by Pol δ preventing re-annealing of the template strand. Surprisingly, Pif1 stimulates the primer extension activity of Pol δ even in the presence of bound Rap1. This provides clear indication that Pif1 can displace bound Rap1 while unwinding the down-

stream duplex. Removal of Rap1 by Pif1 is independent of the nature of the Rap1 site and its orientation, and requires the ATPase activity of Pif1. The ability of Pif1 to remove Rap1 is not limited to the presence of a pre-formed 5'-flap for initial binding. A short 5'-flap transiently generated by the strand displacement activity of Pol δ is sufficient. RPA stimulates the Rap1 displacement activity of Pif1, likely restricting Pif1 binding to the fork junction. The data in this work show that Pif1 stimulates primer extension activity of Pol δ also when the polymerase is not bound to PCNA. Although we cannot exclude that the reported interaction of Pif1 with PCNA (40) has some role in the removal of a Rap1 block, our data indicate that this interaction is not required. Interestingly, the ability of Pif1 to remove Rap1 in front of Pol δ would suggest that the effect of Rap1 on the distribution of Okazaki fragments and the position of the ligation junctions should not be observed *in vivo* (22,23). One simple explanation could be that Okazaki fragment maturation is an efficient process and that flap processing by the Dna2/Pif1 pathway is a rare event.

In *S. cerevisiae*, Rrm3, a second helicase homologue to Pif1, has been proposed to facilitate replication fork progression at specific internal loci and telomeres (13,15,16) and it has been shown *in vitro* that Rrm3 is a 5'-3' helicase (16). Surprisingly all of the Rrm3 constructs we generated so far (including a N-terminal truncated version (16)) show ssDNA dependent ATPase activity, yet they possess poor helicase activity even when coupled to the activity of Pol δ (data not shown). We do not currently know the reason for the limited unwinding activity of the Rrm3 constructs. Whether interaction of Rrm3 with the replisome (14) or other factors activate it for unwinding remains to be determined. However, it has been reported that Pif1 may also facilitate replication fork progression at telomeres (18). In support of this novel function of Pif1, we showed that Pif1 displaces multiple Rap1 molecules, allowing Pol δ to replicate across an array of bound Rap1 that mimics a functional telomere.

Protein barriers may pose a problem not only for normal DNA replication but also during break-induced replication (BIR). In BIR, a replication fork is reassembled to allow copying of the template DNA to the end of the chromosome. Depending on the location of the invasion point the activity of the replicative helicase and Pol δ (or Pol ϵ) may not be sufficient to remove tightly bound proteins. Moreover, completion of BIR would be especially problematic at telomeres, which pose a substantial barrier to progression of replication even during normal replication (13–15,17). Interestingly, it has been shown that Rrm3, the helicase proposed to remove proteins bound to DNA (13,15,16), does not have a significant role in BIR; rather, Pif1 does (40). Although the mechanism whereby Pif1 stimulates DNA synthesis from a migrating D-loop in BIR is not fully established, our data show that the activity of Pif1 in front of Pol δ is sufficient to stimulate kbps of DNA synthesis, even across an array of bound Rap1 that mimics a telomere. It is intriguing to speculate that in BIR one of the roles of Pif1 may be to help remove proteins bound to the DNA, especially at telomeres.

SUPPLEMENTARY DATA

Supplementary Data are available at NAR Online.

FUNDING

National Institutes of Health [GM098509 to R.G. and GM032431 to P.B.]. Funding for open access charge: National Institutes of Health [GM098509 to R.G. and GM032431 to P.B.].

Conflict of interest statement. None declared.

REFERENCES

- MacAlpine, D.M. and Almouzni, G. (2013) Chromatin and DNA replication. *Cold Spring Harb. Perspect. Biol.*, **5**, a010207.
- Corpet, A. and Almouzni, G. (2009) Making copies of chromatin: the challenge of nucleosomal organization and epigenetic information. *Trends Cell Biol.*, **19**, 29–41.
- Groth, A., Corpet, A., Cook, A.J., Roche, D., Bartek, J., Lukas, J. and Almouzni, G. (2007) Regulation of replication fork progression through histone supply and demand. *Science*, **318**, 1928–1931.
- Groth, A., Rocha, W., Verreault, A. and Almouzni, G. (2007) Chromatin challenges during DNA replication and repair. *Cell*, **128**, 721–733.
- Ransom, M., Dennehey, B.K. and Tyler, J.K. (2010) Chaperoning histones during DNA replication and repair. *Cell*, **140**, 183–195.
- Mirkin, E.V. and Mirkin, S.M. (2007) Replication fork stalling at natural impediments. *Microbiol. Mol. Biol. Rev.*, **71**, 13–35.
- Labib, K. and Hodgson, B. (2007) Replication fork barriers: pausing for a break or stalling for time? *EMBO Rep.*, **8**, 346–353.
- Bruning, J.G., Howard, J.L. and McGlynn, P. (2014) Accessory replicative helicases and the replication of protein-bound DNA. *J. Mol. Biol.*, **426**, 3917–3928.
- Brewer, B.J. and Fangman, W.L. (1988) A replication fork barrier at the 3' end of yeast ribosomal RNA genes. *Cell*, **55**, 637–643.
- Linskens, M.H. and Huberman, J.A. (1988) Organization of replication of ribosomal DNA in *Saccharomyces cerevisiae*. *Mol. Cell. Biol.*, **8**, 4927–4935.
- Kobayashi, T. and Horiuchi, T. (1996) A yeast gene product, Fob1 protein, required for both replication fork blocking and recombinational hotspot activities. *Genes Cells*, **1**, 465–474.
- Kobayashi, T. (2003) The replication fork barrier site forms a unique structure with Fob1p and inhibits the replication fork. *Mol. Cell. Biol.*, **23**, 9178–9188.
- Makovets, S., Herskowitz, I. and Blackburn, E.H. (2004) Anatomy and dynamics of DNA replication fork movement in yeast telomeric regions. *Mol. Cell. Biol.*, **24**, 4019–4031.
- Azvolinsky, A., Dunaway, S., Torres, J.Z., Bessler, J.B. and Zakian, V.A. (2006) The *S. cerevisiae* Rrm3p DNA helicase moves with the replication fork and affects replication of all yeast chromosomes. *Genes Dev.*, **20**, 3104–3116.
- Ivessa, A.S., Lenzmeier, B.A., Bessler, J.B., Goudsouzian, L.K., Schnakenberg, S.L. and Zakian, V.A. (2003) The *Saccharomyces cerevisiae* helicase Rrm3p facilitates replication past nonhistone protein-DNA complexes. *Mol. Cell*, **12**, 1525–1536.
- Ivessa, A.S., Zhou, J.Q., Schulz, V.P., Monson, E.K. and Zakian, V.A. (2002) *Saccharomyces Rrm3p*, a 5' to 3' DNA helicase that promotes replication fork progression through telomeric and subtelomeric DNA. *Genes Dev.*, **16**, 1383–1396.
- Ivessa, A.S., Zhou, J.Q. and Zakian, V.A. (2000) The *Saccharomyces Pif1p* DNA helicase and the highly related Rrm3p have opposite effects on replication fork progression in ribosomal DNA. *Cell*, **100**, 479–489.
- Anand, R.P., Shah, K.A., Niu, H., Sung, P., Mirkin, S.M. and Freudenreich, C.H. (2012) Overcoming natural replication barriers: differential helicase requirements. *Nucleic Acids Res.*, **40**, 1091–1105.
- Ayyagari, R., Gomes, X.V., Gordenin, D.A. and Burgers, P.M. (2003) Okazaki fragment maturation in yeast. I. Distribution of functions between FEN1 AND DNA2. *J. Biol. Chem.*, **278**, 1618–1625.
- Jin, Y.H., Ayyagari, R., Resnick, M.A., Gordenin, D.A. and Burgers, P.M. (2003) Okazaki fragment maturation in yeast. II.

- Cooperation between the polymerase and 3'-5'-exonuclease activities of Pol delta in the creation of a ligatable nick. *J. Biol. Chem.*, **278**, 1626–1633.
21. Maga, G., Villani, G., Tillement, V., Stucki, M., Locatelli, G.A., Frouin, I., Spadari, S. and Hubscher, U. (2001) Okazaki fragment processing: modulation of the strand displacement activity of DNA polymerase delta by the concerted action of replication protein A, proliferating cell nuclear antigen, and flap endonuclease-1. *Proc. Natl. Acad. Sci. U.S.A.*, **98**, 14298–14303.
 22. Reijns, M.A., Kemp, H., Ding, J., de Proce, S.M., Jackson, A.P. and Taylor, M.S. (2015) Lagging-strand replication shapes the mutational landscape of the genome. *Nature*, **518**, 502–506.
 23. Smith, D.J. and Whitehouse, I. (2012) Intrinsic coupling of lagging-strand synthesis to chromatin assembly. *Nature*, **483**, 434–438.
 24. Bae, S.H., Bae, K.H., Kim, J.A. and Seo, Y.S. (2001) RPA governs endonuclease switching during processing of Okazaki fragments in eukaryotes. *Nature*, **412**, 456–461.
 25. Pike, J.E., Burgers, P.M., Campbell, J.L. and Bambara, R.A. (2009) Pif1 helicase lengthens some Okazaki fragment flaps necessitating Dna2 nuclease/helicase action in the two-nuclease processing pathway. *J. Biol. Chem.*, **284**, 25170–25180.
 26. Pike, J.E., Henry, R.A., Burgers, P.M., Campbell, J.L. and Bambara, R.A. (2010) An alternative pathway for Okazaki fragment processing: resolution of fold-back flaps by Pif1 helicase. *J. Biol. Chem.*, **285**, 41712–41723.
 27. Fortune, J.M., Stith, C.M., Kissling, G.E., Burgers, P.M. and Kunkel, T.A. (2006) RPA and PCNA suppress formation of large deletion errors by yeast DNA polymerase delta. *Nucleic Acids Res.*, **34**, 4335–4341.
 28. Stith, C.M., Sterling, J., Resnick, M.A., Gordenin, D.A. and Burgers, P.M. (2008) Flexibility of eukaryotic Okazaki fragment maturation through regulated strand displacement synthesis. *J. Biol. Chem.*, **283**, 34129–34140.
 29. Koc, K.N., Stodola, J.L., Burgers, P.M. and Galletto, R. (2015) Regulation of yeast DNA polymerase delta-mediated strand displacement synthesis by 5'-flaps. *Nucleic Acids Res.*, **43**, 4179–4190.
 30. Henricksen, L.A., Umbricht, C.B. and Wold, M.S. (1994) Recombinant replication protein A: expression, complex formation, and functional characterization. *J. Biol. Chem.*, **269**, 11121–11132.
 31. Gomes, X.V., Gary, S.L. and Burgers, P.M. (2000) Overproduction in *Escherichia coli* and characterization of yeast replication factor C lacking the ligase homology domain. *J. Biol. Chem.*, **275**, 14541–14549.
 32. Feldmann, E.A., De Bona, P. and Galletto, R. (2015) The wrapping loop and Rap1 C-terminal (RCT) domain of yeast Rap1 modulate access to different DNA binding modes. *J. Biol. Chem.*, **290**, 11455–11466.
 33. Singh, S.P., Koc, K.N., Stodola, J.L. and Galletto, R. (2016) A monomer of Pif1 unwinds double-stranded DNA and it is regulated by the nature of the non-translocating strand at the 3'-end. *J. Mol. Biol.*, doi:10.1016/j.jmb.2016.02.017.
 34. Burgers, P.M. and Gerik, K.J. (1998) Structure and processivity of two forms of *Saccharomyces cerevisiae* DNA polymerase delta. *J. Biol. Chem.*, **273**, 19756–19762.
 35. Konig, P., Giraldo, R., Chapman, L. and Rhodes, D. (1996) The crystal structure of the DNA-binding domain of yeast RAP1 in complex with telomeric DNA. *Cell*, **85**, 125–136.
 36. Taylor, H.O., O'Reilly, M., Leslie, A.G. and Rhodes, D. (2000) How the multifunctional yeast Rap1p discriminates between DNA target sites: a crystallographic analysis. *J. Mol. Biol.*, **303**, 693–707.
 37. Matot, B., Le Bihan, Y.V., Lescasse, R., Pérez, J., Miron, S., David, G., Castaing, B., Weber, P., Raynal, B., Zinn-Justin, S. *et al.* (2012) The orientation of the C-terminal domain of the *Saccharomyces cerevisiae* Rap1 protein is determined by its binding to DNA. *Nucleic Acids Res.*, **40**, 3197–3207.
 38. Le Bihan, Y.V., Matot, B., Pietrement, O., Giraud-Panis, M.J., Gasparini, S., Le Cam, E., Gilson, E., Sclavi, B., Miron, S. and Le Du, M.H. (2013) Effect of Rap1 binding on DNA distortion and potassium permanganate hypersensitivity. *Acta Crystallogr. D Biol. Crystallogr.*, **69**, 409–419.
 39. Rossi, M.L., Pike, J.E., Wang, W., Burgers, P.M., Campbell, J.L. and Bambara, R.A. (2008) Pif1 helicase directs eukaryotic Okazaki fragments toward the two-nuclease cleavage pathway for primer removal. *J. Biol. Chem.*, **283**, 27483–27493.
 40. Wilson, M.A., Kwon, Y., Xu, Y., Chung, W.H., Chi, P., Niu, H., Mayle, R., Chen, X., Malkova, A., Sung, P. *et al.* (2013) Pif1 helicase and Poldelta promote recombination-coupled DNA synthesis via bubble migration. *Nature*, **502**, 393–396.
 41. Vasianovich, Y., Harrington, L.A. and Makovets, S. (2014) Break-induced replication requires DNA damage-induced phosphorylation of Pif1 and leads to telomere lengthening. *PLoS Genet.*, **10**, e1004679.
 42. Barranco-Medina, S. and Galletto, R. (2010) DNA binding induces dimerization of *Saccharomyces cerevisiae* Pif1. *Biochemistry*, **49**, 8445–8454.
 43. Levikova, M., Klaue, D., Seidel, R. and Cejka, P. (2013) Nuclease activity of *Saccharomyces cerevisiae* Dna2 inhibits its potent DNA helicase activity. *Proc. Natl. Acad. Sci. U.S.A.*, **110**, E1992–E2001.
 44. Grossi, S., Bianchi, A., Damay, P. and Shore, D. (2001) Telomere formation by rap1p binding site arrays reveals end-specific length regulation requirements and active telomeric recombination. *Mol. Cell Biol.*, **21**, 8117–8128.
 45. Garg, P., Stith, C.M., Sabouri, N., Johansson, E. and Burgers, P.M. (2004) Idling by DNA polymerase delta maintains a ligatable nick during lagging-strand DNA replication. *Genes Dev.*, **18**, 2764–2773.
 46. Tishkoff, D.X., Filosi, N., Gaida, G.M. and Kolodner, R.D. (1997) A novel mutation avoidance mechanism dependent on *S. cerevisiae* RAD27 is distinct from DNA mismatch repair. *Cell*, **88**, 253–263.

SUPPLEMENTARY INFORMATION

Pif1 removes a Rap1-dependent barrier to the strand displacement activity of DNA polymerase δ

Katrina N. Koc, Saurabh P. Singh, Joseph L. Stodola, Peter M. Burgers, and Roberto Galletto
 Department of Biochemistry and Molecular Biophysics, Washington University School of Medicine, Saint Louis, MO 63110

SUPPLEMENTARY FIGURES

Figure S1. A single bound Rap1 is a barrier to the strand displacement activity of Pol δ . **A)** Quantitation of the primer extension reactions in Figure 1B using Pol δ . **B)** Quantitation of the primer extension reactions in Figure 1C using Pol δ^{DV} . **C)** Reproducibility of the Rap1 block was tested in independent experiments (n=5) using the indicated substrate.

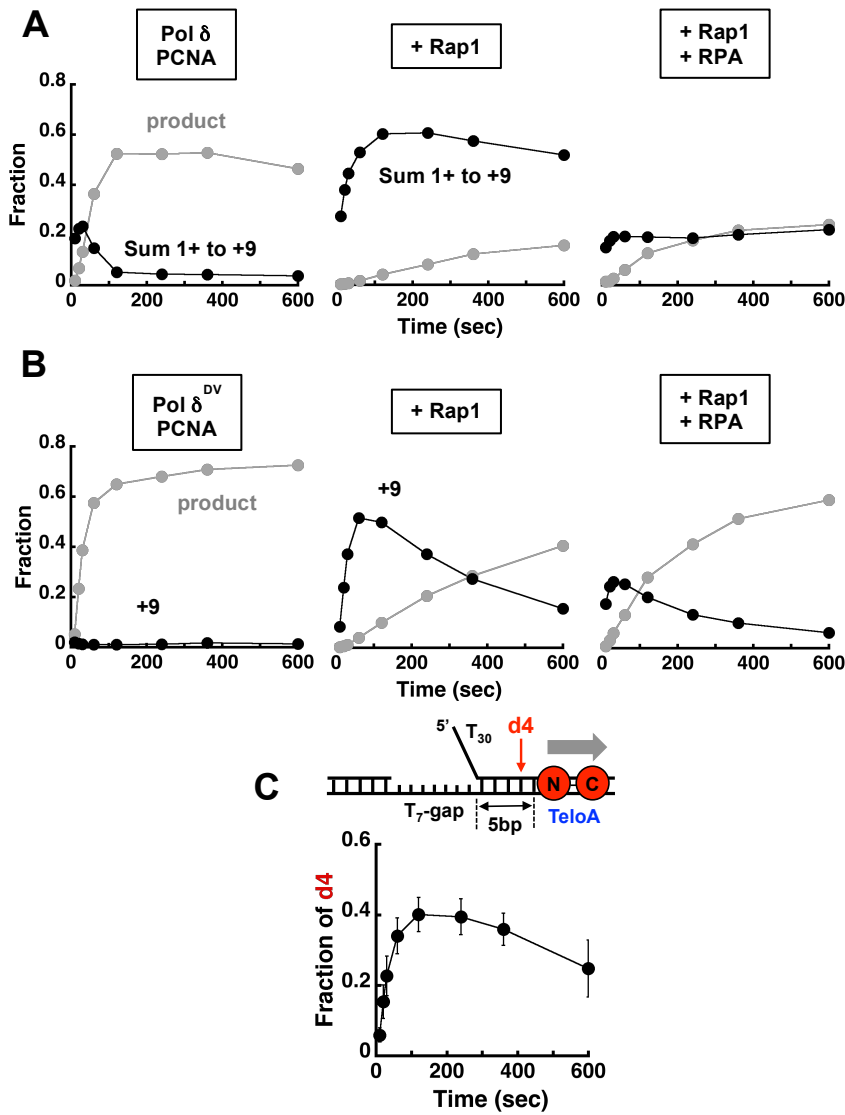


Figure S2. Pif1 stimulates the strand displacement activity of Pol δ^{DV} in the absence of PCNA. Primer extension assays with non-PCNA loaded Pol δ^{DV} (25nM) in the absence (lanes 1,2) and presence of 20nM Pif1 (lanes 5-8). The assays were performed at 40mM NaCl, a condition where Pol δ has slow strand displacement activity. In the presence of Pif1 strand displacement activity is observed at shorter times. The same experiments were also performed in the presence of 100nM Rap1 (lanes 3,4 and 9-12) and show that Pif1 allows bypass of the Rap1 block by Pol δ^{DV} .

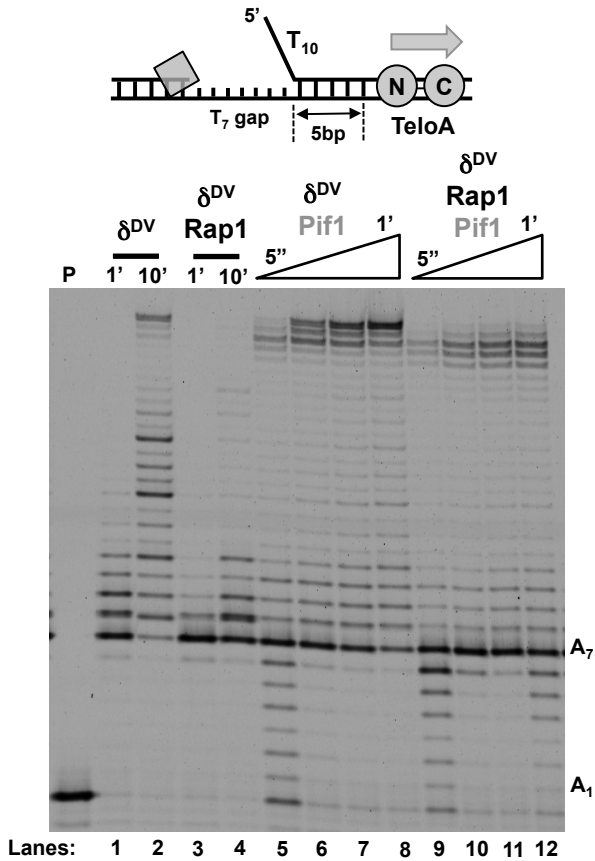
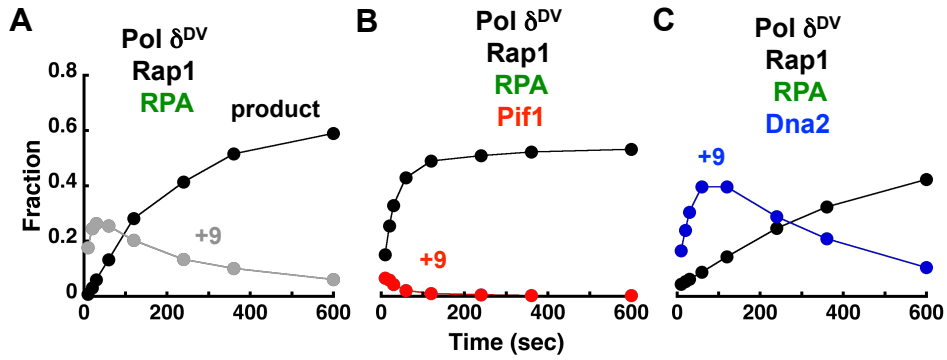


Figure S3. Pif1 stimulates the strand displacement activity of PCNA-loaded Pol δ^{DV} .
Quantitation of primer extension assays as described for Figure 4 but performed in the presence of 50nM RPA.



CHAPTER VIII

Future Directions

The first chapters (II-IV) of this thesis discuss the importance of metal binding structural motifs within Pol δ and the other eukaryotic B-family DNA polymerases. Despite the fact that these enzymes had been the focus of study for many years, these studies yielded new and interesting observations, and in turn more questions that should be addressed in the future. One significant unresolved question with respect to Pol δ is, why is an Fe-S cluster specifically present in the C-terminal domain? We know from the studies discussed here that *some* structural motif is required for interactions between Pol3 and Pol31, but why has evolution favored the formation of a functional group, the Fe-S cluster, that requires a complicated biosynthetic pathway? One possibility is that the Fe-S cluster is redox sensitive in some way, and could be a mechanism by which the general cellular environment could regulate DNA replication.

The base stacking characteristics of DNA enable the double-helix to mediate charge transport, as long as the helix is fully base-paired. The charge carried down the DNA helix has the potential to alter the redox state of proteins bound to the DNA that contain a redox-sensitive functional group. To investigate whether this could be the case with Pol δ , we have initiated a collaboration with the lab of Jacqueline Barton, at the California Institute of Technology. Preliminary results suggest that the Fe-S cluster in Pol δ is capable of cyclic oxidation and reduction when bound to DNA. However, we are only beginning to investigate what residues within the Pol3-CTD may be important for charge transfer from the DNA helix to the Fe-S cluster. Also, we do not currently understand what functional consequences would result from polymerase oxidation or reduction. These will both be areas of active research in the future.

Second, these studies, focusing on the structure-function relationships within the B-family polymerases, highlight the fact that structural information for these multi-subunit complexes is still lacking. In the case of Pol δ , X-ray crystallography has provided structural

information for the core of Pol3 and the human homologues of Pol31 and Pol32. Constructing even a tentative model of the Pol δ holoenzyme required use of the Pol1 C-terminal domain, since it is the only such domain with a known structure. As discussed in the introduction, it is thought that the Pol δ holoenzyme contains two main structural units. The first comprises the Pol3 polymerase core, while the second would contain the Pol3 C-terminal domain, Pol31, and Pol32. It is likely that the enzyme adopts a more structured conformation when in complex with PCNA and template-primer DNA, but until more structural studies are undertaken, that remains a hypothesis.

The Burgers lab has attempted to crystallize a Pol δ -PCNA-DNA complex in the past, but all efforts have been unsuccessful. This largely occurred prior to the knowledge that Pol3 contained an iron-sulfur cluster crucial for forming the multi-subunit Pol δ complex. With this in mind, more careful protein purification techniques could yield a more stable and homogenous polymerase complex more amenable to crystallization. However, I believe it is equally likely that Pol δ -PCNA naturally adopts a conformation on DNA with enough structural heterogeneity that any crystallization may be precluded. Advances in this area may be achieved through cryo-EM; recent advances in this technique make it a good candidate for this project. It is now possible to obtain backbone and in some cases even side-chain resolution for large macromolecular complexes without some of the inherent limits of crystallization.

If a high-resolution structure of the Pol δ -PCNA-DNA complex existed, what information could be gained? First, although multiple PCNA-binding motifs have been identified within Pol δ , it is unclear whether just one, or more of these motifs directly bind PCNA when the complex is bound to DNA. In Chapter II we propose that the CysA motif and the Pol32 PIP-motif are important for interaction with PCNA in different scenarios, either 'on DNA' or 'in

solution', respectively. More complete structural information would shed light onto whether that hypothesis is accurate. Second, it is unclear how many PCNA monomers the different subunits of Pol δ occupy at one time. Using the PCNA heterotrimers, it will be possible to address the functional aspects of this question. However, even if only a single wild-type monomer of PCNA is required for Pol δ activities, this would not preclude the possibility that the mutant monomers were also bound by Pol δ in some manner. Again, additional structural information could shed some light in this area.

In Chapter V, I used molecular biology techniques to evaluate the PCNA tool-belt model. While my studies provide support that this model can exist, this conclusion is still an inference based on replication data. A better approach in the long-term would be to directly observe simultaneous binding of multiple client proteins to PCNA. Using an archaeal replication system, a recent study observed simultaneous binding of the replicative polymerase and FEN1 to PCNA using negative-staining electron microscopy (Cannone et al., 2015). Such structural approaches could also be used with the eukaryotic system. However, the authors used cross-linking to create a stable complex before imaging, raising the question of whether one is simply trapping the proteins in a state that may not frequently exist in actuality. Such a concern is paramount in the case of PCNA–Pol δ –FEN1, where even in the most efficient case FEN1 processivity with PCNA is not complete.

Another option would be to develop single-molecule techniques to address this question. Total internal reflection (TIRF) microscopy, and variations, has been used in recent years to investigate a variety of DNA replication systems; these techniques could possibly be adapted to investigating nick translation. To answer this specific question, the polymerase and FEN1 would both be labeled, and PCNA-dependent co-localization of these proteins while replicating would

indicate that the multi-enzyme complex we propose does indeed exist. Of course, a prerequisite for such a technique is developing a labeling scheme for the various enzymes that retains activity, and does not preclude protein-protein interactions. As even the minimal Okazaki fragment maturation machinery is more complex than some prokaryotic and viral replication systems investigated by these techniques, this goal may be challenging. However, the validity of the tool-belt model will likely remain the subject of some debate in the field until multiple techniques can provide greater clarity.

REFERENCES

- Acharya, N., Klassen, R., Johnson, R.E., Prakash, L., and Prakash, S. (2011). PCNA binding domains in all three subunits of yeast DNA polymerase δ modulate its function in DNA replication. *Proc. Natl. Acad. Sci. U.S.A.* *108*, 17927–17932.
- Ayyagari, R., Gomes, X.V., Gordenin, D.A., and Burgers, P.M.J. (2003). Okazaki fragment maturation in yeast. I. Distribution of functions between FEN1 AND DNA2. *J. Biol. Chem.* *278*, 1618–1625.
- Bae, S.H., Bae, K.H., Kim, J.A., and Seo, Y.S. (2001). RPA governs endonuclease switching during processing of Okazaki fragments in eukaryotes. *Nature* *412*, 456–461.
- Balakrishnan, L., and Bambara, R.A. (2013a). Okazaki fragment metabolism. *Cold Spring Harb Perspect Biol* *5*, a010173–a010173.
- Balakrishnan, L., and Bambara, R.A. (2013b). Flap endonuclease 1. *Annu. Rev. Biochem.* *82*, 119–138.
- Baranovskiy, A.G., Babayeva, N.D., Liston, V.G., Rogozin, I.B., Koonin, E.V., Pavlov, Y.I., Vassilyev, D.G., and Tahirov, T.H. (2008a). X-ray structure of the complex of regulatory subunits of human DNA polymerase delta. *Cell Cycle* *7*, 3026–3036.
- Baranovskiy, A.G., Babayeva, N.D., Pavlov, Y.I., and Tahirov, T.H. (2008b). Crystallization and preliminary crystallographic analysis of the complex of the second and third regulatory subunits of human Pol delta. *Acta Crystallogr. Sect. F Struct. Biol. Cryst. Commun.* *64*, 822–824.
- Bauer, G.A., and Burgers, P.M. (1988). The yeast analog of mammalian cyclin/proliferating-cell nuclear antigen interacts with mammalian DNA polymerase delta. *Proc. Natl. Acad. Sci. U.S.A.* *85*, 7506–7510.
- Beattie, T.R., and Bell, S.D. (2012). Coordination of multiple enzyme activities by a single PCNA in archaeal Okazaki fragment maturation. *Embo J.* *31*, 1556–1567.
- Bell, S.P., and Dutta, A. (2002). DNA replication in eukaryotic cells. *Annu. Rev. Biochem.* *71*, 333–374.
- Boulé, J.-B., and Zakian, V.A. (2006). Roles of Pif1-like helicases in the maintenance of genomic stability. *Nucleic Acids Res.* *34*, 4147–4153.
- Bowman, G.D., O'Donnell, M., and Kuriyan, J. (2004). Structural analysis of a eukaryotic sliding DNA clamp-clamp loader complex. *Nature* *429*, 724–730.
- Budd, M.E., Choe, W.C., and Campbell, J.L. (1995). DNA2 encodes a DNA helicase essential for replication of eukaryotic chromosomes. *J. Biol. Chem.* *270*, 26766–26769.
- Burgers, P.M. (1988). Mammalian cyclin/PCNA (DNA polymerase delta auxiliary protein) stimulates processive DNA synthesis by yeast DNA polymerase III. *Nucleic Acids Res.* *16*, 6297–6307.
- Burgers, P.M., and Gerik, K.J. (1998). Structure and processivity of two forms of *Saccharomyces cerevisiae* DNA polymerase delta. *J. Biol. Chem.* *273*, 19756–19762.
- Burgers, P.M.J. (2009). Polymerase dynamics at the eukaryotic DNA replication fork. *J. Biol. Chem.* *284*, 4041–4045.

- Burgers, P.M.J., Gordenin, D., and Kunkel, T.A. (2016). Who Is Leading the Replication Fork, Pol ϵ or Pol δ ? *Mol. Cell* *61*, 492–493.
- Bylund, G.O., and Burgers, P.M.J. (2005). Replication protein A-directed unloading of PCNA by the Ctf18 cohesion establishment complex. *Mol. Cell. Biol.* *25*, 5445–5455.
- Cannone, G., Xu, Y., Beattie, T.R., Bell, S.D., and Spagnolo, L. (2015). The architecture of an Okazaki fragment-processing holoenzyme from the archaeon *Sulfolobus solfataricus*. *Biochem. J.* *465*, 239–245.
- Chea, J., Zhang, S., Zhao, H., Zhang, Z., Lee, E.Y.C., Darzynkiewicz, Z., and Lee, M.Y.W.T. (2012). Spatiotemporal recruitment of human DNA polymerase delta to sites of UV damage. *Cell Cycle* *11*, 2885–2895.
- Chen, R., and Wold, M.S. (2014). Replication protein A: single-stranded DNA's first responder: dynamic DNA-interactions allow replication protein A to direct single-strand DNA intermediates into different pathways for synthesis or repair. *Bioessays* *36*, 1156–1161.
- Doublé, S., and Zahn, K.E. (2014). Structural insights into eukaryotic DNA replication. *Front Microbiol* *5*, 444.
- Dovrat, D., Stodola, J.L., Burgers, P.M.J., and Aharoni, A. (2014). Sequential switching of binding partners on PCNA during in vitro Okazaki fragment maturation. *Proc. Natl. Acad. Sci. U.S.A.* *111*, 14118–14123.
- Downey, K.M., Tan, C.K., and So, A.G. (1990). DNA polymerase delta: a second eukaryotic DNA replicase. *Bioessays* *12*, 231–236.
- Fan, J., and Pavletich, N.P. (2012). Structure and conformational change of a replication protein A heterotrimer bound to ssDNA. *Genes Dev.* *26*, 2337–2347.
- Filée, J., Forterre, P., Sen-Lin, T., and Laurent, J. (2002). Evolution of DNA polymerase families: evidences for multiple gene exchange between cellular and viral proteins. *J. Mol. Evol.* *54*, 763–773.
- Fragkos, M., Ganier, O., Coulombe, P., and Méchali, M. (2015). DNA replication origin activation in space and time. *Nat. Rev. Mol. Cell Biol.* *16*, 360–374.
- Franklin, M.C., Wang, J., and Steitz, T.A. (2001). Structure of the replicating complex of a pol alpha family DNA polymerase. *Cell* *105*, 657–667.
- Fridman, Y., Palgi, N., Dovrat, D., Ben-Aroya, S., Hieter, P., and Aharoni, A. (2010). Subtle alterations in PCNA-partner interactions severely impair DNA replication and repair. *PLoS Biol.* *8*, e1000507.
- Garg, P., Stith, C.M., Sabouri, N., Johansson, E., and Burgers, P.M. (2004). Idling by DNA polymerase delta maintains a ligatable nick during lagging-strand DNA replication. *Genes Dev.* *18*, 2764–2773.
- Georgescu, R.E., Langston, L., Yao, N.Y., Yurieva, O., Zhang, D., Finkelstein, J., Agarwal, T., and O'Donnell, M.E. (2014). Mechanism of asymmetric polymerase assembly at the eukaryotic replication fork. *Nat. Struct. Mol. Biol.* *21*, 664–670.
- Georgescu, R.E., Schauer, G.D., Yao, N.Y., Langston, L.D., Yurieva, O., Zhang, D., Finkelstein, J., and O'Donnell, M.E. (2015). Reconstitution of a eukaryotic replisome reveals suppression mechanisms that define leading/lagging strand operation. *Elife* *4*.

- Gerik, K.J., Li, X., Pautz, A., and Burgers, P.M. (1998). Characterization of the two small subunits of *Saccharomyces cerevisiae* DNA polymerase delta. *J. Biol. Chem.* *273*, 19747–19755.
- Gibb, B., Ye, L.F., Kwon, Y., Niu, H., Sung, P., and Greene, E.C. (2014). Protein dynamics during presynaptic-complex assembly on individual single-stranded DNA molecules. *Nat. Struct. Mol. Biol.* *21*, 893–900.
- Gordenin, D.A., Kunkel, T.A., and Resnick, M.A. (1997). Repeat expansion--all in a flap? *Nat. Genet.* *16*, 116–118.
- Gulbis, J.M., Kelman, Z., Hurwitz, J., O'Donnell, M., and Kuriyan, J. (1996). Structure of the C-Terminal Region of p21WAF1/CIP1 Complexed with Human PCNA. *Cell* *87*, 297–306.
- Hartwell, L.H. (1976). Sequential function of gene products relative to DNA synthesis in the yeast cell cycle. *J. Mol. Biol.* *104*, 803–817.
- Hedglin, M., Kumar, R., and Benkovic, S.J. (2013a). Replication clamps and clamp loaders. *Cold Spring Harb Perspect Biol* *5*, a010165–a010165.
- Hedglin, M., Perumal, S.K., Hu, Z., and Benkovic, S. (2013b). Stepwise assembly of the human replicative polymerase holoenzyme. *Elife* *2*, e00278.
- Hopfner, K.P., Eichinger, A., Engh, R.A., Laue, F., Ankenbauer, W., Huber, R., and Angerer, B. (1999). Crystal structure of a thermostable type B DNA polymerase from *Thermococcus gorgonarius*. *Proc. Natl. Acad. Sci. U.S.A.* *96*, 3600–3605.
- Indiani, C., McInerney, P., Georgescu, R., Goodman, M.F., and O'Donnell, M. (2005). A sliding-clamp toolbelt binds high- and low-fidelity DNA polymerases simultaneously. *Mol. Cell* *19*, 805–815.
- Ito, J., and Braithwaite, D.K. (1991). Compilation and alignment of DNA polymerase sequences. *Nucleic Acids Res.* *19*, 4045–4057.
- Jain, R., Hammel, M., Johnson, R.E., Prakash, L., Prakash, S., and Aggarwal, A.K. (2009). Structural insights into yeast DNA polymerase delta by small angle X-ray scattering. *J. Mol. Biol.* *394*, 377–382.
- Jin, Y.H., Obert, R., Burgers, P.M., Kunkel, T.A., Resnick, M.A., and Gordenin, D.A. (2001). The 3'→5' exonuclease of DNA polymerase delta can substitute for the 5' flap endonuclease Rad27/Fen1 in processing Okazaki fragments and preventing genome instability. *Proc. Natl. Acad. Sci. U.S.A.* *98*, 5122–5127.
- Jin, Y.H., Ayyagari, R., Resnick, M.A., Gordenin, D.A., and Burgers, P.M.J. (2003). Okazaki fragment maturation in yeast. II. Cooperation between the polymerase and 3'→5' exonuclease activities of Pol delta in the creation of a ligatable nick. *J. Biol. Chem.* *278*, 1626–1633.
- Johansson, E., Majka, J., and Burgers, P.M. (2001). Structure of DNA polymerase delta from *Saccharomyces cerevisiae*. *J. Biol. Chem.* *276*, 43824–43828.
- Johansson, E., and Dixon, N. (2013). Replicative DNA polymerases. *Cold Spring Harb Perspect Biol* *5*, a012799–a012799.
- Johansson, E., and Macneill, S.A. (2010). The eukaryotic replicative DNA polymerases take shape. *Trends Biochem. Sci.* *35*, 339–347.
- Johansson, E., Garg, P., and Burgers, P.M.J. (2004). The Pol32 subunit of DNA polymerase delta contains separable domains for processive replication and proliferating cell nuclear antigen (PCNA)

binding. *J. Biol. Chem.* *279*, 1907–1915.

Johnson, R.E., Klassen, R., Prakash, L., and Prakash, S. (2015). A Major Role of DNA Polymerase δ in Replication of Both the Leading and Lagging DNA Strands. *Mol. Cell*.

Johnson, R.E., Klassen, R., Prakash, L., and Prakash, S. (2016). Response to Burgers et al. *Mol. Cell* *61*, 494–495.

Jónsson, Z.O., Hindges, R., and Hubscher, U. (1998). Regulation of DNA replication and repair proteins through interaction with the front side of proliferating cell nuclear antigen. *Embo J.* *17*, 2412–2425.

Kang, Y.-H., Lee, C.-H., and Seo, Y.-S. (2010). Dna2 on the road to Okazaki fragment processing and genome stability in eukaryotes. *Crit. Rev. Biochem. Mol. Biol.* *45*, 71–96.

Kao, H.-I., Henricksen, L.A., Liu, Y., and Bambara, R.A. (2002). Cleavage specificity of *Saccharomyces cerevisiae* flap endonuclease 1 suggests a double-flap structure as the cellular substrate. *J. Biol. Chem.* *277*, 14379–14389.

Kath, J.E., Jergic, S., Heltzel, J.M.H., Jacob, D.T., Dixon, N.E., Sutton, M.D., Walker, G.C., and Loparo, J.J. (2014). Polymerase exchange on single DNA molecules reveals processivity clamp control of translesion synthesis. *Proc. Natl. Acad. Sci. U.S.A.* *111*, 7647–7652.

Kelch, B.A., Makino, D.L., O'Donnell, M., and Kuriyan, J. (2011). How a DNA polymerase clamp loader opens a sliding clamp. *Science* *334*, 1675–1680.

Kim, C., Paulus, B.F., and Wold, M.S. (1994). Interactions of human replication protein A with oligonucleotides. *Biochemistry* *33*, 14197–14206.

Klinge, S., Núñez-Ramírez, R., Llorca, O., and Pellegrini, L. (2009). 3D architecture of DNA Pol alpha reveals the functional core of multi-subunit replicative polymerases. *Embo J.* *28*, 1978–1987.

Kong, X.P., Onrust, R., O'Donnell, M., and Kuriyan, J. (1992). Three-dimensional structure of the beta subunit of *E. coli* DNA polymerase III holoenzyme: a sliding DNA clamp. *Cell* *69*, 425–437.

Krishna, T.S., Fenyő, D., Kong, X.P., Gary, S., Chait, B.T., Burgers, P., and Kuriyan, J. (1994). Crystallization of proliferating cell nuclear antigen (PCNA) from *Saccharomyces cerevisiae*. *J. Mol. Biol.* *241*, 265–268.

Kubota, T., Katou, Y., Nakato, R., Shirahige, K., and Donaldson, A.D. (2015). Replication-Coupled PCNA Unloading by the Elg1 Complex Occurs Genome-wide and Requires Okazaki Fragment Ligation. *Cell Rep* *12*, 774–787.

Kubota, T., Myung, K., and Donaldson, A.D. (2013a). Is PCNA unloading the central function of the Elg1/ATAD5 replication factor C-like complex? *Cell Cycle* *12*, 2570–2579.

Kubota, T., Nishimura, K., Kanemaki, M.T., and Donaldson, A.D. (2013b). The Elg1 replication factor C-like complex functions in PCNA unloading during DNA replication. *Mol. Cell* *50*, 273–280.

Kumaran, S., Kozlov, A.G., and Lohman, T.M. (2006). *Saccharomyces cerevisiae* replication protein A binds to single-stranded DNA in multiple salt-dependent modes. *Biochemistry* *45*, 11958–11973.

Larrea, A.A., Lujan, S.A., Nick McElhinny, S.A., Mieczkowski, P.A., Resnick, M.A., Gordenin, D.A.,

and Kunkel, T.A. (2010). Genome-wide model for the normal eukaryotic DNA replication fork. *Proc. Natl. Acad. Sci. U.S.A.* *107*, 17674–17679.

Lee, M.Y.W.T., Zhang, S., Lin, S.H.S., Chea, J., Wang, X., LeRoy, C., Wong, A., Zhang, Z., and Lee, E.Y.C. (2012). Regulation of human DNA polymerase delta in the cellular responses to DNA damage. *Environ. Mol. Mutagen.* *53*, 683–698.

Levikova, M., and Cejka, P. (2015). The *Saccharomyces cerevisiae* Dna2 can function as a sole nuclease in the processing of Okazaki fragments in DNA replication. *Nucleic Acids Res.* *43*, 7888–7897.

Li, H., Xie, B., Zhou, Y., Rahmeh, A., Trusa, S., Zhang, S., Gao, Y., Lee, E.Y.C., and Lee, M.Y.W.T. (2006). Functional roles of p12, the fourth subunit of human DNA polymerase delta. *J. Biol. Chem.* *281*, 14748–14755.

Lin, S.H.S., Wang, X., Zhang, S., Zhang, Z., Lee, E.Y.C., and Lee, M.Y.W.T. (2013). Dynamics of enzymatic interactions during short flap human Okazaki fragment processing by two forms of human DNA polymerase δ . *DNA Repair (Amst.)* *12*, 922–935.

Maga, G., Villani, G., Tillement, V., Stucki, M., Locatelli, G.A., Frouin, I., Spadari, S., and Hübscher, U. (2001). Okazaki fragment processing: modulation of the strand displacement activity of DNA polymerase delta by the concerted action of replication protein A, proliferating cell nuclear antigen, and flap endonuclease-1. *Proc. Natl. Acad. Sci. U.S.A.* *98*, 14298–14303.

Maga, G., and Hubscher, U. (2003). Proliferating cell nuclear antigen (PCNA): a dancer with many partners. *J. Cell. Sci.* *116*, 3051–3060.

Majka, J., and Burgers, P.M.J. (2004). The PCNA-RFC families of DNA clamps and clamp loaders. *Prog. Nucleic Acid Res. Mol. Biol.* *78*, 227–260.

Makarova, A.V., and Burgers, P.M. (2015). Eukaryotic DNA polymerase ζ . *DNA Repair (Amst.)* *29*, 47–55.

Makarova, A.V., Stodola, J.L., and Burgers, P.M. (2012). A four-subunit DNA polymerase ζ complex containing Pol δ accessory subunits is essential for PCNA-mediated mutagenesis. *Nucleic Acids Res.* *40*, 11618–11626.

Masai, H., Matsumoto, S., You, Z., Yoshizawa-Sugata, N., and Oda, M. (2010). Eukaryotic chromosome DNA replication: where, when, and how? *Annu. Rev. Biochem.* *79*, 89–130.

Moldovan, G.-L., Pfander, B., and Jentsch, S. (2007). PCNA, the maestro of the replication fork. *Cell* *129*, 665–679.

Montecucco, A., Rossi, R., Levin, D.S., Gary, R., Park, M.S., Motycka, T.A., Ciarrocchi, G., Villa, A., Biamonti, G., and Tomkinson, A.E. (1998). DNA ligase I is recruited to sites of DNA replication by an interaction with proliferating cell nuclear antigen: identification of a common targeting mechanism for the assembly of replication factories. *Embo J.* *17*, 3786–3795.

Netz, D.J.A., Stith, C.M., Stümpfig, M., Köpf, G., Vogel, D., Genau, H.M., Stodola, J.L., Lill, R., Burgers, P.M.J., and Pierik, A.J. (2012). Eukaryotic DNA polymerases require an iron-sulfur cluster for the formation of active complexes. *Nat. Chem. Biol.* *8*, 125–132.

- Neuwald, A.F., Aravind, L., Spouge, J.L., and Koonin, E.V. (1999). AAA+: A class of chaperone-like ATPases associated with the assembly, operation, and disassembly of protein complexes. *Genome Res.* *9*, 27–43.
- Nguyen, B., Sokoloski, J., Galletto, R., Elson, E.L., Wold, M.S., and Lohman, T.M. (2014). Diffusion of human replication protein A along single-stranded DNA. *J. Mol. Biol.* *426*, 3246–3261.
- Nick McElhinny, S.A., Gordenin, D.A., Stith, C.M., Burgers, P.M.J., and Kunkel, T.A. (2008). Division of labor at the eukaryotic replication fork. *Mol. Cell* *30*, 137–144.
- Prakash, A., and Borgstahl, G.E.O. (2012). The structure and function of replication protein A in DNA replication. *Subcell. Biochem.* *62*, 171–196.
- Prelich, G., Kostura, M., Marshak, D.R., Mathews, M.B., and Stillman, B. (1987). The cell-cycle regulated proliferating cell nuclear antigen is required for SV40 DNA replication in vitro. *Nature* *326*, 471–475.
- Pursell, Z.F., Isoz, I., Lundström, E.-B., Johansson, E., and Kunkel, T.A. (2007). Yeast DNA polymerase epsilon participates in leading-strand DNA replication. *Science* *317*, 127–130.
- Reijns, M.A.M., Kemp, H., Ding, J., de Procé, S.M., Jackson, A.P., and Taylor, M.S. (2015). Lagging-strand replication shapes the mutational landscape of the genome. *Nature* *518*, 502–506.
- Rossi, M.L., Pike, J.E., Wang, W., Burgers, P.M.J., Campbell, J.L., and Bambara, R.A. (2008). Pif1 helicase directs eukaryotic Okazaki fragments toward the two-nuclease cleavage pathway for primer removal. *J. Biol. Chem.* *283*, 27483–27493.
- Stewart, J.A., Campbell, J.L., and Bambara, R.A. (2010). Dna2 is a structure-specific nuclease, with affinity for 5'-flap intermediates. *Nucleic Acids Res.* *38*, 920–930.
- Stith, C.M., Sterling, J., Resnick, M.A., Gordenin, D.A., and Burgers, P.M. (2008). Flexibility of eukaryotic Okazaki fragment maturation through regulated strand displacement synthesis. *J. Biol. Chem.* *283*, 34129–34140.
- Sugimoto, K., Sakamoto, Y., Takahashi, O., and Matsumoto, K. (1995). HYS2, an essential gene required for DNA replication in *Saccharomyces cerevisiae*. *Nucleic Acids Res.* *23*, 3493–3500.
- Swan, M.K., Johnson, R.E., Prakash, L., Prakash, S., and Aggarwal, A.K. (2009). Structural basis of high-fidelity DNA synthesis by yeast DNA polymerase delta. *Nat. Struct. Mol. Biol.* *16*, 979–986.
- Tan, C.K., Castillo, C., So, A.G., and Downey, K.M. (1986). An auxiliary protein for DNA polymerase-delta from fetal calf thymus. *J. Biol. Chem.* *261*, 12310–12316.
- Tishkoff, D.X., Filosi, N., Gaida, G.M., and Kolodner, R.D. (1997). A novel mutation avoidance mechanism dependent on *S. cerevisiae* RAD27 is distinct from DNA mismatch repair. *Cell* *88*, 253–263.
- Tsutakawa, S.E., Classen, S., Chapados, B.R., Arvai, A.S., Finger, L.D., Guenther, G., Tomlinson, C.G., Thompson, P., Sarker, A.H., Shen, B., et al. (2011). Human flap endonuclease structures, DNA double-base flipping, and a unified understanding of the FEN1 superfamily. *Cell* *145*, 198–211.
- Vijayakumar, S., Chapados, B.R., Schmidt, K.H., Kolodner, R.D., Tainer, J.A., and Tomkinson, A.E. (2007). The C-terminal domain of yeast PCNA is required for physical and functional interactions with

Cdc9 DNA ligase. *Nucleic Acids Res.* 35, 1624–1637.

Wang, M., Xia, S., Blaha, G., Steitz, T.A., Konigsberg, W.H., and Wang, J. (2011). Insights into base selectivity from the 1.8 Å resolution structure of an RB69 DNA polymerase ternary complex. *Biochemistry* 50, 581–590.

Weinberg, D.H., Collins, K.L., Simancek, P., Russo, A., Wold, M.S., Virshup, D.M., and Kelly, T.J. (1990). Reconstitution of simian virus 40 DNA replication with purified proteins. *Proc. Natl. Acad. Sci. U.S.a.* 87, 8692–8696.

Weinreich, M. (2015). Molecular biology: DNA replication reconstructed. *Nature* 519, 418–419.

Wold, M.S., and Kelly, T. (1988). Purification and characterization of replication protein A, a cellular protein required for in vitro replication of simian virus 40 DNA. *Proc. Natl. Acad. Sci. U.S.a.* 85, 2523–2527.

Yeeles, J.T.P., Deegan, T.D., Janska, A., Early, A., and Diffley, J.F.X. (2015). Regulated eukaryotic DNA replication origin firing with purified proteins. *Nature* 519, 431–435.

Yu, C., Gan, H., Han, J., Zhou, Z.-X., Jia, S., Chabes, A., Farrugia, G., Ordog, T., and Zhang, Z. (2014). Strand-specific analysis shows protein binding at replication forks and PCNA unloading from lagging strands when forks stall. *Mol. Cell* 56, 551–563.

Zhang, S., Zhou, Y., Trusa, S., Meng, X., Lee, E.Y.C., and Lee, M.Y.W.T. (2007). A novel DNA damage response: rapid degradation of the p12 subunit of dna polymerase delta. *J. Biol. Chem.* 282, 15330–15340.

